April 24-25, 2023
CHICAGO
HYATT REGENCY MCCORMICK PLACE

Midwest Clinical & Translational Research Meeting

2023 Annual Meeting Abstracts and Case Reports

Central Society for Clinical and Translational Research

and the

Midwestern Section of the American Federation for Medical Research

2023 Program Committee

Suthat Liangpunsakul, MD, MPH
Jennifer Alexander-Brett, MD, PhD
Dawn Belt Davis, MD, PhD
Steven Dudek, MD
David J. Kennedy, PhD

Anupam Kotwal, MBBS
Jerry A. Krishnan, MD, PhD
Suman Setty, MBBS, PhD
Jeffrey D. Salomon, MD
Terry Unterman, MD

Cardiology / Cardiovascular Disease

1

OUTCOMES IN PATIENTS WITH CARDIAC ARREST NOT UNDERGOING CARDIAC CATHETERIZATION

[1]Suhaib Bajwa, [2]Karthik Gangu, [1]Aniesh Bobba, [2]Sindhu Avula. *[1]University of Missouri; [2]University of Kansas*

Introduction/Background Ventricular tachycardia (VT) and ventricular fibrillation (VF) account for 23-54% of cardiac arrest and are often due to underlying coronary artery disease. Among patients who suffer cardiac arrest secondary to VT/VF, those with evidence of ST segment changes on the post resuscitation electrocardiogram (ECG) had approximately a 70-85% chance of having underlying coronary artery disease. The same patient cohort but without evidence of ST segment changes on the post resuscitation ECG had approximately a 25-50% of having underlying coronary artery disease [1]. A recent nationwide study indicated that post resuscitation for VT or VF arrest, only 87.2% of patients with ST elevation and 33.9% of patients without ST elevation underwent cardiac catheterization in 2016. We aim to study outcomes in patients with cardiac arrest with VT/VF without cardiac catheterization.

Objective(s) - To demonstrate the importance of cardiac catheterization for patients who have cardiac arrest secondary to VT or VF- To highlight the 2019 American Heart Association Scientific Statement recommending urgent cardiac catheterization for patients who suffer cardiac arrest secondary to VT/VF regardless of the presence of ST segment changes.

Methods We conducted a retrospective analysis utilizing 2018 Nationwide readmission database. We included patients with age ≥ 18 yrs who had cardiac arrest secondary to VT/VF and did not undergo cardiac catheterization during index hospitalization. ICD-10 CM (clinical modification) and procedure codes were used to identify the patient population. Primary outcomes were 30-day readmission rate, and the most common cause of readmission. Independent risk factors for readmission were identified using multivariate COX regression analysis.

Results A total of 47,494 patients were included in the study, of which 4,431 died during the index admission. Of patients who were discharged alive, 5,543 (12.86%) were readmitted within 30-days with the most common reason being recurrent ventricular tachycardia (34.4%). Patient characteristics and the most common reasons for readmission were represented in Table 1 & 2.

Table 1: Patient characteristics (N= 47494)	
Variable	**N (%)**
Age (years)	
18-44	3704 (7.8)
45-64	16366 (34.46)
65-84	23848 (50.21)
≥85	3576 (7.53)
Mean Age (SD)	
Female	64.38 (16.4)
Male	66.32 (13.9)
Sex (Female)	26.53%
Median income ($)	
<$45,999	12697 (26.73)
46,000 – 58,999	13481 (28.38)
59,000 - 78,999	12146 (25.57)
>79,000	9170 (19.3)
Insurance	
Medicare	30669 (64.57)
Medicaid	4317 (9.09)
Private	11364 (23.92)
Uninsured	1144 (2.41)

Table 2: Most common all cause 30-day readmission	N (%)
1. VT	1909 (34.3%)
2. Hypertensive heart and chronic kidney disease	496 (8.9%)
3. Hypertensive heart disease with heart failure	267 (4.8%)
4. Sepsis, unspecified	189 (3.4%)
5. VF	153 (2.8%)
6. Acute Kidney Failure	130 (1.2%)
7. Acute on chronic systolic heart failure	76 (1.2%)
8. Supraventricular Tachycardia	68 (1.2%)
9. Paroxysmal atrial fibrillation	64 (1.2%)
10. NSTEMI	63 (1.1%)

Conclusion Our study shows that 34.4% of patients with cardiac arrest due to VT/VF without subsequent cardiac catheterization who were readmitted within 30 days had recurrent VT which demonstrates the importance of urgent cardiac catheterization. This affirms the 2019 American Heart Association Scientific Statement recommending that patients post resuscitation for VT/VF would benefit from urgent cardiac catheterization regardless of the presence of ST segment changes on the post resuscitation ECG.

REFERENCE(S)

1. Yannopoulos D, Bartos JA, Aufderheide TP, et al. The Evolving Role of the Cardiac Catheterization Laboratory in the Management of Patients With Out-of-Hospital Cardiac Arrest: A Scientific Statement From the American Heart Association. Circulation 2019;Feb 14

2

RIGHT VENTRICULAR FUNCTION ON CARDIOVASCULAR MAGNETIC RESONANCE IMAGING AND LONG-TERM OUTCOMES IN STABLE HEART TRANSPLANT RECIPIENTS.

[1]Collin Barrett, [1]Parag Bawaskar, [2]Andrew Hughes, [1]Pal Satyajit Singh Athwal, [1]Khaled Ismail, [1]Tamas Alexy, [1]Chetan Shenoy. [1]*University of Minnesota Medical School;* [2]*Vanderbilt University Medical Center*

Introduction/Background In stable heart transplant recipients, right ventricular (RV) dysfunction may occur for a variety of reasons, including pulmonary hypertension, tricuspid regurgitation, rejection(s), and cardiac allograft vasculopathy. Whether RV dysfunction in the stable phase after heart transplantation is associated with long-term adverse outcomes is unknown. This knowledge has the potential to improve the long-term outcomes of heart transplant recipients.

Objective(s) We sought to determine the long-term prognostic significance of RV dysfunction identified using cardiovascular magnetic resonance imaging (CMR) at least one year after heart transplantation.

Methods We performed a retrospective cohort study of consecutive heart transplant recipients who had CMR for routine surveillance between July 2001 and December 2020 at our institution. We assessed two CMR measures of RV function: RV ejection fraction (RVEF) and RV global longitudinal strain (RVGLS). We investigated associations between RV dysfunction and a composite endpoint of death or major adverse cardiac events (MACE), including re-transplantation, non-fatal myocardial infarction, coronary revascularization, and heart failure hospitalization. Kaplan–Meier analyses and multivariable Cox proportional hazards regression analyses were used for these analyses.
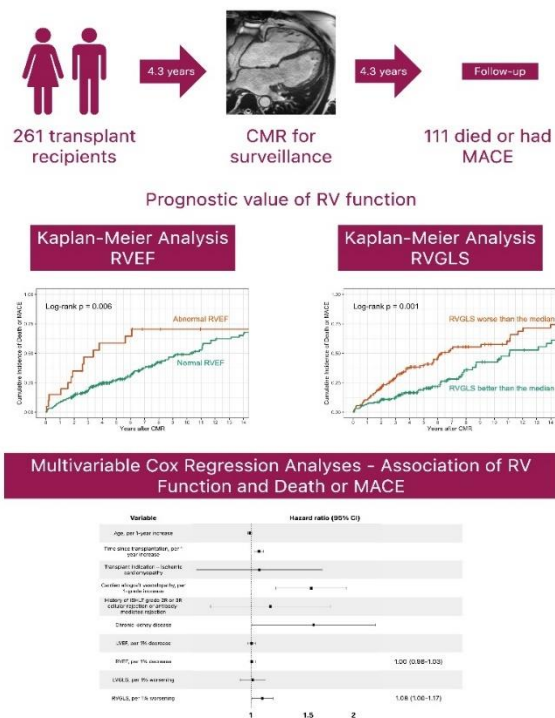
Abstract 2 Figure 1

Results 261 heart transplant recipients (median age 59.1 years; 75.5% men) who had CMRs at a median of 4.3 years after heart transplantation were included. Over a median follow-up of 4.3 years after the CMR, 111 recipients experienced the study outcome of death or MACE. On Kaplan-Meier analyses, recipients with abnormal RVEF had a greater estimated cumulative incidence of the composite endpoint compared with recipients with normal RVEF (log-rank p=0.006), and recipients with RVGLS worse than the median had a greater estimated cumulative incidence of the composite endpoint compared with recipients with RVGLS better than the median (log-rank=0.001). On multivariable Cox regression, RVEF was not associated with the composite endpoint, but RVGLS was independently associated with the composite endpoint with a hazard ratio of 1.08 for every 1% worsening in RVGLS (95% confidence interval: 1.00 to 1.17; p=0.041). The association was replicated in subgroups of recipients with normal RVEF and those with late gadolinium enhancement imaging. RVGLS provided incremental prognostic value over other variables in the multivariable analyses.

Conclusion CMR feature tracking-derived RVGLS assessed at least one year after heart transplantation was independently associated with the long-term risk of death or MACE, while RVEF was not. Future studies should investigate the role of CMR feature tracking-derived RVGLS in guiding clinical decision-making in heart transplant recipients.

3

EFFECT OF DIFFERENT LIGATION TIMES AND MOUSE STRAINS ON LEFT VENTRICULAR FUNCTIONS: A MOUSE MODEL OF MYOCARDIAL INFARCTION

Ayman Isbatan, Ming Tang, Maricela Castellon, Zhigang Hong, Sang Ging Ong, Jalees Rehman, Jiwang Chen. *University of Illinois at Chicago*

Introduction/Background The mouse model of myocardial infarction (MI) has been widely used to study prevention, diagnosis and therapy of human MI. Different mouse strains with different ligation times have been traditionally used in cardiac infarct studies.

Objective(s) In this study, we aim to examine the effect of two different mouse strains (C57Bl6 and an immunodeficient mouse called NOD-SCID) and different ligation times (30 min and permanent) on the left ventricular functions with echocardiography.

Methods All the procedures were approved by the Ethics / Animal Care Committee of the University of Illinois at Chicago.Mice: C57BL/6 and NOD/SCID mice were purchased from Jackson Laboratories (Sacramento, CA).Myocardial infarction (MI): Adult mice weighing 25–30g were anesthetized and ventilated. A left thoracotomy was performed via the fourth intercostal space to expose the heart. The left anterior descending coronary artery (LAD) was identified and ligated. Ligation was released after 30 minutes or left intact (permanent ligation). The lungs were inflated by increasing positive end-expiratory pressure and the thoracotomy site closed. Animals that had sham surgery underwent the same procedure with the exception of LAD ligation. The animals were observed and studied for six weeks post-surgery. Echocardiography was performed with the VEVO2100 (Visualsonics, Inc) using a 550Hz transducer.

Results Our data demonstrates that, in the groups with 30 min ligation, C57Bl6 mice have significantly lower ejection fraction (EF) and fraction shortening (FS) values at Day 2 and Day 7 after MI surgeries, compared to NOD-SCID mice. In addition, NOD-SCID mice have no significant difference of EF and FS values between pre-MI and 48 hrs after MI, but both EF and FS values significantly decrease at Day 7 after MI. We also found that, in NOD-SCID mice, EF and FS values significantly decreased in permanent ligation group compared to 30 min ligation at either Day 2 or Day 7 after MI surgeries, however in C57Bl6 mice we did not observe significant decrease of EF and FS values in the permanent ligation group, compared to 30-min ligation group.

Abstract 3 Table 1
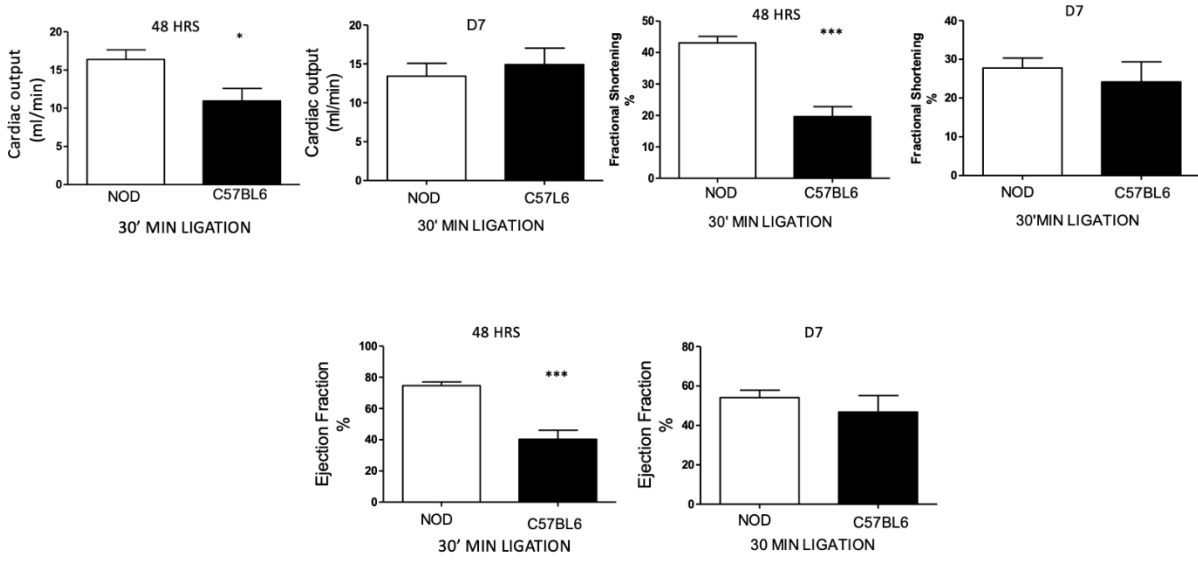
Abstract 3 Table 2
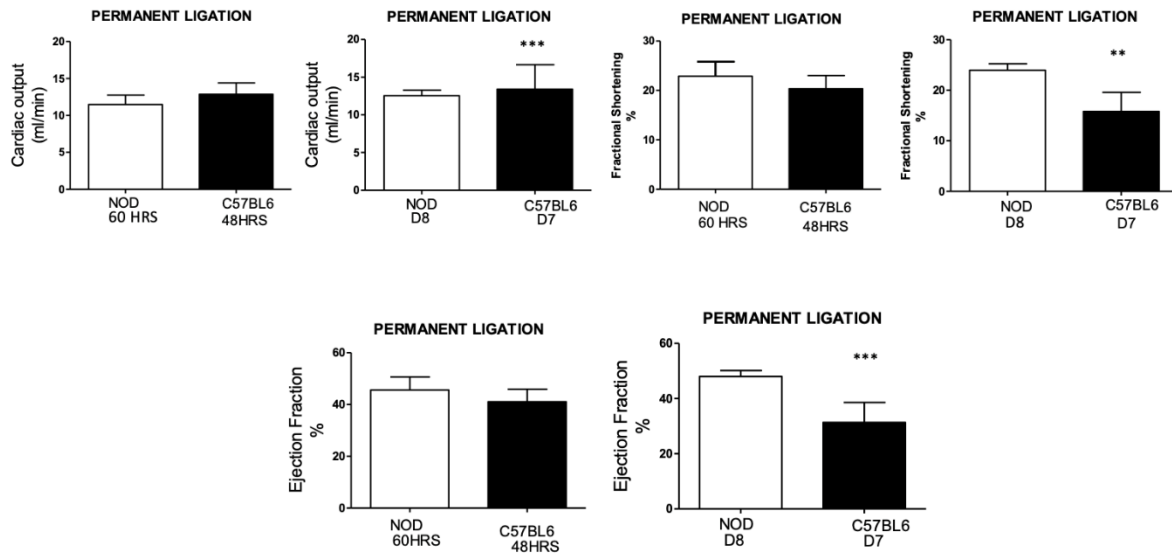
Conclusion This study will be essential for experimental design of MI studies.

4

CASPASE 12 DEFICIENCY IS PROTECTIVE FOR HEART FAILURE

[1]Dan Marian, [2]Ayman Isbatan, [2]Ali Imran Sarwar, [2]Maricela Castellon, [2]Jiwang Chen. [1]*Cardiovascular Research Core at UIC;* [2]*University of Illinois at Chicago*

Introduction/Background Caspase-12 has long been used as an upregulation marker for endoplasmic reticulum (ER) stress, a key apoptotic pathway in cells. In addition, ER stress is believed to have a significant role in mediating ischemic heart failure.

Objective(s) We seek to examine whether or not caspase-12 deficiency is protective for heart failure.

Methods To test this hypothesis, caspase-12 knockout (KO) mice and their wild-type siblings (WT) were used. Each of these mice were subjected to the permanent ligation of the left anterior descending coronary artery (LAD), resulting in induced myocardial infarction (MI). Subsequently, heart function was monitored over several time intervals (24hrs, 48hrs, 72hrs, 7 days, and 1 month) via echocardiography, using the Fujifilm Vevo 2100.

Results M-mode analysis of parasternal short-axis views of left ventricular function showed that ejection fraction (EF) values are significantly higher in caspase-12 KO than in WT mice (49.82% vs 34.66% (± 6.775%), p=.033) after 24 hours and after a month (41.34% vs 32.11% (± 3.397%), p=.021); the fractional shortening (FS) values were also significantly higher in caspase-12 KO mice after a month (20.18% vs 15.01% (± 1.975%), p=.024); and their CO values were significantly higher in KO mice (17.72 mL/min vs 12.72 mL/min (± 1.756 mL/min), p=.011) after a month. All statistical results were obtained using unpaired one-tailed t-tests with comparison to student's t-table values.

Conclusion In light of these results, we conclude that caspase-12 deficiency offers a protective effect against the development of severe acute heart failure. Inhibition of the caspase-12 pathway may have a therapeutic effect in the treatment of heart failure.

5

LONG-TERM PROGNOSTIC VALUE OF LEFT AND RIGHT VENTRICULAR SYSTOLIC FUNCTION ON CARDIOVASCULAR MAGNETIC RESONANCE IMAGING IN SYSTEMIC SCLEROSIS

Parag Bawaskar, Sanya Chhikara, Adinan Kanda, Chetan Shenoy. *University of Minnesota*

Introduction/Background Systemic sclerosis (SSc) is rare autoimmune disorder that is associated with a high risk of cardiovascular disease. Previous studies on the prognostic significance of ventricular systolic function have shown inconsistent results, mainly because of their small size. Therefore, a large study is needed to better understand the value of ventricular systolic function in identifying SSc patients at risk of adverse outcomes.

Objective(s) We aimed to determine the long-term prognostic value of left and right ventricular (LV and RV) systolic dysfunction detected on cardiovascular magnetic resonance imaging (CMR) in a large cohort of SSc patients.

Methods In this retrospective cohort study, we included consecutive adults with SSc who had CMR imaging for suspected cardiac disease from 2005 to 2020. We assessed two CMR measures of ventricular systolic function for each ventricle—ejection fraction (EF) and feature tracking-derived global longitudinal strain (GLS)—and investigated their associations with the long-term incidence of a composite endpoint of death or major adverse cardiac events (MACE) using Kaplan–Meier analyses and multivariable Cox proportional hazards regression analyses. MACE was defined as one or more occurrences of heart failure hospitalization, ventricular assist device implantation, heart transplantation, and sustained ventricular tachycardia.

Results 130 SSc patients (median age 58 years; 80% female) with suspected cardiac involvement had CMR for clinical indications at a median of 3.6 years after diagnosis. The median LVEF was 57.5% and the median LVGLS was −15.1%. The median RVEF was 57.0% and the median RVGLS was −16.3%. Abnormal LVEF and RVEF were present in 22% and 20% of patients, respectively. Over a median follow-up of 3.6 years after the CMR, 49 patients experienced the composite endpoint of death or MACE. On Kaplan-Meier analyses, abnormal LVEF and RVEF were associated with greater cumulative incidence of death or MACE compared to normal LVEF (log-rank p = 0.026) and normal RVEF (log-rank p = 0.003), respectively. In addition, LVGLS and RVGLS less than median were associated with a greater cumulative incidence of death or MACE compared to LVGLS more than median (log-rank p = 0.020) and RVGLS more than median (log-rank p = 0.013), respectively. On multivariable Cox regression, after adjustment for established clinical and imaging risk factors, a 1% worsening in LVGLS was independently associated with a 11% increased risk of the primary end point [(hazard ratio [HR] 1.11 per 1% worsening; 95% confidence interval [CI] 1.02-1.22; p = 0.022), while LVEF was not associated with the composite endpoint of death or MACE (HR 1.01 per 1% decrease; 95% CI 0.98-1.05; p = 0.41). Similarly, a 1% worsening in RVGLS was independently associated with a 13% increased risk of the primary end point [(hazard ratio [HR] 1.13 per 1% worsening; 95% confidence interval [CI] 1.04-1.23; p = 0.003), while RVEF was not associated with the composite endpoint of death or MACE (HR 0.99 per 1% decrease; 95% CI 0.96-1.03; p = 0.69).

Conclusion In a large cohort of patients with SSc investigated by CMR, LVGLS and RVGLS were independently associated with death or MACE while LVEF and RVEF were not. CMR feature tracking-derived GLS shows promise in guiding clinical decision-making in SSc, which needs to be investigated further.

6

## SYMPATHETIC NERVOUS SYSTEM AS A POTENTIAL NEW THERAPEUTIC TARGET FOR ABDOMINAL AORTIC ANEURYSM

Calvin Chao, Caitlyn Dang, Taylor Brown, Bin Jiang. *Northwestern University*

Introduction/Background Abdominal aortic aneurysms (AAA) are defined as localized dilation of the infrarenal aorta to greater than 3.0 cm and remain a leading cause of premature death worldwide. The primary risk of this condition is aortic rupture and subsequent massive hemorrhage with a mortality rate of 85-90% after rupture. Strategies for repair broadly consist of open aortic surgery or endovascular aneurysm repair (EVAR), which has become the predominant treatment modality. Yet, despite remarkable advancements in surgical technique, particularly in the endovascular space, no pharmacologic therapy has successfully slowed or halted AAA growth. There is thus an unmet clinical need to develop novel therapeutics that could limit the growth and rupture of AAA.

Objective(s) The paucity of medical therapies for the management of AAA and negative clinical trials have prompted significant interest in elucidating novel mechanisms in the pathogenesis and thus new therapeutic targets of this condition. Aortic wall stress, or vascular tone, is highly regulated by neural innervation from the sympathetic nervous system (SNS). Despite recognition that SNS innervation to vascular smooth muscle cells (VSMC) mediates cell phenotype, how SNS dysfunction contributes to AAA pathogenesis remains unknown. This study aims to evaluate the role of the perivascular SNS during AAA formation as a potential therapeutic target. We hypothesize that dysfunction of sympathetic innervation to the abdominal aortic smooth muscle is crucial to the onset of aortic dilatation and progression of aneurysmal disease.

Methods To generate experimental AAA, male ApoE-/- mice (n=5) underwent subcutaneous osmotic pump implantation for continuous Angiotensin II (AngII) infusion (1 µg/kg/min). Animals were monitored through 4 weeks with necropsies conducted after any mortality to confirm aortic rupture as cause of death. At 4 weeks, animals were sacrificed for aortic tissue harvest and subsequent morphologic, histologic, and immunohistochemical analysis. For systemic denervation, ApoE-/- mice underwent serial intraperitoneal injection (100 mg/kg, 250 mg/kg) of 6-hydroxydopamine (6-OHDA) (n=7) or vehicle control (n=3). Denervated animals were sacrificed at 2 weeks or 4 weeks to assess sustained denervation via morphologic, histologic, and immunohistochemical analysis. Our combination model utilizing AngII infusion and 6-OHDA administration is underway. Male ApoE-/- mice underwent subcutaneous osmotic pump implantation with serial 6-OHDA denervation (n=5) or delayed denervation (n=5). The results of this experiment are pending and will conclude prior to this meeting.

Results Tyrosine hydroxylase (TH), an SNS-specific marker, was utilized to visualize nerve fibers (Figure 1). AngII group aortic walls demonstrated significantly increased nerve fibers (n=32.3 ± 7.1) and density (154.4 ± 47.2 fibers/mm2) as compared to healthy controls (n=3.7 ± 1.7, 53.5 ± 19.2 fibers/mm2) (Figure 2). 6-OHDA administration produced sustained denervation of mesenteric branch arteries through two weeks with evidence of some neural regeneration at four weeks (Figure 1). No mortality or weight loss was observed after 6-OHDA administration. Analysis of our combination AngII infusion and 6-OHDA denervation model results are on-going and anticipated to conclude prior to this meeting.
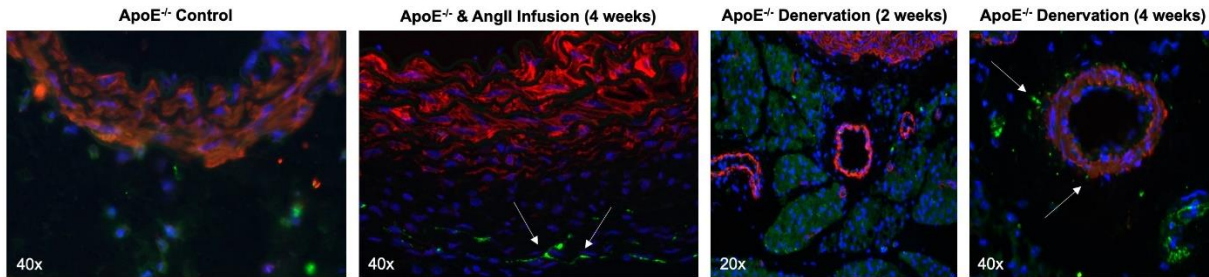
Figure 1: Representative IHC of control aorta (left), experimental aorta after AngII infusion (left middle), mesenteric branch artery after denervation (right middle), and mesenteric branch artery after four weeks (right). Red=αSMA; Blue=DAPI; Green=Tyrosine Hydroxylase (TH).

Abstract 6 Figure 1
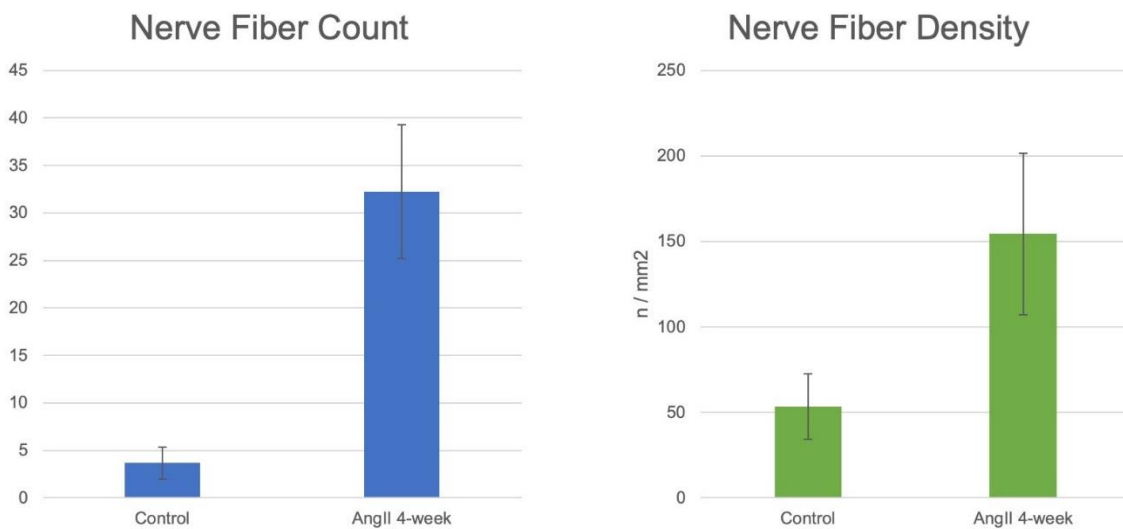
Figure 2: Quantification of nerve fiber count (left) and density (right).

Abstract 6 Figure 2

Conclusion Our findings suggest an evolving role of SNS dysregulation in AAA pathogenesis and the utility of systemic vascular denervation in elucidating the function of the perivascular SNS in aortic pathologies. Ultimately, our results highlight the SNS as a potential therapeutic target in the treatment of AAA.

7

A LIPIDOMICS APPROACH TO PREDICTING PULMONARY HYPERTENSION IN HUMAN HEART FAILURE WITH PRESERVED EJECTION FRACTION

Vaishnavi Aradhyula, Rohit Vyas, Prabhatchandra Dube, Rajesh Gupta, Steven Haller, David Kennedy, Samer Khouri. *University of Toledo College of Medicine and Life Sciences*

Introduction/Background Pulmonary hypertension (PH) in heart failure with preserved ejection fraction (HFpEF; PH-HFpEF) is associated with high morbidity and mortality; however, the pathophysiology of disease is unknown. The development of PH is a continuum of disease processes initiated by HFpEF, where patients initially develop isolated postcapillary PH (ipc-PH) which can transform to the more fatal combined pre and postcapillary PH (cpc-PH). This transformation of PH does not occur in all patients and is not explained by traditional risk factors alone, necessitating the need to examine novel regulatory mechanisms. Polyunsaturated Fatty Acid (PUFA) metabolites play a vital role in cardiovascular health by regulating balance between anti-inflammatory, pro-inflammatory, and pro-resolutory lipid mediators. An imbalance of lipid metabolites has been previously shown to predispose PH.

Objective(s) Here, we sought to characterize PUFA-derived mediators that distinguish PH in patients with HFpEF.

Methods Pulmonary arterial and venous serum samples were collected during right heart catheterization from 88 HFpEF patients without PH (control, n=40), HFpEF with ipc-PH (ipc-PH-HFpEF, n=30), and HFpEF with cpc-PH (cpc-PH-HFpEF, n=18). 143 PUFA metabolites were analyzed using mass spectroscopy with Multiple Reaction Monitoring. A series of regression models was conducted to assess which molecules were predictive of PH.

Results The ipc-PH-HFpEF model was characterized by low pro-resolutory 7(S)-Maresin1 (p=0.0003), low anti-inflammatory 11(12)-EpETrE (p=0.02), and low 8(S)-HETrE (p=0.02) PUFA metabolites compared to control. The cpc-PH-HFpEF model was characterized by low pro-resolutory 7(S)-Maresin1 (p=0.004), high pro-inflammatory 5,6-DiHETrE (p=0.001), and high pro-inflammatory tetranor prostaglandin E metabolite, a major metabolite of Prostaglandin E2 (p=0.007) compared to control. Additionally, cpc-PH-HFpEF was characterized by high PGF2a, both a pro- and anti-inflammatory metabolite, compared to pc-PH-HFpEF patients (p=0.006).

Conclusion These findings support the hypothesis that distinct PUFA metabolites may play a significant role in mediating PH in HFpEF. Our study introduces a novel lipidomics framework for the diagnostic and prognostic assessment of PH in HFpEF patients (figure 1), which can be validated in prospective clinical and translational studies.
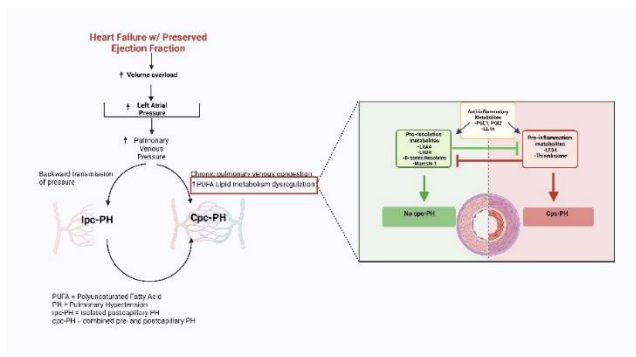
Abstract 7 Figure 1 Dysregulated Lipid Metabolism Predisposing Development of Combined Pre and Postcapillary Pulmonary Hypertension in Patients with Heart Failure with Preserved Ejection Fraction

This figure demonstrates how dysregulated lipid metabolism may predispose development of combined pre and postcapillary pulmonary hypertension (cpc-PH), which carries a greater morbidity and mortality risk compared to isolated postcapillary pulmonary hypertension (ipc-PH) in patients with existing heart failure with preserved ejection fraction (HFpEF).

8

IMPACT OF MODE OF TRANSPORTATION ON THE OUTCOMES IN STEMI PATIENTS: A SYSTEMIC REVIEW AND META-ANALYSIS OF 36557 PATIENTS

[1]Abdulmajeed Alharbi, [1]Halah Alfatlawi, [2]Mohammed Mhanna, [3]Azizullah Beran, [1]Allison Franz, [1]Ehab Altahawy. [1]*University of Toledo;* [2]*Iowa Univiersity;* [3]*Indiana University*

Introduction/Background Introduction: Cardiovascular disease, particularly acute coronary syndrome (ACS), is a leading cause of mortality worldwide. Currently, emergency revascularization with primary percutaneous coronary intervention (PCI), has been established to improve clinical outcomes for patients with ACS especially ST-elevation myocardial infarction (STEMI). For acute coronary syndromes such as STEMI, healthcare facilities allot and utilize resources to practice the guideline recommendation of minimizing delays to percutaneous coronary intervention. Numerous observational studies have attempted to compare the efficiency of widely-used transport modalities around the world. To our knowledge, this is the first meta-analysis that evaluates the data from these research studies collectively.

Objective(s) Information from a collective study such as this would potentially allow for establishing a transportation protocol for healthcare facilities to implement when transporting STEMI patients from a non-PCI facility to a PCI-capable facility. The present meta-analysis focused on evaluation of modalities for emergency transport systems for patients with STEMI.

Methods We performed a comprehensive literature search for published studies indexed in PubMed, Embase, and Web of Science. A total of 273 studies were retrieved by our search strategy. Among these, 49 were eligible for the systematic review. Twelve studies met our inclusion criteria and were included in the meta-analysis. All studies were observational in nature. Our primary outcomes of interest were the door to balloon time and EMS call to PCI time. Secondary outcomes we evaluated were time from arrival at non-PCI facility to PCI within 90 minutes and within 120 minutes. We also evaluated mortality from cardiac death at 1 year after PCI.

Results The major findings for STEMI patients transported by air using helicopter compared with those transported by ground ambulance were as follows: First, air transportation had shorter time from door to balloon. Second, EMS call to PCI was shorter in air transportation compared to ground transportation. Third, when comparing air to ground transfer from non-PCI to PCI-capable facilities within 90 minutes and 120 minutes in particular, transfer via air transportation was less likely to achieve the target timeline.

Conclusion Data included in this metanalysis show that air transport saves time for STEMI patients requiring PCI, especially in long-distance primary transport (from home to the nearest PCI-capable center). However, for secondary transfer (from a non-PCI center to a PCI-capable center) air transportation was not superior for achieving guideline-recommended goal times. Finally, the outcome of cardiac death one year after PCI, was not significantly reduced based on the mode of transportation.

9

HEART FAILURE HOSPITALIZATION OUTCOMES DURING COVID-19 PANDEMIC

[1]Halah Alfatlawi, [1]Abdulmajeed Alharbi, [2]Mohammed Mhanna, [1]Abdurahman Mohammed, [1]rawnag el sheikh, [1]Ragheb Assaly. [1]*University of Toledo; [2]Iowa University*

Introduction/Background Background: Heart failure (HF) was designated as an epidemic in 1997 due to an observed exponential increase in hospitalization rate. From 2014 to 2017, there was a 26% increase in observed HF-related hospitalizations, further highlighting the public health concern and economic burden of this condition. In the year 2020, hospitalizations related to the COVID-19 pandemic created a global health emergency further straining the healthcare sector and exacerbating the public health burden of conditions such as heart failure. The focus of this study is to examine how a secondary COVID-19 diagnosis affects the outcome of HF patients, and how a pre-existing diagnosis of heart failure impacts outcomes of patients hospitalized with COVID-19 infection.

Objective(s) The focus of this study is to examine how a secondary COVID-19 diagnosis affects the outcome of HF patients, and how a pre-existing diagnosis of heart failure impacts outcomes of patients hospitalized with COVID-19 infection.

Methods This was a retrospective observational study of adult patients hospitalized with heart failure and COVID-19 infection within the United States in the years 2020 and 2019. Analysis was conducted using the National Inpatient Sample (NIS) database of the Healthcare Utilization Project (HCUP). The total number of patients included in this study from the NIS database 2020 was 94,745. Of those, 93,798 had heart failure without a secondary diagnosis of COVID-19; 947 had heart failure along with a secondary diagnosis of COVID-19. The primary outcome of our study was in-hospital mortality, length of stay, total hospital charges and time from admission to right heart catheterization, which was compared between the two cohorts. The exposure of interest was COVID-19 infection.

Results Our main study findings are that mortality in HF patients with secondary diagnosis of COVID-19 infection was not statistically different compared to those who were without a secondary diagnosis of COVID-19. Our study findings also showed that length of stay (LOS) and hospital costs in HF patients who had a secondary diagnosis of COVID-19 was not statistically different compared to those who did not have the secondary diagnosis. Time from admission to right heart catheterization (RHC) in HF patients who had a secondary diagnosis of COVID-19 was shorter in HFrEF but not in HFpEF compared to those without secondary diagnoses of COVID-19. Finally, when evaluating hospital outcomes for patients admitted with COVID-19 infection, we found that inpatient mortality increased significantly when they had a pre-existing diagnosis of heart failure.

Conclusion The COVID-19 pandemic significantly impacted hospitalization outcomes for patients admitted with heart failure. This meta-analysis provides a nationwide retrospective study of a large number of patients with heart failure during the COVID-19 pandemic to evaluate the effect of the pandemic on hospital outcomes. The time from admission to right heart catheterization was significantly shorter in patients admitted with heart failure reduced ejection fraction who also had a secondary diagnosis of COVID-19 infection. When evaluating hospital outcomes for patients admitted with COVID-19 infection, we found that inpatient mortality increased significantly when they had a pre-existing diagnosis of heart failure. Length of hospital stay and hospital charges also were higher for patients with COVID-19 infection who had pre-existing heart failure. Further studies should focus not just on how medical comorbidities like COVID-19 infection, affect outcomes of heart failure but also on how overall strains on the healthcare system, such as pandemics, may affect the management of conditions such as heart failure.

10

DIMINISHED ACTIVITY OF HDL-ASSOCIATED ENZYME PARAOXONASE IS ASSOCIATED WITH AORTIC AND CORONARY ARTERY VASCULAR CALCIFICATION IN PATIENTS WITH HEART FAILURE

Prabhatchandra Dube, Vaishnavi Aradhyula, Chandramohan Meenakshisundaram, Eve Schodowski, Konrad Katterle, Shangari Varatharajan, Steven Haller, Samer Khouri, David Kennedy, Rajesh Gupta.
University of Toledo College of Medicine and Life Sciences

Introduction/Background Vascular calcification is a significant risk factor for adverse cardiovascular outcomes and is positively correlated with atherosclerotic plaque burden, increased risk of myocardial infarction (MI), and plaque instability. The pathogenesis of vascular calcification is multifactorial. Clinical and experimental evidence has previously demonstrated that diminished activity of the HDL-associated enzyme Paraoxonase (PON) is associated with vascular dysfunction and increased cardiovascular morbidity and mortality in the setting of heart failure (HF), although the exact mechanism is unclear.
Objective(s) In the present study, we tested the hypothesis that diminished PON activity is associated with increased levels of vascular calcification in patients with a new diagnosis of HF with preserved ejection fraction (HFpEF) and no history of prior MI.
Methods Pulmonary arterial and venous serum samples were collected during right heart catheterization from 90 HFpEF patients with a new diagnosis of HFpEF and no history of prior MI. PON lactonase activity was measured from serum samples. CT scans were scored for vascular calcification as 0 (none), 1 (50%; severe).
Results Compared to patients with no or mild aortic vascular calcification, circulating PON levels were decreased in patients with severe aortic vascular calcification ($p < 0.05$). Similarly, compared to patients with no or mild coronary artery calcification, circulating PON levels were decreased in patients with severe coronary artery calcification ($p = 0.03$).
Conclusion Decreased circulating PON lactonase activity, a measure of diminished HDL-associated antioxidant properties, in patients with new onset HFpEF is associated with both severe aortic vascular calcification and severe coronary artery calcification. Our study warrants further research aimed at understanding the potential mechanistic role of PON activity in the prevention of vascular calcification in HFpEF patients.

11

PHOSPHORYLATION OF MITOCHONDRIAL CALCIUM UNIPORTER IN HEART FAILURE

Madeline Kelly, Jin OUchi. *University of Minnesota*

Introduction/Background In addition to their role as a cellular powerhouse, mitochondria are recognized as key players in cell death signaling via reactive oxygen species (ROS). Increased ROS and mitochondrial damage are proposed to be involved in the pathology of various cardiovascular diseases such as heart failure (HF), but there are no therapies available in the clinical setting that can directly target/treat cardiac mitochondria. Mitochondrial Ca2+ (mtCa2+) overload via the mtCa2+ uniporter (MCU) in cardiomyocytes (CMs) is frequently observed in HF, which induces overproduction of ROS, promoting CM damage, and subsequently leading to HF. Our recent characterization of tyrosine phosphorylation (P-Tyr) and activation of MCU under the activation of oxidation-sensitive protein Tyr kinases (PTK) including proline-rich PTK 2 (Pyk2) in primary CMs represents an opportunity to overcome a major roadblock in the understanding of the role of mtCa2+ for mitochondrial ROS (mROS) generation in cardiac pathology. However, it is still unclear how Pyk2 accesses MCU structure, phosphorylates MCU, and modulates its channel function as well as mitochondrial Ca2+ uptake profile.

Objective(s) To clarify the detailed molecular mechanism for Pyk2-MCU signaling-mediated HF development.

Methods HEK293T cells stably expressing wild-type (WT) MCU, dephospho-mimetic mutants of MCU (MCU-YFs), or empty vector were used for biochemical and physiological assays. To assess MCU phosphorylation levels in stable cell lines, immunoprecipitation and a phosphate-affinity electrophoresis technique (Phos-tag SDS-PAGE) were employed. To assess the levels of MCU phosphorylation in vivo settings, ventricular tissue lysates from transgenic mice with cardiac-specific overexpression of constitutively active Galphaq and from human HF patients were used. To measure mitochondrial Ca2+ fluctuations, cells transfected with a mitochondria-specific Ca2+ biosensor were plated on glass bottom dishes, and observed under an epifluorescence or confocal microscope.

Results Overexpression of Pyk2 increased MCU phosphorylation in HEK293T cells, indicating that Pyk2 can access MCU structure, and directly phosphorylate MCU. Two computational programs for phosphorylation site prediction, NetPhos2.0 and Group-Based Prediction System (GPS) 2.1.2 predicted three PTK phosphorylation sites within MCU structure. Using the dephospho-mimetic mutants of MCU (MCU-YFs), we identified two PTK-specific P-Tyr sites in N- and C-terminal tails of MCU. Our data showed that P-Tyr of MCU at N- and/or C-terminal tails activates mtCa2+ uptake and P-Tyr at the C-terminus of MCU enhances MCU oligomerization. In addition, we found that this signaling cascade (Pyk2 activation, P-Tyr of MCU, activation of apoptotic signaling) in the heart exists in a mouse nonischemic HF model and human HF.

Conclusion Pyk2-dependent P-Tyr of MCU promotes mtCa2+ overload, mROS overproduction, and activates apoptotic signaling in the HF. Elucidation of the pathological importance of Pyk2-MCU signaling may help to develop the genetic or pharmacological tools for mitochondria-targeted therapies (i.e., targeting Pyk2 and MCU function within the mitochondria), for preventing CMs from further damage during HF.

RELATIONSHIP OF INTESTINAL DYSBIOSIS AND BARRIER DYSFUNCTION WITH FEEDING INTOLERANCE IN CONGENITAL HEART DISEASE PATIENTS UNDERGOING CARDIOPULMONARY BYPASS

[1]Jacob Owens, [2]Haowen Qiu, [1]Cole Knoblich, [1]Robin High, [2]Jean-Jack Riethoven, [2]Jacques Izard, [1]Jeffrey Salomon. *[1]University of Nebraska Medical Center*; *[2]University of Nebraska Lincoln*

Introduction/Background Congenital heart disease (CHD) is the most common birth defect, occurring in around 1 in 40,000 births annually in the US. Infants with CHDs will often have increased metabolic demands from increased cardiac workload and work of breathing, and they can also see increases in intestinal inflammatory states due to hypoxemia and/or reduced mesenteric blood flow from systemic hypoperfusion. This can lead to intestinal dysbiosis, intestinal epithelial barrier dysfunction (EBD), and increased gut permeability. Pediatric patients with CHDs will often require surgical correction with cardiopulmonary bypass (CPB). This procedure has been shown to cause a systemic inflammatory response syndrome and can result in further intestinal inflammation. This can exacerbate problems with intestinal homeostasis and result in post-operative feeding intolerance (FI).

Objective(s) The objective of this study was to determine the relationship of feeding intolerance with intestinal dysbiosis and EBD in the post-operative period after CPB.

Methods Patients were enrolled into two arms: a control group undergoing neurosurgery and/or orthopedic surgery, and a group undergoing cardiac surgery with CPB, CPB group. Stool and blood samples were taken pre-operative and at multiple time points post-operatively and evaluated for the microbiome, markers of EBD, and inflammatory cytokines. Demographic and clinical variables were collected from the medical record. An FI score was calculated from clinical variables and documentation (table 1) to obtain objective data to determine the degree of, and duration of, FI in the post-operative period in both groups.

Abstract 12 Table 1 Feeding intolerance scoring
Variables included in feeding intolerance scoring. A score ≥2 within a 24-hour period is considered positive for feeding intolerance.

| Feeding Intolerance Scoring Variables	Score
Abdominal distention	1
Diarrhea	1
Emesis	1
GI bleed	1
Use of antiemetic >24 hours after surgery	1

Results Preliminary data for 26 CPB patients and 11 controls have been evaluated to date, with 11 CPB and 2 control patients demonstrating FI. Microbial analysis demonstrated patients with FI had reductions in the multiple organisms when evaluated with both groups (Figure 1) combined and within the CPB group (Figure 2). Many of these organisms are producers of short-chain fatty acids (SCFA), such as ¬¬Peptostreptococcus, Fusobacterium, and Prevotella 9. The genus Paeniclostrodium was increased in FI patients when looking at both groups together (p=0.0094) and within the CPB group (p=0.016). The CPB group also had an increase in Flavonifractor (p=0.03). All other significant genera were reduced, but despite this, alpha diversity metrics were not statistically significant between FI vs no FI either between groups or within CPB. When evaluating laboratory markers (table 2) and clinical variables, we noted an

association with fatty acid binding protein (FABP) 2 on post-op day #1 and FI in both groups (AUC 0.66) and FI within the CPB group (AUC 0.75). There was also a slight association with interleukin (IL)-1ß 1-hour post-op and FI in both groups (AUC 0.64) and IL-6 1-hour post-op within the CPB group (AUC 0.62). Other clinical variables with association include BUN on post-op day #2 in both groups (AUC 0.7) and within the CPB group (AUC 0.66) and post-op day #1 hematocrit in the CPB group (AUC 0.73).

Abstract 12 Table 2 CPB and control microbial abundance changes
Data plot showing the changes in abundance of different microbial phyla and genera in patients with FI within both the CPB and control arms. Listed are the organisms with statistically significant shifts in relative abundance in feeding intolerance vs no feeding intolerance with adjusted p-value <0.05.
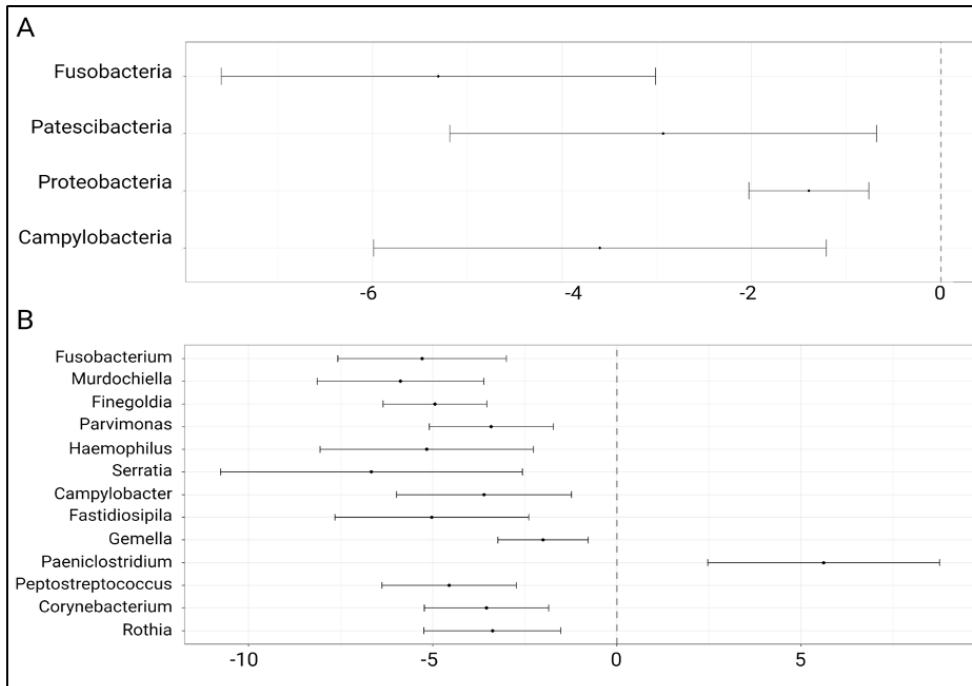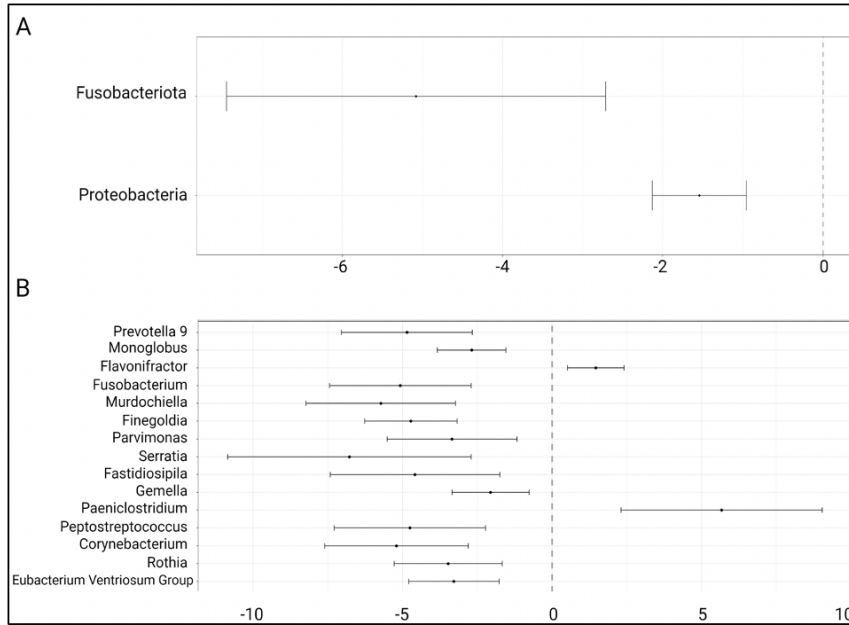
Abstract 12 Figure 1 CPB only microbial abundance changes
Data plot showing the changes in abundance of different microbial phyla and genera in patients with FI within the CPB arm. Listed are the organisms with statistically significant shifts in relative abundance in feeding intolerance vs no feeding intolerance with adjusted p-value <0.05.
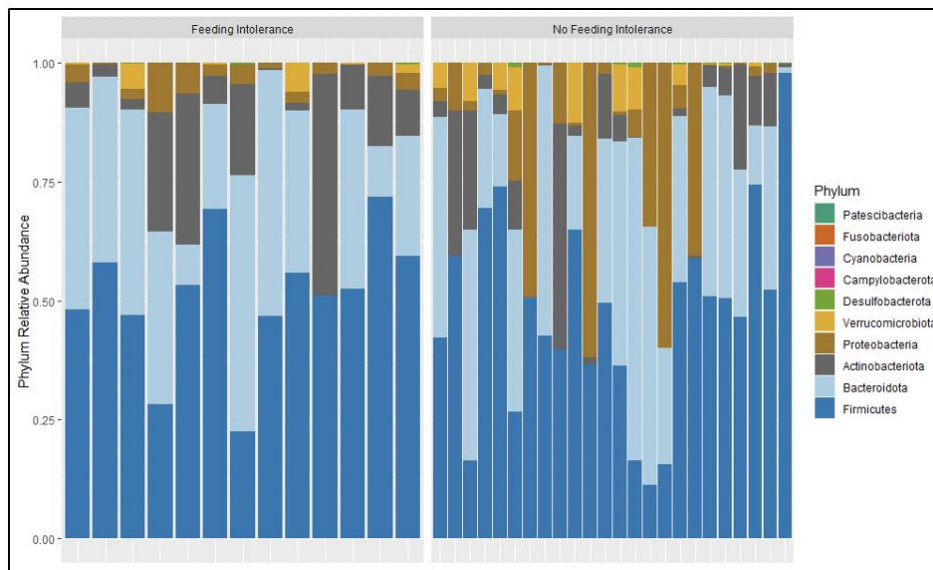
Abstract 12 Figure 2 FI vs no FI microbiome composition Bar graph visualization of microbiome composition between patients with and without feeding intolerance.

Abstract 12 Table 2 Levels for markers of intestinal barrier dysfunction and cytokines
A t-test or Mann-Whitney-U test used for normal and non-normally distributed data, respectively. CPB, cardiopulmonary bypass; FABP2, Intestinal fatty acid binding protein 2; EBD, Epithelial barrier dysfunction; SD, standard deviation; POD, post-op day; IL, interleukin; TNF, tumor necrosis factor.

| Lab Value and Collection Time	CPB Group		Control		
	n	Mean (SD)	n	Mean (SD)	p-value*
FABP2 pre-op, ng/mL	26	7.37 (10.67)	11	5.29 (7.5)	0.441
FABP2 1-hour post-op, ng/mL	26	14.08 (10.75)	11	7.31 (8.33)	0.013
FABP2 POD #1, ng/mL	26	12.25 (10.33)	11	7.07 (7.58)	0.0418
FABP2 POD #2, ng/mL	26	7.36 (9.81)	11	7.67 (9.18)	0.911
FABP2 POD #3, ng/mL	26	6.46 (6.95)	11	6.72 (8.48)	0.909
Claudin-2 pre-op, ng/mL	26	5.91 (4.57)	11	4.31 (2.01)	0.24
Claudin-2 1-hour post-op, ng/mL	26	9.37 (6.67)	11	4.32 (2.12)	0.006
Claudin-2 POD #1, ng/mL	26	9.69 (7.91)	11	4.42 (2.15)	0.008
Claudin-2 POD #2, ng/mL	26	11.13 (8.06)	11	4.25 (2.21)	0.001
Claudin-2 POD #3, ng/mL	26	10.91 (7.66)	11	3.65 (1.82)	<0.001
Claudin-3 pre-op, ng/mL	26	6.05 (3.99)	11	4.25 (2.34)	0.104
Claudin-3 1-hour post-op, ng/mL	26	10.67 (9.35)	11	3.43 (2.06)	0.002
Claudin-3 POD #1, ng/mL	26	12.07 (10.94)	11	4.43 (2.48)	0.003
Claudin-3 POD #2, ng/mL	26	13.91 (10.99)	11	4.50 (2.81)	0.001
Claudin-3 POD #3, ng/mL	26	14.65 (11.68)	11	3.94 (2.21)	<0.001
Interleukin 1-beta pre-op	26	0.960 (0.454)	11	0.605 (0.319)	0.016
Interleukin 1-beta, 1-hour post-op	26	1.885 (0.750)	11	0.975 (0.569)	<0.001
Interleukin 1-beta POD #1	26	1.159 (0.646)	11	1.069 (0.467)	0.672
Interleukin 1-beta POD #2	26	1.301 (0.624)	11	1.178 (0.579)	0.590
Interleukin 1-beta POD #3	26	1.083 (0.615)	11	1.013 (0.454)	0.721
Interleukin 6 pre-op	26	15.229 (28.796)	11	11.482	0.663
Interleukin 6 1-hour post-op	26	215.878 (137.947)	11	44.048	<0.001
Interleukin 6 POD #1	26	95.006 (59.947)	11	47.428	0.039
Interleukin 6 POD #2	26	53.064 (66.987)	11	48.153	0.815
Interleukin 6 POD #3	26	22.471 (25.986)	11	19.461	0.683
Interleukin 8 pre-op	26	3.750 (5.223)	11	5.122 (6.441)	0.559
Interleukin 8 1-hour post-op	26	52.379 (54.741)	11	13.853	0.003
Interleukin 8 POD #1	26	31.344 (58.170)	11	13.349 (9.561)	0.147
Interleukin 8 POD #2	26	15.640 (15.646)	11	11.483 (8.296)	0.328
Interleukin 8 POD #3	26	10.824 (10.610)	11	13.907	0.551
TNF-alpha pre-op	26	4.235 (5.339)	11	2.934 (2.947)	0.377
TNF-alpha 1-hour post-op	26	32.927 (29.877)	11	14.770 (6.165)	0.01
TNF-alpha POD #1	26	14.239 (8.682)	11	8.761 (5.353)	0.037
TNF-alpha POD #2	26	8.156 (6.841)	11	7.367 (3.734)	0.673
TNF-alpha POD #3	26	4.887 (3.495)	11	5.366 (2.191)	0.650

Conclusion Feeding intolerance remains a prevalent issue in CHD patients post-operatively after CPB. We showed specific changes to the microbiome associated with FI in both CPB patients and in other surgical controls. We also demonstrated an association with early post-op IL-1ß and IL-6, post-op day #1 FABP2 and hematocrit, and post-op day #2 BUN. These markers combined may help guide clinicians on the early identification of patients at risk for FI to guide management in the post-operative period. Future models to evaluate these markers and monitor potential interventions to the microbiome could be used improve feeding and nutrition post-operatively after cardiac surgery with CPB.

ACHALASIA CAUSING ACUTE HEART FAILURE AND CHEST PAIN: A RARE ENCOUNTER

Gorgina Barsoum, Talal Asif. *University of Missouri- Kansas City*

Introduction/Background Achalasia, a rare esophageal abnormality, when severe can cause left atrial compression. In theory, this can contribute to hemodynamic compromise and acute heart failure, but there are no reported cases in literature. We present a case of acute hypoxemia and resulting acute heart failure from severe achalasia causing obstructive physiology. We highlight the importance of mechanical decompression when encountered by such a case.

Case Presentation A 31-year-old male patient, with no significant past history, presented to the emergency room with sudden onset chest pain and dyspnea for one day. The patient was satting at 84% on room air at presentation and was placed on four liters of oxygen by nasal cannula. Electrocardiogram demonstrated no acute ischemic changes (figure). Due to hypoxemia and chest pain, patient underwent computed tomographic pulmonary angiography (CTPE) in the emergency room that showed no acute pulmonary embolism but demonstrated bilateral pulmonary edema and markedly dilated thoracic esophagus filled with particulate matter to the level of the thoracic inlet (figure). There was concern for left atrial (LA) compression (figure 1). Patient's brain natriuretic peptide (BNP) level was elevated at 450 pg/mL (normal < 100 pg/mL). Patient's initial high sensitivity troponin was markedly elevated at 374 pg/mL (normal < 4 pg/mL). Transthoracic echocardiography (TTE) was then performed that showed a normal left ventricular ejection fraction and normal wall motion but with left atrial compression and dilated inferior vena cava, indicating elevated central venous pressures. The left ventricular outflow tract velocity time integral (LVOT VTI) showed evidence of pulsus alternans (figure 1). Gastroenterology (GI) team were emergently consulted due to concern for acute heart failure from mass effect on the left atrium. Patient underwent emergent removal of retained food with resolution of his hypoxemia and improvement in his chest pain. Patient was placed on liquid diet and is scheduled to undergo peroral endoscopic myotomy (POEM) by bariatric surgery.
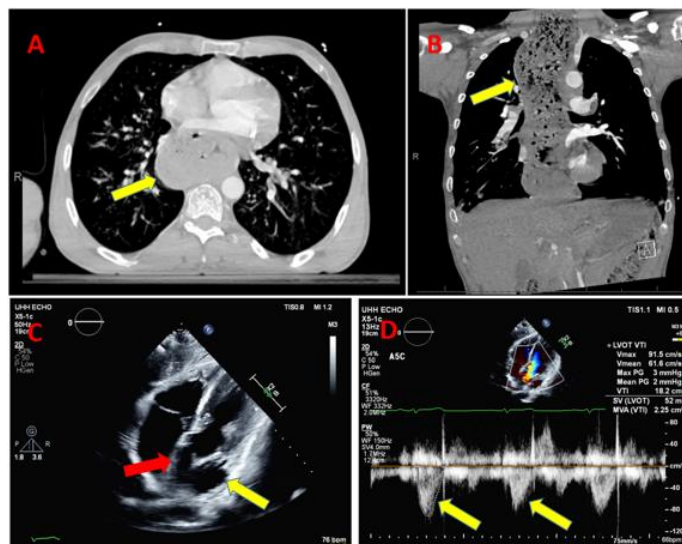
Abstract 13 Figure 1 Figure A, B showing markedly dilated esophagus with retained food, causing left atrial compression (yellow arrows). Figure C showing air filled dilated esophagus (yellow arrow) compressing the true left atrium (red arrow). Figure D demonstrates pulsus alternans on left ventricular outflow tract spectral doppler.

Discussion Extra-cardiac mass effect on left atrium from achalasia is an uncommon cause of acute heart failure and chest pain. When encountered, immediate measures to remove the obstruction should be taken to prevent obstructive shock.

14

IMPORTANCE OF REVIEW OF NON-GATED CT CHEST IMAGES: A DIAGNOSTIC TREASURE

Ali Naveed, Gorgina Barsoum, Aamer Ubaid, Talal Asif. *University of Missouri, Kansas City.*

Introduction/Background Non-gated chest CT scans are frequently performed for numerous clinical conditions in patients presenting to the emergency department (ED). Attention is seldom given to cardiac structures as these scans are not aimed at cardiac evaluation. We present a case to emphasize review of images.

Case Presentation A 46-year-old female presented to the ED with retrosternal chest pain for 2 days. ECG showed sinus rhythm with no ischemic changes. Serial high-sensitivity cardiac troponins were below the limit of detection. CT pulmonary angiography (CTPA) was performed due to elevated D-dimer levels which ruled out acute pulmonary embolism. Patient was discharged with follow-up arranged in the cardiology clinic the following morning for further decision making on ischemic evaluation. We reviewed patient's CTPA images that demonstrated a large right ventricular (RV) mass and no thrombus in transit (Figure A and B). The radiology report remarked only on cardiac size as per departmental protocols since this was a non-gated study. We proceeded with urgent transthoracic echocardiogram that demonstrated the large RV mass and was seen obstructing the RV cavity (Figure C, D and E). Patient was admitted for further work up. The primary tumor was deemed to be hepatocellular carcinoma (Figure F) with cardiac metastasis to the RV. Patient is currently undergoing aggressive chemotherapy.
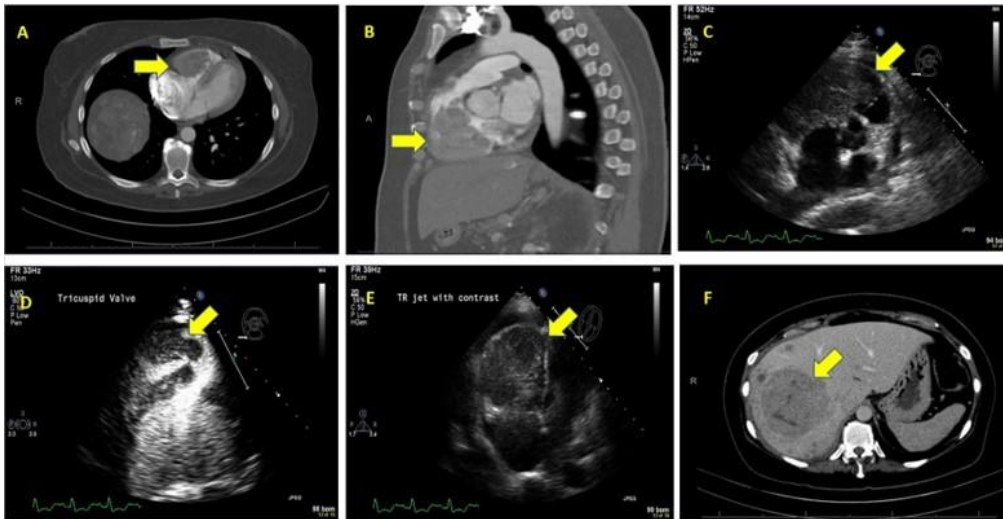
Abstract 14 Figure 1 NON-GATED CT ANGIOGRAM AND ECHOCARDIOGRAM WITH RIGHT VENTRICULAR MASS
A. Large right ventricular (RV) mass seen on axial slices of Non gated CT pulmonary angiogram (arrow). B. The RV mass seen on sagittal plane (arrow). C. Parasternal short axis (PSAX) view on transthoracic echocardiogram demonstrating the RV mass almost occluding the RV cavity. D. PSAX view with contrast showing the large irregular RV mass. E. The primary tumor, large hepatocellular carcinoma as seen on CT abdomen. The diagnosis was confirmed on Biopsy.

Discussion Non-gated chest CT scans should be routinely reviewed not just for coronary calcifications but for additional cardiac structural abnormalities.

PERICARDIAL EFFUSION MASKING ACUTE RUPTURE OF SINUS OF VALSALVA ANEURYSM: ROLE OF POINT OF CARE ULTRASOUND AND MULTIMODALITY IMAGING

Gorgina Barsoum, Talal Asif. *University of Missouri- Kansas City*

Introduction/Background The sinus of Valsalva aneurysm (SOVA) is a rare cardiac anomaly characterized by dilation of the aortic root between the aortic valve annulus and the sinotubular junction. Rupture of SOVA into the pericardial space is a very rare but life-threatening complication and delays diagnosis due to diversion of attention to the pericardial effusion. The role of multimodality imaging becomes central in these cases to facilitate early diagnosis. We present a case to highlight the advantages of readily available multimodality imaging techniques for rapid diagnosis in these uncommon but life-threatening cases. We also emphasize the importance of following up critical findings on cardiac point of care ultrasound (POCUS) with more formal imaging.

Case Presentation A 44-year-old female patient with no prior medical history, presented to the emergency room with two-day history of pleuritic type chest pain. The patient at presentation was in atrial fibrillation with rapid ventricular rate of 127 beats per minute as seen on electrocardiogram with blood pressure of 135/80 mmHg and oxygen saturation of 99% on room air. Bedside echocardiogram performed by emergency room (ER) physicians demonstrated a moderate pericardial effusion. Markers of inflammation including erythrocyte sedimentation rate and C-reactive protein were markedly elevated. Initial high sensitivity troponins were negative. With the possible diagnosis of acute pericarditis, a formal transthoracic echocardiogram (TTE) was ordered. The TTE revealed a non-coronary SOVA (NC-SOVA) with moderate aortic regurgitation and a moderate fibrinous pericardial effusion (figure 1). There was no evidence of cardiac tamponade. This finding raised a strong concern for acute rupture of the NC-SOVA. An urgent computed tomographic angiography (CTA) of the aorta was obtained that displayed a large aneurysmal outpouching of the NC-SOVA measuring 3.8 X 3.5 X 2.8 cm (figure). Patient was emergently taken to the operating room where intra-operative transesophageal echocardiogram confirmed acute rupture of the NC-SOVA into the pericardial space (figure 1). The patient underwent aortic root and mechanical aortic valve replacement and is doing well on follow up.
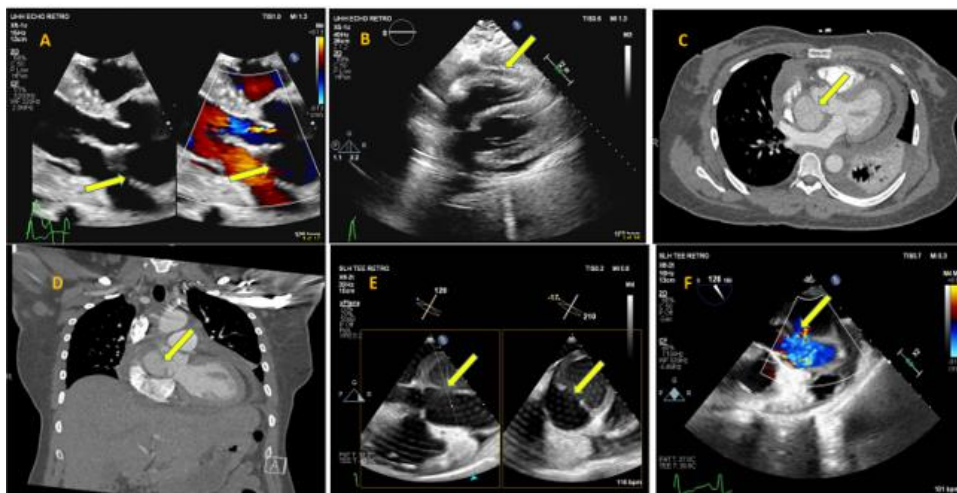
Abstract 15 Figure 1
A: Transthoracic echocardiogram showing dilated aortic root and dilated non-coronary sinus of Valsalva (yellow arrow). B: Transthoracic echocardiogram showing hemorrhagic pericardial

effusion (yellow arrow). C, D: CT aortic angiogram showing the dilated non-coronary sinus of Valsalva aneurysm (yellow arrows). E, F: Intraoperative transesophageal echocardiogram showing the ruptured sinus of Valsalva aneurysm (yellow arrows).

Discussion This case highlights the benefits of using readily available multimodality imaging techniques to arrive at the rapid and correct diagnosis of ruptured SOVA. Although cardiac POCUS is being used increasingly in our ERs, this case also emphasizes the importance of using formal imaging techniques once critical findings on POCUS have been identified.

MARATHON MADNESS: AN UNUSUAL PRESENTATION OF ST-SEGMENT ELEVATED MYOCARDIAL INFARCTION IN A YOUNG ATHLETE TAKING CREATININE SUPPLEMENTATION

Alexander Shinn, Max Isaac, Mohammad Al Bataineh, Adam Russell, Suhaib Bajwa, Brian Bostick.
University of Missouri Healthcare

Introduction/Background ST-Segment Elevation Myocardial Infarction (STEMI) is a result of acute plaque rupture and total occlusion of a coronary artery. Clinically, these occur in older patients and those with significant risk factors. We present a case of a young athletic patient who experienced a STEMI while training for a marathon.

Case Presentation A 23-year-old healthy athletic male presents to the emergency room after experiencing sudden onset chest pain at rest. During the past four months, he has been training for a marathon and taking creatine supplementation. Electrocardiogram demonstrated ST-segment elevation in leads II, III and AVF with no previous ECGs. Troponin level was < 0.01 ng/mL and creatinine 0.89 mg/dL. The cardiac cath lab was activated, and invasive coronary angiogram severe distal occlusions of Right Posterior Descending Artery and branches of the Right Posterolateral arteries with thrombus concerning for embolic disease. Left ventricular ejection fraction (LVEF) measured via angiography was 50% with severe apical hypokinesis. Aspiration thrombectomy was performed with EXPORT catheter without ballooning or stenting. There was significant improvement in flow with 0% residual stenosis. After the intervention, he was started on Aspirin, Plavix and Metoprolol. Follow up echocardiogram (ECHO) demonstrated LVEF 60-65% with no wall motion abnormalities and a small Patent foramen ovale (PFO).
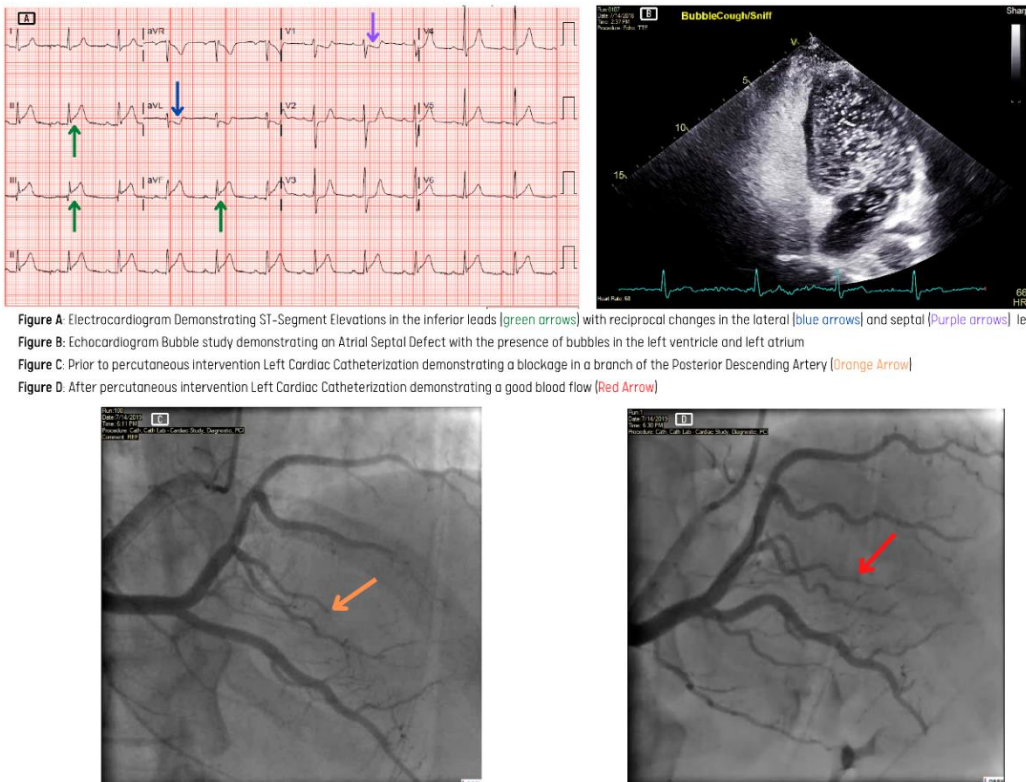
Figure A: Electrocardiogram Demonstrating ST-Segment Elevations in the inferior leads (green arrows) with reciprocal changes in the lateral (blue arrows) and septal (Purple arrows) leads
Figure B: Echocardiogram Bubble study demonstrating an Atrial Septal Defect with the presence of bubbles in the left ventricle and left atrium
Figure C: Prior to percutaneous intervention Left Cardiac Catheterization demonstrating a blockage in a branch of the Posterior Descending Artery (Orange Arrow)
Figure D: After percutaneous intervention Left Cardiac Catheterization demonstrating a good blood flow (Red Arrow)

Abstract 16 Figure 1

Discussion Hematology was involved for further work up for hypercoagulable disorders which was negative. Additionally, Rheumatology was consulted but did not recommend any further workup nor therapy for vasculitis. The etiology was due to creatinine supplementation which placed this athlete in a temporarily hypercoagulable state, predisposing him to intravascular clot formation. With the presence of his PFO seen on ECHO, it is likely that a peripheral thrombus developed, crossed his PFO and lodged into his right coronary artery.

This case is an example of an athletic patient who experienced a STEMI secondary to embolic disease. It is important to consider embolic disease in younger patients experiencing chest pain and taking various supplements to enhance their athletic performance.

17

DIAGNOSING CARDIAC CONDITIONS ON NON-GATED CT CHEST: A CASE OF INFECTIVE ENDOCARDITIS

Ali Naveed, Bazigh Naveed, Gorgina Barsoum, Talal Asif. *University of Missouri, Kansas City.*

Introduction/Background Non-gated computed tomographic scans (CT) of the chest are the mainstay of initial diagnostic work-up in patients who present to the emergency department (ED) with undifferentiated dyspnea. Generally, cardiac structures are not reviewed in detail during the reporting of these studies as electrocardiographic gating is not performed. We present a case of acute infective endocarditis (IE) initially recognized on non-gated CT chest. We aim to highlight the diagnostic value of non-gated CTs acquired in the ED and importance of visualizing valvular structures during reviewing these studies.

Case Presentation A 27-year-old female in 24th week of gestation presented to the ED with one week history of exertional dyspnea and right sided chest pain. Patient endorsed active intravenous (IV) drug abuse. Initial temperature was 101.5°F, blood pressure 98/55 mmHg and heart rate of 116 beats/minute. CT pulmonary angiography (CTPA) was performed which ruled out acute pulmonary embolism but demonstrated multifocal pulmonary nodules. Blood cultures were obtained, and the patient was initiated on broad spectrum antibiotics. On day two of admission, blood cultures returned positive for methicillin resistant staphylococcus aureus (MSSA). Only then was this followed up with a transthoracic echocardiogram (TTE) as per protocol for MSSA bacteremia. The TTE identified large vegetations on the tricuspid valve (TV) after which cardiology consultation was requested. We reviewed the patient's non-gated CTPA that demonstrated the large TV vegetations but had not been recognized on admission. This was followed up with a transesophageal echocardiogram (TEE) that confirmed the large vegetations on the TV and severe tricuspid regurgitation and excluded complications of IE such as valvular abscesses, aneurysms, pseudoaneurysms and fistulae formation. Patient had a prolonged hospital stay in which patient was delivered safely. Due to active IV drug use, the multidisciplinary heart team determined that percutaneous vegectomy with AngioVac cannula was the best temporizing measure and patient underwent the procedure successfully. She was discharged and on follow-up is planned to undergo bioprosthetic TV replacement.
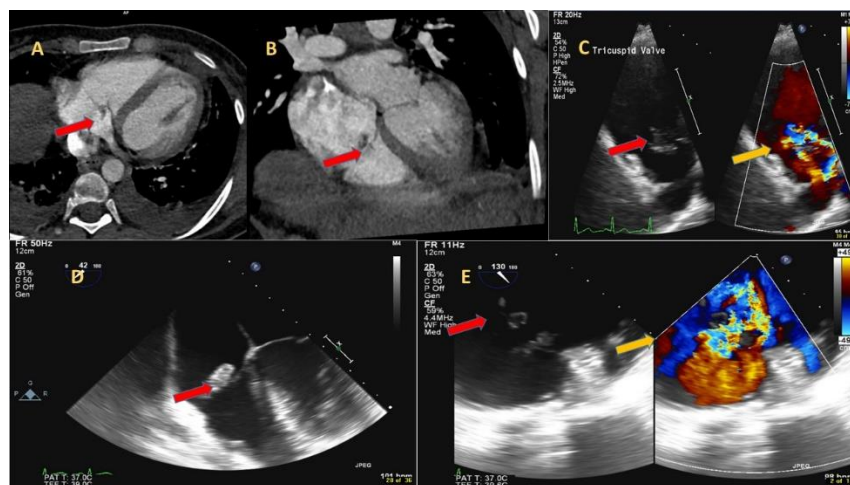
Abstract 17 Figure 1 NON GATED CT ANGIOGRAM AND ECHOCARDIOGRAM SHOWING INFECTIVE ENDOCARDITIS.

A: Non-gated computed tomographic pulmonary angiography (CTPA) axial images showing tricuspid valve (TV) vegetation (red arrow).

B: Coronal images of the non-gated CTPA reconstructed to demonstrate the TV vegetation (red arrow). C: Transthoracic echocardiogram (TTE) in the short-axis views revealing vegetations on the posterior and the septal leaflet of the TV (red arrow). The yellow arrow demonstrates severe tricuspid regurgitation (TR).

D: Transesophageal echocardiogram showing the large TV vegetation.

E: TEE demonstrating large vegetation on the TV (red arrow) and severe TR (yellow arrow).

Discussion It is important to comprehensively review valvular structures on non-gated chest CTs to expedite the diagnosis of IE, especially in high-risk patients, to minimize the complications associated with this disease entity. Additionally, in patients with fever of unknown origin undergoing CT chest, this serves as an important diagnostic tool and is easy to apply in clinical practice.

18

EXPANDING ON NON-COMPACTION: A RARE CASE OF A CARDIAC DEVELOPMENTAL DISORDER ASSOCIATED WITH NEUROMUSCULAR DISEASES

[1]Adam Russell, [1]Alexander Shinn, [2]Brian Bostick. *[1]University of Missouri – Columbia;*
[2]MU Health Care

Introduction/Background Left ventricular hyper-trabeculation or noncompaction (LVHT) is a cardiomyopathy with altered myocardial wall due to arrest of compaction during uterine development. This results in deep intra-trabecular recesses and has been described in association with multiple neuromuscular diseases (NMD), with some studies showing up to 80% of patients with LVHT having an associated NMD. We present a case of a male with type I muscular dystrophy who was diagnosed with LVHT.

Case Presentation This case concerns a 37-year-old white male with hypertension and recent diagnosis of myotonic dystrophy type I who presented for routine cardiac screening. At the time, patient complained of fatigue, weakness with exertion, dizziness, and palpations. Patient was able to walk 1 block on flat ground. Patient denied any orthopnea, peripheral edema, chest pain, or episodes of syncope. As part of his cardiac screening patient underwent a transthoracic echocardiogram which was remarkable for low normal LVEF of 50% as well as apical trabeculations suggestive of LVHT. This was followed by a cardiac MRI which was remarkable for a ratio of noncompacted to compacted myocardium consistent with LVHT. There were no findings of infiltration or scars secondary to his neuromuscular disease. Holter monitoring for 48 hours showed no signs of ventricular arrhythmias. At this time patient was started on Losartan for aggressive blood pressure control. A repeat echocardiogram several months later showed improvement in his LVEF to 62%. Subjectively, patient reported an increase in ambulation distance on level surfaces. LVHT is usually asymptomatic but can be complicated by heart failure, thromboembolism, or ventricular arrhythmias. Currently, the ideal therapy for patients with LVHT is unknown. The decision was made to proceed with aggressive risk factor mitigation with guideline directed medical therapy for heart failure with close follow up to screen for potential complications. Patient was continued on Losartan with blood pressure goal < 130 mm Hg systolic. Serial echocardiograms with strain imaging analysis were planned with follow up every 3-6 months.

**Discussion** This case is an example of a patient with a NMD who was found to have a LVHT. Patients with NMD are screened routinely for cardiomyopathies, with dilated cardiomyopathy and conduction abnormalities being the most common cardiac abnormalities. This case highlights the importance of screening for other forms of cardiomyopathy. Specifically non-compaction cardiomyopathy, which has a significant association with NMDs.

19

THE HAPPY HEART PARADOX

[1]Nicholas Zingas, [2]Vaskar Mukerji, [3]Damian Valencia. [1]*Wright State University Boonshoft SOM Internal Medicine Residency Program;* [2]*Wright State University Boonshoft School of Medicine*; [3]*Kettering Health*

Introduction/Background The relationship between takotsubo cardiomyopathy and negative stressors, such as sorrow or fear, has been recognized for many years, hence the term "broken heart syndrome" (BHS). More recently an association with joyful triggers, such as good news or a celebration, has also been described, referred to as the "happy heart syndrome" (HHS). According to reports, this represents less than 5% of the cases of stress cardiomyopathy. It affects men more often than in BHS, and frequently the ventricle demonstrates a ballooning pattern that is atypical. We present here a case demonstrating the challenge of identifying the trigger and categorizing these cases.

Case Presentation A 67-year-old man presented to the Emergency Department at 6:00 AM with severe persistent chest pain and was found to have an acute anterior STEMI. He was taken for emergent cardiac catheterization, during which he was found to have a 100% thrombotic occlusion of the proximal left anterior descending artery. During percutaneous intervention, the patient experienced an episode of ventricular fibrillation requiring defibrillation. The patient's wife was updated on his diagnosis and the events which occurred in the catheterization lab. Following successful revascularization, the patient was transferred to the intensive care unit. The patient's wife was informed that his status was critical and that he needed close monitoring at that time. The following morning at 9:00 AM, the patient's condition appeared stable with no further complication. Again, the patient's wife was updated, although now tearful and overwhelmed with joy, she hugged every team member in gratitude. At approximately 1:00 PM, the patient's wife complained of mid-anterior retrosternal chest pressure associated with shortness of breath and diaphoresis. An EKG revealed mild ST segment elevation in the anterior leads. Troponin was mildly elevated. She too was then taken emergently for cardiac catheterization. Angiography revealed the absence of any epicardial coronary disease. Ventriculogram showed apical ballooning with a hyperkinetic base (Figure), consistent with Takotsubo. The patient was medically managed and repeat echocardiography four weeks later showed recovered ventricular function with normal wall motion.
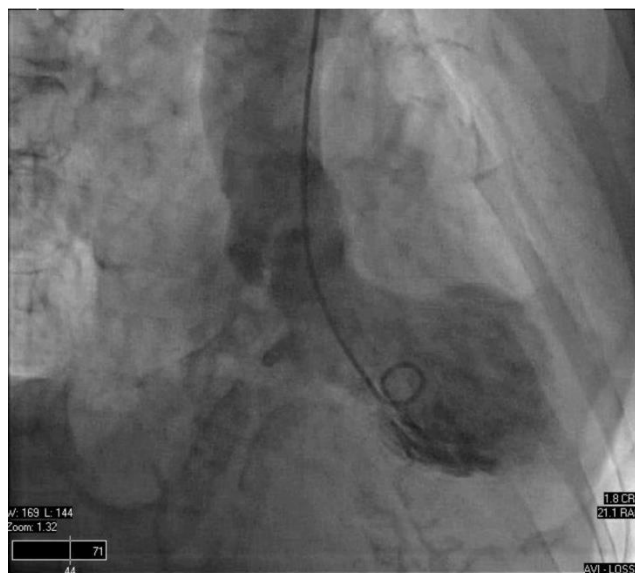
Abstract 19 Figure 1 Ventriculogram

Discussion The patient's wife developed symptoms approximately 28 hours after the negative stressor and 4 hours after the positive stressor. It is unclear whether the patient developed her condition secondary to the joyful news she received regarding her husband's recovery or had resulted from the preceding stress and anxiety related to his acute illness. In reviewing reported cases of HHS, it appears that the celebratory event is frequently preceded by a period of stress and concern. Hence, there is a predicament in identifying the actual trigger and differentiating between BHS and HHS. This case suggests that additional criteria need to be defined to clarify the diagnosis.

REFERENCE(S)
1. S Hassan, P Tornvall. Epidemiology, pathogenesis, and management of takotsubo syndrome. Clin Auton Res. 2018;28(1):53-65. doi: 10.1007/s10286-017-0465-z.
2. Stiermaier T, Walliser A, El-Battrawy I, Patz T, Mezger M, Rawish E, et. al. Happy Heart Syndrome: Frequency, Characteristics, and Outcome of Takotsubo Syndrome Triggered by Positive Life Events. JACC Heart Fail. 2022;10(7):459-466. doi: 10.1016/j.jchf.2022.02.015.

20

ANESTHETIC MANAGEMENT OF A PATIENT WITH SEVERE PULMONARY ARTERIAL HYPERTENSION FOR INCARCERATED UMBILICAL HERNIA REPAIR

[1]Leena Penumalee, [2]Allison Dalton. [1]*University of Chicago Pritzker School of Medicine;* [2]*University of Chicago Medical Center*

Introduction/Background Pulmonary arterial hypertension (PAH), defined as a mean pulmonary arterial pressure ≥ 25 mmHg, is a disorder with a reported incidence of 15 to 50 individuals per million. (1) PAH is associated with perioperative changes in hemodynamics and the risk of acute right ventricular decompensation. (2,3) Anesthetic plans for these patients often involve careful risk assessment, invasive cardiopulmonary monitoring, and anticipation of possible pulmonary hypertension crises. (3)

Case Presentation We present the case of a 66-year-old female with severe pulmonary hypertension and RV failure who presented with an incarcerated umbilical hernia requiring emergent operative repair. Her past medical history was remarkable for pulmonary hypertension (WHO Group I, II, and III), COPD, tracheobronchomalacia, history of unprovoked pulmonary embolism, and cervical disc disease requiring cervical spine fusion. Prior to admission, patient was taking ambisentran, sildenafil, and apixaban in addition to medications for management of other medical conditions. A right heart catheterization from about one year prior revealed elevated RA (19 mmHg), RV (80/19 mmHg), PA (78/30/50 mmHg), and PCWP (25 mmHg) pressures. Initially, the anesthesia team considered regional anesthesia, but since the use of apixaban is a contraindication to neuraxial anesthesia, the team decided to proceed with a general anesthetic. Given the patient's degree of pulmonary hypertension, right ventricular failure, and emergent nature of the surgery, the institution's ECMO team was contacted prior to proceeding to the operating room. After discussion with the cannulating physician, we decided to proceed to surgery with ECMO on standby for worsening RV function. Pre-induction radial arterial line access was obtained. The patient then underwent a topicalized, sedated (0.5 mg midazolam) fiberoptic intubation given her history of cervical spine fusion and tracheobronchomalacia. Following intubation, patient was induced with an additional 1.5 mg midazolam and sevoflurane prior to the administration of rocuronium. A right internal jugular double lumen 9 Fr catheter was placed to allow for invasive hemodynamic monitoring, and transesophageal echocardiography was used throughout the procedure. Intraoperatively, systolic blood pressures ranged from 120-160 mmHg on approximately 0.5-0.6 MAC of sevoflurane with one brief period of decreased SBP to 97 mmHg, which was treated with vasopressin. Central venous pressure remained < 10 mmHg throughout the procedure. The surgery lasted 104 minutes during which the patient received a total of 100 mL of lactated ringers with intraoperative urine output of 400 mL. Given patient co-morbidities, she was kept intubated and admitted to the SICU. She was extubated on post-operative day 1.

Discussion This case illustrates a successful anesthetic regimen for a patient with severe pulmonary arterial hypertension. PAH is associated with increased incidence of intra-operative and post-operative adverse events in non-cardiac surgery. A literature review finds several cases of patients with severe disease who have successfully undergone complex surgeries and high risk transplant procedures. (4,5) This patient's case was uniquely challenging because of the severity of pulmonary hypertension as well as the emergent nature of the operation. The anesthetic regimen was crafted to maintain adequate preload, limit the use of agents that compromise right ventricular contractility, and minimize increases in pulmonary vascular resistance. Further considerations included the use of invasive monitoring to quickly address changes in hemodynamics and extensive communication with the surgical and ECMO teams regarding potential intra-operative challenges.

REFERENCE(S)

1. Levine DJ. Pulmonary arterial hypertension: updates in epidemiology and evaluation of patients. Am J Manag Care 2021; 27: S35–S41
2. Rosenkrans S, Howard L S, Gomberg-Matland M, et al. Systemic Consequences of Pulmonary Hypertension and Right-Sided Heart Failure. Circulation, 2020, 141(8): 678-93.
3. Price LC, Martinez G, Brame A, et al. Perioperative management of patients with pulmonary hypertension undergoing non-cardiothoracic, non-obstetric surgery: a systematic review and expert consensus statement. Br J Anaesth. 2021;126(4):774–90
4. Zhou Y, Chen H, Zhang H, Li M, Guo J, et al. (2017) Anesthesia for a Patient with Severe Pulmonary Hypertension Undergoing Laparoscopic Cholecystectomy: A Case Report. J Pulm Respir Med 7: 403
5. Swamy MC, Mukherjee A, Rao LL, Pandith S. Anaesthetic management of a patient with severe pulmonary arterial hypertension for renal transplantation. Indian J Anaesth. 2017;61(2):167-169

21

MATERNAL MONITORING FOR MULTI-DRUG REGRACTORY FETAL SUPRAVENTRICULAR TACHYCARDIA: A MANAGEMENT CHALLENGE

Gorgina Barsoum, Asif Talal. *University of missouri- Kansas City*

Introduction/Background There are no current recommendations for general cardiologists and internists practicing in the community on maternal monitoring of patients being treated for fetal supraventricular tachycardia (SVT). Fetal SVT, though rare, is a significant source of life-threatening complications such as hydrops fetalis and intrauterine fetal demise. It is treated with various combinations of maternal antiarrhythmic therapy and transplacental administration of antiarrhythmic medications. We present a case to guide physicians practicing in community hospitals on how to approach these complex patients and highlight the challenges of maternal monitoring during management of refractory fetal SVT.

Case Presentation A 38-year-old female patient was admitted with recurrent fetal SVT as a transfer from an outside hospital. Patient had been tried on sotalol which had led to QTc interval prolongation and had to be discontinued. Patient had also been given digoxin which she was unable to tolerate due to severe nausea, anorexia, vomiting and abdominal pain. A multi-disciplinary team approach involving maternal-fetal medicine, pediatric cardiology, adult cardiology and pediatric electrophysiology team was adopted. Perinatal ultrasound at presentation revealed persistent fetal SVT with evidence of hydrops fetalis. Patient was placed on continuous telemetry monitoring. Electrocardiogram (ECG) showed normal sinus rhythm with normal QTc interval. Transthoracic echocardiogram demonstrated normal left ventricular ejection fraction and no cardiac structural abnormalities. Baseline blood counts, electrolytes, thyroid, liver and renal functions were within normal limits. Daily maternal ECGs were obtained to monitor QTc interval. Patient was started on flecainide but immediately developed blurry vision, nausea and vomiting, and the medication was discontinued. Patient was then initiated on amiodarone. Digoxin was carefully reintroduced with close monitoring of maternal serum therapeutic levels. Patient had hypokalemia and hypomagnesemia which were aggressively addressed. Fetal SVT did not resolve after 48 hours of maternal oral therapy at which point amiodarone was administered transplacentally with conversion to fetal sinus rhythm in 48 hours.

Discussion There is insufficient data to guide physicians practicing in our communities on approach to maternal monitoring during treatment of refractory SVT with combination antiarrhythmic therapy. Our case provides an algorithmic approach to maternal monitoring in such cases. We also advocate a multidisciplinary approach to ensure maternal cardiac safety.
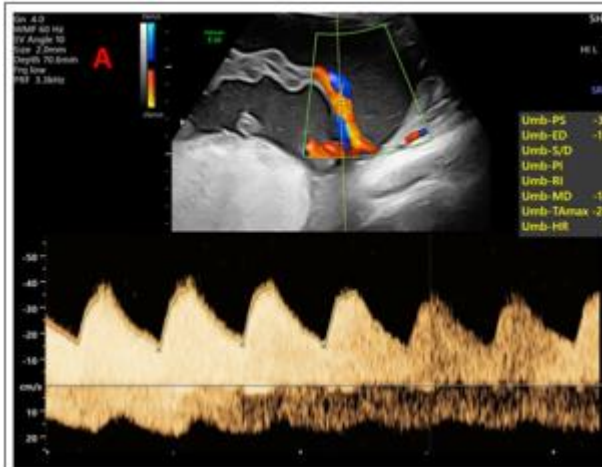
Abstract 21 Figure 1 Fetal ultrasound demonstrating fetal supraventricular tachycardia (SVT)
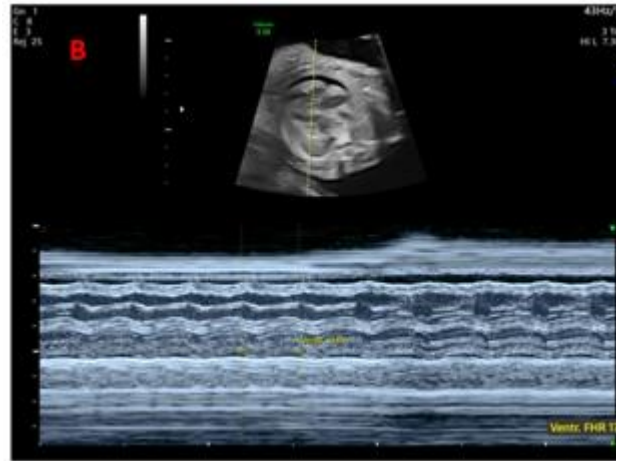
Abstract 21 Figure 2 Fetal ultrasound demonstrating fetal supraventricular tachycardia (SVT)

Abstract 21 Figure 3 Continuous fetal heart rate monitoring before transplacental amiodarone infusion showed persistent fetal SVT despite oral antiarrhythmic therapy

Abstract 21 Figure 4 Post transplacental infusion of amiodarone, fetal SVT resolved

22

STRESS INDUCED RECURRENCE OF SYMPTOMATIC NON-SUSTAINED VENTRICULAR TACHYCARDIA

Austin Meehl, *The University of Toledo Residency Program*

Introduction/Background Non-Sustained Ventricular Tachycardia (NSVT) is widely defined as an arrhythmia with a heart rate greater than 100 beats per minute lasting for three or more consecutive beats but for a duration of less than 30 seconds.[1] It is recognized as relatively common, often found incidentally and without appreciable symptoms although symptoms may range from palpitations to syncope, and albeit less frequently, sudden cardiac arrest.[1] Idiopathic VT and Premature Ventricular Contractions (PVCs) frequently originate from the right ventricular outflow tract (RVOT), aortic cusps, tricuspid anulus, right or left ventricle, inferoapical septum, and LVOT.[2,3] Treatment with radiofrequency ablation for symptomatic arrhythmia in patients without structural heart disease has been found to be effective in eliminating arrhythmia in up to 90% of patients.[2] In patients with refractory arrhythmia, sotalol and amiodarone are preferred.[4]

Case Presentation Patient is a 42-year-old female who presented to the emergency department with chief complaints of dizziness and palpitations. She has a medical history significant for non-sustained ventricular tachycardia beginning 2 years prior, and a recent cardiac ablation procedure performed 1 month before the current presentation due to a high burden of PVCs. Her symptoms had been well controlled on metoprolol since the ablation and had only recently recurred. Further questioning elicited that symptom of dizziness was not experienced prior to ablation and that the patient was experiencing tremendous new onset stress due to the recent death of a loved one. Telemetry showed intermittent runs of NSVT lasting for 5-10 seconds with spontaneous conversion to sinus rhythm. During each episode the patient remained hemodynamically stable and oriented to conversation but reported feeling the arrhythmia coming on moments before converting to NSVT and described a distractingly anxious feeling which then resolved upon conversion to sinus rhythm. One episode of syncope was reported prior to ablation and she endorses no pertinent family history and no arrythmia until 2 years prior after recovering from a viral illness. Patient was admitted to the Cardiac ICU where she remained on telemetry and was loaded with sotalol with resolution of NSVT without recurrence after initial dose. Patient continued to experience intermittent PVCs and sotalol dose was optimized before being discharged in stable condition with plans for close monitoring and cardiac MRI with possible future revision of ablation.

Discussion This case serves to exemplify the presentation, diagnosis, and stabilization of a patient experiencing symptomatic runs of NSVT non-sustained ventricular tachycardia.

REFERENCE(S)
1) American College of Cardiology/American Heart Association Task Force on Clinical Data Standards (ACC/AHA/HRS Writing Committee to Develop Data Standards on Electrophysiology); Buxton AE, Calkins H, Callans DJ, DiMarco JP, Fisher JD, Greene HL, Haines DE, Hayes DL, Heidenreich PA, Miller JM, Poppas A, Prystowsky EN, Schoenfeld MH, Zimetbaum PJ, Goff DC, Grover FL, Malenka DJ, Peterson ED, Radford MJ, Redberg RF. ACC/AHA/HRS 2006 key data elements and definitions for electrophysiological studies and procedures: a report of the American College of Cardiology/American Heart Association Task Force on Clinical Data Standards (ACC/AHA/HRS Writing Committee to Develop Data Standards on Electrophysiology). Circulation. 2006 Dec 5;114(23):2534-70. doi: 10.1161/CIRCULATIONAHA.106.180199. Epub 2006 Nov 27. PMID: 17130345.
2) Tada H, Tadokoro K, Ito S, Naito S, Hashimoto T, Kaseno K, Miyaji K, Sugiyasu A, Tsuchiya T, Kutsumi Y, Nogami A, Oshima S, Taniguchi K. Idiopathic ventricular arrhythmias originating from the tricuspid

annulus: Prevalence, electrocardiographic characteristics, and results of radiofrequency catheter ablation. Heart Rhythm. 2007 Jan;4(1):7-16. doi: 10.1016/j.hrthm.2006.09.025. Epub 2006 Sep 28. PMID: 17198982.

3) Callans, DJ. Ventricular tachycardia in the absence of apparent structural heart disease. In: UpToDate, Estes, NAM & Parikh, N (Eds), UpToDate, Waltham, MA, 2023.

4) Mont L, Seixas T, Brugada P, Brugada J, Simonis F, Kriek E, Smeets JL, Wellens HJ. The electrocardiographic, clinical, and electrophysiologic spectrum of idiopathic monomorphic ventricular tachycardia. Am Heart J. 1992 Sep;124(3):746-53. doi: 10.1016/0002-8703(92)90286-5. PMID: 1514503.

23

CORONARY ARTERY TO LEFT VENTRICULAR FISTULA MASQUERADING HYPERTROPHIC CARDIOMYOPATHY: A RARE CASE OF HEART FAILURE

Gorgina Barsoum, Asif Talal. *University of Missouri- Kansas City*

Introduction/Background Coronary artery fistula (CAF) is an abnormal connection between a coronary artery and another vessel or cardiac chamber. The majority of CAF are congenital and often have no hemodynamic consequences. However, when large, these can lead to significant left to right shunting and resultant heart failure and pulmonary hypertension. CAF are rare and there is limited understanding of their phenotype, natural history and indications for percutaneous closure. We present a case of congenital CAF that was initially diagnosed as hypertrophic cardiomyopathy (HCM). To our knowledge, this is the first case of CAF mimicking HCM, adding new knowledge to literature on its phenotypic characteristics and improving our understanding of this rare clinical entity.

Case Presentation A 57-year-old female patient with a history of HCM, hypertension and obstructive sleep apnea, presented to the emergency room with chest pain and worsening dyspnea for 2 days. Patient's presenting blood pressure was 118/61 mmHg, heart rate 136 bpm, respiratory rate 24/min with oxygen saturation (SaO2) of 70% on room air. The patient was placed on bilevel positive airway pressure (BiPAP) ventilation and administered 40 mg of intravenous furosemide with which SaO2 improved to 90%. ECG demonstrated sinus tachycardia, non-specific T wave changes and right axis deviation (Figure). CT pulmonary angiography was obtained that showed no evidence of pulmonary embolism but demonstrated significant pulmonary edema. Initial high sensitivity troponin was markedly elevated at 1200 pg/mL. Transthoracic echocardiogram (TTE) was obtained that showed severely increased left ventricular (LV) wall thickness (Figure) and right ventricular dilatation. Decision was made to proceed with invasive coronary angiography (ICA) given patient's markedly elevated troponin levels and chest pain. ICA showed markedly dilated left coronary artery system with intramyocardial arterio-arterial coronary loops (AACL) arising from left anterior descending and left circumflex coronary arteries. There was then a fistulous connection of the AACL to the left ventricle (Figure). The presence of intramyocardial AACL gave the impression of marked myocardial hypertrophy. The case is being discussed in our heart team regarding options of percutaneous closure and the challenges it poses due to the risk of large iatrogenic post closure myocardial infarction.

Abstract 23 Figure 1 ECG showing sinus tachycardia.
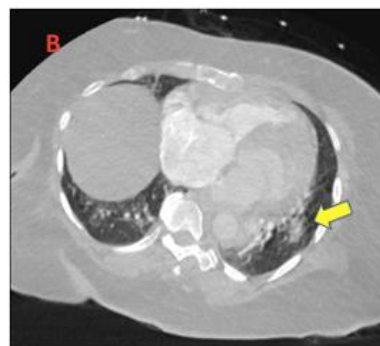
Abstract 23 Figure 2 CT pulmonary angiography showing no pulmonary embolism but demonstrating pulmonary edema (arrow)

Abstract 23 Figure 3 & 4 Severely increased left ventricular wall thickness on transthoracic echocardiography (arrows)
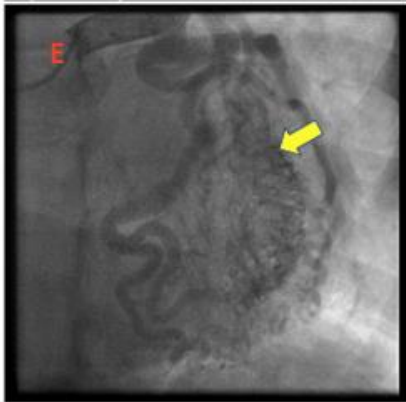
Abstract 23 Figure 5 Intramyocardial arterio-arterial loops (arrow) from the left coronary system

Abstract 23 Figure 6 Arterio-arterial loops from the left coronary system communicating with the left ventricular cavity (arrow)

Discussion Through this case we raise awareness of the rare presentation of congenital CAF simulating HCM and the challenges it presents in terms of diagnosis and percutaneous closure planning. Additionally, undiagnosed congenital heart disease should be considered in adult patients presenting with acute heart failure.

LEFT VENTRICULAR NARROW-NECK PSEUDOANEURYSM FOLLOWING A REDO MITRAL VALVE REPLACEMENT

[1]Abdel-Rhman Mohamed, [2]Abdulmajeed Alharbi, [3]Robert Grande, [2]Abdelmoniem Moustafa, [2]Omar Sajdeya, [3]Stephanie Younes. [1]*Internal Medicine;* [2]*The University of Toledo;* [3]*Promedica Toledo Hospial*

**Introduction/Background** A cardiac pseudoaneurysm is defined as a contained rupture of the myocardium by the pericardium[1]. This is differentiated by a true aneurysm that contains all layers of myocardial tissue. It is of vital importance to be able to diagnose pseudoaneurysms as they require urgent surgical intervention and carry a high risk of rupture and mortality[8]. Most commonly, pseudoaneurysms are associated with myocardial infarctions, particularly of the inferior wall[2].

Case Presentation We present a rare case of a pseudoaneurysm arising from a bioprosthetic mitral valve that developed after a redo mitral valve replacement (MVR). The patient is a 78-year-old female with a medical history significant for mitral valve prolapse, tricuspid valve regurgitation repaired with a 26mm Contour ring, aortic stenosis, atrial fibrillation on Apixaban, insulin dependent type 2 diabetes mellitus, hyperlipidemia, gastroesophageal reflux disease, and obstructive sleep apnea. She had undergone a bioprosthetic mitral valve replacement 11 years prior to presentation for the mitral valve prolapse and severe mitral regurgitation. She initially presented with progressive shortness of breath and dyspnea on exertion. She underwent a transesophageal echocardiogram (TEE) that demonstrated presence of severe prosthetic mitral valve stenosis with moderate to severe tricuspid insufficiency and normal left ventricular systolic function with an ejection fraction (EF) of 50-55%. Cardiac catheterization demonstrated no evidence of coronary artery disease. She was then scheduled for a redo replacement of the mitral valve without immediate postoperative complications. During her follow up five months later, she was still complaining of shortness of breath and a CT Angiogram of the chest showed evidence of a new thin-walled narrow-neck, 0.987cm, pseudoaneurysm 3.4cm in width originating from the lateral margin of the mitral prosthesis at the inferolateral base of the left ventricle (figure 1). Subsequently, the patient underwent a TEE and a cardiac CTA that confirmed the findings (figures 2). The TEE showed an ejection fraction (EF) of 55-60%, a 27mm Mosaic bioprosthetic mitral valve, moderate left atrial dilation, mild tricuspid regurgitation through a 26mm Contour ring, and mild aortic regurgitation. Ultimately, she underwent a successful percutaneous closure of the pseudoaneurysm with a 16mm Amplatzer, (Abbott- Park, IL, USA) (figures 3,4 showing left ventricular angiogram before and after deploying Amplatzer occluding device). The highlight of our case is not only the interesting presentation of the pseudoaneurysm following a mitral valve surgery, but also the method of therapeutic intervention. The mainstay of treatment for a cardiac pseudoaneurysm is surgical intervention. However, this procedure was done percutaneously utilizing an Amplatzer occlude device.Cardiac CTA after the procedure showed thrombosing of the pseudoaneurysm, with a resolving small leak around the Amplatzer plug (figure 5). Patient followed up in clinic with Cardiology following her percutaneous closure with improvement in her shortness of breath and has not had any chest pain, palpitations, or any other concerning symptoms. She underwent a repeat CT one month later which showed further resolution of the residual leak around the device.

Abstract 24 Figure 1 LV pseudoaneurysm on CT
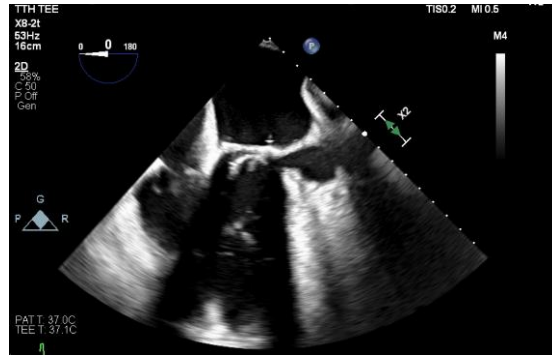
Abstract 24 Figure 2 LV pseudoaneurysm on TEE
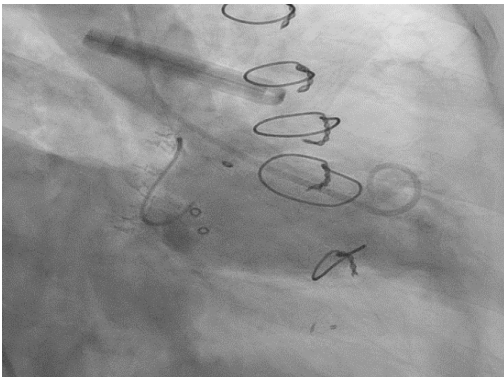
Abstract 24 Figure 3 LV angiogram showing LV pseudoaneurysm

Abstract 24 Figure 4 LV angiogram post LV pseudoaneurysm occlusion by Amplatzer occlude device
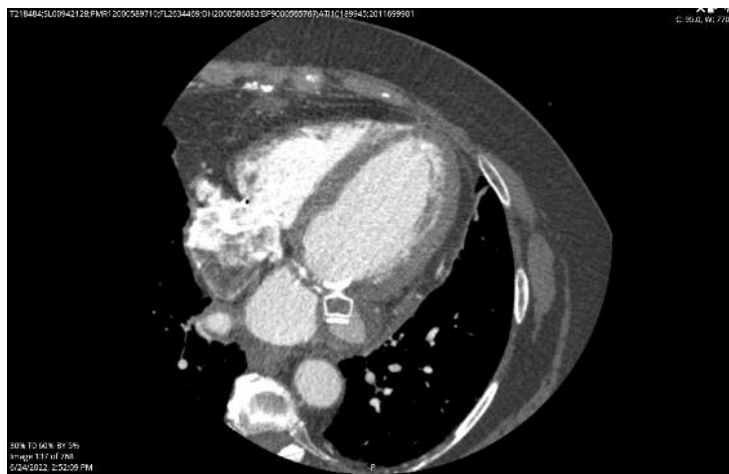
Abstract 24 Figure 5 LV pseudoaneurysm on CT in follow up post Amplatzer device implantation

Discussion Pseudoaneurysms are rare complications of MVR and prosthetic mitral valve infective endocarditis (IE). Studies have reported that pseudoaneurysms are most commonly caused by myocardial infarction followed by IE resulting in an abscess cavity. The incidence of LV pseudoaneurysms

occurs in 0.8% of cases after MVR, and the incidence is 8-times higher than that of pseudoaneurysm development after myocardial infarction2.Rupture of the left ventricle (LV) is infrequent but one of the life-threatening complications after mitral valve replacement. Left ventricular pseudoaneurysm (LVPA) due to incomplete or late rupture after mitral valve replacement is very rare7. However, if LVPA develops into pericardial tamponade it may lead to mortality. Rupture of the LV after mitral valve replacement can present as: early rupture, delayed rupture, or late rupture. Late rupture in particular appears days to years after mitral valve replacement and presents as a pseudoaneurysm of the LV. LVPA may develop de novo after the surgical procedure or may be a sequela of an earlier rupture5.The clinical presentations of LVPA are shortness of breath, heart failure symptoms, chest pain, endocarditis, and pericardial tamponade. However, it can also have an asymptomatic course. The recommended treatment is surgical repair. Conservative follow-up is an alternative approach for those patients who refuse surgical treatment or are considered as high risk for re-operation7.Predisposing risk factors of LVPA are female gender, advanced age, mitral stenosis, small-volume LV, and small body size. Resection of excessive mitral tissue during the removal of the diseased mitral valve can cause injury to the annulus. The greatest injury during debridement is probably seen with heavy calcified mitral valves, especially with calcification in the posterior leaflet. The same injury can also be caused during the removal of a noncalcified mitral valve by inadvertent incision and/or forced traction of the annulus. Deeply placed sutures or excessive traction on sutures in the annulus can cause a tear through the myocardium and create small tracts in the myocardium. With elevated LV pressure, blood enters these small tracts and can dissect through the wall to the pericardial space. Insertion of an oversized mitral prosthesis can stretch the annulus and thus leads to rupture of the posterior wall of the LV. Untethering of the LV by excision of the mitral valve with the chordae tendineae and papillary muscles can cause an increase in the pressure stress on the myocardium. This stretch effect can lead to transverse midventricular endomyocardial disruption. Untethered myocardium promotes extension of the myocardial thickness defects produced by mechanical injury and converts these to transmural ruptures. Insertion of oversized mitral prosthesis can stretch the mitral annulus and can lead to rupture of the LV, which can result in pseudoaneurysm6.LVPA can present at any time: early rupture, delayed rupture, or late rupture. Late rupture in particular manifests days to years after mitral valve replacement and presents as a pseudoaneurysm of the LV. Pankaj and his team reported a late rupture with LVPA that happened 4 years after mitral valve replacement4. LVPA can happen earlier like our case which developed 5 months post MVR.A such surgical complication as in our case is not uncommon and echocardiography is the most widely used method for the diagnosis of LVPA. The typical finding on echocardiography is an echo-free annular aneurysmal sac that is adjacent to the posterior wall of the LV [1, 30]. A turbulent flow on the orifice of the pseudoaneurysm can be seen with two-dimensional color Doppler echocardiography (Fig.3). Color Doppler echocardiography can help in the visualization of blood flowing forward into the pseudoaneurysm with systole and backflow into the LV with diastole5.This rare case demonstrates the importance of routine imaging and follow up especially after surgical intervention. It also demonstrates the importance of keeping a broad differential diagnosis and to use objective data to confirm diagnoses. This case highlights another option to treating cardiac pseudoaneurysms as the mainstay treatment is surgical. There are not many cases of percutaneous plugging closure, especially with an Amplatzer occlude device, so this successful case sheds light into different modalities of treatment for future cases. Through these modalities and following up, a rare presentation of a pseudoaneurysm was able to be identified and promptly treated through percutaneous closure that resolved the patient's clinical symptoms.

REFERENCE(S)

1. Dachman AH, Spindola-Franco H, Solomon N. Left ventricular pseudoaneurysm. Its recognition and significance. JAMA. 1981;246(17):1951-1953.

2. Frances C, Romero A, Grady D. Left ventricular pseudoaneurysm. J Am Coll Cardiol. 1998;32(3):557-561. doi:10.1016/s0735-1097(98)00290-3

3. Kim M, Park YJ, Yu HT, Kim T-H, Uhm J-S, Joung B, et al. Case Report: Delayed Ventricular Pseudoaneurysm After Radiofrequency Ablation of Left Posteromedial Papillary Muscle Ventricular Tachycardia. Front Cardiovasc Med [Internet]. 2022 Jun 15 [cited 2022 Sep 27];9. Available from: https://pubmed.ncbi.nlm.nih.gov/35783824/

4. Malhotra P, Han D, Kwan AC, Skaf S, Siegel R, Trento A, et al. CASE REPORT CLINICAL CASE A Rare Case of Post-Mitral Valve Replacement Ventricular Pseudoaneurysm, Bioprosthetic Dehiscence, and Paravalvular Mitral Regurgitation. JACC Case Reports [Internet]. 2022 [cited 2022 Sep 27];4:449–54. Available from: https://doi.org/10.1016/j.jaccas.2022.02.006

5. Neupane S, Kommuri NVA, Kazanji N, Chowdhury P. Left ventricular pseudoaneurysm after mitral valve replacement. Echocardiography [Internet]. 2016 Nov 1 [cited 2022 Sep 27];33(11):1788–9. Available from: https://pubmed.ncbi.nlm.nih.gov/27400412/

6. Şahan E. Linksventrikuläres Pseudoaneurysma nach Mitralklappenersatz: Übersichtsarbeit über Pseudoaneurysmen als Spätfolge nach Mitralklappenersatz. Herz [Internet]. 2015 Aug 18 [cited 2022 Sep 27];40(5):778–82. Available from: https://link.springer.com/article/10.1007/s00059-015-4302-7

7. Sakai K, Nakamura K, Ishizuka N, Nakagawa M, Hosoda S. Echocardiographic findings and clinical features of left ventricular pseudoaneurysm after mitral valve replacement. Am Heart J [Internet]. 1992 [cited 2022 Sep 27];124(4):975–82. Available from: https://pubmed.ncbi.nlm.nih.gov/1529909/

8. Vlodaver Z, Coe JI, Edwards JE. True and false left ventricular aneurysms. Propensity for the latter to rupture. Circulation. 1975;51(3):567-572. doi:10.1161/01.cir.51.3.567

Dermatology

25

SHAVE REMOVAL OF SQUAMOUS CELL CARCINOMA AND BASAL CELL CARCINOMA

[1]Aishwarya Sharma, [2]Thomas Matzke. [1]*Univerity of North Dakota School of Medicine and Health Sciences;* [2]*Sanford Health*

Introduction/Background Based on the American Academy of Dermatology, the current standard of care for a lesion suspicious for a basal cell carcinoma (BCC) or squamous cell carcinoma (SCC), is first performing a biopsy, and then if diagnosis is confirmed as either BCC or SCC the patient would be scheduled for definitive treatment[1]. Depending on risk factors such as size, location, or aggressive histological features, treatment options include excision with standard margins, mohs surgery, destruction such as electrodessication and cauterization (ED&C), or radiation. In select cases, superficial nonmelanoma skin cancer [NMSC] 1.5 cm or less in diameter can be excised using a disposable #15 scalpel blade and followed up with routine pathology and twice-annual follow up[2]. This expedient alternative modality saves time for the patient, cost for the hospital and conserves provider resources in better service to others in need without compromising on the healing cosmetically [2]. We aim to prove that when approaching a lesion suspicious for BCC or SCC starting instead with a shave procedure with the intent to remove the lesion entirely can be definitive treatment if the histological margins are reported as uninvolved and there aren't aggressive histological features.

Objective(s) To determine the outcome of shave removal of BCC and SCC.

Methods We conducted a retrospective chart review of 507 patients who were diagnosed with either BCC or SCC based on pathology case numbers and received a shave removal during the year 2017 in our dermatology clinic. Any patient with a diagnosis of BCC or SCC during the period of January 2017-December 2017 who underwent shave removal by this provider in our clinic was included in the study. Any patient with a diagnosis of melanoma or a diagnosis of BCC/SCC outside of 2017 were excluded from this study. Data that was recorded included demographic information, clinical characteristics, and management outcome. Patient demographic information included age, sex, and race. Clinical characteristics included the diagnosis of BCC or SCC, size and location of the lesion. Management outcomes included any additional interventions, presence/absence of recurrence, and time to recurrence. Analysis was performed using summary statistics and bivariate comparisons (Chi-square tests and GLM means). All significance tests were two-sided, P-value < 0.05 for significance.

Results Of the 507 patient encounters in 2017, there ended up being 794 shave removals for BCC or SCC. The average age of the patient was 75. There was a roughly equal number of males (57%) and females (43%). 99% of the patients were Caucasian. 9 lesions were excluded because the biopsy results confirmed melanoma. Of the 785 remaining, 364 were BCC, 93 were SCC, and 328 were SCCIS. The average size of the lesions was < 6mm with a majority of them (72%) located on the face. Patients were followed up for an average of 65 months. Of the 785 remaining, 298 were watch for recurrence and 487 lesions recurred. Of the 487 recurrences, 139 had ED&C, 37 had cryotherapy, 49 underwent wide re-excisions, and 286 underwent MOHS surgery with no further recurrence at 5 years. The overall recurrence rate of those that were watch for recurrence was 0% (p< 0.05).

Conclusion While the use of shave biopsy for BCC and SCC isn't presently in the main dermatological or surgical literature, we have practiced this approach for over 15 years involving over 10,000 skin cancers with high cure rates and excellent patient satisfaction. The NCCN guidelines outlines a similar approach (initial shave removal / saucerization with a 2mm margin) as one of the methods for first performing removal of lesions clinically suspicious for thin melanoma within. In addition, in the NCCN on BCC and

SCC they comment that some of the authors advocate performing destruction/ED&C at time of biopsy and not performing additional treatment if high risk historical features are not identified on pathology. Our approach is that one is better off trying to remove the lesion with the shave than partial biopsy with ED&C, with the added benefit of having more histology to review. While some argue that shave margins are not reliable, they are superior to having less of the lesion to evaluate as some skin cancers can appear more banal superficially and show more ominous features within the deeper aspects of the lesion. This approach is especially useful for SCCIS with an average diameter of < 6mm, located on the chest, back, or extremities. Also, our approach of trusting shave margins has been supported in the literature for atypical nevi. Given the benefit of preventing some patients from undergoing additional treatments resulting in a savings of money, time, and improved patient access, we recommend shave removal for similar lesions suspicious for BCC and SCC.

REFERENCE(S)
1. HARRISON, P. V. MD1. Shave Excision for Basal Cell Carcinoma. The Journal of Dermatologic Surgery and Oncology: May 1994 - Volume 20 - Issue 5 - p 350 doi: 10.1111/j.1524-4725.1994.tb01637.x
2. Abramson AK, Krasny MJ, Goldman GD. Tangential shave removal of basal cell carcinoma. Dermatol Surg. 2013 Mar;39(3 Pt 1):387-92. doi: 10.1111/dsu.12106. Epub 2012 Dec 27. PMID: 23279298.

CHARACTERIZATION OF M6A RNA METHYLATION IN CUTANEOUS SQUAMOUS CELL CARCINOMA

[1]Grace Duan, [2]Jake Lazaroff, [2]Michelle Verghese, [2]Breanna Bertacchi, [2]Seungwon Yang, [2]Yu-Ying He, [2]Diana Bolotin. [1]*University of Chicago Pritzker School of Medicine; [2]University of Chicago*

Introduction/Background Cutaneous squamous cell carcinoma (SCC) is among the most common malignancies in the United States[1]. Carcinogenesis of SCC progresses through precursor dysplastic lesions, full thickness SCC in situ (SCCis) tumor, and eventually invasive and metastatic SCC. Exposure to ultraviolet radiation (UVR) is a well-established pathogenic factor in the development of SCC, and recent studies have suggested the importance of m(6)A RNA methylation in regulation of UVR-induced DNA damage response [2]. This modification process subjected to dynamic control via positive regulators ("writers") such as METTL14 and negative regulators ("erasers") such as ALKBH5 and FTO[3]. Although m(6)A RNA methylation has been described in the initiation, progression and drug response of various malignancies, its role in cutaneous SCC carcinogenesis is not well-understood.

Objective(s) This study aims to characterize m(6)A RNA methylation in cutaneous squamous cell carcinoma (SCC) tumorigenesis and identify potential regulatory players mediating its role in cutaneous UVR-damage response.

Methods This is a prospective study approved by the institutional review board. Patients who presented to at University of Chicago for Mohs surgery for the treatment of cutaneous SCC or SCCis on the head and neck were screened for eligibility. Patients between 18-95 years of age, diagnosis of cutaneous SCC or SCCis, and clinically evident residual tumor on the day of the procedure were eligible. After informed consent, tissue samples were obtained from each patient including 1) Mohs debulk of the primary tumor, 2) adjacent, normal-appearing sun-exposed skin (SE-skin) and 3) punch biopsy of the participant's proximal inner upper arm to serve as sun-protected control (SP-skin). Immunohistochemistry was performed to measure m(6)A RNA methylation levels in the three skin samples. Western blot analysis was performed to quantify levels of m(6)A effector proteins, including METTL14, ALKBH5, and FTO, in those samples. Statistical comparisons were conducted using paired t-tests with alpha set to 0.05. A total of 28 participants and 32 tumor specimens were included in the analysis.

Results Immunohistochemical analysis revealed that normalized mean signal intensity of m(6)A RNA methylation was significantly decreased in SCC (0.72) compared to SE-skin (0.88; P=0.02) and SP-skin (1.00; P< 0.0001). Additionally, m(6)A induction was significantly lower in SE-skin relative to SP-skin (P=0.04). Western blot analysis demonstrated METTL14 had decreased expression in SCC compared to SE-skin and SP-skin. Conversely, ALKBH5 was expressed at higher levels in SCC than in SE-skin and SP-skin and FTO was expressed at higher levels in SCC compared to SP-skin.

Conclusion In this translational study, we characterize m(6)A RNA methylation in cutaneous SCC carcinogenesis using immunohistochemistry and Western blot techniques with correlation to clinical and pathologic findings of SCC using patient-derived samples. We report that m(6)A RNA methylation is lowest in SCC/SCCis tumoral tissue, followed by SE-skin, and subsequently highest in SP-skin. This suggests that impairment in m(6)A induction in chronically UVR-damaged skin may disrupt innate mechanisms that normally protect against SCC carcinogenesis [4]. Furthermore, altered m(6)A RNA methylation in SE-skin and SCC/SCCis may be mediated by the disruption in m(6)A effector proteins. Our finding that METTL14, a m(6)A methyltransferase, is downregulated in SE-skin and SCC/SCCis is consistent with previous reports in melanoma that METTL14 normally localizes to UVR damage sites to prevent cell proliferation, migration, and invasion [5]. Conversely, we found that m(6)A demethylases ALKBH5 and FTO were upregulated in SE-skin and SCC/SCCis. Prior studies in cervical SCC [6] and

melanoma [5] suggest FTO has an important role in tumorigenesis, whereby the knockdown of FTO has a tumor-suppressive effect. ALKBH5 is less understood. Neither FTO nor ALKBH5 have been previously reported in cutaneous SCC. This study introduces translational evidence that UVR-induced dysregulation of m(6)A RNA methylation play a role in cutaneous SCC pathogenesis. Further characterization is needed and may drive innovation in the prevention and treatment of cutaneous SCC.

REFERENCE(S)
1. Rogers HW, Weinstock MA, Feldman SR, Coldiron BM. Incidence estimate of nonmelanoma skin cancer (keratinocyte carcinomas) in the U.S. population, 2012. JAMA Dermatol. 2015;151(10):1081-1086.
2. Rigel DS. Cutaneous ultraviolet exposure and its relationship to the development of skin cancer. J Am Acad Dermatol. 2008;58(5 Suppl 2):S129-132.
3. Zhao BS, Roundtree IA, He C. Post-transcriptional gene regulation by mRNA modifications. Nat Rev Mol Cell Biol. 2017;18(1):31-42.
4. Xiang Y, Laurent B, Hsu CH, et al. RNA m(6)A methylation regulates the ultraviolet-induced DNA damage response. Nature. 2017;543(7646):573-576.
5. Yang S, Wei J, Cui YH, et al. m(6)A mRNA demethylase FTO regulates melanoma tumorigenicity and response to anti-PD-1 blockade. Nat Commun. 2019;10(1):2782.
6. Zhou S, Bai ZL, Xia D, et al. FTO regulates the chemo-radiotherapy resistance of cervical squamous cell carcinoma (CSCC) by targeting beta-catenin through mRNA demethylation. Mol Carcinog. 2018;57(5):590-597.

27

A COMPARATIVE STUDY OF REVIVIFY TO RESTORE SKIN WELL-BEING AMONG POPULATION SUFFERING FROM ACNE VULGARIS

[1]Wahida Chowdhury, [1]Nashida Chowdhury, [2]Syeda Hussain, [2]Liaquat Hossain, [3]Mohammad Uddin. [1]*Orion Institute for Translational Research;* [2]*Advance Pharmaceuticals Inc*; [3]*Texas A&M University School of Medicine*

Introduction/Background Acne vulgaris is a common chronic inflammatory skin disease of pilosebaceous units. It affects both male and females in different times of their lives, but more commonly in adolescents. It primarily affects the face, upper part of the chest, back, arm and thigh. This happens from a complex pathogenesis of overproduction of sebum by the sebaceous gland, clogging of hair follicles leading to formation of plug, and accumulation of bacteria namely Propionibacterium. Thereafter, there occurs an inflammatory reaction leads to reactive species (ROS) production by the damaged follicular walls. In addition, Propionibacterium bacteria produces some enzymes like lipases, protease, hyaluronidases which play an important role in the inflammatory process. Oxygen, which is an important and vital component for human, can produce reactive types like super-oxide anions, hydroxyl radicals. Super-oxide dismutase (SOD), catalase (CAT) and glucose 6 phosphate dehydrogenase are some of the antioxidant enzymes. Currently, there is a new medication, namely Revivify which is a dietary supplement based on primary antioxidant superoxide dismutase, prebiotic fiber, diverse polyphenols from various fruits juice. It stimulates the immune system by activating T-cell, and acts as an antioxidant and anti-inflammatory product. It works on the cellular level to help to repair damage cells, caused by free radicals. It also increases oxygen, reduce inflammation, and promote skin well-being by promoting healthy digestion and gut flora.

Objective(s) The study objective is to evaluate the effect of Revivify on Bangladeshi population to restore skin well-being suffering from acne vulgaris.

Methods We conducted a case and control study in the different clinics under the Dhaka North City Corporation, Bangladesh. In total, 20 patients joined who were equally and randomly assigned in case and control groups i.e., 10 in each group. The selection criteria: male and female aged 20 years and above irrespective of marital status who were suffering from moderate to severe ranges of acne vulgaris with post inflammatory hyper-pigmentation, scars and uneven skin tone. In the case group, study respondents used Revivify along with Oral Doxycycline and tropical therapy, whereas the control group used only Oral Doxycycline and tropical therapy.

Results During the clinical assessment, we found that the number and size of blemishes, level of inflammation and post inflammatory effect including hyperpigmentation and scars reduced substantially and their skin tone improved noticeably among the study respondents who used Revivify along with Oral Doxycycline and tropical therapy comparing to the control group.

Conclusion Though, this small-scale study findings suggested that Revivify is useful to re-establish skin well-being among Bangladeshi population, yet it also highlighted the necessity of conducting a large-scale study to measure the significant impact of this medication on the Bangladeshi population having acne vulgaris with complications, so that the dermatologists can avoid over-use of antibiotics.

Diagnosis or Treatment of a Disease Process or Clinical Syndromes

28

MACHINE VISION ESTIMATION OF HEMOGLOBIN CONCENTRATION IN HOSPITALIZED PATIENTS WITH ANEMIA.

[1]Mohammed Lone, [1]Edvardine Joseph, [2]Bryan Huang, [3]Mustafa Alam, [4]Shaveta Khosla, [5]Micah Prochaska, [2]Mark Hasegawa-Johnson, [2]Narendra Ahuja, [5]David Beiser. [1]*The University Of Chicago*; [2]*UIUC Grainger College of Engineering*; [3]*Howard University College of Medicine*; [4]*University of Illinois at Chicago*; [5]*UChicago Medicine*

Introduction/Background Anemia is an important global health problem that affects nearly a third of the world population. Chronic anemia has a significant disease burden and is associated with increased morbidity, early mortality, and adverse economic impacts. Laboratory screening, diagnosis and monitoring of anemia requires the use of capillary puncture or venipuncture hemoglobin (hematocrit) assays that are typically performed during in-person healthcare visits. The rise of telemedicine healthcare visits during the recent COVID-19 pandemic highlighted the need to develop non-invasive methods, appropriate for virtual patient assessments, to reduce the need for in-person clinic visits and laboratory blood draws.Previous groups have utilized laboratory-grade optical devices and machine vision approaches for noninvasive estimation of hemoglobin concentration in healthy caucasian students. We hypothesized that similar accuracy could be achieved on image samples acquired using consumer-grade cameras in a diverse population of chronically-ill hospitalized patients with anemia.
Objective(s) The objective of this study is to collect a dataset of visual samples of hospitalized anemic patients for development of an automated machine-vision based hemoglobin concentration estimator.
Methods Patients admitted to the general medicine or hospitalist service with a hemoglobin (Hb) concentration below 10 gm/dL were approached for study participation. Standardized views of the left and right eye conjunctival surfaces were captured with a consumer-grade digital SLR camera under standardized lighting conditions. Demographic information and laboratory-based Hb concentration values were abstracted from the patient's electronic medical record.Two regions of interest (ROI), the anterior and posterior rims of the conjunctiva, were manually segmented from the images. Color vectors were extracted for each ROI using 2 different color spaces. The resulting 12 features were color-corrected and fit to the true Hb levels in a linear regression model and a support vector regression (SVR) model. Leave-one-out cross validation was applied to the SVR model. The SVR model's hyperparameters were manually tuned to improve the coefficient of determination between the true Hb levels and leave-one-out test Hb levels.
Results A total of 27 hospitalized patients were enrolled, 20 of whom had distinguishable anterior and posterior rims. The population consisted of 56% men and 81% African-Americans, with a median age of 57, and median Hb concentration of 8.7g/dL (6.8 – 11 g/dL). A total of 91 conjunctiva images were collected, of which 61 contained distinguishable subregions. In the SVR regression model with color correction, the coefficient of determination (R-squared) between the predicted and actual hemoglobin level was 0.6614 (figure 1). In the linear regression model, the coefficient of determination was 0.5285 (figure 2).
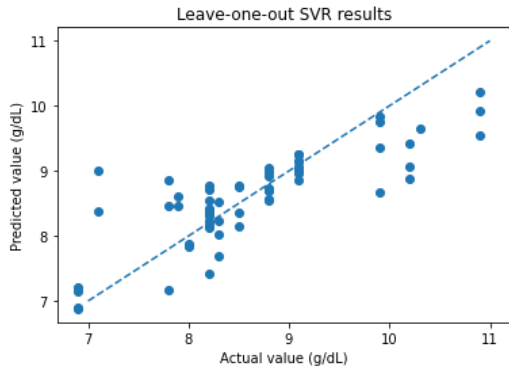
Abstract 28 Figure 1 Predicted Hb by Actual Hb in SVR model.
Individual images were plotted by predicted Hb from the model vs. corresponding true Hb value. Line of best fit was depicted as a blue dashed line. R-Squared = .6614
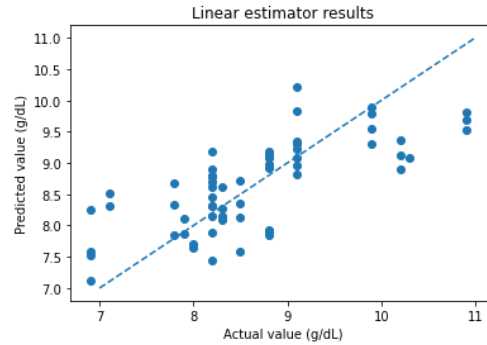
Abstract 28 Figure 2 Predicted Hb by Actual Hb in Linear Regression model.
Individual images were plotted by predicted Hb from the model vs. corresponding true Hb value. Line of best fit was depicted as a blue dashed line. R-Squared = .5285

Conclusion These preliminary results demonstrate the feasibility of utilizing machine-vision techniques for the non-invasive estimation of Hb in a diverse population of chronically-ill patients with consumer-grade equipment. With improved accuracy through further algorithmic optimization, such an approach may be utilized as a low-cost, non-invasive, method for estimating Hb concentration in patients during telemedicine visits.

URINARY LEVELS OF ANGIOGENIC FACTORS AND MARINOBUFAGENIN IN URINE OF PREGNANT PATIENTS WITH AND WITHOUT PREECLAMPSIA

[1]India Morgan, [2]Thomas Kuehl, [2]Ahmed Pantho, [1]Mohammad Uddin, [3]Niraj Vora, [1]David Zawieja. [1]*Texas A&M University School of Medicine*; [2]*Orion Institute for Translational Medicine*; [3]*Baylor Scott & White Health, Temple, Texas*; [1]*Texas A&M University School of Medicine*

Introduction/Background Preeclampsia is a syndrome which occurs in 3-10% of pregnancies and is a leading cause of maternal and fetal morbidity and mortality. This syndrome is characterized by the de novo development of hypertension and proteinuria after 20 weeks of gestation. The precise etiology (etiologies) of this syndrome remain(s) unknown. it seems clear that preeclampsia is not a single disorder, but a syndrome with multiple pathophysiologic factors and mechanisms. There is no single biomarker for detection of the syndrome.

Objective(s) To measure angiogenic factors, anti-angiogenic factors, and marinobufagenin (MBG) in urine of pregnant patients with and without preeclampsia.

Methods A prospective cohort of patients with normal pregnancies and of those with preeclampsia were recruited to provide urine samples, sFlt-1, soluble endoglin (sEng), PIGF, TGF-B, VEGF, and marinobufagenin (MBG) were assayed using ELISA and results corrected to units per mg creatinine. Patient characteristics were compared using Chi-square tests for proportions, Student's t-test for parametric data, and Mann-Whitney U-test for non-parametric data. $P < 0.05$ was taken as significant. Variation associated with gestational age was examined using correlations, and, when appropriate, linear regression equations were obtained. Receiver operator curves (ROC) were examined to establish criteria levels for those factors that varied with preeclampsia.

Results In total, 23 patients with normal pregnancies were sampled between 22 and 39 weeks gestation, and 17 patients with preeclampsia were sampled between 28 and 39 weeks gestation. As expected, groups differed (p0.14). Only urinary MBG was found to vary with gestational age in normal pregnancies (p=0.0009). MBG, sFlt-1, PIGF, and sFlt-1/PIGF ratio had significant ROC area under the curve measurements (p< 0.02) with criteria for preeclampsia that provided sensitivities between 65-88%, and specificities between 74-96%.

Conclusion Urinary levels of certain angiogenic factors and anti-angiogenic factors demonstrated differences in patients with a clinical diagnosis of preeclampsia. Urine specimen procurement and assay are a less invasive and potentially more acceptable for assessment of preeclampsia.

30

PROLONGED HOSPITAL COURSE LEADING TO DELAYED IDENTIFICATION OF TOXIC EPIDERMAL NECROLYSIS WITH FATAL COMPLICATIONS

Shelby Schuh, Austin Reed, Suhaib Bajwa, Tinashe Maduke. *University of Missouri-Columbia*

Introduction/Background Toxic epidermal Necrolysis (TENS) is a desquamative necrotic rash encompassing 30 percent or more of the body's surface area. Without prompt identification of triggers, TENS can progress to distributive shock and multi-organ failure. We present a unique case of a patient with acute hypoxic respiratory failure, distributive shock, and a desquamative rash secondary to TENS. Careful review of outside records revealed Augmentin as the likely culprit agent. A maximal supportive care strategy across a multidisciplinary team was employed. High clinical suspicion for TENS is imperative to allow for timely removal of causative agent and initiation of supportive care as the management of TENS is complex and best well managed in critical care units.Toxic Epidermal Necrolysis (TENS) and Stevens-Johnson Syndrome (SJS) are severe mucocutaneous reactions characterized on histopathology as having keratinocyte necrosis with partial to full thickness necrosis of epidermis[1]. TENS normally covers greater than 30% of the body surface area whereas SJS covers less than 10% [2]. While the exact pathophysiology remains unclear, many drugs such as sulfonamide antimicrobials, phenobarbital, carbamazepine, and lamotrigine are well known triggers[3]. Furthermore, not only is pathophysiology unclear but the management of TENS remains controversial. The mainstay of treatment continues to be prompt withdrawal of possible offending agents and supportive care, however, IVIG, steroids and other medications are frequently trialed[1]. Although the treatment remains controversial, a retrospective case study completed at a national referral center for TENS/SJS in Singapore demonstrated the patients still do have improved overall outcomes with early referral. Early referral was defined as patients seen within 4 days of developing blistering lesions[4]. The improved outcomes from early referral were likely due to prompter withdrawal of offending medications and the possibility of immunomodulatory therapy use which has been shown to be more effective in the progressive phase of disease.

Case Presentation The patient is a 52-year-old male that presented as a transfer for acute hypoxic respiratory failure in the setting of extensive rash concerning for Stevens-Johnson syndrome (SJS) versus toxic epidermal necrolysis syndrome (TENS). Past medical history included end-stage renal disease (ESRD) on Monday-Wednesday-Friday dialysis, hypertension, paroxysmal atrial fibrillation on apixaban, seizure disorder on levetiracetam, and hypothyroidism. Prior to presentation, the patient had a prolonged hospital course for syncope. During this stay, the patient received numerous antibiotics including Vancomycin, Ceftriaxone, Aztreonam and 2 separate courses of Augmentin for concern of pneumonia in the setting of persistent fevers. The patient was eventually discharged but subsequently was reevaluated in the emergency department for diffuse desquamating rash and hypoxia 5 days later. The patient was subsequently transferred to a tertiary care center and was noted to have vitals with a heart rate of 110 bpm, blood pressures of 110/80 mmHg, and oxygen saturation of 100% on room air on initial presentation. However, during the initial evaluation, the patient desaturated and required intubation. The chest x-ray demonstrated multifocal airspace opacities. Skin examination revealed numerous eroded bullae and exfoliative desquamation accounting for >30% of patient's body surface area with positive Nikolsky's sign (figure 1). Physical exam was also notable for diffuse 3+ lower extremity pitting edema up to his lower abdomen. Management: Given the high suspicion for epithelial sloughing in the setting of TENS leading to the acute hypoxic respiratory failure, urgent bronchoscopy with bronchoalveolar lavage (BAL) was performed and demonstrated mild bruising in the upper right lobe with thick secretions in the right and left lower lobes. Immediately following the procedure, the

patient was noted to be hypotensive requiring vasopressor support. Although supportive care with aggressive fluid resuscitation remains first line for distributive shock in the setting of TENS, our avenue for fluid resuscitation remained limited given the diffuse pitting edema in setting of ESRD the patient already had. Linezolid and meropenem were chosen as broad spectrum antibiotics in order to avoid antibiotics with associations with TENS. Of note, the patient's respiratory status continued to decline and was concerning for ARDS given the worsening P/F ratios. A subsequent decision was made to prone and paralyze the patient prone via the ARDS protocol at our hospital. Over the course of the next few days, multiple medical and surgical subspecialties were consulted for further evaluation and management. Dermatology was consulted and completed a punch biopsy with results positive for TENS. Given the severity and extent of desquamation, dermatology recommended starting the patient on IVIG. Nephrology was consulted and assisted with IVIG administration and management of the patient's hemodialysis. General Surgery was consulted for wound care management and performed multiple bedside debridement. Despite multiple aggressive interventions, the patient's clinical status continued to decline and eventually died less than a week into his admission at our tertiary care facility.

Abstract 30 Figure 1 Area of desquamation on patient's arm.

Discussion TENS occurs after a trigger leading to keratinocyte apoptosis by a mechanism not yet fully understood. Some patients have a genetic predisposition to development of TENS through various HLA class subtypes. Although diagnosis of TENS remains infrequent, there are well documented reports linking sulfonamide antibiotics, phenobarbital, carbamazepine, and lamotrigine as triggers for the onset of TENS. Less common but additional medications that can trigger TENS include levetiracetam and penicillin antimicrobials. In this case, the patient was taking levetiracetam and could be an inciting factor but given the long-term use of levetiracetam by this patient, it remains as an unlikely trigger for TENS in this case. The more likely offending agent, however, was Augmentin as it was given on 2 separate occasions and the patient's rash developed nearly 1-3 weeks after initiation of the medication. With the patient's prolonged outside hospital course and unclear timeline to the onset of the rash, it was difficult to identify Augmentin as the offending agent and thus remove it in a timely manner. Prior to dermatologic involvement, TENS typically presents as fevers with generalized malaise and myalgias[5]. Laboratory abnormalities for TENS typically include anemia, and lymphopenia. Neutropenia is also present in approximately one-third of patients and correlated with a poor prognosis [6]. The patient in this case was noted to have persistent fevers and had received filgrastim at the previous hospital for neutropenia of unknown etiology. Given SJS/TENS diagnosis remains rare and thus not well studied, no exact treatment protocol has been developed. One case-control study completed in Europe found that neither corticosteroids nor intravenous immunoglobulins had a significant effect on mortality as

compared to supportive care alone[7]. Another retrospective study conducted at a burn center using a treatment algorithm focusing on supportive care and early utilization of intravenous immunoglobulins demonstrated significant improvement in mortality beyond what was predicted from mortality scores[8]. The mainstay of therapy and the focus in the literature continues to be early identification and removal of offending agents. In the case of our patient, the patient was initially started on supportive care with pressor support and eventually trialed on IVIG due to the extensiveness of the dermatologic findings and the late progression of the disease. Not only is there no exact treatment method, but the mortality rates also remain high for TENS. On average for TENS, the mortality is about 23% at six weeks and 34% at one year[9]. Part of the reason the mortality rate is so high in this patient population is due to the serious complications that can occur with TENS including ARDS, mucosal bleeding, and epithelial dysfunction leading to septic shock. Our patient was noted to have septic shock secondary to epithelial dysfunction leading to bacterial translation, and ARDS secondary to epithelial sloughing. Furthermore, our patient was noted to have a history of ESRD on HD, was grossly fluid overloaded, and had developed ARDS on presentation which limited an aggressive fluid resuscitative approach. Several studies have attempted to elucidate the likelihood of developing these severe complications in TENS patients. A prospective study performed in South Africa over a 3-year period found that of the total 75 patients included in the study, 2 developed ARDS and 28 developed severe sepsis [10]. Furthermore, a review of the literature demonstrated that only a few other instances have been documented of TENS patients developing concomitant septic shock and ARDS albeit these reports are exclusively with patients significantly younger and with fewer comorbidities [11]. We present in a rare and challenging case of a patient presenting with TENS complicated by ARDS and septic shock compounded by the patient's underlying history of ESRD requiring HD and hypervolemic status on presentation.

REFERENCE(S)
1. Stern RS, Divito SJ. Stevens-Johnson Syndrome and Toxic Epidermal Necrolysis: Associations, Outcomes, and Pathobiology-Thirty Years of Progress but Still Much to Be Done. Journal of Investigative Dermatology. 2017;137(5):1004-1008.
2. Bastuji-Garin S, Rzany B, Stern RS, Shear NH, Naldi L, Roujeau JC. Clinical classification of cases of toxic epidermal necrolysis, Stevens-Johnson syndrome, and erythema multiforme. Archives of Dermatology. 1993;129(1):92-96.
3. Mockenhaupt M, Viboud C, Dunant A, et al. Stevens-Johnson syndrome and toxic epidermal necrolysis: assessment of medication risks with emphasis on recently marketed drugs. The EuroSCAR-study. Journal of Investigative Dermatology. 2008;128(1):35-44.
4. Clark AE F-CS, Choo K, et al. Delayed admission to a specialist referral center for Stevens-Johnson syndrome and toxic epidermal necrolysis is associated with increased mortality: A retrospective cohort study. Journal of American Academy of Dermatology International. 2021;4:10-12.
5. Roujeau JC, Stern RS. Severe adverse cutaneous reactions to drugs. New England Journal of Medicine. 1994;331(19):1272-1285.
6. Westly ED, Wechsler HL. Toxic epidermal necrolysis. Granulocytic leukopenia as a prognostic indicator. Archives of Dermatology. 1984;120(6):721-726.
7. Schneck J, Fagot J-P, Sekula P, Sassolas B, Roujeau J-C, Mockenhaupt M. Effects of treatments on the mortality of Stevens-Johnson syndrome and toxic epidermal necrolysis: A retrospective study on patients included in the prospective EuroSCAR Study. Journal of the American Academy of Dermatology. 2008;58(1):33-40.
8. McCullough M, Burg M, Lin E, Peng D, Garner W. Steven Johnson Syndrome and Toxic Epidermal Necrolysis in a burn unit: A 15-year experience Burns. 2017;43(1):200-205.

9. Sekula P, Dunant A, Mockenhaput M, et al. Comprehensive survival analysis of a cohort of patients with Stevens-Johnson syndrome and toxic epidermal necrolysis. Journal of Investigative Dermatology. 2013;133(5):1197-1204.
10. Kannenberg S.M.H., Jordaan H.F., Koegelenberg C.F.N., Von Groote-Bidlingmaier F., Visser W.I. Toxic epidermal necrolysis and Stevens–Johnson syndrome in South Africa: a 3-year prospective study, QJM: An International Journal of Medicine, 2012;105(9):839–846.
11. Roeleveld YWF, Cleffken BI, Dokter J, Oen IMMMH, Van Der Vlies CH. A 19-year old Female wit Toxic Epidermal Necrolysis and Acute Pulmonary Failure was Successfully Treated with Extracorperoreal Membrane Oxygenation: A case report and Review of the Literature. Journal of Clinical Dermatology and Therapy. 2015;2(1):1-3.

ALLOPURINOL HYPERSENSITIVITY SYNDROME COMPLICATED BY RESPIRATORY DISTRESS, TOXIC EPIDERMAL NECROLYSIS AND MULTI-ORGAN FAILURE

Andrew Campbell, Austin Meehl. *University Toledeo Medical Center*

Introduction/Background Allopurinol-induced drug reactions are related to a hypersensitivity syndrome characterized by fever, skin rash and multiple organ involvement. Pulmonary manifestations of allopurinol hypersensitivity syndrome (AHS) are not often described in previous studies, however a 2019 literature review reported symptoms of cough and dyspnea were present in 72% of patients at the time of presentation.[1] Almost half of the cases in this 2019 study were initially treated with empiric antibiotics for suspected pneumonia prior to reaching the correct diagnosis. AHS associated mortality has been reported as high as 18-32% and its long latency period can present a challenge to timely diagnosis and treatment.[2]

Case Presentation We present a case of an 81-year-old man who presented to the emergency department with chief complaints of shortness of breath and headache for several days. He has a past medical history of hypertension and chronic kidney disease on diuretic therapy. He was found to be hypoxemic in the emergency department and started on high-flow oxygen. The patient was otherwise hemodynamically stable. He was admitted and treated with empiric antibiotics for suspected pneumonia based on interstitial infiltrates on radiography. Upon admission he noticed a diffuse maculopapular rash involving his face, trunk and extremities (Fig. 1). Serial examinations revealed worsening rash and oral mucosal ulceration. While liver function tests were initially normal, subsequent labs showed elevated transaminases, alkaline phosphatase, and hyperbilirubinemia. Labs were negative for eosinophilia, abdominal ultrasound found no biliary dilation, and viral/autoimmune hepatitis panel was negative. Further questioning elicited that the patient had started allopurinol 100 mg daily for gout 4 weeks prior to onset of the rash, although it was not listed on his medication reconciliation upon admission. Treatment was started for suspected allopurinol drug reaction with intravenous steroids and a calcineurin inhibitor. Although his dyspnea, hypoxemia, rash, and liver function studies had improved after treatment, the patient developed oliguric acute renal failure requiring hemodialysis. Patient was discharged in stable condition but without recovery of renal function.

Discussion Based on the temporal relation between drug initiation and clinical symptoms, allopurinol was implicated as the cause for this patient's respiratory distress, morbilliform rash, and multi-organ dysfunction. The case met all three major criteria for AHS, including rash, renal failure, and liver dysfunction. His risk factors were older age, concomitant diuretic use, and chronic kidney disease. The patient's initial presentation with dyspnea and cough is significant because they have been reported as common presenting symptoms and are not included in the diagnostic criteria. Pulmonary symptoms in AHS are often accompanied by imaging findings of pleural effusion and interstitial infiltrates, both of which were present in our case. Taweesedt et al. suggest that pulmonary involvement in AHS is often present on admission and initially misdiagnosed as pneumonia, only to be followed later by the more classic AHS presentation meeting diagnostic criteria.(1) Increased recognition that AHS may present with pulmonary symptoms may improve time to diagnosis and overall outcomes.

REFERENCE(S)
1. Taweesedt PT et al. Pulmonary Manifestations of Drug Reaction with Eosinophilia and Systemic Symptoms (DRESS) Syndrome: A Systematic Review. Biomed Res Int. 2019 Sep 24;2019:7863815.
2. Kim, S.C., et al.; (2013), Severe Cutaneous Reactions Requiring Hospitalization in Allopurinol Initiators: A Population-Based Cohort Study. Arthritis Care Res, 65: 578-584.
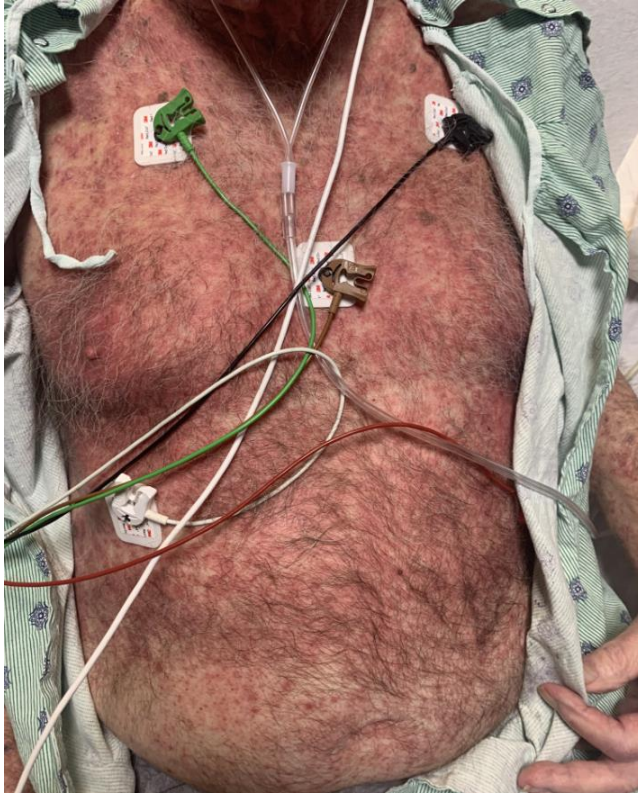
Abstract 31 Figure 1: Morbilliform Rash Attributed to Allopurinol Hypersensitivity Reaction. Photo taken on hospital day 3. The rash also involved the patient's back and all four extremities.

Educational / Outcome Research

32

THE RELATIONSHIP OF THE EARLY EDUCATION OF THE DANGERS OF VAPING/E-CIGARETTE USES IN TEENS.

Rukmini Surnedi.

Introduction/Background As most likely known, vape use is extremely popular in the United States. Many most likely know how much of a problem vaping is as well. As of December 2018, youth e-cigarette use was declared a national epidemic by the United States Surgeon General. The Food and Drug Administration(FDA) wrote as of December 12, 2022, one in six high school students uses a vape, and one in twenty-five middle school students vape. For me, learning this information was quite confusing. In the society I live in, teen vaping/e-cigarette use was normalized. Causing students like me to think that vaping/e-cigarette use was no big deal. The American Academy of Pediatrics(AAP) stated that more than 2,500 kids alone are hospitalized due to e-cigarette or vaping-related lung injuries.
Objective(s) The objective of this project is whether educating children about vaping/e-cigarette use would help prevent them from using a vape/e-cigarette later down the line.
Methods This study was designed as an anonymous survey approved by the Institutional Review Board. The survey was posted around the Veterans Memorial High School campus. Students could optionally fill out the survey, keeping it completely random and anonymous as well. To complete the survey, students would have to fill out the following questions, do you vape or use e-cigarettes, why or how did you start vaping/using an e-cigarette, what grade did you start vaping/using an e-cigarette, were you ever told about the health risks of vaping/using an e-cigarette before you started, and if you were told about vaping/using an e-cigarette and the health risks, would you have started at all? The data was then analyzed after the survey was up for four continuous days.
Results Around sixty-seven percent of students would still use vape/e-cigarettes whether they were educated about vaping/e-cigarettes use beforehand. While around thirty-three percent of students said they would not know if they would use vape/e-cigarettes or not without prior knowledge of the dangers of vaping/e-cigarettes uses.
Conclusion The data shows that in this experiment the prior knowledge of the health risks and dangers of vaping would have no effect on whether or not a student starts vaping later in life. This contradicts my hypothesis that telling students about vaping would help prevent students from vaping in the future. It is also contradict a larger and more reliable experiment done by the CDC. Based on the data further investigations between the correlation of vaping and prior knowledge of the dangers of vaping needs to occur.

33

HIGH FAT DIETS WITH CHOLESTEROL AND FRUCTOSE HAVE A DIFFERENTIAL IMPACT IN NASH AND ADIPOSITY IN MICE WITH PRE-ESTABLISHED DIET-INDUCED OBESITY.

Jose Cordoba-Chacon, Samuel Lee, Jose Muratalla, Marta Sierra-Cruz. *University of Illinois at Chicago*

Introduction/Background Non-alcoholic fatty liver disease (NAFLD) is characterized by excess storage of fat in hepatocytes. NAFLD has a prevalence over 30% in the US that increases to 70% in overweight/obese individuals. About 25% of patients with NAFLD progress to non-alcoholic steatohepatitis (NASH), a condition that may lead to fibrosis, cirrhosis, hepatocellular carcinoma, cardiovascular disease, and increase risk of mortality. NAFLD/NASH is associated with obesity and increased expression of hepatic peroxisome proliferator-activated receptor gamma (PPARg) in mice and humans.

Objective(s) In mice, it is challenging to induce human-like NASH and obesity with formulated diets. In this study, we assessed the effect of two different NASH-inducing high-fat diets supplemented with cholesterol and fructose in mice with pre-established high-fat diet (HFD)-induced obesity. To test the effect of these diets, PPARg was knocked out in hepatocytes (Pparg-HepKO) of male mice with pre-established HFD (60% Kcal from fat, 16 weeks)-induced obesity, or in male and female chow-fed mice.

Methods A group of control and Pparg-HepKO diet-induced obese mice was either maintained on the HFD or switched to NASH inducing diets for an additional 8 weeks. Specifically, a cohort of diet-induced obese mice was fed a high fat (40% Kcal fat, partially hydrogenated corn oil), cholesterol (2%) and fructose (22%, in pellets) (HFCF) diet, whereas a second cohort of diet-induced obese mice was fed a high fat (60% Kcal from fat, lard) and cholesterol (2%) diet with fructose (10%, in drinking water) (HFC+Fr). In addition, we also assessed if HFC+Fr diet feeding for 24 weeks promotes obesity and NASH in a different cohort of control and Pparg-HepKO adult male and female chow-fed mice.

Results Our results show that hepatic PPARg expression was increased in diet-induced obese mice and, independent of diet, was reduced in Pparg-HepKO mice. In the first set of studies, HFD induced both obesity and liver steatosis. Interestingly, the HFCF diet reduced adipose tissue weight, and prevented body weight increase in diet-induced obese mice whereas adiposity and body weight were maintained in HFC+Fr-fed obese mice. However, both HFCF and HFC+Fr diets increased liver weight and promoted histological features of NASH. Pparg-HepKO did not alter adiposity but it reduced steatosis in HFD-fed mice. Furthermore, Pparg-HepKO reduced NASH progression without reducing steatosis in HFC+Fr-fed mice. This positive effect of Pparg-HepKO was associated with reduced expression of the hepatic fibrotic markers and the collagen-stained fibrotic area in liver sections. In the second set of studies, we show that HFC+Fr diet for 24 weeks increased obesity and insulin resistance in both male and female mice. HFC+Fr diet increased liver weight and steatosis in male and female mice. Pparg-HepKO reduced liver triglycerides in male and female mice, the expression of hepatic fibrotic markers, as well as the collagen-stained fibrotic area in male mice.

Conclusion Overall, the dietary composition of NASH-inducing diets influences adiposity in mice fed these diets and can regulate the negative effect of hepatocyte PPARg in the development of liver fibrosis under conditions of NASH.

34

THE IMPACT OF PARENT-OF-ORIGIN ON CHILDHOOD GROWTH TRAJECTORIES AND SULFONYLUREAS USE IN CHILDREN WITH HNF1A-MODY IN THE U.S. MONOGENIC DIABETES REGISTRY.

[1]Maria Salguero Bermonth, [2]Louis Philipson, [2]Rochelle Naylor. [1]*University of Chicago Hospitals;* [2]*University of Chicago*

Introduction/Background MODY (autosomal dominant diabetes) accounts for ~3% of pediatric diabetes.[1,2] Precision therapy for HNF1A-MODY is sulfonylureas (SU).[3] There are gaps in understanding the impact of in-utero maternal hyperglycemia on childhood weight and SU efficacy.[4]

Objective(s) Assess the impact of parent-of-origin on childhood growth trajectories and SU use in pediatric HNF1A-MODY in the U.S. Monogenic Diabetes Registry.

Methods Cross-sectional analysis of Registry data on 23 pediatric participants with HNF1A-MODY. We compared BMI percentiles at birth, diabetes diagnosis, and most recent Registry survey as well as rates of precision therapy using non-parametric methods.

Results There were 7 males (30%), 16 females (70%). 12 inherited HNF1A-MODY maternally (MAT), 10 paternally (PAT). One mutation was spontaneous. Birth weight percentile was 72 MAT vs 56 PAT, p=0.16. BMI percentile at diabetes diagnosis was 76 MAT vs 64 PAT, p=0.20. Most recent BMI percentile was 84 MAT vs 66 PAT, p=0.44). 33% of MAT participants vs 44% of PAT participants had ever taken SU. On most recent Registry survey, 33% of MAT participants were taking SU compared to 60% of PAT. Specific data for SU failure was absent in most participants. One male patient with maternally-inherited HNF1A-MODY and weight and BMI percentiles >99th, failed treatment after 1 year.

Conclusion There was higher weight/BMI percentiles in MAT group compared to PAT, but this did not reach statistical significance. We note a trend toward less SU use in MAT group. Conclusions cannot be drawn based on small numbers and limitations of missing data. Future studies will collect detailed information to test the hypothesis that negative fetal programming from in utero maternal hyperglycemia decreases SU efficacy of in pediatric HNF1A-MODY.

REFERENCE(S)

1. Shepherd M, Shields B, Hammersley S, Hudson M, McDonald TJ, Colclough K, Oram RA, Knight B, Hyde C, Cox J, Mallam K, Moudiotis C, Smith R, Fraser B, Robertson S, Greene S, Ellard S, Pearson ER, Hattersley AT. Systematic Population Screening, Using Biomarkers and Genetic Testing, Identifies 2.5% of the U.K. Pediatric Diabetes Population With Monogenic Diabetes. Diabetes Care. 2016;39(11):1879-88. Epub 20160606. doi: 10.2337/dc16-0645. PubMed PMID: 27271189; PMCID: PMC5018394.

2. Shields BM, Hicks S, Shepherd MH, Colclough K, Hattersley AT, Ellard S. Maturity-onset diabetes of the young (MODY): how many cases are we missing? Diabetologia. 2010;53(12):2504-8. Epub 20100525. doi: 10.1007/s00125-010-1799-4. PubMed PMID: 20499044.

3. Hattersley AT, Patel KA Precision diabetes: learning from monogenic diabetes. Diabetologia 2017;60(5):769-77.4. Bianco ME, Josefson JL. Hyperglycemia During Pregnancy and Long-Term Offspring Outcomes. Curr Diab Rep. 2019 Nov 21;19(12):143. doi: 10.1007/s11892-019-1267-6. PMID: 31754898; PMCID: PMC7008468.

GLUCOSE AVAILABILITY CONTROLS PROTEIN STABILITY OF HEXOKINASE DOMAIN CONTAINING 1 (HKDC1)

Md. Wasim Khan. *University of Illinois at Chicago*

Introduction/Background Glucose is essential for various metabolic pathways, acting as a nutrient and a signaling molecule. Its dysregulated metabolism leads to metabolic disorders like hyperglycemia, type II diabetes, and obesity. Metabolic disorders are prevalent in 90-95% of adults worldwide, and hyperglycemia is an independent risk factor for cardiovascular disease, contributing significantly to morbidity and mortality. Hexokinases catalyze the first committed step of glucose metabolism. The novel hexokinase, hexokinase domain containing 1 (HKDC1), is dramatically overexpressed in the liver in conditions like type II diabetes mellitus (T2D), non-alcoholic steatohepatitis (NASH), non-alcoholic fatty liver disease (NAFLD), and most recently hepatocellular carcinoma (HCC) where HKDC1 plays a role in modulating glucose metabolism and/or flux. However, the mechanism by which HKDC1 expression is regulated in these pathological conditions remains unknown.

Objective(s) Our aim is to reveal the specific elements underlying HKDC1 regulation is significant as it could lead to ways to control its expression in pathological conditions where it is overexpressed and therefore bring forward novel treatment avenues.

Methods We used both in vivo and in vitro models to study the effect of glucose levels on HKDC1 protein and mRNA expression.

Results Our novel data indicate that glucose levels in hepatocyte cell lines directly control HKDC1 protein stability. Our discovery that HKDC1 protein stability is linked to glucose availability provides a unique, innovative mechanism for HKDC1 regulation in HCC.

Conclusion Our data shows that while high glucose levels enhance the mRNA expression of HKDC1 in a mouse model of hyperglycemia, short-term deprivation of glucose led to enhanced protein degradation of HKDC1 via the proteasomal pathway.
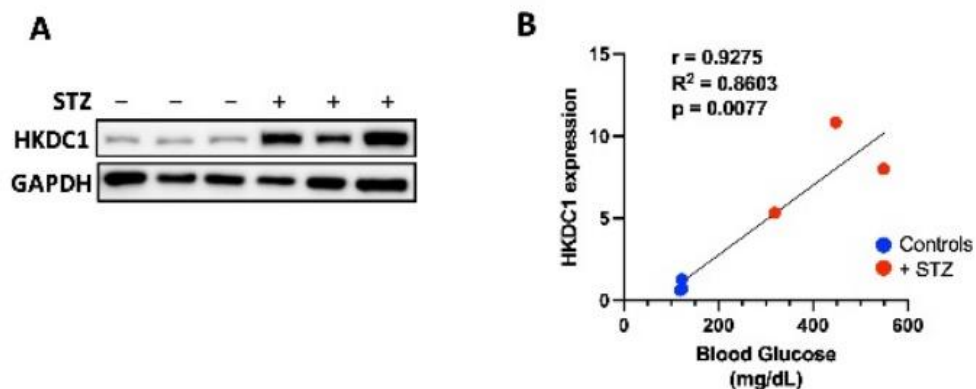
Fig 1. HKDC1 expression correlates with blood glucose levels.
6 weeks old male C57Bl6/J mice (n=3) were injected 50mg/kg STZ (streptozotocin) intra-peritoneally. Mice were monitored for 8 weeks, after which they were sacrificed. The liver was harvested, and HKDC1 protein (A) and mRNA (B) were assessed by immunoblot and qPCR, respectively. Values are Mean ± SD; * p<0.05.
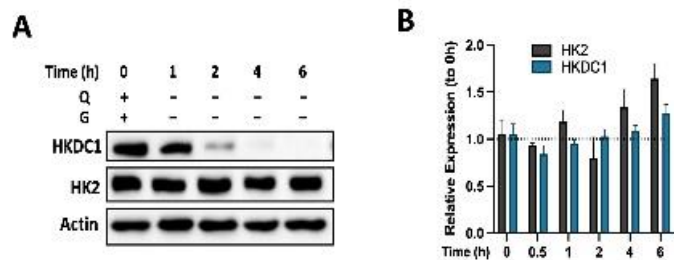
Fig 2. HKDC1 is degraded in the absence of glucose.

HepG2 cells growing in 5.5 mM glucose were starved of glucose (G) in the presence of glutamine (Q) for the indicated periods, followed by immunoblot (representative of 3 blots) or qPCR (n=5); to assess changes in protein **(A)** and mRNA **(B)** levels of HKDC1.

Fig 3. Glucose deprivation decreases HKDC1 protein half-life.

A) HepG2 cells growing in 5.5 mM glucose were treated with 50ug/ml cycloheximide (CHX) in the presence or absence of glucose for the indicated periods, followed by immunoblot to assess change in HKDC1 protein levels. **B)** Half-life of HKDC1 calculated from A. Values are Mean ± SD.
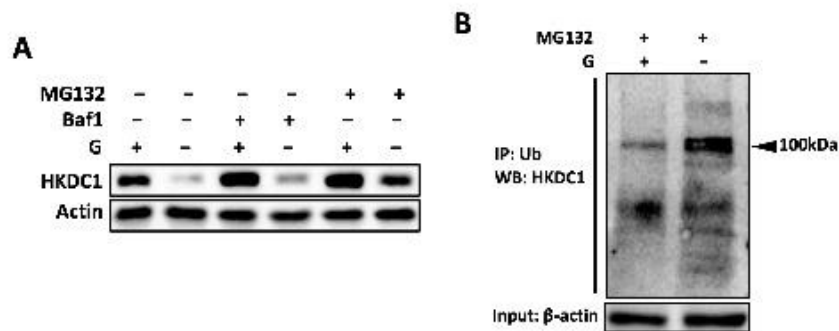
Fig 4. HKDC1 is degraded by the proteasome pathway in the absence of glucose.

A. HepG2 cells were starved of glucose (G) for 4h in the presence or absence of autophagy inhibitor Bafilomycin A1 (BafA1) or proteasomal inhibitor MG132 followed by immunoblot to assess change in HKDC1 protein levels. **B)** HepG2 cells growing in 5.5 mM glucose were starved of glucose (G) for 4h in the presence or absence of proteasomal inhibitor MG132, followed by immunoprecipitation of ubiquitin and immunoblot of HKDC1.
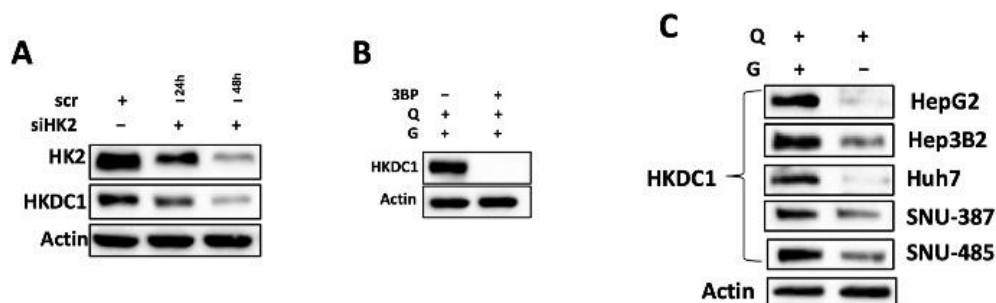
Fig 5. Glucose metabolism is required for HKDC1 protein stability.

A) siRNAs against HK2 for 24-48h in the presence of glucose. Immunoblot was done to assess change in HK2 and HKDC1 protein. **B)** HepG2 cells were treated with 100 µM 3-BP for 2 hrs. **C)** HCC (HepG2, Hep3B2, Huh7, SNU-387, SNU-485) cell lines growing in 5.5mM glucose were starved of glucose (G) for 4 h, followed by immunoblot to assess change in HKDC1 protein levels.

36

CHARACTERIZING CLINICAL CHARACTERISTICS OF 6Q24-RELATED TRANSIENT NEONATAL DIABETES

Michael McCullough, Lisa Letourneau-Freiberg, Tiana Bowden, Balamurugan Kandasamy, Daniela Del Gaudio, Kristen Wroblewski, Louis Philipson, Siri Greeley. *University of Chicago*

Introduction/Background Transient neonatal diabetes mellitus (TNDM) is a heterogeneous subtype of neonatal diabetes that usually presents within the first days or weeks of life, spontaneously remits in infancy, but can recur in childhood or adolescence as a permanent form of diabetes. Approximately 70% of TNDM cases are due to overexpression of genes at chromosome 6q24 caused by one of three potential mechanisms: uniparental disomy (UPD6), paternal duplication, or hypomethylation of the maternal allele.

Objective(s) Our aim was to further elucidate clinical characteristics of a relatively large group of individuals with this rare condition.

Methods Participants with a confirmed or suspected diagnosis of 6q24 TNDM were identified through the University of Chicago Monogenic Diabetes Registry. Research based genetic testing was provided. Clinical information was extracted from survey responses and medical records.

Results There were 33 participants with 6q24-TNDM (58% male). Eight (24%) had hypomethylation of the maternal allele, seven (21%) had paternal duplication, seventeen (52%) had UPD6, and one had UPD6 vs. hypomethylation of the maternal allele. The mean age of initial diabetes presentation was 4.6 days (n=33). Remission occurred at a mean age of 4.5 months (n=28). Nine participants reported having relapse of diabetes, with a mean age of relapse of 17.4 years (range 12 - 31 years). There were six participants who reported umbilical hernia (22%, n=27), fifteen participants reported macroglossia (54%, n=27), and ten (36%, n=28) indicated speech therapy was required. No significant differences in clinical characteristics were identified across the three mechanisms (UPD6, paternal duplication, hypomethylation).

Conclusion Clinical characteristics were not different across mechanism groups, suggesting that genetic testing is required to definitively determine a mechanism and diagnosis of 6q24 TNDM. Early assessment for speech therapy should be considered for this patient population.

37

FGF21 HAS A SEX-SPECIFIC ROLE IN CALORIE-RESTRICTION-INDUCED BEIGING OF WHITE ADIPOSE TISSUE IN MICE

[1]Mariah Calubag, [1]Ismail Ademi, [1]Chung-Yang Yeh, [1]Reji Babygirijia, [2]Heidi Pak, [1]Alyssa Bhoopat, [1]Ildiko Kasza, [1]Cara Green, [1]Michelle Sonsalla, [2]Dudley Lamming. [2]*University of Wisconsin-Madison;* [2]*University of Texas Southwestern*

Introduction/Background Calorie restriction (CR), defined as a dietary regimen in which calories are reduced without malnutrition, promotes healthspan and increases lifespan in diverse organisms ranging from yeast to mice and non-human primates. Despite almost a century of effort, the physiological and molecular mechanisms by which CR functions are still not totally understood, stymieing efforts to develop CR mimetics which could promote health in the rapidly aging global populace. As CR works to slow aging in all tissues, it has been suggested that CR may work in part through endocrine factors. Some studies have demonstrated that CR induces, to different extents, fibroblast growth factor 21 (FGF21), a hormone that regulates energy balance and that when overexpressed, promotes metabolic health and longevity in mice. However, the role of FGF21 in the response to CR has not been fully investigated.

Objective(s) We directly examined the role of FGF21 in the physiological and metabolic response to a CR diet in male and female mice as well as assessed its role in white adipose tissue adaptations to this diet.

Methods We fed 10-week-old Fgf21-/- and wild-type control mice either an ad libitum (AL) diet or a 30% CR diet for 15 weeks. Starting at 8 weeks, metabolic phenotyping through the assessment of glucose homeostasis and energy regulation was performed prior to sacrifice and tissue collection.

Results We find that FGF21 is largely dispensable for CR-induced improvements in body composition and energy balance, but that lack of Fgf21 blunts CR-induced changes aspects of glucose regulation and insulin sensitivity in females. Surprisingly, despite not affecting CR-induced changes in energy expenditure, loss of Fgf21 significantly blunts CR-induced beiging of white adipose tissue in male but not female mice.

Conclusion Our results shed new light on the molecular mechanisms involved in the beneficial effects of a CR diet, clarify that FGF21 is largely dispensable for the metabolic effects of a CR diet, and highlight a sex-dependent role for FGF21 in the molecular adaptation of white adipose tissue to CR.

Figure 8

A
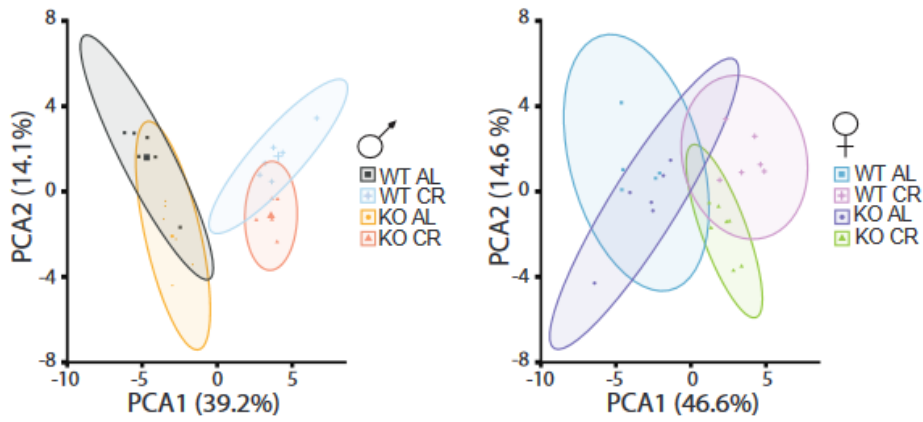
B
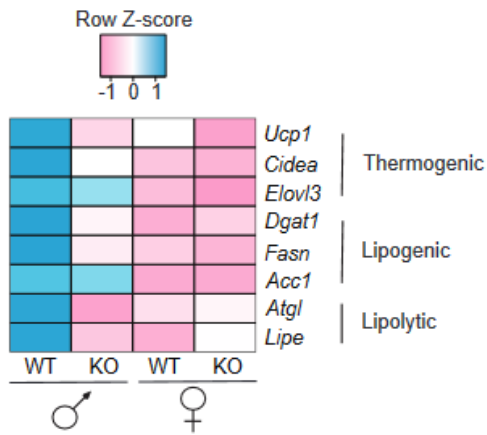
Figure 8: Loss of *Fgf21* does not largely affect the overall phenotypic response to CR, but blunts the induction of iWAT genes in a sex-specific manner.

(A) Phenotypic measurements of individual mice visualized by genotype and diet groups and split by sex indicating separation along PC1 and PC2; 95% confidence ellipses are indicated. (B) Log$_2$ fold changes in gene expression induced by CR in the iWAT of each genotype and sex of mice were z-scaled normalized.

Abstract 37 Figure 1

38

EVALUATION OF URINARY TRACT INFECTIONS IN MALES WITH LOWER URINARY TRACT SYMPTOMS AND CONCOMITANT SGLT2 INHIBITOR USE

Austin Reed, Suhaib Bajwa, Tun Tun Aung, Ishani Shah, Waqar Salam. *University of Missouri-Columbia*

Introduction/Background Excluding dapagliflozin, a meta-analysis in 2017 looking at outcomes for patients on SGLT2 inhibitors (SGLT2i) found no significant difference in UTI rates when compared to placebo [1]. The meta-analysis did not further stratify these patients based on history of benign prostatic hypertrophy (BPH) which is a risk factor for UTIs.

Objective(s) Our aim was to determine if patients who had lower urinary tract symptoms (LUTS) from BPH to the point where they required medication management, would be at higher risk or at risk in general of urinary tract infections when placed on an SGLT2i. It's theorized that the stasis of bladder outlet obstruction could predispose patients to more frequent UTIs. Now is this risk compounded by being on an SGLT2i needed further analysis.

Methods We conducted a retrospective cohort study of male patients ≥ 49 years old from 2017-present with treatment by SGLT2 inhibitors for at least 6 months and/or diagnosis of clinically significant BPH. Clinically significant BPH was defined as individuals requiring therapy with alpha blockers and/or 5alpha-reductase inhibitors. Patients were grouped into being treated with SGLT inhibitors only, BPH medications only, or being on treated with both SGLT inhibitors and BPH medications. Patients with a history of ureteral, bladder, prostate or urethral surgery were excluded. Primary outcomes were frequency of UTIs, and sepsis secondary to a urinary source. Secondary outcomes were hospitalization, length of stay, rate of antibiotic failure, Fornier's gangrene, and death. Multivariate logistic analysis was used to control for patient characteristics to assess for the independent association between simultaneous treatment with SGLT2i and BPH medications simultaneously and UTIs.

Results 237 patients were identified with 176 being treated with SGLT2 inhibitors only, and 61 on both SGLT2 inhibitors and BPH medications. The BPH only group had 8 patients and as such was excluded from the analysis. The average age was 69.77 for SGLT inhibitors only vs 64.02 for SGLT2 + BPH (p-value < 0.001).The average BMI was 34.89 vs 33.61 (p-value=0.27). Primary outcomes included no instances of sepsis secondary to UTI. For frequency of UTIs, 11 individuals in the SGLT2 + BPH groups and 5 individuals in the SGLT2 were identified (p-value < 0.001). Multivariate analysis demonstrated that being on SGLT2 and BPH medications simultaneously was independently associated with UTIs as compared to being on SGLT2 medications alone (95% confidence interval) 4.59 (1.48 - 15.53, p value = 0.008). For secondary outcomes, no instances of hospitalization, antibiotic failure, Fornier's gangrene, or death were identified.

Abstract 38 Table 1 Baseline Demographic Data and Rates of UTIs

Characteristic	Total	SGLT2+BPH	SGLT2 only
N	237	61	176
Age (years)	65.50 ± 8.32	69.77 ± 8.62	64.402 ± 7.771
BMI	33.94 ± 7.81	34.89 ± 8.36	33.61 ± 7.61
Race			
Whites	212 (89.45%)	52 (85.25%)	160 (90.91%)
Non-Whites	25 (10.55%)	9 (14.75%)	16 (9.09%)
Insurance Type			
Private	119 (50.21%)	26 (42.62%)	93 (52.84%)
Medicare	86 (36.29%)	25 (40.98%)	61 (34.66%)
Unknown	32 (13.50%)	10 (16.39%)	22 (12.50%)
Indications for SGLT2			
DM	187 (78.90%)	49 (80.33%)	138 (78.41%)
HF	25 (10.55%)	2 (3.28%)	23 (13.07%)
Both	25 (10.55%)	10 (16.39%)	15 (8.52%)
SGLT2 Inhibitors			
Canagliflozin	17 (7.17%)	6 (9.84%)	11 (6.25%)
Dapagliflozin	64 (27%)	14 (22.95%)	50 (28.41%)
Empagliflozin	156 (65.82%)	41 (67.21%)	115 (65.34%)
UTI Occurrence	16 (6.75%)	11 (18.03%)	5 (2.84%)
1 episode	10 (65.2%)	6 (54.55%)	4 (80%)
2 episodes	5 (31.25%)	4 (36.36%)	1 (20%)
4 episodes	1 (6.25%)	1 (9.09%)	0 (0%)

Conclusion Our study reveals novel findings showing that being treated with SGLT2 inhibitors in the context of clinically significant BPH (pharmacotherapy with alpha blockers and/or 5 alpha reductase inhibitors) appears to be an independent risk factor for developing UTIs as compared to being treated with SGLT2 inhibitors alone when controlling for patient demographics. Recognition that patients on BPH medications are possibly at increased risk for UTIs if placed on SGLT2 inhibitors could further help risk stratify patient selection for placement on SGLT2 inhibitors. Of note, outcomes could not be compared to patients on BPH medications alone due to the small sample size. Further larger retrospective cohort studies or prospective studies are needed to evaluate these relationships.

REFERENCE(S)

1. Liu J, Li L, Li S, Jia P, Deng K, Chen W, Sun X. Effects of SGLT2 inhibitors on UTIs and genital infections in type 2 diabetes mellitus: a systematic review and meta-analysis. Sci Rep. 2017 Jun 6;7(1):2824. doi: 10.1038/s41598-017-02733-w. PMID: 28588220; PMCID: PMC5460243.

39

NOVEL MUTATIONS IN GLIS3/TRMT10A AS A CAUSE OF CONGENITAL HYPERINSULINISM

Mansa Krishnamurthy, Lily Deng, Holly McGarvey. *Cincinnati Children's Hospital Medical Center*

Introduction/Background Congenital hyperinsulinism (CHI) is a heterogeneous group of disorders characterized by hypoglycemia and inappropriate insulin secretion. Prompt identification of CHI and its genetic causes are essential to minimize the risk of permanent neurological damage as well as guide treatment options for these patients. Although, there are 15 known monogenic forms of CHI, there remain 50% of patients without an identified genetic diagnosis, suggesting that there are genetic loci that remain yet to be discovered.
Objective(s) We describe a 4 month old male presenting with new-onset seizures due to hypoglycemia. Lab evaluation was consistent with hyperinsulinism and a trial of diazoxide was pursued. He developed severe thrombocytopenia and was switched to octreotide and continuous feeds. A 98% pancreatectomy was performed and the resected pancreas was consistent with diffuse CHI.
Methods Targeted genetic evaluation was negative and whole exome sequencing of the patient and parents revealed a novel heterozygous mutation in GLIS3 (c.835G>A, p.Glu279Lys) and an extra copy of TRMT10a (entire coding sequence). Using the resected pancreas, we performed deep histological characterization to better understand changes in islet architecture and alterations in transcription factor expression profiles when compared to age matched islet controls.
Results We observed a significant increase in insulin positive cells, along with an increase in polyhormonal cells expressing insulin/glucagon and insulin/somatostatin. Moreover, there was a reduction in pancreatic polypeptide expressing cells. Interestingly, we also observed an increase in ductal marker CK19 expression throughout all regions of the pancreas and increased co-expression of CK19 with single insulin positive cells consistent with nesidioblastosis. Proliferative index through Ki67 labelling was much higher in beta cells of the resected pancreas when compared to age matched controls. Finally, we observed a statistically significant increase in key beta cell transcription factors including FOXA2, PDX1 and NKX6.1.
Conclusion For the first time, we demonstrate the connection between GLIS3/TRMT10a and CHI, expanding the list of known genetic causes. This case highlights the utility of whole exome sequencing in further identifying novel genetic causes for CHI and the benefits of deep histological characterization to better understand changes in islet architecture and gene expression.

40

ARYL HYDROCARBON RECEPTOR ACTIVATION PROTECTS AGAINST PREGNANCY INDUCED INSULIN RESISTANCE

Medha Priyadarshini, Husena Electricwala, Bader Abdel-Hadi, Brian Layden. *University of Illionois at Chicago*

Introduction/Background Increase in insulin resistance, during later stages of pregnancy is a physiologic adaptation, that returns to normal in the postpartum period. Exact mechanisms underlying the regulation of pregnancy insulin resistance are not clearly defined. We recently identified that precursors of insulin resistance during pregnancy may originate in the gut microbiota. We observed marked decline in gut microbially generated indole metabolites in feces and modest gut inflammation in pregnant mice at gestation day 15, G15, (phenotypically analogous to insulin resistant phase of human pregnancy). Of note, gut microbial indole derivatives serve as ligands for aryl hydrocarbon receptor (AHR), and their impaired production is a key factor in development of metabolic disorders.
Objective(s) Based on these data we hypothesized that restoration of these derivatives will impact insulin resistance during pregnancy.
Methods 10-11-week-old C57BL/6J female mice were fed a diet either supplemented with 200ppm of phytochemical indole-3-carbinol (I3C) or devoid of I3C (control, AIN-76A) prior to mating and throughout the course of pregnancy. Metabolic outcomes (glucose tolerance and insulin resistance by tolerance tests), and intestinal inflammation and AHR induction (by qPCR) were analyzed at G0 and G15. Data was analyzed by two-way ANOVA or t-test.
Results I3C supplementation during pregnancy lead to improved glucose tolerance and reduced insulin resistance as compared to control diet. Pregnancy induced modest inflammation in the gut was noted as increased mRNA levels of proinflammatory cytokines (Tnfa, Ifng, Lcn2) in the ileum of control diet fed mice at G15. I3C diet attenuated this increase in pro-inflammatory cytokine mRNA expression. Inflammation driven increase in mRNA expression of indoleamine 2,3-dixoygenase 1 (Ido1) in the ileum at G15 compared to G0 was observed in control diet fed mice. I3C supplementation prevented such an increase in Ido1 mRNA levels. As expected, significant AHR induction (analyzed as induction of its target genes Cyp1a1 and Cyp1b1) was observed in the intestine of I3C fed mice.
Conclusion Our results indicate that restoration of indole metabolites during pregnancy prevents insulin resistance associated with pregnancy. These changes appear to be due to activation of AHR in the intestine. Mechanistic evaluation of the beneficial effects of indoles and intestinal AHR activation is underway. (Support: DRTC P&F grant-MP).

REFERENCE(S)
1.   Barbour LA, McCurdy CE, Hernandez TL, et al. Cellular mechanisms for insulin resistance in normal pregnancy and gestational diabetes. Diabetes Care 2007;30 Suppl 2:S112-9.Priyadarshini M, Navarro G, Reiman DJ, et al. Gestational Insulin Resistance Is Mediated by the Gut Microbiome-Indoleamine 2,3-Dioxygenase Axis. Gastroenterology 2022;162:1675-1689 e11.
2.   Natividad JM, Agus A, Planchais J, et al. Impaired Aryl Hydrocarbon Receptor Ligand Production by the Gut Microbiota Is a Key Factor in Metabolic Syndrome. Cell Metab 2018;28:737-749 e4.

41

BIOLOGICAL SEX AND GENETIC BACKGROUND DETERMINE THE METABOLIC OUTCOMES OF DIETARY ISOLEUCINE RESTRICTION

Michaela Trautman, Cara Green, Reji Babygirija, Esther Zelenovskiy, Madelyn Green, Chung-Yang Yeh, Michelle Sonsalla, Mariah Calubag, Dudley Lamming. *University of Wisconsin Madison*

Introduction/Background While calorie restriction (CR) is the gold standard for prolonging mammalian health and lifespan, adhering to CR diets is difficult for humans. Protein restriction (PR) replicates some of the theorized CR mechanisms and promotes health and longevity in mice; lower consumption of dietary protein is also associated with positive outcomes in humans. We have found that the key mediators of these benefits are the three branched-chain amino acids (BCAAs), leucine, isoleucine (ile), and valine. Restriction of all three BCAAs promotes metabolic health, fitness, and lifespan in C57BL/6J male mice, and we recently discovered that restriction of ile is necessary and sufficient for the effects of a PR diet in mice.

Objective(s) Here, we investigate the long-term metabolic impact of different levels (low, control, excess) of dietary ile on the response of both sexes of two different inbred strains of mice in the context of a high-fat, high sucrose diet.

Methods We measured body composition at regular intervals with EchoMRI and assessed glucose homeostasis with intraperitoneal glucose and insulin tolerance tests. HOMA-IR was calculated by measuring fasting blood sugar via glucometer and fasting insulin via Crystal Chem mouse insulin ELISA kit. Gas exchange was measured in metabolic chambers to assess effects on metabolism. All metabolic phenotypes were compared via principal component analysis and hepatic samples were utilized for transcriptomic analysis.

Results Global improvements were observed in body composition and reduced fat mass in the low ile-fed groups despite increased food consumption. Intriguingly, only C57BL/6J males gained significantly more fat mass in the excess ile diet group. Glucose tolerance and HOMA2-IR were improved in the low ile groups, but DBA/2J females failed to reach statistical significance. PCA plots reveal dramatic similarities in the low ile diet groups, which are distinct from the excess and control ile diet groups in males. In females, there are discrete similarities in the excess and control ile groups, but with less overlap between the low ile diet groups. This indicates that the overall metabolic phenotype in the excess and control ile group is not very different, which is supported by hepatic transcriptomic analysis. Differences in the PCA plots of the low ile group also are supported by transcriptomics, which reveal unique signatures both between males and females and also between strains.

Conclusion Together, this data indicates that dietary ile restriction results in both shared and unique metabolic effects. Excess ile surprisingly does not appear to be additionally detrimental. Future directions include further analysis the hepatic landscape via lipidomics and correlation of all 3 -omics studies. Additionally, we will examine control versus low ile diets in genetically heterogenous BXD strains for QTL mapping. Overall, these results demonstrate that biological sex and genetic background should be considered when evaluating the efficacy, translatability, and clinical application of dietary interventions.

Abstract 41 Table 1

	Control AA	WD Low Ile	WD AA	WD High Ile
Protein (% kcal)	22.0	19.0	20.7	19.0
CHO (% kcal)	59.4	39.3	38.5	39.1
Fat (% kcal)	18.6	41.7	40.9	41.9
Ile (g/kg)	7.8	2.54 (1/3x)	7.8 (1x)	23.4 (3x)
kcal/g	3.9	4.5	4.6	4.5

Table 1. Macronutrient distribution and calorie density of the experimental diets.
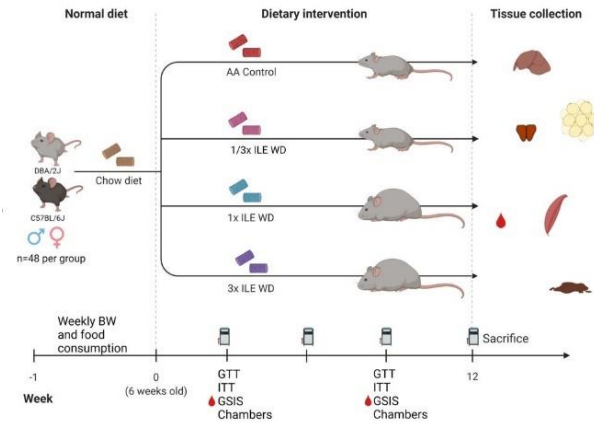
Abstract 41 Figure 1. Experimental design.
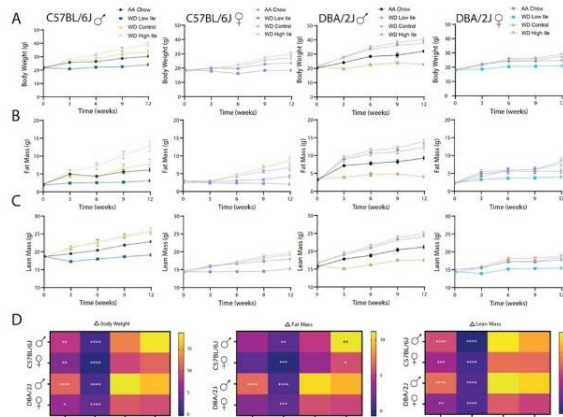
Abstract 41 Figure 2. Body composition over time and change from the beginning to end of the study.
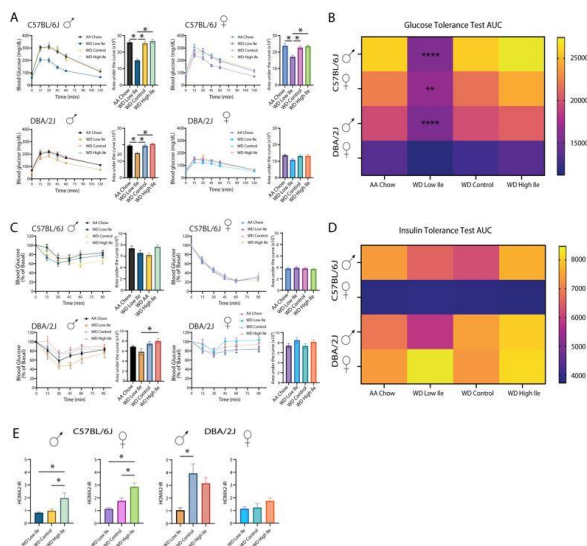
Abstract 41 Figure 3. Glucose homeostasis is improved by a low isoleucine diet.
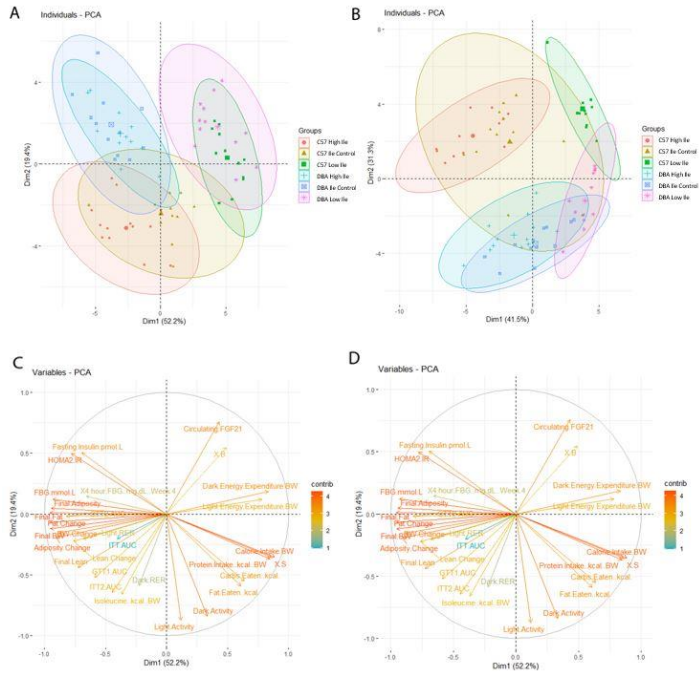
Abstract 41 Figure 4 PCA plots reveal unique changes by low ile diets.
A) Glucose tolerance tests and corresponding AUC (B).
C) Insulin tolerance tests and corresponding AUC (D).
E) HOMA2-IR.

42

LIPOLYSIS AS A REGULATORY FOCUS IN GEROPROTECTIVE DIETARY INTERVENTIONS

[1]Chung-Yang Yeh, [1]Lucas CS Chini, [1]Isaac Freichels, [1]Lexi Borgelt, [1]Mariah Calubag, [1]Cara Green, [1]Reji Babygirija, [1]Michelle Sonsalla, [2]Heidi Pak, [1]Michaela Trautman, [1]Dudley Lamming. *[1]University of Wisconsin-Madison; [2]UT Southwestern*

Introduction/Background The push for real-world applications of pro-longevity therapies must consider the contribution of environmental factors and the possibility of combining multiple geroprotective treatments for even greater benefits. One variable that fits both criteria is diet. Amongst the lifespan-extending dietary interventions, caloric restriction (CR) remains the gold standard in effectiveness, followed by its more tenable derivative, protein restriction (PR). The restriction of dietary isoleucine (IleR) is a critical component of PR and recapitulates its longevity and metabolic benefits, including improvement in glycemic control, weight loss, and energy expenditure. These dietary restrictions are thought to elicit their benefits through the inhibition of the nutrient-sensing master regulator mechanistic target of rapamycin complex 1 (mTORC1). Rapamycin, the putative pharmacological inhibitor of mTORC1, is one of the most robust treatments evaluated in the Interventions Testing Program (ITP) for healthy aging across sexes, throughout age ranges, and in various dosages. However, rapamycin elicits undesirable side effects due to its inhibition of mTORC2, causing glucose dyshomeostasis and poor metabolic health. The prospect of avoiding these side effects of rapamycin by simultaneously combining a dietary promoter of metabolic health represents an exciting, highly promising approach to provide a comprehensive geroprotective treatment regimen.

Objective(s) The overarching goal of this study is to determine the diet-drug interaction between rapamycin and the prominent dietary interventions as an investigation into the combinatory effects of geroprotective treatments.

Methods In this study, we utilized male C57BL/6J mice at 9 weeks of age and exposed them to amino acids-defined diets of isoleucine restriction, protein restriction, and methionine restriction. We simultaneously began to treat them with daily injections of rapamycin (4 mg/kg; i.p.). Subsequently, we tracked the physiological outcome of these combinatory treatments and performed metabolic tests, healthspan evaluations, and molecular profiling.

Results Surprisingly, our preliminary data found rapamycin to overwhelm the benefits of IleR. In mice treated with rapamycin and fed an IleR diet with a reduction of dietary isoleucine by 67%, the predominate physiological signature was identical to a rapamycin-injected mouse fed the control diet. The dual-treatment blunted the gross effects of the diet. The rapamycin treatment prevented the IleR-induced improvements in glycemic control, body composition, and energy expenditure of these animals. Circulating levels of fibroblast growth factor 21 (FGF21), a beneficial energy balance hormone, was suppressed by the drug. However, in the inguinal white adipose tissue, adipocyte thermogenesis and lipogenesis gene programs remained highly elevated by IleR. Interestingly, rapamycin only selectively blocked adipocyte lipolysis genes.

Conclusion These results showed that simultaneous initiation of IleR and rapamycin treatments resulted in a gross phenotype resembling that of a rapamycin-treated animal. Further, we identified the previously under-appreciated role of the inguinal white adipose tissue lipolysis gene program as a potential focal point in metabolism and healthspan regulation. This study revealed a clear molecular mechanism that may prove to be a critical feature of geroprotective treatments. Future studies will isolate and define the role of adipocyte lipolysis in physiology and lifespan, as well as determine the contribution of lipolysis in other therapeutic options.
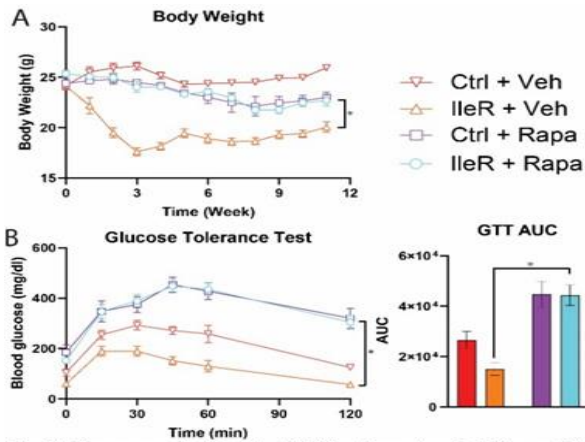
Fig 1: Rapamycin blocks IleR-induced weight loss (A) and improvement in glucose tolerance (B). Significance indicated from pair-wise and two-way ANOVA, p<0.05, n=10 each.

Abstract 42 Figure 1

Fig 1: Rapamycin prohibits IleR's ability to induce an increase in energy expenditure (A) and respiratory exchange ratio (B). Black arrows highlight differences between IleR+Vehicle (orange) and IleR+Rapamycin (Blue). Two-way ANOVA, p<0.05, n=8-10 each.

Abstract 42 Figure 2

Fig. 1: Rapamycin blocks IleR-induced loss in absolute fat mass (left) and also % body composition (right). Significance indicates two-way ANOVA. p<0.05. n=10 each.

Abstract 42 Figure 3
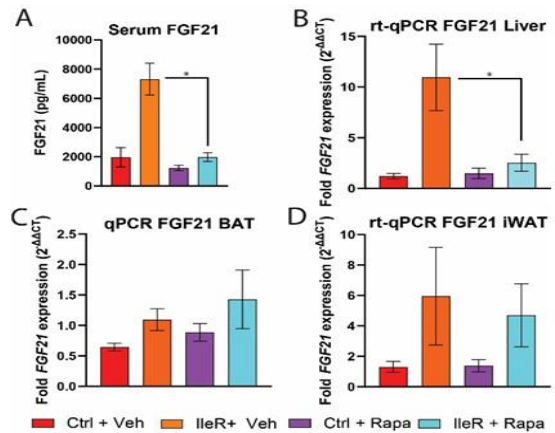
Fig 1: Rapamycin prevents the IleR-induced increase in serum FGF21 (A) and FGF21 expression in the liver (B), but not in the BAT (C) or the iWAT (D). Two-way ANOVA, p<0.05, n=8-10.

Abstract 42 Figure 4

Fig. 1: Rapamycin selectively blocks the IleR-induced increase in expression of iWAT lipolytic program genes Atgl (left) and Lipe (right). Two-way ANOVA, p<0.05, n=8-10.

Abstract 42 Figure 5

43

REVIVIFY REDUCE FASTING GLUCOSE: HUMAN CASE STUDY

[1]Ahmed Pantho, Syeda Afroze, *PhD,* [2]Syed Hussain, [1]Thomas Kuehl, [2]Liaquat Hossain, [3]Mohammad Uddin. [1]*Orion Institute for Translational Medicine*; [2]*Advance Pharmaceutical Inc.*; [3]*Texas A&M University School of Medicine*

Introduction/Background Increased fasting glucose is associated with diabetic patient having type 2 diabetes. The impaired glucose metabolism and its improper utilization of glucose by the body cells are the main reason of increased fasting glucose. We believe, glucose homeostasis depends on many organ/tissue/cells integration process. If body cell's integrity is not compromised or altered by free radicals induced oxidative stress, the pancreas, the liver, the brain, the muscle cells and other cell combined would maintain desired level of fasting glucose. Based on this hypothesis, we have chosen a patented dietary supplement called Revivify, which study showed as a strong antioxidant, diverse anti-inflammatory properties, and enhanced immunity capabilities. Revivify composition focus on integrating the cellular health intigrity as well as gut microbes good eco-system, both are involved in glucose metabolism. In addition, some polyphenols are added value in both cellular health and gut-microbes eco-system. Thus Revivify compositions can improve slowly the pancreatic cell to produce adequate insulin and release as needed. Its anti-inflammatory property can reduce insulin resistance. and increase uptake of glucose by muscle cells. Gut-microbe production of vitamins may bring efficiency in glucose utilization in energy ATP production. Modulation of beneficial microbes, production of Short Chain Fatty acid all in combination can play role in reducing fasting glucose.

Objective(s) To evaluate if REVIVIFY is capable to utilize all the properties to maintain cellular health integrity slowly and reduce the fasting glucose of diabetic patent

**Methods** We conducted a case and control study in the population of Williamson County, Texas. In total, 30 patients joined who were equally and randomly assigned in the case study: 18 males and 12 females. The selection criteria: male and female aged 20 years with type to diabetes 2 diabetes. The patients had average Fasting Blood Glucose (mmol/l): 7.8 ± 1.2 and HbA1c: 8.2 ± 2.1. The study respondents used one pouch of REVIVIFY Pro-Vitality Fruit Blend with Superoxide Dismutase (SOD) and dietary fiber daily after breakfast and one revivify Pro-Energy stick contains dietary fiber with SOD and Resveratrol dissolved in water along with oral diabetic medications for three months.

Results After three months of taking Revivify gel and stick, we found that a significant decrease of average Fasting Blood Glucose (mmol/l) and HbA1c. The Fasting Blood Glucose (mmol/l) was decreased from 7.8 ± 1.2 (initial; beginning of study) to 5.4 ± 0.4 (after three months of study) and HbA1c was decreased from 8.2 ± 2.1 (initial; beginning of study) to 6.8 ± 2.4 (after three months of study). Moreover, the patients reported the improvement of their General Health, Fatigue Status and Sleeping Pattern.

Conclusion: The study results showed that Revivify patented composition is capable of reducing cellular stress, maintain desired cellular inflammation level, maintain cellular communication process by repair of cellular damages, bring efficiency in using glucose in ATP production efficiency, modulate beneficial microbes lactobacillus [as other study showed]. The study not only showed reduction of fasting glucose, more importantly feeling better and less fatigue. Revivify can be platform for heal.

44

MONSTER IN DISGUISE A CASE OF LARGE METASTATIC ADRENAL CORTICAL CARCINOMA

Sreekant Avula, Ammar Ahmed, Michael Salim, Kidmealem Zekarias. *University of Minnesota*

Introduction/Background Adrenal tumors are common; prevalence is estimated to be 3% to 10%. Most adrenal tumors are found incidentally during routine imaging and the majority are benign nonfunctional adrenocortical adenomas. Adrenal cortical carcinoma (ACC), in contrast, is a very rare disease with an incidence believed to be 1 to 2 per million per year. The diagnosis of malignancy relies on careful investigations of clinical, biological, and imaging features before surgery and pathological examination after tumor removal. Most patients present with steroid hormone excess or abdominal mass effects, but 15% of ACC are discovered incidentally. We present a rare case of metastatic adrenal carcinoma in a young male who presented with back pain and elevated blood pressure and on workup was found to have a very large adrenal mass with possible metastasis.

Case Presentation A 30-year-old young male with no significant past medical history presented to his Primary care physician (PCP) with low back pain, headaches, and lower extremities edema for 3 months which continued to worsen. At the PCP office, he had elevated blood pressure (BP) of 210/120 mmHg with lower leg edema. He was immediately referred to the emergency department and was in hypertensive urgency with a BP of 214/144 mg Hg, Heart rate of 102 beats/minute. CT and MRI abdomen demonstrated a very large left adrenal mass of size 28cm with mass effect on adjacent structures as well as left adrenal, renal vein, and IVC thrombus, possible metastatic lesion in liver and para-aortic nodes. His blood work revealed slightly elevated urine dopamine, Hypercortisolism [blood cortisol 31 mcg/dl, 24-hour urine cortisol 742 mcg/24 hours (3.5-45), late-night salivary cortisol 1070 ng/dL (reference range < 100)] with low ACTH, low aldosterone and renin, high DHEAS, high estradiol, and low testosterone. He didn't have any cushingoid features even with elevated cortisol levels. For elevated blood pressure, he was on doxazocin, metoprolol, and amlodipine. He underwent left nephrectomy/adrenalectomy, renal vein thrombectomy, pancreatectomy, splenectomy, vena cava thrombectomy closure of IVC with a patch, and segment 4B lesion wedge resection. Histopathology was consistent with Adrenocortical carcinoma (ACC), tumor extending into major veins, unremarkable splenic and pancreatic parenchyma, and liver wedge resection 4B showed metastatic adrenocortical carcinoma with a pathological staging of pT4pN0pM1. He was placed on glucocorticoid replacement for adrenal insufficiency due to HPA axis suppression secondary to hypercortisolism from the ACC. He was followed by the Oncology team for his metastatic ACC and was planned to start chemotherapy with Mitotane. He was referred to a genetic counselor for a genetic workup as there was a significant family history of multiple cancers. Overall patient's prognosis seems to be guarded.

Discussion Most ACC is sporadic; rarely it is associated with hereditary syndromes like Li-Fraumeni syndrome, Beckwith-Wiedemann syndrome, and Multiple endocrine neoplasia type 1 (MEN1). Surgery is the next step for suspected or confirmed ACC. Histopathology is the gold standard for diagnosis. Resection status, tumor stage, mitotic count, autonomous cortisol secretion, and patient's general condition are prognostic markers. High-risk patients for recurrence, metastatic disease, or patients with advanced ACC not amenable to complete resection are treated with Mitotane alone or Mitotane plus chemotherapy or radiation.Conclusion:ACC is rare. Treatment of advanced ACC not amenable to complete resection or metastatic disease is palliative and research that addresses.
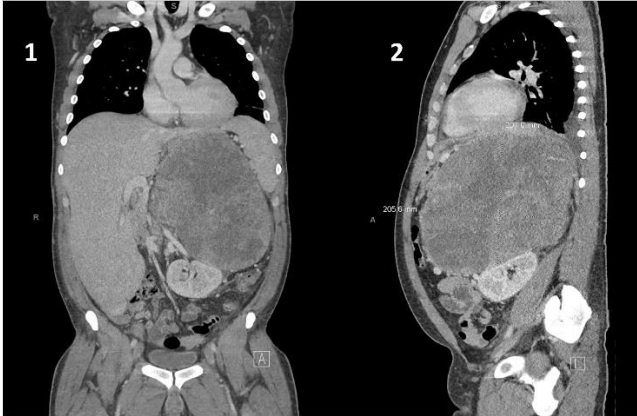
Abstract 44 Figure 1 Coronal (1) & Sagittal(2) CT image of the Adrenal Cortical Carcinoma
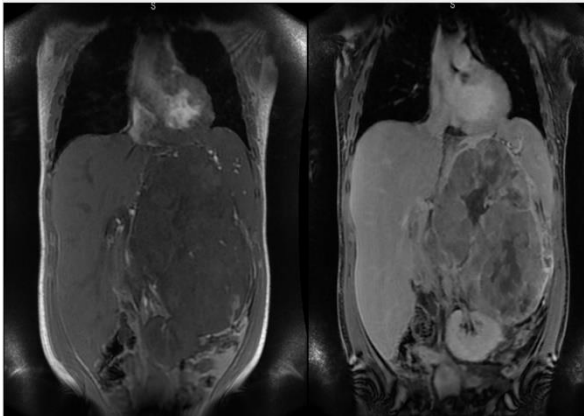
Abstract 44 Figure 2 Coronal View of MRI Abdomen of Adrenal Cortical Carcinoma
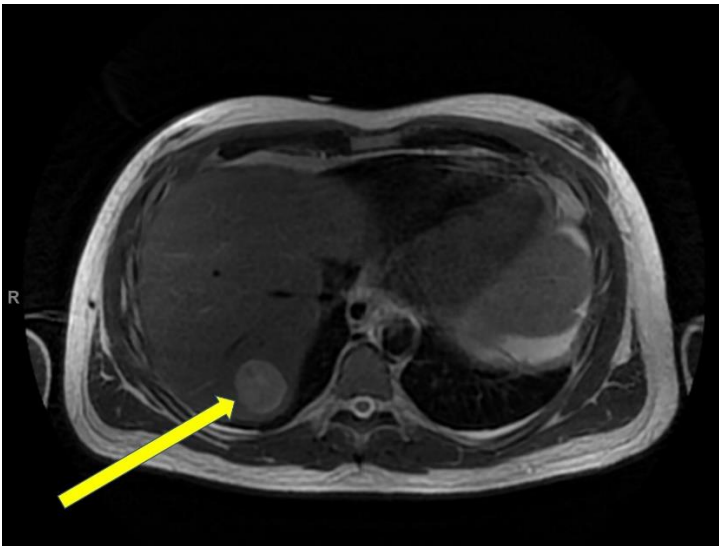
Abstract 44 Figure 3 Axial view of MRI Abdomen showing Metastatic Lesion in Liver

45

VALIDATING A NEW METHOD OF APPROXIMATING CATEGORICAL INDIVIDUAL-LEVEL INCOME USING COMMUNITY-LEVEL INCOME FROM THE CENSUS (WEIGHTING BY INCOME PROBABILITIES)

Uriel Kim, Johnie Rose, Weichuan Dong, Kurt Stange, James Spilsbury, Siran Koroukian. *Case Western Reserve University School of Medicine*

Introduction/Background Individual-level income is an important but often missing variable in biomedical research studies. To surmount this issue, "indirect estimation" methods have been used, often imputing this missing information by joining community-level data from the US census using a patient's community of residence. Central tendency measures of community-level data from the census (i.e. "median income of a census tract") are often used in the indirect estimation of income, though this approach may lead to substantial misclassifications. Weighting by "income probabilities" is a newly described (1) advancement in indirect estimation of income that may improve estimations. It involves using data from the US census to calculate the probability of having a certain user-defined income category in each census tract ("income probabilities"). Then, patients are assigned these income probabilities based on their census tracts of residence. Finally, the income probabilities are used as observation weights in calculations, facilitating a broad range of income-stratified statistical tasks.
Objective(s) Here we further evaluate the accuracy of the weighting by income probabilities method by conducting an external validation on a "real-world" dataset of non-elderly colorectal cancer patients who were enrolled in Medicaid.
Methods We applied the traditional approach of income approximation using median census-tract income along with two income probabilities-based approaches to estimate the proportion of patients with incomes < 100% of the Federal Poverty Level (FPL) versus 100-138% FPL. The validation data consisted of non-elderly Medicaid beneficiaries diagnosed with colorectal cancer in 2015-2017, sourced by linking the Ohio Cancer Incidence Surveillance System to Medicaid Enrollment Files. The reference income data were encoded in the Medicaid Enrollment Files.
Results In the validation data (N=862), 77.5% (N=668) of individuals had incomes < 100% FPL. The traditional approach had an error rate of 14.6%, overpredicting the number of individuals with incomes < 100% FPL by N=126; the best performing weighting by income probabilities approach had a statistically significant (p< 0.05) lower error rate of 9.2%, underpredicting the number of individuals with incomes of < 100% FPL by N=80. Thus, weighting by income probabilities represents at 37% relative improvement compared to the traditional approach. Race/ethnicity, sex, and diagnosis year-stratified analyses revealed that in most instances, weighting by income probabilities approaches had a significantly lower error rate compared to the traditional approach, while in the remaining instances, the differences in error rates were non-significant.
Conclusion This external validation demonstrates that weighting by income probabilities meaningfully improves income estimations compared to the traditional approach. In studies where income is a key variable, the balance between the incremental increase in methodological complexity and the improved accuracy of income estimates likely will favor using the weighting by income probabilities estimation approach. As socioeconomic status is a key predictor of health, the weighting by income probabilities method has potential use in a broad range of biomedical research studies, especially those focusing on reducing income-based health disparities.
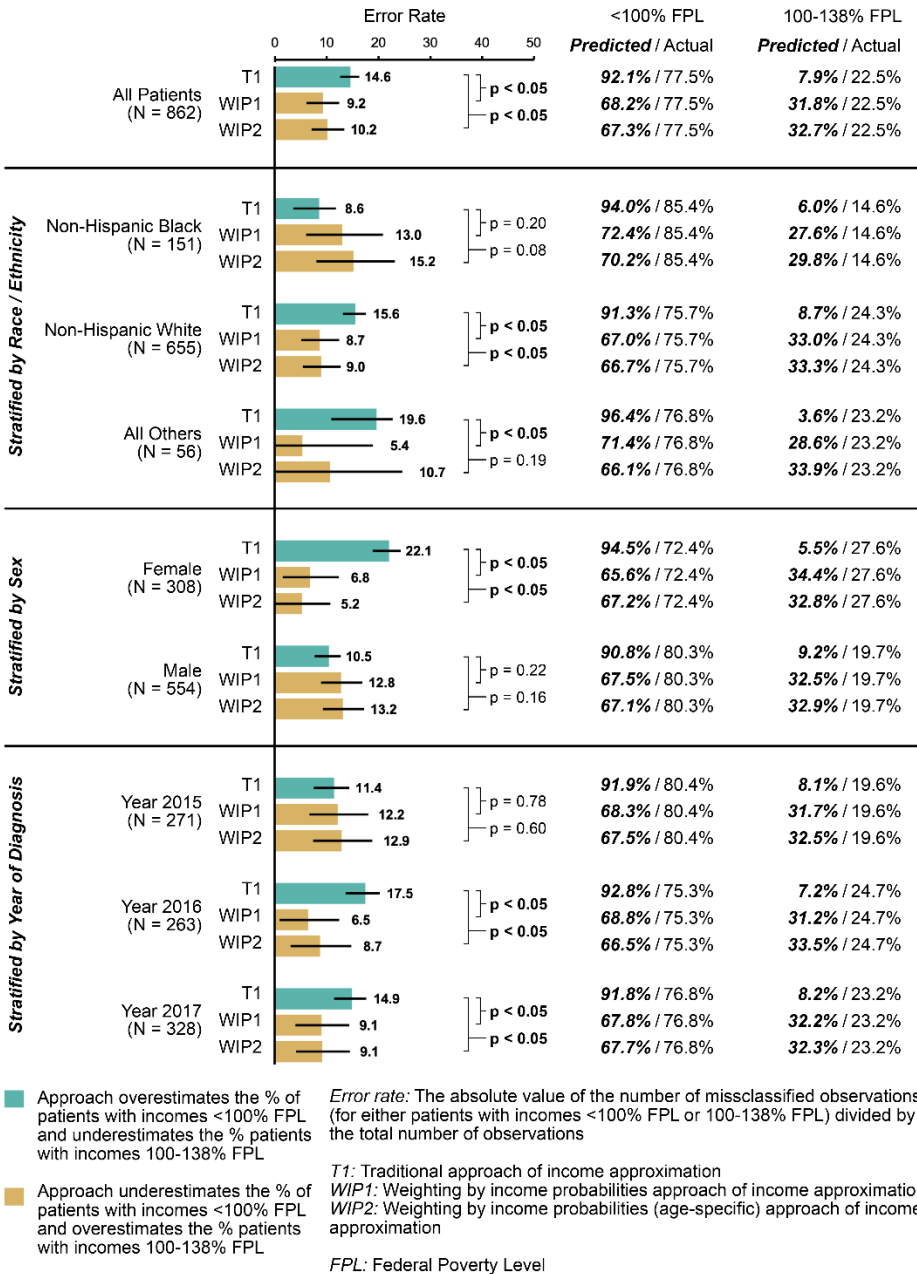
Abstract 45 Figure 1. Error rates for traditional versus weighting by income probabilities approaches to income

REFERENCE(S)
1. Kim, U, Koroukian, SM, Stange, KC, Spilsbury, JC, Dong, W, Rose, J. Describing and assessing a new method of approximating categorical individual-level income using community-level income from the census (weighting by income probabilities). Health Serv Res. 2022; 57(6): 1348- 1360. doi:10.1111/1475-6773.14026

46

EPIDEMIOLOGICALLY SIGNIFICANT AND GEOGRAPHICALLY EQUITABLE COVID-19 WASTEWATER-BASED EPIDEMIOLOGY (WBE) SITE SELECTION STRATEGY FOR THE STATE OF ILLINOIS

[1]Anuj Tiwari, [2]Aditya Nair, [3]Katelyn Leisman, [3]Aaron Packman, [4]Charles Williams, [2]Rachel Poretsky, [5]Sarah Owens, [1]Sandra Gesing, [5]Charlie Catlett. [1]*Discovery Partners Institut, University of Illinois System;* [2]*University of Illinois;* [3]*Northwestern University;* [4]*Illinois Department of Public Health (IDPH);* [5]*Argonne National Laboratory*

Introduction/Background Wastewater-Based Epidemiology (WBE) provides an opportunity for near real-time, cost-effective monitoring of community-level transmission of SARS-CoV-2. It typically focuses on wastewater treatment plants (WWTPs) and the corresponding community. However, many public health questions require insight across many communities such as at the county or state level. What is the optimal sampling strategy in regions such as rural counties with dozens of WWTPs and private septic systems, or in entire states with many such counties? Selecting WWTPs to perform COVID-19 WBE at the state, or county level is no trivial task given the rural-urban health disparities, geographical complexities in the WWTPs boundaries, and the multiple demographic, socioeconomic, and epidemiological constraints involved. In the last three years, CDC-driven nationwide or public health departments-enabled statewide WBE programs used different analytical and qualitative techniques to determine the most favorable locations for COVID-19 WBE. Some of the most frequently used site-selection techniques include the largest population centers in each county, the largest population centers in COVID-19 risk regions, and COVID-19 hotspots. population-centric techniques fail to provide coverage in large rural regions whereas pandemic-centric techniques daily update with frequently updating pandemic statistics and can not be used directly for stable site selection.

Objective(s) In the current research work, we present an epidemiologically defined and geographically equitable site selection strategy for implementing COVID-19 WBE in the state of Illinois. The objectives are as follows: 1. COVID-19 Impact Assessment using Modified SIR Epidemiological Modeling 2. COVID-19 Vulnerability Modeling using CatBoost Machine Learning 3. Using COVID-19 Vulnerability Index for selecting WWTPs for COVID-19 WBE.

Methods Epidemiological modeling involves the development and use of mathematical and computational techniques to describe the spread of the pandemic whereas non-linear (machine learning) vulnerability models are powerful tools for describing the impact of the pandemic and identifying communities that are at persistent risk. We integrated a modified SIR epidemiological model with the CatBoost machine learning-based vulnerability model in a geospatial environment, which led to identifying the WWTPs serving the most vulnerable communities. Detail description of COVID-19 Impact Assessment and Vulnerability Modeling is as follows: COVID-19 Impact Assessment Step 1: Plot time series between Susceptible and Recovered Populations. Step 2: Compute the trend of the Susceptible-Recovery time series and find all change points using homogeneity analysis. Step 3: For each phase of the regular trend calculate the reproduction number using the SIR model. Step 4 (optional): Customize the trend phase (week/month or specific time period) and calculate the reproduction number. Step 5: Compute the reproduction number for all counties and classify them to produce a COVID-19 Impact map.COVID-19 Vulnerability ModelingCOVID-19 vulnerability modeling: COVID-19 vulnerability modeling was implemented using the CatBoost machine learning technique. This model predicts the vulnerability of a given county on a continuous scale of 0 (least vulnerable) to 1 (most vulnerable). The map was graded according to the COVID-19 Vulnerability Index into five vulnerability classes: very high (>80%), high (80%–60%), moderate (60%–40%), low (40%–20%) and very low (< 20%).

Results Our 'COVID-19 Impact Assessment' algorithm performed a county-wise assessment of the pandemic using the confirmed cases, deaths, and recovery counts from the day the first COVID-19 case was reported in the county. Figure 1 describes the model output for Cook County. Daily reported cases and deaths from February 2020 to August 2021 are used in the modified SIR model for preparing a phase-dependent Susceptible-Recovery Trend Graph and then for every phase of homogeneous trend, Reproduction Number (R0) and Infection Fatality Rate (IFR) were computed. Phase-dependent Reproduction Number (R0) and Infection Fatality Rate (IFR) are presented in table 1 and Table 2, respectively. After integrating the spread of the pandemic (R0) and mortalities (IFR), a combined county-level COVID-19 Impact was generated. Figure 2 presents the COVID-19 Impact Map for every county of Illinois. COVID-19 Impact Map was further processed with COVID-19 causal and resilience criteria (presented in Table 1) for COVID-19 Vulnerability Modeling. Figure 3 presents the COVID-19 Vulnerability of each county in Illinois by 31st Aug 2021. The COVId-19 Impact and Vulnerability maps were internally shared on a Web Map Viewer (Figure 4) for selecting WWTPs in the COVID-19 WBE program. Using this site selection strategy we have enrolled the WWTPs in the Illinois COVID-19 WBE program. Wastewater samples were collected from the selected WWTPs twice a week and SARS-CoV-2 RNA was consistently found. Selected WWTPs and corresponding viral levels can be accessed using Illinois Wastewater Surveillance System Dashboard (https://il-nwss-dashboard-staging.herokuapp.com/).
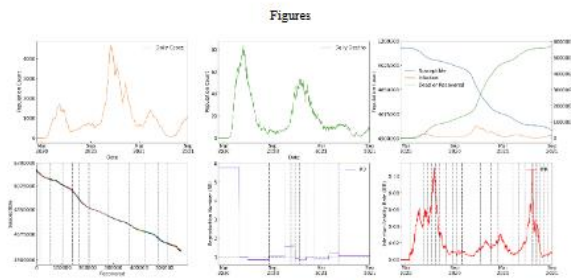
Figure 1 Cook County daily report (a) cases and (b) deaths from February 2020 to August 2021 (c) Susceptible-Infection-Dead or Recovered Graph (c) Phase-dependent Susceptible-Recovery Trend Graph, (c) Phase-dependent Reproduction Number (R0) and Phase-dependent Infection Fatality Rate (IFR)
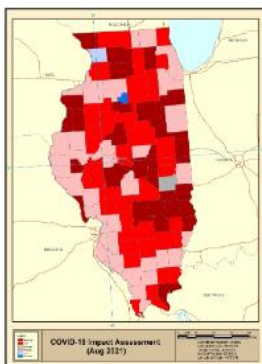
Figure 2 COVID-19 Impact (combined Impact of R0 and IFR) Assessment for Illinois State computed in August 2021

Abstract 46 Figure 1 & 2
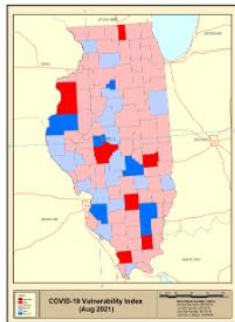
Figure 3 COVID-19 Vulnerability Index for Illinois State computed in August 2021
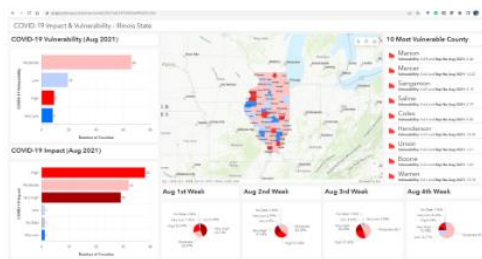
Figure 4. COVID-19 Web Map Viewer. This figure illustrates snapshots of the COVID-19 web map viewer used for internally communicating COVID-19 Impact and Vulnerability information for selecting WWTPs

Abstract 46 Figure 3 & 4

Conclusion In this research, we proposed an innovative approach to conduct the vulnerability assessment of COVID-19 within Illinois at the county level. This approach integrates the reliable and high-functioning domains of machine learning and compartmental epidemiology modeling. CatBoost machine learning technique in conjunction with the epidemiology modeling constituted the basis of our COVID-19 WBE site selection strategy. Results described that the developed site selection strategy provides a promising approach for state-wide pandemic surveillance in wastewater, thus better guiding spatially targeted public health monitoring and mitigation planning.

REFERENCE(S)

1.   Tiwari, Anuj, Arya V. Dadhania, Vijay Avin Balaji Ragunathrao, and Edson RA Oliveira. "Using machine learning to develop a novel COVID-19 Vulnerability Index (C19VI)." Science of The Total Environment 773 (2021): 145650.
2.   Tiwari, A., Leisman, K. P., Shrestha, A., Poretsky, R., Owens, S., Dorevitch, S., Grippo, M., Packman, A., Gesing, S., Catlett, C. (2022). "A Science Gateway for Wastewater-based Epidemiology - a Case Study of the World's Largest Wastewater Treatment Plant in Chicago". Gateways; 2022 Oct 18-20; San Diego, California.
3.   ZenodoTiwari, A., Catlett, C., Poretsky R., Packman, A., Jasmin, W., Williams, C., Duffus, W., Patrick, S., Wendt, J., Wise, L., "Optimizing Sampling Strategies for Large Rural Regions", DHS/NIST Workshop: Standards to Support an Enduring Capability in Wastewater Surveillance for Public Health from 14th JUN - 18th JUN 2021.

4.   Azar, Kristen MJ, Zijun Shen, Robert J. Romanelli, Stephen H. Lockhart, Kelly Smits, Sarah Robinson, Stephanie Brown, and Alice R. Pressman. "Disparities In Outcomes Among COVID-19 Patients In A Large Health Care System In California: Study estimates the COVID-19 infection fatality rate at the US county level." Health Affairs 39, no. 7 (2020): 1253-1262.

5.   Meyerowitz-Katz, Gideon, and Lea Merone. "A systematic review and meta-analysis of published research data on COVID-19 infection-fatality rates." International Journal of Infectious Diseases (2020).

6.   Streeck, Hendrik, Bianca Schulte, Beate M. Kümmerer, Enrico Richter, Tobias Höller, Christine Fuhrmann, Eva Bartok et al. "Infection fatality rate of SARS-CoV2 in a super-spreading event in Germany." Nature communications 11, no. 1 (2020): 1-12.

7.   Campbell, Harlan, L. Maxwell, Jong VMd, T. Debray, T. Jänisch, and P. Gustafson. "Bayesian adjustment for preferential testing in estimating the COVID-19 infection fatality rate: Theory and methods." (2020).

8.   M. J. Keeling and P. Rohani, Modeling Infectious Diseases in Humans and Animals, Princeton (2007).

Abstract 46 Table 1 Cook County Reproduction Number (R0) variations in different phases of the Susceptible-Recover trend

Segment	Start	End	R0
Initial	10-Feb-20	29-Apr-20	5.78
1st	30-Apr-20	29-May-20	1
2nd	30-May-20	17-Aug-20	0.85
3rd	18-Aug-20	16-Oct-20	1.04
4th	17-Oct-20	7-Nov-20	1.58
5th	8-Nov-20	22-Nov-20	1.6
6th	23-Nov-20	10-Dec-20	0.94
7th	11-Dec-20	5-Jan-21	0.86
8th	6-Jan-21	2-Feb-21	1.03
9th	3-Feb-21	31-Mar-21	0.91
10th	1-Apr-21	5-May-21	1.22
11th	6-May-21	31-Aug-21	1.06

Abstract 46 Table 2 Cook County Infection Fatality Rate (IFR) trend variations in different phases of the Susceptible-Recovery trend

Segment	Start	End	Trend
Initial	10-Feb-20	5-May-20	no trend
1st	6-May-20	20-May-20	increasing
2nd	21-May-20	4-Jun-20	increasing
3rd	5-Jun-20	19-Jun-20	no trend
4th	20-Jun-20	4-Jul-20	no trend
5th	5-Jul-20	29-Jul-20	no trend
6th	30-Jul-20	23-Aug-20	no trend
7th	24-Aug-20	7-Sep-20	decreasing
8th	8-Sep-20	27-Sep-20	decreasing
9th	28-Sep-20	6-Dec-20	increasing
10th	7-Dec-20	15-Jan-21	no trend
11th	16-Jan-21	9-Feb-21	increasing
12th	10-Feb-21	5-Apr-21	no trend
13th	6-Apr-21	30-Apr-21	decreasing
14th	1-May-21	20-May-21	decreasing
15th	21-May-21	19-Jun-21	no trend
16th	20-Jun-21	4-Jul-21	increasing
17th	5-Jul-21	19-Jul-21	increasing

18th	20-Jul-21	3-Aug-21	increasing
19th	4-Aug-21	18-Aug-21	no trend
20th	19-Aug-21	31-Aug-21	decreasing

Abstract 46 Table 3 Details of causal and resilience parameters used for COVID-19 Vulnerability Modeling

No	Parameter	Theme	Type	Description
1	Population Count	Population	Static	Number of people living in the county
2	Population Density		Static	Number of individuals divided by the size of the county
3	Population 65 <	Aged People	Static	Aged 65 or Older
4	Population 10 >	Children	Static	Aged 10 or Younger
5	Single Parent Household		Static	Percentage of single parent households
6	Children in Poverty		Static	Percent of children under age 18 who are living in families with incomes below the federal poverty threshold
7	Severe Housing Problem		Static	Percentage of households with housing problems: overcrowding, high housing costs, lack of kitchen facilities, or lack of plumbing facilities.
8	Socioeconomic Status	Social Vulnerability	Static	Status of family income, parents' education, and parents' employment.
9	Household Composition & Disability		Static	Status of age, disability, and household composition
10	Housing Type and Transportation		Static	Status of house type and transportation medium
11	Minority Status and Language		Static	Percentage of minorities and non-fluent English-speaking individuals
12	Unemployed Population		Static	Percentage Unemployed residents
13	Epidemiological Factor	Health and Disease	Static	High risk populations as elderly adults and individuals with conditions related to immunodeficiency
14	Healthcare System Factor		Static	Capacity, strength, accessibility and preparedness of the healthcare system regarding COVID-19.
15	Hospital Beds		Dynamic	Summation of hospital beds for hospitals
16	Hospital Ventilator		Dynamic	Percentage of ventilators in use
17	Uninsured Population		Static	Percentage uninsured residents
18	Vaccines	COVID-19	Dynamic	Percentage of unvaccinated residents
19	Social Distancing		Dynamic	People interacting with other
20	Air Pollution	Pollution	Dynamic	Average daily density of fine particulate matter
21	Baseline Traffic		Dynamic	Average traffic volume per meter of major roadways
22	Smoker Percentage		Static	Percentage of adults who are current smokers

47

HMGB2 IN MEDIATING HEPATIC STELLATE CELLS ACTIVATION AND LIVER FIBROSIS

[1]Zhihong Yang, [2]Yi Huang, [1]Nazmul Huda, [1]Suthat Liangpunsakul, [1]Jing Ma. [1]*Indiana University School of Medicine; [2]University of Connecticut*

Introduction/Background Liver fibrosis is characterized by the excessive accumulation of extracellular matrix (ECM) in response to liver injury, which is mainly produced by hepatic stellate cells (HSCs). Liver fibrosis can progress to cirrhosis leading to an increase in morbidity and mortality. High-mobility group box 2 (HMGB2) is a chromatin protein that belongs to the HMG protein family and is involved in gene transcription and repair processes. The role of HMGB2 in the pathogenesis of liver fibrosis is elusive.
Objective(s) We aimed to explore the role of HMGB2 in mediating liver fibrosis and its potential as the therapeutic target for liver fibrosis.
Methods Human liver specimens from controls and those with various chronic liver diseases were obtained. Liver fibrosis was induced by carbon tetrachloride (CCl4) treatment for six weeks in mice. We used AAV8-Hmgb2 with a specific thyroxine binding globulin promoter to specifically overexpress Hmgb2 in the liver. The loss of function experiments were performed in Hmgb2−/− mice. HMGB2 inhibitor Inflachromene (ICM) and liposome-shHMGB2 (lipo-shHMGB2) were used to inhibit HMGB2 for the translational experiments. Primary mouse HSCs from wild type (WT) or Hmgb2−/− mice were isolated for in vitro experiments.
Results HMGB2 mRNA and protein expression were significantly induced in the liver of patients with advanced fibrosis and cirrhosis, but not with hepatic steatosis. Interestingly, hepatic HMGB2 was also markedly elevated in mice treated with CCl4. These results implied an important role of HMGB2 in liver fibrosis and cirrhosis. Hepatic overexpression of Hmgb2 significantly enhanced liver fibrosis induced by CCl4. In contrast, Hmgb2-/- mice treated with CCl4 did not develop fibrosis. Plasma ALT and AST levels were elevated in AAV8-Hmgb2 mice treated with CCl4 and decreased in Hmgb2-/- mice. The increased protein expression of α-SMA, a marker for the transdifferentiation of HSC to myofibroblast-like cells, by CCl4 in WT mice was further enhanced in AAV-8-Hmgb2 mice but diminished in Hmgb2-/- mice. For the translational experiments, we generated liposome-mediated delivery of shHmgb2 (Lipo-shHmgb2) to specific knockdown of HMGB2 as well as treated mice with ICM to inhibit HMGB2. Both Lipo-shHmgb2 and ICM ameliorated liver fibrosis in CCl4-treated mice as determined by Masson Trichrome staining, prevented liver injury as determined by plasma AST and ALT, diminished HSC activation as determined by ⍺-SMA expression, and reduced inflammation as determined by a decrease in the expression of IL-4, Mip2, and iNos2. For the invitro experiments, primary HSCs were isolated and culture-activated on uncoated plastic dishes and coverslips for 7 days. On day 1, HMGB2 protein was detected in the nucleus of quiescent HSCs. By day 3, we started to observe α-SMA expressing cells, indicating the early activation of HSCs. At day 5 of activation, many cells showed markedly increased staining of α-SMA and HMGB2 was found mostly in the nucleus. By day 6 of culture, HSCs became activated by showing further induction of α-SMA. HMGB2 protein was also observed in the cytoplasmic compartment in addition to its nuclear localization by day 7. HSCs isolated from Hmgb2-/- mice showed little activation after 5 days of culture compared with WT HSCs and were associated with marked reduction of α-SMA, suggesting that HMGB2 is required for stellate cell activation.
Conclusion HMGB2 is indispensable for stellate cell activation. Targeting HMGB2 may provide a potential therapeutic strategy to prevent HSCs activation and liver fibrosis during chronic liver injury.

48

ALDH2 DEFICIENCY EXACERBATES BINGE ALCOHOL-INDUCED GUT LEAKINESS, ENDOTOXEMIA, AND ACUTE LIVER INJURY THROUGH THE GUT-LIVER AXIS.

Wiramon Rungratanawanich, Byoung-Joon Song. *National Institute on Alcohol Abuse and Alcoholism (NIAAA), NIH*

Introduction/Background More than 560 million people worldwide have inactive mitochondrial aldehyde dehydrogenase 2 (ALDH2), a major enzyme metabolizing alcohol-derived acetaldehyde to acetate, due to a dominant-negative ALDH2*2 gene mutation. This leads to an accumulation of toxic acetaldehyde and lipid aldehydes after alcohol consumption. These individuals are susceptible to alcohol-induced tissue injury, notably in the gut and liver. Aldh2-knockout (KO) mice also exhibit increased sensitivity to alcohol-mediated tissue damage compared with that of wild-type (WT), indicating a conserved system among species. However, the underlying mechanisms by which ALDH2 deficiency enhances alcohol-induced tissue damage remain unclear.

Objective(s) We aimed to investigate the role of ALDH2 in protecting against alcohol-induced liver injury using a binge ethanol (EtOH) model in mice, by focusing on post-translational protein modifications (PTMs) and the crosstalk between the gut-liver axis.

Methods WT and Aldh2-KO mice were gavaged with a single dose of EtOH at 3.5, 4.0, or 5.0 g/kg. Liver and intestinal tissues were collected after 1 and 6 h. Histological analyses were determined using H&E and TUNEL staining. Liver injury was evaluated by serum transaminases, pro-inflammatory cytokines, and markers for apoptosis and oxidative/nitrative stress. Gut dysbiosis was measured via 16s metagenomic sequencing of fecal samples from the cecum. Gut leakiness was assessed by measuring serum endotoxin. Immunoblots and immunoprecipitation were performed to detect protein alterations and PTMs. CRISPR/Cas9-mediated ALDH2-knockout T84 human colonic cells were generated and treated with EtOH (40 mM, 1-2 h). In parallel experiments, T84 cells were pretreated with Daidzin (ALDH2 inhibitor) or Alda-1 (ALDH2 activator) followed by EtOH treatment (40-130 mM, 1-2 h) to determine the function of ALDH2 on gut permeability using biochemical and confocal analyses.

Results EtOH significantly induced gut and liver inflammation and apoptosis of enterocytes and hepatocytes in Aldh2-KO compared with WT mice in a dose-dependent manner (Fig.1). Aldh2-KO mice treated with EtOH showed significantly increased gut oxidative/nitrative stress and PTMs, specifically nitration of gut tight junction and adherent junction proteins (TJ/AJs), leading to their degradation via ubiquitin-dependent proteolysis. The degradation of TJ/AJs resulted in elevated gut permeability, serum endotoxin, and acute liver injury in Aldh2-KO mice, even treated with EtOH as low as 3.5 g/kg. These alterations were not observed in those of EtOH-treated WT mice. Aldh2-KO mice exhibited significantly higher abundance of pathogenic microbiota, Proteobacteria, with lower contents of health-promoting beneficial bacteria, Verrucomicrobia, than those of WT mice. The mechanism by which ALDH2 protects gut permeability was also studied by the loss-of-function approaches using CRISPR/Cas9-mediated ALDH2-knockout or a pharmacological inhibitor of ALDH2 (Daidzin) in human T84 colonic cells. ALDH2 deficiency from both methods exacerbated EtOH-induced cell death and permeability with the reduction of TJ/AJs and disruption of their distribution. These alterations were prevented in the gain-of-function experiments by pretreating T84 cells with an ALDH2 activator (Alda-1).

Abstract 48 Figure 1. ALDH2 deficiency exacerbates binge alcohol-induced gut leakiness, endotoxemia, and acute liver injury through the gut-liver axis.

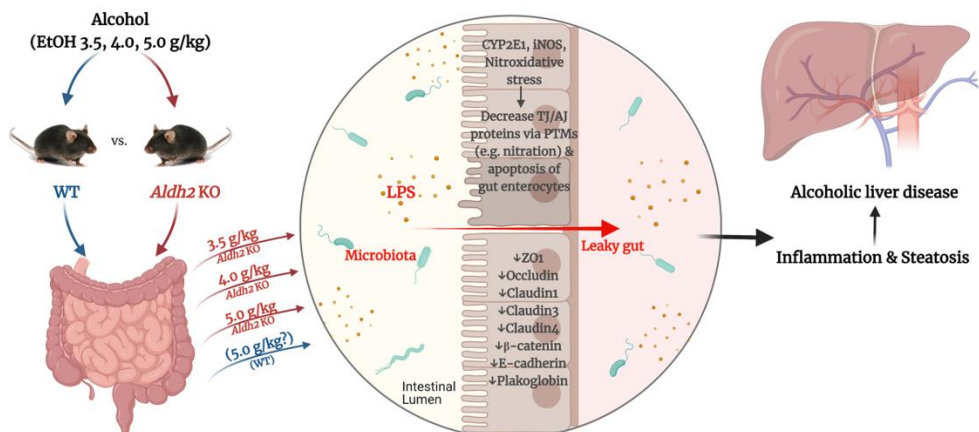The deletion of Aldh2 gene in Aldh2-KO mice contributes to greater production of oxidative and nitrative stress markers, which result in elevated PTMs, such as nitration, followed by ubiquitin-dependent proteasomal degradation of gut TJ/AJ proteins, apoptosis of enterocytes, and intestinal barrier dysfunction, ultimately leading to gut leakiness and endotoxemia after exposure to a single dose of ethanol even at 3.5 g/kg. In contrast, no or little changes were observed in the corresponding WT mice. Consequently, elevated endotoxemia and/or bacterial translocation can cause inflammation, oxidative stress, apoptosis, hepatic steatosis, and acute liver injury through the gut-liver axis.

Conclusion ALDH2 is crucial in maintaining gut barrier integrity, microbiome eubiosis, and hepatic function. It also protects against alcohol-induced liver injury through the gut-liver axis by preventing gut leakiness and endotoxemia. These protective roles of ALDH2 likely underlie the susceptibility of ALDH2-deficient people to alcohol-induced tissue injury. Thus, targeting ALDH2 is an attractive therapeutic strategy for preventing alcohol-induced gut and liver injury.

MELATONIN TREATMENT PROTECTS AGAINST THIOACETAMIDE (TAA)-MEDIATED LIVER FIBROSIS BY SELECTIVELY ACTIVATING SIRT1 DEACETYLASE AND PROTEIN DEACETYLATION

Wiramon Rungratanawanich, Karli LeFort, Byoung-Joon Song. *National Institute on Alcohol Abuse and Alcoholism (NIAAA), NIH*

Introduction/Background More than 1.5 billion people worldwide are suffering from chronic liver diseases, including liver fibrosis, an excessive extracellular matrix deposition. Once developed, the disease may progress from advanced fibrosis to cirrhosis and subsequent liver failure. There is no FDA-approved drug for effectively treating or preventing liver fibrosis. Melatonin (MT), a generally recognized as safe (GRAS) agent by the FDA, has been considered not only a circadian rhythm regulator, but also an anti-inflammatory and antioxidant agent. However, the mechanism underlying liver fibrosis and the beneficial role of a physiologically relevant MT dose as a potential therapeutic agent are still elusive.

Objective(s) We aimed to investigate the mechanisms for liver fibrosis using thioacetamide (TAA) in rodent models by focusing on liver protein post-translational modifications (PTMs) and the protective effects of MT against liver fibrosis.

Methods Young male Sprague-Dawley rats were randomly divided into 12 groups (4 groups x 3 timepoints): Control (vehicle), MT (10 mg/kg/day orally), TAA (200 mg/kg/dose twice a week via i.p.), and MT+TAA for 1, 2, and 4 weeks (n=6-8/group). Liver fibrosis and hepatocyte apoptosis were determined using Picrosirius red staining and TUNEL assay, respectively. Liver injury was determined by serum transaminases (ALT and AST). Liver cytokines involved in fibrosis were measured with a cytokine array kit. Liver protein alterations and PTMs were examined by immunoblots. For additional mechanistic studies, we also conducted similar experiments in wild-type (WT) and liver specific Sirt1-KO mice (Sirt1-LKO) by injecting with TAA 200 mg/kg/dose, twice a week for 5 weeks. Significant differences between groups (mean ± SD) were determined by ANOVA, and $p < 0.05$ was considered significant.

Results Liver fibrosis and hepatocyte apoptosis were developed as early as 1 week after TAA exposure. The severity of fibrosis and apoptosis was markedly worsened after 2 and 4 weeks post-TAA injection. TAA-treated rats had significant increases in the levels of liver fibrosis protein markers (collagen-1, α-SMA, vimentin, and TGF-β) and liver chemokines involved in fibrosis development (CCL5, CCL20, and CCL21) after 1 week as well as serum transaminases (AST and ALT) 2 weeks post-TAA exposure. Pre-treatment with MT significantly ameliorated these changes at 1, 2, and 4 weeks. Mechanistically, TAA-exposed rats had significant increases in the levels of liver protein acetylation, specifically acetylated lysine (Ac-Lys) proteins related to cellular apoptosis (Ac-p53), inflammation (Ac-NFκB), and liver metabolism (Ac-FOXO1). Since protein acetylation is regulated by acetyltransferases and deacetylases using acetyl-CoA and NAD+ as substrates, the levels of acetyltransferase, acetyl-CoA, and NAD+/NADH ratio were also evaluated, but no changes were observed. However, liver SIRT1 activity and protein levels, but not other six SIRT isoforms, were significantly decreased in TAA-exposed rats, while their decrements were restored by MT administration. To confirm the functional significance of SIRT1 in liver fibrosis, WT and Sirt1-LKO mice were treated with TAA for 5 weeks. TAA-exposed Sirt1-LKO mice exhibited markedly elevated liver fibrosis, apoptosis, hepatic injury markers, and protein acetylation compared to those of WT counterparts.

Conclusion TAA-induced liver fibrosis is mediated by decreased SIRT1 deacetylase, resulting in elevated acetylation of specific hepatic proteins involved in cellular apoptosis, inflammatory, and liver metabolic pathways. MT exerts its protective effects against liver fibrosis through SIRT1 activation and protein deacetylation, suggesting MT as a potential therapeutic option for liver fibrosis.

50

OPPOSING FUNCTIONS OF GALECTIN-3 AND -8 IN MODULATING DIFFERENTIATION STATES AT HOMEOSTASIS AND IN METAPLASIA

Jeffrey Brown, Xiaobo Lin*. Washington University in St. Louis, School of Medicine*

Introduction/Background Although aberrant expression of neoglycosylation epitopes is widely recognized to occur in metaplasia and cancer where they serve as important biomarkers to (1) diagnose these tissue transformations, (2) monitor therapeutic response, and (3) evaluate for recurrence, the functional consequences of these post-translational modifications are under- and/or unstudied. In the gastrointestinal foregut, galactose containing Lewis antigens are prominent examples of such neoglycosylation epitopes in metaplasia and cancer of the esophagus, stomach, and pancreas [e.g., 3'-Sulfo-LeA/C that we have recently described in addition to others like 3'-Sialyl-LeA (CA19-9)].
Objective(s) To learn why such neoglycosylation epitopes are stereotypically expressed during tissue metaplastic and oncogenic transformation.
Methods Murine model of gastric intestinal metaplasia in the background of Galectin-3 and Galectin-8 knockout mice (two proteins previously shown to bind sulfated mucins). IHC, IF, Pulldown, Mass Spectroscopy, Western blot.
Results We observed mice null for Lgals3 are unable to efficiently secrete these sulfomucins as they downscale their cellular architecture en route to a metaplastic phenotype. In contrast, Lgals8–/– mice exhibit a significant delay in cellular maturation as judged by the absent expression of gastric intrinsic factor or sulfomucins in the zymogenic granules of the gastric chief cells until ~4 weeks of age.
Conclusion Thus, galectins 3 and 8 appear to have fundamentally opposite effects on cellular differentiation, with galectin 3 overexpressed in cancer driving the cells towards a dedifferentiated state, while galectin 8 whose expression is decreased in cancer favors a mature homeostatic phenotype. The molecular mechanisms (autophagy, vesicular trafficking, exocytosis) responsible for these phenotypes will be discussed. Overall, the results presented here suggest that the expression of neoglycosylation epitopes along with their receptors plays an important role in modulating cellular architecture both at homeostasis and in processes like paligenosis. As such, neoglycosylation epitopes appear to confer unique cellular plasticity to cells enabling them to undergo metaplastic and oncogenic transformation.

51

NOVEL APPLICATION OF NUTRIMETABOLOMICS - A NEW WINDOW FOR THE BIOMEDICAL SCIENCES AND CLINICAL NUTRITION RESEARCH

[1]Sugasini Dhavamani, [1]Prasanth Kumar [1]Punathil Kannan, [1]Anchal Sharma, [1]Anuj Tiwari, [2]Raja Lakshitha, [2]Ilamaran Muthu. [1]*University of Illinois at Chicago*; [2]*Tamilnadu Agricultural University*

Introduction/Background Nutrimetabolomics helps to study the molecular and bioactive lipids, proteins, and carbohydrates in plant, algal and animal foods, cells, tissues, and biological fluids. Targeted and untargeted metabolites of lipidomics, proteomics, and glycomics play a crucial role in biomedical science and nutrition for the maintenance of good health.
Objective(s) This nutrimetabolomic approach of lipidomics, proteomics, and glycomics help to analyze the interactions with other lipids, proteins, and carbohydrates help to with targeted analysis, metabolite profiling, and metabolic fingerprinting. Metabolomic approaches are driven based on Gas chromatography-mass spectrometry (GCMS), high-performance or ultra-performance Liquid chromatography (HPLC, UPLC), and mass spectrometry (LCMS/MS) and Nuclear magnetic resonance spectroscopy (NMR). The unending knowledge of metabolomics in biomedical science and nutrition research has been expanded substantially.
Methods Those approaches are the identification of novel bioactive food components, screening of bioactive lipids and proteins or peptides from various resources, toxicity, measurement the food safety and Quality assurance, Assessment of bioactive function, measure the nutrition levels of triglyceride molecular species, phospholipids, sphingolipids, eicosanoids and exploring the new classes and metabolites of bioactive lipids.
Results Metabolomics provokes various bioactive lipids and proteins which is mediated by several signaling pathways and act as vital compound for cell membranes. Any transformation in lipid, protein, and glucose metabolism leads to an alteration of membrane composition, permeability, and disruption of the signaling network which causes cardiovascular disease, inflammation, neurodegeneration, cancer, and metabolic diseases.
Conclusion Hence, the metabolomic analysis is considered an important tool to study the triglyceride molecular species, fatty acids, and bioactive lipids like phospholipidomics, glycolipidomics, sphingolipidomics, eicosanomics, Neurolipidomics, Neuroprotectins, resolvins, maresins, and cardiolipins. The current lack of metabolomic data in nutraceuticals, nutritional and clinical studies can be critically evaluated both at a biological pathway, biophysical and technological level. Hence, Nutrimetabolomics with mathematics, statistics, and bioinformatics tools can also be utilized for the identification of clinical endpoints of dietary interference and the identification of novel biomarkers.

52

PRE-CUT PAPILLOTOMY VS EUS-RENDEZVOUS- A SYSTEMATIC REVIEW AND META-ANALYSIS

Amna Iqbal, Zohaib Ahmed, Kirubel Zerihun, Manesh Gangwani, Sara Stanley, Anas renno, Mona hassan, Yaseen alastal, Ali Nawras, Tossef javaid, Abdallah kobeissy. *University of Toledo*

Introduction/Background ERCP is now used more commonly as a therapeutic procedure rather than a diagnostic procedure for hepatobiliary and pancreatic diseases. Recently, European Society of Gastrointestinal Endoscopy (ESGE) defined Difficult Biliary Cannulation (DBC) as one of the following: more than 5 contacts with papilla when trying to cannulate, more than 5 minutes spent to cannulate after visualization of papilla, or more than one inadvertent cannulation or opacification of pancreatic duct. (2) Various endoscopic techniques are employed to achieve biliary cannulation when confronted with difficult biliary access. Every technique carries its own risk of complications. We aim to perform meta-analysis to compare pre-cut papillotomy and EUS-Rendezvous technique for difficult biliary cannulation.
Objective(s) To compare pre-cut papillotomy to EUS-Rendezvous for Difficult Biliary Cannulation (DBC)
Methods A comprehensive literature search was performed from inception through August 9, 2022. After applying inclusion and exclusion criteria, three observational studies were included. The primary outcome was technical success by achieving biliary cannulation. Secondary outcomes were postoperative pancreatitis and bleeding. A random-effects model was used to calculate the risk ratios (RR), mean differences (MD), and confidence intervals (CI). A P-value < 0.05 was considered statistically significant.
Results Three studies comparing pre-cut papillotomy and EUS Rendezvous approach were included. The studies included a total of 4933 total ERCP procedures, of whom 567 patients underwent alternate biliary cannulation procedures due to DBC. The included studies consisted of 2 retrospective cohort studies and 1 prospective cohort study. The mean age of patients was 49.5 years and males represented 53.3% of the total participants. Our meta-analysis found that both techniques were similar in terms of clinical success (RR 0.98, 95%CI 0.94-1.02). No difference was found between rates of post procedure pancreatitis (RR 1.60, 95% CI 0.52, 4.94) and post procedure bleeding (RR 3.94, 95% CI 0.53, 29.39).
Conclusion Our meta-analysis shows no significant difference in terms of technical success rate between the pre-cut papillotomy and EUS-Rendezvous techniques. There was no difference in terms of post procedure pancreatitis and bleeding. More Randomized controlled trials are needed to compare different techniques for difficult biliary cannulation.

REFERENCE(S)
1.   Endoscopic retrograde cholangiopancreatography: Current practice and future research. David J Sanders, Shivanand Bomman, Rajesh Krishnamoorthi, Richard A Kozarek. World J Gastrointest Endosc. 2021 Aug 16;13(8):260-274. doi: 10.4253/wjge.v13.i8.260.
2.   Papillary cannulation and sphincterotomy techniques at ERCP: European Society of Gastrointestinal Endoscopy (ESGE) Clinical Guideline. Pier Alberto Testoni, Alberto Mariani, Lars Aabakken, Marianna Arvanitakis, Erwan Bories, Guido Costamagna, Jacques Devière, Mario Dinis-Ribeiro, Jean-Marc Dumonceau, Marc Giovannini, Tibor Gyokeres, Michael Hafner, Jorma Halttunen, Cesare Hassan, Luis Lopes, Ioannis S. Papanikolaou, Tony C. Tham, Andrea Tringali, Jeanin van Hooft, Earl J. Williams. http://dx.doi.org/10.1055/s-0042-108641.Published online: 2016 Endoscopy© Georg Thieme Verlag KG Stuttgart · New York ISSN 0013-726X

53

PROTEIN RESTRICTION AUGMENTS WEIGHT LOSS AND GLUCOSE CONTROL FOLLOWING SLEEVE GASTRECTOMY

Julia Illiano, David Harris, Dudley Lamming, Luiz Lopez, Odin Schaepkens. *University of Wisconsin Madison*

Introduction/Background Sleeve gastrectomy (SG) improves obesity and Type 2 diabetes (T2D). The added therapeutic potential of post-operative dietary interventions on obesity and T2D are understudied. Following SG, patients increase dietary protein consumption, however, protein restriction induces weight loss, improves metabolic health, and extends lifespan in mice and humans.
Objective(s) We hypothesized reducing dietary protein intake following SG would improve post-operative weight loss, glucose tolerance, and metabolism.
Methods Sixty-four, C57BL/6J mice were preconditioned on high-fat, western diet (WD) starting at 5 weeks of age. At 17 weeks, mice were weight-matched and received SG or sham surgery. After recovery, mice were placed into 1 of 4 dietary groups: High (36%), medium (21%), or low protein (7%), or WD. All protein diets were isocaloric. A separate control group of 16 mice were preconditioned on normal chow diet (NCD; 5% fat, 24% protein), received SG or sham, and were maintained on NCD. Weights and food intake were tracked longitudinally. Glucose tolerance and insulin sensitivity were assessed via oral glucose and insulin tolerance testing, respectively. Body composition was determined through MRI spectroscopy. Energy expenditure (EE) was quantified using indirect calorimetry and normalized to lean mass. Grip strength was assessed using an inverted cling assay. Area under the curve analysis, one-way ANOVA with Dunnett corrections, and t-tests were used.
Results SG induced weight loss across all groups compared to their respective Shams. SG mice on 7% protein had higher percent weight loss compared to other SG groups despite having increased daily food intake compared to SG mice on 36% protein (p=0.02) or WD (p=0.01). SG mice on 36% protein and NCD had the lowest fat mass and 36% SG mice had significantly elevated lean mass compared to other SG groups. Notably, 7% SG mice had equivalent lean mass to NCD and 21% SG groups. All SG mice had improved glucose tolerance compared to their respective shams. 7% SG mice trended toward improved glucose tolerance (compared to WD p=0.08, 36% protein p=0.066, 21% protein p=0.019) and had significantly reduced fasting glucose compared to all SG groups (36% protein p=0.0217). This occurred independent of changes in insulin sensitivity, which was similar across all groups. EE per gram of lean mass was increased in all mice consuming 7% compared to 36% protein in light and dark cycles (Sham p=0.0082, SG p=0.04). Across both surgical groups, there is a step-wise decrease in EE as the percent of protein in the diet increases. Strength (Cling time) did not differ between sham and SG mice in any diet group or when comparing 36% and 7% SG mice.
Conclusion Protein restriction enhances weight loss and improves T2D control after SG. This occurs independent of changes in insulin sensitivity and has minimal effects on overall lean mass or grip strength. However, high protein diets after SG may promote maximal lean mass gains, potentially contributing to improved insulin sensitivity. As a result, manipulating protein intake after SG may improve metabolic health outcomes for patients and will likely need to be individually tailored.

54

IS INPATIENT FECAL IMMUNOHISTOCHEMICAL TESTING (FIT) USEFUL FOR PREDICTING COLONOSCOPY OUTCOMES

[1]Katherine Janike, [1]Dexter Nwachukwu, [1]Hasan Raza, [1]Claire Shin,[2]Gabriel Marrero-Rivera, [1]Keith Naylor.
[1]*University of Illinois At Chicago;* [2]*University of Pittsburgh Medical Center*

Introduction/Background Evidence supports fecal immunohistochemical testing (FIT) for routine screening of colorectal cancer (CRC) in asymptomatic patients, however FIT is often used in the inpatient setting to evaluate the source of symptoms in patients with acute illness. Studies have shown that inpatient FIT has led to extended hospital stay and increased use of unnecessary procedures. We studied colonoscopy outcomes after inpatient FIT to better understand FITs utility in predicting disease at our tertiary care center.
Objective(s) To review inpatient FIT results, colonoscopy outcomes, and evaluate FITs utility in screening for CRC and sources of bleeding in acute illness.
Methods We conducted a retrospective cross-sectional study by reviewing electronic health records (EHR) of patients aged 45-75 who underwent FIT between January 1, 2016 and December 31, 2020. The study population was further narrowed to patients who had FIT while inpatient and had a colonoscopy completed after FIT resulted. We collected data on age, gender, ethnicity, reason for fit, and colonoscopy outcomes including presence of tubular adenomas, advanced adenomas, colorectal cancer, hemorrhoids, and diverticulosis . We used SAS, version 9.5 (SAS Institute Inc., Cary, North Carolina) for data analysis. Differences in colonoscopy outcomes associated with fit tests were assessed using Chi-Square test. Mean number of days from fit test to colonoscopy was compared by t-test.
Results Of the 656 patients with FIT test completed in the study period, we identified 157 FITs that had been completed while a patient was in the ER or admitted to the hospital. Of the 157 FITs completed inpatient, 89 had colonoscopies after FIT results. The most common reasons for obtaining inpatient FIT was anemia (56%), gastrointestinal bleeding (16%), abdominal pain (5%), and diarrhea (5%) (Table 3). There was no difference in subsequent colonoscopy outcomes between patients with positive FIT and those with negative FIT results (Table 2). The average number of days between positive FIT and colonoscopy was 191 days (SD 308) compared to negative FIT 298 days (SD 320), which was not statistically significant (Table 2). None of the patients who had inpatient FIT were diagnosed with colorectal cancer.

Abstract 54 Table 1 Demographics (N=89)

Demographic variable	
Age, years ± SD	61.52 ± 8.19
Female, n (%)	45 (50.56)
Race/ethnicity, n (%)	
Non-Hispanic White	7 (7.87)
African American	47 (52.81)
Asian/Pacific Islander	2 (2.25)
Hispanic	28 (31.46)
Other (e.g., decline to state, multirace)	5 (5.62)

Abstract 54 Table 2 Association between FIT test and colonoscopy results

Colonoscopy result	All (n=89)	FIT Test Result		Chi-square analysis or ttest analysis	Logistics regression analysis[1]
		Positive (n=54)	Negative (n=35)		
Abnormal colonoscopy	68 (76.40)	43 (79.63)	25 (71.43)	χ^2=0.7923; P=0.3734	χ^2=1.0299; P=0.3102
Tubular adenoma	27 (30.34)	16 (29.63)	11 (31.43)	χ^2=0.0325; P=0.8569	χ^2=0.0063; P=0.9367
Advanced adenoma	2 (2.25)	2 (3.70)	0 (0)	χ^2=1.3261; P=0.2495	χ^2=0.0155; P=0.9008
Colorectal Cancer	0 (0)	0 (0)	0 (0)	NA	NA
Hemorrhoids	51 (57.30)	33 (61.11)	18 (51.43)	χ^2=0.8137; P=0.3670	χ^2=1.5273; P=0.2165
Diverticulosis	26 (29.21)	16 (29.63)	10 (28.57)	χ^2=0.0115; P=0.9146	χ^2=0.0000; P=0.9950
Days between FIT test and colonoscopy test, days, mean±SD	233.67 ± 315.79	191.59 ± 308.40	298.60 ± 320.47	t= -1.57; df=87; P=0.1190	

Abstract 54 Table 3 Associations between FIT indication and colonoscopy results.[1] Other include constipation, weight loss, CRC screening, and ileus

Colonoscopy result	FIT Indication					
	Anemia (n=56)	GI bleeding (n=16)	Abdominal pain (n=5)	Diarrhea (n=5)	Other[1] (n=7)	
Abnormal colonoscopy	43 (76.79)	13 (81.25)	5 (100.00)	4 (80.00)	3 (42.86)	p= 0.1873
Tubular adenoma	18 (32.14)	5 (31.25)	1 (20.00)	2 (40.00)	1 (14.29)	p=0.8407
Advanced adenoma	1 (1.79)	1 (6.25)	0 (0)	0 (0)	0 (0)	p=0.8066
Colorectal Cancer	0 (0)	0 (0)	0 (0)	0 (0)	0 (0)	NA
Hemorrhoids	29 (51.79)	13 (81.25)	3 (60.00)	4 (80.00)	2 (28.57)	p=0.0962
Diverticulosis	15 (26.79)	4 (25.00)	4 (80.00)	2 (40.00)	1 (14.29)	p=0.1087
Days between FIT test and colonoscopy test, days, mean±SD	261.25 ± 350.69	230.94 ± 312.60	197.20 ± 210.52	143.00 ± 143.27	110.147 ± 121.92	p=0.3181

Conclusion The intended use of FIT is colorectal cancer screening. The majority of inpatient FITs in this study were ordered for reasons other than colorectal cancer screening. Though the testing mechanism is identifying hemoglobin in the stool, there was no significant difference in outcomes of colonoscopy that cause occult or non-occult bleeding between positive and negative FIT groups. FIT testing inpatient is not an effective tool to screen for sources of bleeding or colorectal cancer.

REFERENCE(S)

1.   Cancer Facts and Figures: 2020. (2020). Accessed July 23, 2021.
       https://www.cancer.org/content/dam/cancer-org/research/cancer-facts-and-statistics/annual-cancer-facts-and-figures/2020/cancer-facts-and-figures-2020.pdfYang DX, Gross CP, Soulos PR, Yu JB.

2. Estimating the magnitude of colorectal cancers prevented during the era of screening: 1976 to 2009. Cancer 2014;120(18):2893–901.   Noone A., Howlader N, Krancho M et al. SEER

3. Cancer Statistics Review 1975-2015. National Cancer Institute, Bethesda, MD.US Preventive Services Task Force. Screening for Colorectal Cancer: US Preventive Services Task Force Recommendation Statement. JAMA. 2021;325(19):1965–1977. Quintero E., Castells A., Bujanda L. et al.

4. Colonoscopy versus Fecal immunochemical Testing in Colorectal Cancer Screening. N Engl J Med 2012; 366:697-706.Gupta S, Halm EA, Rockey DC, et al.

5. Comparative Effectiveness of Fecal Immunochemical Test Outreach, Colonoscopy Outreach, and Usual Care for Boosting Colorectal Cancer Screening Among the Underserved: A Randomized Clinical Trial. JAMA Intern Med. 2013; 173(18):1725-1732.Lee YC, Li-Sheng Chen S, Ming-Fang Yen A, et al.

6. Association Between Colorectal Cancer Mortality and Gradient Fecal Hemoglobin Concentration in Colonoscopy Noncompliers. Journal of the National Cancer Institute. 2017;109(5):djw269. Flugelman AA, Stein N, Segol O, et al.

7. Delayed Colonoscopy Following a Positive Fecal Test Result and Cancer Mortality. JNCI Cancer Spectr. 2019;3(2):pkz024. Corley DA, Jensen CD, Quinn VP et al.

8. Association Between Time to Colonoscopy After a Positive Fecal Test Result and Risk of Colorectal Cancer and Cancer Stage at Diagnosis. JAMA. 2017; 317(16):1631–41.

9. Cusumano VT and May FP. Making FIT Count: Maximizing Appropriate Use of the Fecal Immunochemical Test for Colorectal Cancer Screening Programs. J Gen Intern Med. 2020; 35(6):1870-4Robertson, Douglas J., and Kevin Selby.

10. "Fecal Immunochemical Test: The World's Colorectal Cancer Screening Test." Gastrointestinal Endoscopy Clinics of North America, vol. 30, no. 3, 2020, pp. 511–26, https://doi.org/10.1016/j.giec.2020.02.011.Bhatti, Umer MD1; Jansson-Knodell, Claire MD1; Saito, Akira MD1; Han, Andrew MD1; Krajicek, Edward MD2; Imperiale, Thomas F. MD3; Fayad, Nabil MD1. S1259

11. Inappropriate Use of Fecal Immunohistochemical Testing (FIT) in the Hospital and Emergency Department: FIT Is Un-FIT for Inpatient and Emergency Use. The American Journal of Gastroenterology 115():p S632, October 2020. | DOI: 10.14309/01.ajg.0000707084.49259.f7 Soin S, Akanbi O, Ahmed A, Kim Y, Pandit S, Wroblewski I, Saleem N.

12. Use and abuse of fecal occult blood tests: a community hospital experience. BMC Gastroenterol. 2019 Sep 3;19(1):161. doi: 10.1186/s12876-019-1079-9. PMID: 31481027; PMCID: PMC6724234. Narula N, Ulic D, Al-Dabbagh R, Ibrahim A, Mansour M, Balion C, Marshall JK.

13. Fecal occult blood testing as a diagnostic test in symptomatic patients is not useful: a retrospective chart review. Can J Gastroenterol Hepatol. 2014 Sep;28(8):421-6. doi: 10.1155/2014/189652. Epub 2014 Jul 11. PMID: 25014182; PMCID: PMC4210232.Mosadeghi S, Ren H, Catungal J, Yen I, Liu B, Wong RJ, Bhuket T.

14. Utilization of fecal occult blood test in the acute hospital setting and its impact on clinical management and outcomes. J Postgrad Med. 2016 Apr-Jun;62(2):91-5. doi: 10.4103/0022-3859.180553. PMID: 27089107; PMCID: PMC4944357.Bhatti U, Jansson-Knodell C, Saito A, Han A, Krajicek E, Han Y, Imperiale TF, Fayad N.

15. Not FIT for Use: Fecal Immunochemical Testing in the Inpatient and Emergency Settings. Am J Med. 2022 Jan;135(1):76-81. doi: 10.1016/j.amjmed.2021.08.004. Epub 2021 Sep 9. PMID: 34508698.

55

COMPARISON OF THE UTILIZATION, QUALITY, AND FOLLOW UP OF FECAL IMMUNOCHEMICAL TEST IN COLORECTAL CANCER SCREENING AND NON-COLORECTAL CANCER SCREENING.

[1]Claire Shin, [2]Gabriel Marrero-Rivera, [1]Katherine Janike, [1]Hasan Raza, [1]Dexter Nwachukwu, [1]Keith Naylor.
[1]*University of Illinois at Chicago*; [2]*University of Pittsburg*

Introduction/Background Colorectal cancer (CRC) is the second leading cause of cancer-related mortality in the US, with over 50,000 deaths expected in the year 2020 [1]. Despite its disease burden in our population, effective colorectal cancer screening and surveillance programs have been shown to reduce CRC incidence and mortality [2,3]. The fecal immunochemical test (FIT) is one mode of first-line CRC screening that has resulted in higher screening participation due to its cost-effectiveness, accessibility, and noninvasive approach, especially in underserved communities [4,5]. Despite its only indication for CRC screening, FIT has been widely used inappropriately [6-8].

Objective(s) Our aim was to compare the utilization, quality, and follow-up of FIT for CRC screening and non-CRC screening.

Methods A total of 581 patients from a single tertiary center who have received FIT leading to colonoscopy were included in the study. Exclusion criteria included patient age less than 45, age greater than 75, personal history of malignant neoplasm of large intestine, rectum, rectosigmoid junction, and anus, adenomatous colonic polyps, inflammatory bowel disease, and genetic susceptibility to other malignancies. Patients were divided into two groups: FIT positive for CRC screening and FIT positive for non-screening. Demographics, insurance, colonoscopy findings, bowel preparation quality, and time to colonoscopy were analyzed using a chi-square test and t-test. Association with adenoma detection for CRC screening vs. non-screening indication was analyzed using the multivariate analysis using STATA.

Results The comparison of demographics of the two groups shown in table 1 did not differ significantly. There were no differences based on race or insurance. The CRC screening group had a higher likelihood of having an adenoma on their colonoscopy. The non-screening group (204.1 days ± 253) took longer time for colonoscopy compared to the screening group (121.3 days ± 161). Table 2 shows that factors positively associated with adenoma presences are increasing age, and good bowel prep; while, poor prep, inadequate prep, and a non-screening indication were negatively associated with having an adenoma. Colonoscopy indications for FIT for the non-screening group include anemia (34.9%), hematochezia (32.6%), bowel habit change (12.2%), abdominal pain (8.7%), weight loss (5.2%), abnormal CT findings (1.7%), and miscellaneous (4.7%).

Abstract 55 Table 1 The comparisons of demographics, health insurance, colonoscopy findings, bowel preparation quality, and time-to-colonoscopy.

	Total n = 581 (%)	FIT for CRC screening n = 453 (%)	FIT for non-screening n = 128 (%)	p-Value
Age Mean (± S. D.)	58.2 ± 7.2	58.4 ± 7	57.3 ± 8	0.137
Sex				
Female	238 (41.0)	183 (40.4)	55 (43.0)	0.601
Race				
White	83 (14.3)	60 (13.3)	23 (18.0)	0.439
Black	313 (53.9)	246 (54.3)	67 (52.3)	
Asian	17 (2.9)	15 (3.3)	2 (1.6)	
Not recorded	168 (28.9)	132 (29.1)	36 (28.1)	
Ethnicity				
Hispanic	162 (27.9)	124 (27.4)	38 (29.7)	0.423
Non-Hispanic	408 (70.2)	322 (71.1)	86 (67.2)	
Not recorded	11 (1.9)	7 (1.6)	4 (3.1)	
Health Insurance				
Private	273 (47.0)	224 (49.5)	49 (38.3)	0.149
Medicare	153 (26.3)	117 (25.8)	36 (28.1)	
Medicaid	140 (24.1)	101 (22.3)	39 (30.5)	
Charity care	13 (2.2)	9 (2.0)	4 (3.1)	
Self-pay	2 (0.3)	2 (0.4)	0 (0)	
Colonoscopy findings				
Adenomatous polyp	223 (38.4)	194 (42.8)	29 (22.7)	<0.001
Advanced adenoma	18 (3.1)	15 (3.3)	3 (2.3)	0.577
Colon cancer	1 (<1.0)	1 (<1.0)	0 (0)	0.764
Diverticulosis	213 (37.1)	164 (36.8)	49 (38.3)	0.989
Hemorrhoids	303 (52.5)	233 (51.9)	70 (54.7)	0.577
Bowel preparation quality				
Excellent	353 (60.9)	282 (62.4)	71 (55.5)	0.056
Good	152 (26.2)	120 (26.6)	32 (25.0)	
Fair	34 (5.9)	21 (4.7)	13 (10.2)	
Poor	20 (3.5)	16 (3.5)	4 (3.1)	
Unsatisfactory	21 (3.6)	13 (2.9)	8 (6.3)	
Time-to-colonoscopy				
Mean (± S. D.)	132.4 ± 177	121.3 ± 161	204.1 ± 253	0.049

Abstract 55 Table 2 Odds ratios for the multivariate analysis of factors associated with adenoma detection during colonoscopy following FIT for CRC screening or a non-screening indication.

Characteristic	Categories	OR	95% CI
Age		1.03	(1.00, 1.05)
Sex	Male	1.00	Reference
	Female	1.08	(0.75, 1.55)
Bowel preparation quality	Excellent	1.00	Reference
	Good	1.63	(1.10, 2.43)
	Fair	1.15	(0.53, 2.50)
	Poor	0.10	(0.01, 0.78)
	Unsatisfactory	0.11	(0.01, 0.88)
Hemorrhoids found	No	1.00	Reference
	Yes	1.09	(0.75, 1.56)
Diverticula found	No	1.00	Reference
	Yes	1.10	(0.76, 1.58)

Indication	CRC Screening	1.00	Reference
	Non-screening indication	0.39	(0.25, 0.63)

Conclusion The comparison of the two groups shows that the FIT for CRC screening group was more likely to receive better preparation and to have adenoma detected on their colonoscopy. 22.0% of FIT tests were being ordered for non-CRC screening purposes with the most ordered indication of anemia followed by hematochezia.

REFERENCE(S)
1. Cancer Facts and Figures: 2020. (2020). Accessed July 23, 2021. https://www.cancer.org/content/dam/cancer-org/research/cancer-facts-and-statistics/annual-cancer-facts-and-figures/2020/cancer-facts-and-figures-2020.pdf
2. Yang DX, Gross CP, Soulos PR, Yu JB. Estimating the magnitude of colorectal cancers prevented during the era of screening: 1976 to 2009. Cancer 2014;120(18):2893–901.
3. Noone A., Howlader N, Krancho M et al. SEER Cancer Statistics Review 1975-2015. National Cancer Institute, Bethesda, MD.
4. US Preventive Services Task Force. Screening for Colorectal Cancer: US Preventive Services Task Force Recommendation Statement. JAMA. 2021;325(19):1965–1977.
5. Quintero E., Castells A., Bujanda L. et al. Colonoscopy versus Fecal immunochemical Testing in Colorectal Cancer Screening. N Engl J Med 2012; 366:697-706.
6. Masood, U., Bernshteyn, M., Pavelock, N., Singh, K., Schad, L. A., Morley, C. P., Gupta, A., Jasti, V., & Murthy, U. (2022). Appropriateness of fecal immunochemical testing utilization for colorectal cancer screening at an academic center. Proceedings (Baylor University. Medical Center), 36(1), 20–23. https://doi.org/10.1080/08998280.2022.2123667
7. Bhatti, U., Jansson-Knodell, C., Saito, A., Han, A., Krajicek, E., Han, Y., Imperiale, T. F., & Fayad, N. (2022). Not FIT for Use: Fecal Immunochemical Testing in the Inpatient and Emergency Settings. The American journal of medicine, 135(1), 76–81. https://doi.org/10.1016/j.amjmed.2021.08.004
8. Gluskin, A. B., Dueker, J. M., & Khalid, A. (2021). High Rate of Inappropriate Fecal Immunochemical Testing at a Large Veterans Affairs Health Care System. Federal practitioner : for the health care professionals of the VA, DoD, and PHS, 38(6), 270–275. https://doi.org/10.12788/fp.0142

56

PASSAGE OF FOOD BOLUS USING GLUCAGON IN THE PRESENCE OF A SCHATZKI RING

[1]Austin Reed, [1]Suhaib Bajwa, [1]Sanket Basida, [1]Emily Reznicek, [1]Ahmad Ali, [2]Daniel Lovinger. [1]*University of Missouri-Columbia;* [2]*Harry S. Truman VA*

Introduction/Background A 73-year-old male was admitted for concern of food bolus impaction. Medical management with glucagon was initiated. The subsequent EGD performed demonstrated a lower esophageal Schatzki ring with esophagitis located both proximal and distal to the Schatzki ring, consistent with passage of a food bolus. This case represents successful medical management of a food bolus impaction in the setting of a Schatzki ring. Food bolus impactions are an increasingly common reason for hospital admissions. Typically, food bolus impactions are treated with therapeutic endoscopy, although on occasion medical management with glucagon can be trialed. Glucagon has been chosen previously for its proposed effect of the relaxation of the structures of the esophagus. We present a case of the passage of a food bolus using glucagon as medical therapy in the setting of a Schatzki ring.
Case Presentation A 73-year-old male presented to the Emergency Department (ED) for globus sensation of one day in duration. He had consumed a large dinner the night prior and reported symptom onset shortly after swallowing some ribs. Other symptoms reported included generalized chest discomfort, regurgitation of all liquids, and sialorrhea. His medical history included small cell lung cancer status post chemotherapy and radiation, coronary artery disease status post stenting, and chronic gastroesophageal reflux disease (GERD). Vital signs on initial presentation were noted to be afebrile with a temperature of 36.6 C, hypertensive at 177/72 mmHg, with a heart rate of 59 bpm, and saturating 94% on room air. Initial laboratory work demonstrated a normal amylase at 62 U/L, negative troponin at Gastroenterology was consulted for esophogastroduodenoscopy (EGD) evaluation of food bolus impaction. The patient was placed on a strict nothing by mouth diet in anticipation for an EGD to be performed the following morning. Given the patient's history of coronary artery disease, other etiologies of his symptoms including myocardial infarction were ruled out with a negative troponin and an ECG demonstrating normal sinus rhythm. Prior to the EGD evaluation, the patient overnight was given 1 milligram of intravenous glucagon to aid in passage of bolus. The next morning, upon inspection via endoscopy, the patient was noted to have passed the food bolus. There was mucosal irritation seen where food bolus was present (figure 2). Remaining EGD findings included a Schatzki ring and esophagitis located both proximal and distal to the ring where the food bolus had likely been impacted (figure 1 and 3). The Schatzki ring was broken via passage of the EGD scope. The patient tolerated the procedure without complications and was discharged the following day. A follow-up EGD six weeks later showed resolution of esophagitis.

Abstract 56 Figure 1
Distal esophagus with presence of a Schatzki ring

Abstract 56 Figure 2
Mucosal irritation likely at the site of impaction of the food bolus
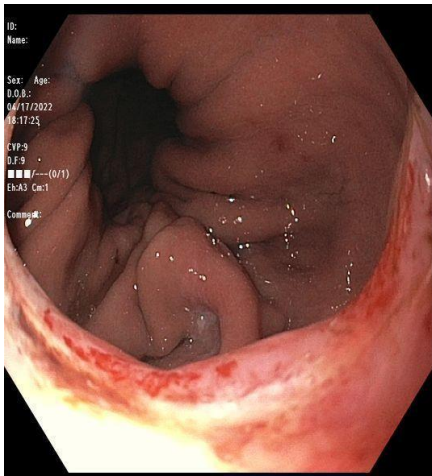
Abstract 56 Figure 3
LES with inflammation where food bolus had likely been impacted by Schatzki Ring. Large hiatal hernia likely precipitating reflux / schatzki ring formation

Discussion A Schatzki ring is a band of connective tissue and muscularis mucosa that forms under the normal esophageal mucosa at the level of the distal esophagus resulting in mechanical compression of the esophagus4. Often patients with a Schatzki ring present with dysphagia and are often treated with mechanical dilation to break the ring, which results in improvement in the size of the esophageal lumen5. Data from a retrospective review by Gurala et al. demonstrated that Schatzki rings account for roughly 8.6% of possible causes for food bolus impactions. Additional data from Gurala et al. showed the success rate of resolution of food bolus after utilization of glucagon ranged from 12 to 50%. The wide variability of the study was attributed to the high prevalence of strictures and Schatzki rings which significantly reduced the effectiveness of glucagon administration6. Glucagon is often trialed as a first line agent in the passage of a food bolus impaction due to its inhibitory effects on the smooth muscle of the gastrointestinal tract. This inhibitory effect is thought to be secondary to the release of nitric oxide and prostaglandin E2 after glucagon binds to receptors located in the smooth muscle of the gastrointestinal tract8. Specifically, when dosed at 0.25mg to 0.5mg, Glucagon has been shown to reduce the pressure across the lower esophageal sphincter (LES)1. The LES is a high-pressure zone that

separates the esophagus from the stomach, and overcoming this pressure allows for passage of food into the stomach. The pressure across the LES is primarily dictated by the smooth muscles comprising the LES, and relaxation of these smooth muscles due to inhibitory signals results in a decrease of pressure at the level of LES7. In the case of our patient, a Schatzki ring was located near the LES which further increased the LES pressure resulting in a food bolus impaction as the food bolus was unable to overcome the LES pressure with peristalsis. Glucagon usage in the case of our patient resulted in LES relaxation leading to decreased LES pressures allowing the food bolus to pass. This case represents the only report of successful medical management of a food bolus impaction in the setting of a Schatzki ring. Conclusion While endoscopy is the mainstay of treatment in management, glucagon remains a safe and often more affordable option for initial treatment of food bolus impaction2. Patients with anatomical variants, such as rings, webs, and strictures of the lower esophagus, are negative predictors of successful treatment of food bolus impaction through medical management with glucagon3. However, this should not discourage consideration of glucagon trial, as this case demonstrated successful passage of food bolus impaction with glucagon while in the presence of Schatzki ring.

REFERENCE(S)
1. Khayyat YM. Pharmacological management of esophageal food bolus impaction. Emerg Med Int. 2013;2013:924015. doi: 10.1155/2013/924015. Epub 2013 May 13. PMID: 23738071; PMCID: PMC3666276.
2. Haas J, Leo J, Vakil N. Glucagon Is a Safe and Inexpensive Initial Strategy in Esophageal Food Bolus Impaction. Dig Dis Sci. 2016 Mar;61(3):841-5. doi: 10.1007/s10620-015-3934-z. Epub 2015 Oct 24. PMID: 26500116.
3. Sodeman TC, Harewood GC, Baron TH. Assessment of the predictors of response to glucagon in the setting of acute esophageal food bolus impaction. Dysphagia. 2004 Winter;19(1):18-21. doi: 10.1007/s00455-003-0019-5. PMID: 14745641.
4. DeVault KR. Lower esophageal (Schatzki's) ring: pathogenesis, diagnosis and therapy. Dig Dis. 1996 Sep-Oct;14(5):323-9
5. Gonzalez A, Sullivan MF, Bonder A, Allison HV, Bonis PA, Guelrud M. Obliteration of symptomatic Schatzki rings with jumbo biopsy forceps (with video). Dis Esophagus. 2014 Sep-Oct;27(7):607-10
6. Gurala D, Polavarapu A, Philipose J, Amarnath S, Avula A, Idiculla PS, Demissie S, Gumaste V. Esophageal Food Impaction: A Retrospective Chart Review. Gastroenterology Res. 2021 Jun;14(3):173-178
7. Bajwa S, Toro F, Kasi A. Physiology, Esophagus. Statpearls. 2022 Jan. 8. Insuela, D. B. R., Daleprane, J. B., Coelho, L. P., Silva, A. R., e Silva, P. M. R., Martins, M. A., & Carvalho, V. F. (2015). Glucagon induces airway smooth muscle relaxation by nitric oxide and prostaglandin E2, Journal of Endocrinology, 225(3), 205-217.

57

METASTATIC DUODENAL SIGNET RING CELL ADENOCARCINOMA PRESENTING AS AN OBSTRUCTING COLONIC MASS: A CASE REPORT.

[1]Wasef Sayeh, [1]Omar Sajdeya, [1]Ziad Abuhelwa, [1]Sahithi Chinnam, [1]Ajit Ramadugu, [2]Mohammad Alshoha, [2]Tarik Alhmoud. [1]*University of Toledo Medical Center;* [2]*Toledo Hospital*

Introduction/Background Signet ring cell adenocarcinomas (SRCC) are a rare histological subtype of adenocarcinoma with a poor prognosis, typically due to advanced disease at the time of diagnosis. The stomach is considered the most common site for primary tumors in SRCC with more than 50% of cases of SRCC usually originating from the stomach1. However, other sites mainly in the gastrointestinal (GI) tract were identified. Here, we are presenting a rare case of duodenal SRCC with metastasis.

Case Presentation A 51-year-old female patient with a known past medical history significant for chronic gastroesophageal reflux disease (GERD), gastric ulcers, gastric bypass surgery with Roux-en-Y and cigarette smoking was complaining for abdominal pain of one month duration prior to her presentation. The pain was bandlike, stabbing in character, radiating to the back, and not associated with nausea or vomiting. Pain intensity was not changing in relation to food intake. Abdominal CT scan with IV contrast didn't reveal any acute pathology that could explain the pain. She was admitted to the hospital and was scheduled for a diagnostic endoscopic gastroduodenoscopy (EGD) which was performed on the next day and showed a healthy mucosal tissue along the esophagus, the gastrojejunostomy and the anastomotic limbs with no evidence of masses or malignancy. Patient returned to the ward after the procedure for further investigations of the pain. The patient's pain was increasing in intensity and became more severe. A repeat abdominal CT scan with IV contrast was done on day 7 of hospitalization and showed findings suggestive of hepatic flexure obstructing colonic mass causing dilation of the ascending colon, cecum, and small bowel proximally (figure 1). A diagnostic colonoscopy was scheduled after two days after having adequate bowel preparation. The colonoscopy showed a benign appearing colonic mass in the ascending colon with erythema and edema that couldn't be traversed (Figure 2). Biopsies were taken and the procedure was aborted without assessing the ascending colon. Biopsy results came back later showing atypical cells with findings suggestive of carcinoma. A few days later, an exploratory laparotomy was performed which revealed the presence of right upper quadrant mass extending from the duodenum and gastric remnant to the inferior surface of the liver and hepatic flexure resulting in complete colonic obstruction. Multiple biopsies were taken from the colonic mass, mesentery, omentum and peritoneum which all came back consistent with signet ring cell adenocarcinoma. The colonic biopsy showed that the signet ring cell adenocarcinoma has extensive infiltration into the submucosa, muscularis and subserosa, with unremarkable overlying colonic mucosa. Therefore, patient was diagnosed with metastatic signet ring cell adenocarcinoma with the duodenum suspected to be the primary origin of the malignancy.
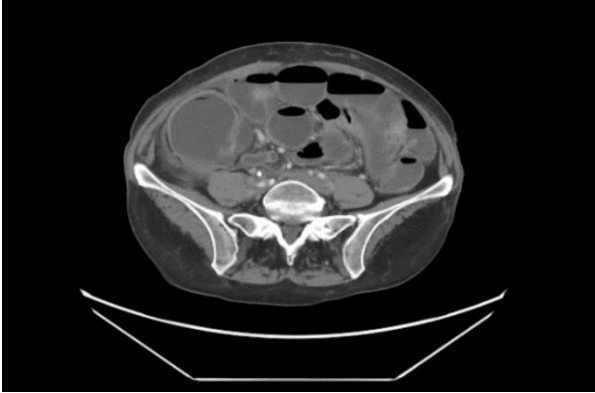
Abstract 57 Figure 1. Abdominal CT scan with IV contrast
Abdominal CT scan with IV contrast showing multiple air fluid levels and bowel dilation due to ascending colon obstruction.
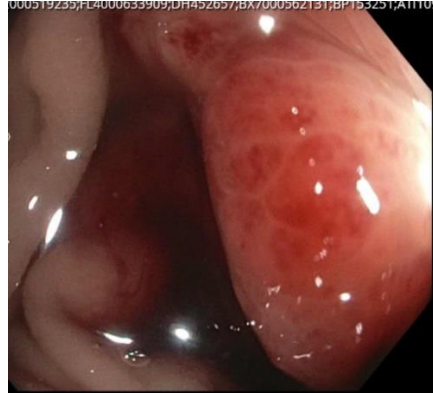
Abstract 57 Figure 2. colonoscopy picture of hepatic flexure. Colonoscopy showing a mass in the ascending colon.

Discussion We described a rare case of metastatic SRCC which was originating from the duodenum and caused a metastatic obstructing colonic mass. This type of cancer mainly originates from the GI tract with few cases reported to originate from other sites outside the GI track such as the breast, lungs, or ovaries. The stomach remains the most common origin for the cancer overall1. It is believed that around 90% of cases originates from stomach, esophagus, colon, and rectum. Very few cases were reported to be originating from other sites in the GI track such as in our case.

REFERNECE(S)
1.   Benesch MGK, Mathieson A. Epidemiology of Signet Ring Cell Adenocarcinomas. Cancers (Basel). Jun 11 2020;12(6)doi:10.3390/cancers12061544

58

A HETEROZYGOUS VARIANT OF TGFB3 IN A PATIENT WITH AN ATYPICAL PRESENTATION OF LOEYS-DIETZ SYNDROME: CASE REPORT AND REVIEW OF THE LITERATURE

[1]Meagan McNicholas, [2]Tarika Patel, [1]Christina Laukaitis. [1]*Carle Illinois College of Medicine*; [2]*University of Illinois Urbana-Champaign*

Introduction/Background Loeys-Dietz syndrome (LDS) is an autosomal-dominant connective tissue disorder characterized by the clinical triad of hypertelorism, bifid uvula or cleft palate, and aortic aneurysm.[1, 2] Mutations of genes encoding components of the transforming growth factor beta (TGFβ) signaling pathway are implicated in LDS. (1)LDS5 (Rienhoff syndrome), caused by TGFB3 mutations, is characterized by the syndromic presentation of early-onset of aortic aneurysms with a risk of dissections and rupture but clinical features vary among patients.[3]

Case Presentation A 42-year-old female born to nonconsanguineous parents with a history of persistent back and hip pain, hypermobile joints, and scoliosis treated with cervical spine fusion was referred to genetics for a connective tissue disorder evaluation.The patient denied a history of joint dislocation, pectus excavatum, wound dehiscence, hip dislocation or dysplasia, club feet, and heart murmurs. She was not aware of any pregnancy or birth complications and met appropriate milestones but was hospitalized for failure to thrive at age 2. She has pes planus, an umbilical hernia, and moderate myopia. Despite two uncomplicated pregnancies, a septate uterus was identified that complicated ablation for excessive bleeding leading to a hysterectomy.A physical exam revealed an arm span-to-height ratio of 1.07, a high-arched palate with crowding, and left corneal clouding. She had an increased range of motion but normal strength in the elbows, hips, and knees, and decreased motion with surgical scarring in the low back. The patient's skin was doughy with palpable bilateral piezogenic papules. Other examination findings were normal. An echocardiogram was normal with a tricuspid aortic valve and normal aortic measurements. Computed tomography of the brain was likewise normal.A four-generation pedigree showed a maternal aunt with a history of a cerebral aneurysm but no family history of thoracic aortic aneurysms, dissections, or other presentations of connective tissue disorders.The patient was evaluated using the 2017 diagnostic criteria for hypermobile Ehlers-Danlos Syndrome, however, the criteria were not fulfilled. Sequence analysis revealed a pathogenic variant, c.427A>T (p.Arg143*), in the TGFB3 gene, clarifying the diagnosis of LDS5.

Discussion Only a few studies have been published reporting patients with LDS5. TGFB3 mutations display reduced penetrance with variable expressivity both among families and unrelated probands. Two clinical triad features, hypertelorism and bifid uvula/cleft palate, were observed in 40% of patients but were not observed in this patient. Arachnodactyly, pes planus, joint laxity, scoliosis, and dental crowding are observed frequently in people with LDS5 and are also seen in our proband (table 1).The most interesting phenotypic variation is cardiac involvement. Out of 68 patients with TGFB3 mutations, dissections and aneurysms affected only 24% of people, even with case findings focused on cohorts ascertained for aneurysms (table 2) (4-11). Patients with LDS5 without cardiac/vascular involvement are enriched for children with the mutation, possibly because children are too young to have developed cardiac involvement. Our patient does not display any vascular changes but could still experience cardiac involvement in the future. When evaluating a patient for hypermobility, referral to genetics and the use of molecular sequencing help to clarify the diagnosis in people with atypical symptoms. The comparison of our patient with others with TGFB3 mutations illustrates that LDS5 can manifest with various clinical

features and vascular involvement. This highlights the value of more investigations to define the specific phenotype of LDS5 and further advance patient management in clinical practice.

Abstract 58 Table 1 *TGFB3* Phenotype Frequency in Reported Patients (n=68)

Feature	Frequency of feature (%)
Aortic dilation	42
Aneurysm & dissection	24
Dental Crowding	10
Bifid Uvula	40
Cleft palate	13
Hypertelorism	40
Micrognathia/retrognathia	31
Myopia	21
Tall stature/overgrowth/Marfanoid Habitus	51
Scoliosis	28
Pectus carinatum/excavatum	38
Pes planus	49
Arachnodactyly	54
Decreased muscle mass/muscular hypotonia	21
Reduced subcutaneous fat	16
Hernia	22
Joint laxity	49

Abstract 58 Table 2 Frequency of cardiac and vascular involvement categorized by age of *TGFB3* mutation report.

Age at report	Frequency of dilation (%)	Frequency of aneurysm/dissection (%)
0-10 years	1/11 (9)	1/11 (9)
11-20 years	4/9 (44)	0/9 (0)
21-30 years	6/10 (60)	0/10 (0)
31-40 years	2/6 (33)	1/6 (17)
41-50 years	5/14 (36)	4/14 (29)
>50 years	11/18 (61)	10/18 (56)

REFERENCE(S)

1.   MacCarrick, G., Black, J. H., 3rd, Bowdin, et al. (2014). Loeys-Dietz syndrome: a primer for diagnosis and management. Genetics in medicine : official journal of the American College of Medical Genetics, 16(8), 576–587. https://doi.org/10.1038/gim.2014.11

2.   Van Laer, L., Dietz, H., & Loeys, B. (2014). Loeys-Dietz syndrome. Advances in experimental medicine and biology, 802, 95–105. https://doi.org/10.1007/978-94-007-7893-1_7

3.   Hussein, D., Olsson, C., Lagerstedt-Robinson, K., & Moreira, T. (2021). Novel Mutation of the TGF-β 3 Protein (Loeys-Dietz Type 5) Associated With Aortic and Carotid Dissections: Case Report. Neurology. Genetics, 7(6), e625.

4.   Rienhoff, H. Y., Jr, Yeo, C. Y., Morissette, R., et al. (2013). A mutation in TGFB3 associated with a syndrome of low muscle mass, growth retardation, distal arthrogryposis and clinical features overlapping with Marfan and Loeys-Dietz syndrome. American journal of medical genetics. Part A, 161A(8), 2040–2046. https://doi.org/10.1002/ajmg.a.36056

5.   Bertoli-Avella, A.M., Gillis, E., Morisaki, H., et al. "Mutations in a TGF-β ligand, TGFB3, cause syndromic aortic aneurysms and dissections." Journal of the American College of Cardiology vol. 65,13 (2015): 1324-1336. doi:10.1016/j.jacc.2015.01.040

6.   Schepers, D., Tortora, G., Morisaki, et al. (2018). A mutation update on the LDS-associated genes TGFB2/3 and SMAD2/3. Human mutation, 39(5), 621–634. https://doi.org/10.1002/humu.23407

7.   Marsili, L., Overwater, E., Hanna, N., et al. (2020). Phenotypic spectrum of TGFB3 disease-causing variants in a Dutch-French cohort and first report of a homozygous patient. Clinical genetics, 97(5), 723–730. https://doi.org/10.1111/cge.13700

8.   Gouda, P., Kay, R., Habib, M., et al. (2022). Clinical features and complications of Loeys-Dietz syndrome: A systematic review. International journal of cardiology, 362, 158–167. https://doi.org/10.1016/j.ijcard.2022.05.065

9.   Kuechler, A., Altmüller, J., Nürnberg, P., et al. (2015). Exome sequencing identifies a novel heterozygous TGFB3 mutation in a disorder overlapping with Marfan and Loeys-Dietz syndrome. Molecular and cellular probes, 29(5), 330–334. https://doi.org/10.1016/j.mcp.2015.07.003

10.   Ziganshin, B. A., Bailey, A. E., Coons, C., et al. (2015). Routine Genetic Testing for Thoracic Aortic Aneurysm and Dissection in a Clinical Setting. The Annals of thoracic surgery, 100(5), 1604–1611. https://doi.org/10.1016/j.athoracsur.2015.04.106

11.   Matyas, G., Naef, P., Tollens, M., et al. (2014). De novo mutation of the latency-associated peptide domain of TGFB3 in a patient with overgrowth and Loeys-Dietz syndrome features. American journal of medical genetics. Part A, 164A(8), 2141–2143. https://doi.org/10.1002/ajmg.a.36593

Geriatrics

59

THE EXPERIENCES OF HIGH UTILIZERS WITH END-OF-LIFE CARE AND ADVANCE CARE PLANNING AS REPORTED BY PROXIES

Jamie Zeng, Makayla Betancourt, Omar Marin, Sriya Bandi, Alexandra Tate. *University of Chicago*

Introduction/Background Advance care planning (ACP) is defined as a process used to address, comprehend, and support an individual's preferences and goals for future medical care. This is particularly relevant in the event that an individual is in or approaching a sustained altered mental status while dealing with chronic or serious illness.[1] ACP is essential to prepare for the growing aging population who are high utilizers of the healthcare system particularly in providing EOL (end-of-life) care aligned with wishes and goals that also consider a palliative, quality-of-life based approach rather than simply defaulting to aggressive care.[2,3] ACP has been argued to be essential for psychosocial well-being in late life because patients and their caregivers report feeling more prepared for difficult EOL decisions.[4,5,6,7] This pilot study seeks to address the need for further investigation into the factors that facilitate or inhibit better ACP between patients and their care team and the various motivations behind deciding to prioritize quantity or quality of life at different stages of the EOL care process.

Objective(s) Aim 1: To explore factors that shaped EOL care experiences among high healthcare utilizers in their last year of life as reported by proxies after death. Aim 2: To examine whether and how ACP affected EOL care experiences of high healthcare utilizers in their last year of life as reported by proxies after death.

Methods This study utilized proxy postmortem interviews in which we interviewed caregivers and proxies identified by decedents at the time of their earlier enrollment into the Comprehensive Care Program (CCP) at UCMC. CCP is a care model that seeks to de-fragment care by randomizing high healthcare utilizers to two groups: treatment, in which their PCP administers care both in and out of the hospital, or control, in which their PCP only sees them for outpatient care. This defragmented model of care began in 2012. All enrollees are covered by Medicare or Medicaid and 90% of patients in this program self-identified as Black or African American, the majority hailing from the South side of Chicago. The study consisted of semi-structured qualitative interviews (n=6) conducted with proxies at least 4 months and no more than 2 years from the CCP patient's death. Interviews were conducted via Zoom meeting or phone. Proxies were asked a series of questions about the last year of the decedent's life, including frequency and nature of healthcare utilization, palliative and/or hospice use, other EOL care experiences—including facilitators and barriers to EOL care—and trust in providers, and the decedent's use of the healthcare system. After interviews were transcribed, we employed abductive analysis, a commonly-used social science approach to coding qualitative data.[8] This allowed us to establish a priori themes based on the literature and supported identification of new surprising themes as we coded interviews.

Results The following themes emerged: (1) trust/confidence in healthcare providers, (2) support of multiple social ties in end-of-life decision-making, (3) individual principles motivating pursuing certain types of care, (4) proxy confidence in decision-making and (5) orientation towards the treatment imperative. 1) Trust or lack thereof in the authority or expertise of doctors and perceptions of the hospital institution or individual healthcare providers (physicians, nurses, home health aides, etc.) influenced some patients' decisions regarding ACP and EOL care. 2) Most participants had at least one or multiple close familial caregiver(s) or other close social ties involved in caregiving and shared decision-making near the EOL, which both facilitated seeking treatment for acute health concerns and

coordinating EOL care. 3) Individual principles influenced by religion, spirituality, and financial concerns undergirded patients' or caregivers' decisions regarding ACP or desired end-of-life care. These were cited as reasons to both pursue or avoid aggressive life-sustaining treatments by different interviewees. In particular, faith/religion helped facilitate ACP documentation because of particular religious beliefs, such as attitudes towards transfusion. In others, it supported their acceptance of their decline. 4) Discussions and/or documentation of ACP preferences between patients, proxies, and healthcare providers prior to the patient's passing increased the proxies' confidence in making EOL decisions on behalf of the patient, with several interviewees feeling that they abided by their loved ones' wishes at the EOL. 5) Participants demonstrated an orientation toward the treatment imperative, a theoretical framework established by Shim, Russ and Kaufman (2008) describing the "inescapable obligation" to pursue medical treatment at any cost.9 Specifically, there was a willingness to seek medical care in hopes of remedying current medical conditions. Even within the last 12 months of life, whether or not there was ACP or formal discussion with doctors about prognostication, proxies reported that patients defaulted to medical intervention, particularly viewing hospital visits as having an important role in improving or maintaining their health.

Conclusion These preliminary findings have the potential to inform larger studies seeking to understand the relevant experiences of high healthcare utilizers in their last 12 months of life.

REFERENCE(S)
1.   Sudore RL, Lum HD, You JJ, et al. Defining advance care planning for adults: a consensus definition from a multidisciplinary delphi panel. Journal of Pain and Symptom Management. 2017;53(5):821-832.e1. doi:10.1016/j.jpainsymman.2016.12.331
2.   Medina L, Sabo S, Vespa J. Living Longer: Historical and Projected Life Expectancy in the United States, 1960 to 2060. US Department of Commerce, US Census Bureau; 2020.
3.   Bees J. The Coming "Silver Tsunami" of Dementia Patients. NEJM Catalyst. 2(9). doi:10.1056/CAT.21.0296
4.   Institute of Medicine. Dying in America: Improving Quality and Honoring Individual Preferences near the End of Life. National Academies Press; 2015.
5.   Dixon J, Karagiannidou M, Knapp M. The Effectiveness of Advance Care Planning in Improving End-of-Life Outcomes for People With Dementia and Their Carers: A Systematic Review and Critical Discussion. Journal of Pain and Symptom Management. 2018;55(1):132-150.e1. doi:10.1016/j.jpainsymman.2017.04.009
6.   Song JA, Oh Y. The Association Between the Burden on Formal Caregivers and Behavioral and Psychological Symptoms of Dementia (BPSD) in Korean Elderly in Nursing Homes. Archives of Psychiatric Nursing. 2015;29(5):346-354. doi:10.1016/j.apnu.2015.06.004
7.   Sautter JM, Tulsky JA, Johnson KS, et al. Caregiver Experience During Advanced Chronic Illness and Last Year of Life. Journal of the American Geriatrics Society. 2014;62(6):1082-1090. doi:10.1111/jgs.12841
8.   Timmermans S, Tavory I. Theory Construction in Qualitative Research: From Grounded Theory to Abductive Analysis. Sociological Theory. 2012;30(3):167-186. doi:10.1177/0735275112457914
9.   Shim JK, Russ AJ, Kaufman SR. Late-life cardiac interventions and the treatment imperative. PLoS medicine. 2008;5(3):e7.

60

REASONS FOR PT NON-TREATMENT IN PATIENTS WITH FUNCTIONAL IMPAIRMENT DURING HOSPITALIZATION FOR MEDICAL ILLNESS

[1]Mahnoor Baig, [2]Daniel Young, [1]David Meltzer, [1]Maylyn Martinez. [1]*University of Chicago, Medicine*; [2]*University of Nevada, Las Vegas*

Introduction/Background Hospitalized patients spend 87-100% of their time in bed. This prolonged immobility contributes to the development of hospital-associated disability (HAD), defined as the new inability to perform one or more activities of daily living (ADLs) after discharge from the hospital without assistance. HAD is associated with increased readmissions, institutionalization, and death. Physical therapy (PT) is an invaluable tool to treat and prevent HAD but is a constrained resource in most hospitals. Given their limited numbers, it is important to optimize the time of physical therapists. Patients miss over 15% of inpatient PT sessions but little is known about the reasons for missed sessions, termed PT "non-treatment", in patients with specific indicators of the need for PT. Knowing this could contribute to the optimization of inpatient PT protocols, maximizing the time therapists spend with patients in need.

Objective(s) We aimed to identify reasons for PT nontreatment in patients hospitalized for acute medical illness using validated mobility measurement tools to indicate PT needs.

Methods We conducted a retrospective analysis of patients admitted to the University of Chicago Hospital's medical services between 8/2018 - 3/2021. We limited our cohort to patients ≥ 65 years old, with a length of stay of 7-10 days. To further limit our cohort to patients likely to need physical therapy, we selected patients with an Activity Measure Post-Acute Care (AM-PAC) mobility assessment scores of ≤ 18 at the time of admission, indicating functional impairment. The main outcome measures were the number of missed PT sessions and the reasons for missed PT sessions. We coded reasons for missed sessions as: 1 = patient declined due to symptoms/ condition, 2 = patient declined for non-medical reasons, 3 = patient gone for imaging/treatment/busy with healthcare providers, 4 = therapist deferred due to patient condition, 5 = no PT needed, and 6 = other. If a missed session was completed later the same day this was noted. Descriptive statistics were used to assess frequency and proportions of reasons for PT non-treatment.

Results Charts for 885 patients were reviewed based on eligibility criteria. In total, 2,100 PT sessions were completed including missed sessions that were completed later on the same day. A total of 461 sessions (22.0%) were missed without a makeup session later the same day. The most common reason for a missed PT sessions was "therapist deferred due to patient condition" (38.6%) followed by "patient gone for imaging/treatment/busy with healthcare providers" (27.5%), "patient declined for non-medical reasons" (14.9%), "patient declined due to symptoms/ condition" (8.4%), and "other" (5.5%). Sessions were not completed due to the therapist deeming treatment unnecessary in 5.2% of cases. The percentage of missed consultations that were completed later the same day was 0.8%.

Conclusion Our study demonstrates that patients miss nearly one out of every four PT sessions and more than 30% of these missed sessions are potentially avoidable. Improving ordering provider knowledge of what constitutes the need for PT and coordinating patient scheduling between all providers could optimize the use of PT time and facilitate the completion of PT sessions, which may reduce the development of HAD in patients with functional impairment on admission.

61

MOTIVATING SMOKING CESSATION IN AGING AFRICAN AMERICANS WHO SMOKE: FINDINGS FROM A CULTURALLY-SPECIFIC MESSAGE DEVELOPMENT STUDY

[1]Adrienne Johnson, [2]Lorraine Lathen. [1]*University of Wisconsin Center for Tobacco Research and Intervention; [2]Jump at the Sun Consultants, LLC*

Introduction/Background While the U.S. adult population has shown significant reduction in cigarette smoking since 2000, older adults who smoke remain stagnant in their cessation rates. Older adults who smoke are half as likely to quit smoking than younger counterparts, but more likely to succeed in quit attempts when using evidence-based smoking treatment. Recent research suggests the potential utility of dementia prevention messaging to motivate smoking cessation among older adults, but there are unique smoking-related factors associated with the African American/Black (AA/Black) community (i.e., later smoking onset, lower daily smoking rate, increased menthol cigarette use, and lower smoking cessation success than White counterparts) that suggest older AA/Black adults who smoke may benefit from tailored interventions. Culturally-specific interventions for AA/Black adults who smoke are beneficial in terms of intentions to quit, utilization of evidence-based smoking treatment resources, and cessation success. However, there has yet to be a culturally-specific message for older adult AA/Black people who smoke to motivate cessation attempts and increase the use of evidence-based smoking treatment.

Objective(s) Develop culturally-specific, patient-centered health-related messages for older adult AA/Black individuals with especially high potential to motivate smoking cessation attempts and increase evidence-based smoking treatment use.

Methods 8 focus groups and key informant interviews were conducted between February and March, 2022. Eligibility criteria included: self-identification as AA/Black, between 50-80 years old, no history of dementia or mild cognitive impairment (confirmed via MOCA-BLIND score > 19), self-reported current cigarette smoker. Interviews lasted ~60 minutes, used a semi-structured interview guide, were recorded and transcribed, were completed in person or virtually (via Zoom) and led by a trained moderator knowledgeable of smoking in AA/Black communities. All procedures were approved by the local Institutional Review Board and participants were compensated for their time and efforts.

Results Directed content analyses using a combination of deductive and inductive coding identified themes in 5 domains: concerns about aging, smoking and health risks, previous tobacco prevention messages, smoking cessation treatments, and recommendations for future tobacco prevention messages. Participants reported a variety of concerns about aging, recognizing many of them were related to their smoking. Contrary to previous research with primarily White older adults who smoke, dementia was no more important than any other health condition in motivating cessation attempts. Although participants were familiar with existing cessation advertisements, they did not feel represented in these advertisements and wanted more treatment guidance. Most participants reported a strong existing motivation to quit, but multiple barriers impeded their cessation success. One key barrier to quitting was access to cessation resources, and participants reported a strong desire for support groups with similar aged and race-concordant peers trying to quit smoking. Recommendations for future advertisements included highlighting the role of the tobacco industry in getting them addicted to smoking and profiting from them, monetary gain from quitting, and benefits of quitting at older age. Preliminary messages developed from these findings are presented in Figures 1-4.

Abstract 61 Figure 1.
Message highlighting tobacco industry profiting from African American/Black older adults who smoke.

Abstract 61 Figure 2.
Message highlighting benefit of quitting at older age.

Abstract 61 Figure 3.
Message highlighting financial burden of smoking and tobacco industry profiting from continued use.

Abstract 61 Figure 4.
Message highlighting tobacco industry targeting and profiting from African American/Black older adults who smoke.

Conclusion Findings highlight a need for increased resources to support cessation efforts in older adult AA/Black communities and the utility of developing culturally-specific messages. Future work should develop and test the acceptability and initial efficacy of these messages among an older AA/Black community.

62

TRAUMA, SUBSTANCE USE, AND SEXUAL RISK BEHAVIORS: ASSOCIATIONS EXAMINED AMONG SEXUAL AND GENDER MINORITIZED YOUTH

[1]Faith Summersett Williams, [2]Lisa Kuhns, [1]Nikki Iancki, [3]Sneha Pamulapati, [4]Niranjan Karnik, [4]Geri Donenberg, [2]Robert Garofalo. [1]*Northwestern University Feinberg School of Medicine*; [2]*Ann & Robert H.Lurie Childrens Hospital*; [3]*Midwestern University*; [4]*University of Illinois of Chicago*; [2]Robert Garofalo,

Introduction/Background In recent years, trauma exposure has emerged as a consistent correlate of sexual risk behaviors among adolescents and young adults who are vulnerable to HIV infection. It is unclear, however, whether substance use changes the strength of the association between trauma exposure and sexual risk-taking behaviors. Furthermore, these associations have not been explored among sexual minoritized populations such as young men who have sex with men (YMSM) and young transgender women (YTW), as these populations have been found to have an increased risk of trauma exposure and HIV infection compared to those identifying as heterosexuals. Most studies have examined sexual risk behaviors and trauma exposure among heterosexuals who engage in substance use, which may not capture the complexities and vulnerabilities of sexual minoritized groups. To our knowledge no studies have examined sexual risk behaviors, substance use, and trauma exposure in a community-recruited sample of sexual minoritized youth.

Objective(s) In this study, we examine whether the relationship between trauma exposure and sexual risk behaviors is moderated by substance use in YMSM and YTW.

Methods This study was designed as a retrospective cross-sectional analysis using baseline data previously gathered from 450 participants in a randomized trial of the effect of electronic screening and brief intervention on alcohol misuse, embedded in a community-based HIV rapid testing environment. Trauma was assessed with the Life Events Checklist (range=0-17), which screens for lifetime traumatic events, both direct and indirect (witnessed). Sexual risk behaviors were measured as the number of unprotected insertive or receptive sexual acts while under the influence in the past 3 months. We used regression models to examine the associations between trauma, substance use, and sexual risk behavior. Separate negative binomial regression models were fit for each substance of interest with and without the interaction terms. The likelihood ratio using chi-squared test for the model with and without the interaction term were compared to determine if the interaction term improved overall model fit.

Results The sample had a mean age of 22.7 (SD=2.1, range=16-25) and the vast majority identified as male (86.2%) in terms of gender, and gay or bisexual (85.8%) in terms of sexual orientation. Physical and sexual assault were the most frequently reported traumatic events experienced and witnessed. Median total trauma was 2, with mean of 2.99 (SD=2.90). Drug use in the study population varied with cannabis having the highest proportion of ever use (83%) and ever using street opioids having the lowest proportion (4%). Just over a quarter (25.8%) of the study population reported ever using stimulants. In addition, 44% reported binge drinking in the past month. Among those with reported binge drinking in the past month, as direct trauma score increased, the number of reported risky sexual acts increased to a greater extent compared to those who did not report binge drinking. No moderation was found for other substance misuse.

Conclusion The results of this study suggest binge drinking plays a crucial role in the relationship between trauma exposure and sexual risk-taking behaviors among sexual and gender minoritized youth. This study reaffirms the importance of screening for alcohol use and alcohol use disorders to help promote safe sex practices and prevent sexual-risk-taking behaviors in a population vulnerable to HIV exposure.

63

COULD RELAXIN BE A MARKER FOR PRO-TUMORAL MICROENVIRONMENT OF THYROID CANCER?

[1]Anupam Kotwal, [1]Robert Bennett, [2]Nicholas Whiteman, [3]Rhonda Simpson, [1]Swanson Benjamin, [1]Ana Yuil-Valdes, [1]Whitney Goldner. [1]*University of Nebraska Medical Center/Nebraska Medicine*; [2]*Gustavus College*; [3]*Omaha VA*

Introduction/Background Differentiated thyroid cancer (DTC) generally has a favorable prognosis, however, 30% have recurrence and progression hence there is a critical need to identify additional prognostic and potentially therapeutic markers. Relaxin inhibits the inflammatory macrophage type (M1) but promotes the anti-inflammatory macrophage type (M2) which is favorable for tumor growth, hence deserves to be investigated in the DTC tumor microenvironment (TME). We hypothesize that Relaxin is expressed in DTC and is associated with pro-tumoral macrophage infiltration.
Objective(s) To evaluate the role of Relaxin in relation to macrophage infiltration in human thyroid cancer tissue.
Methods A tissue microarray (TMA) with cores per specimen was created from surgical thyroid tissue from 55 adults with DTC localized to the neck. Fluorescent immunohistochemistry (FIHC) using antibodies against nucleus (DAPI), macrophage (CD68), M2 macrophage (CD163), and relaxin (RLN2) was performed on this TMA. Gene (qPCR) and protein (Western blot) expression of RLN2 and its receptor RXFP1 in thyroid cell lines were also identified.
Results The median age was 50 years (range 19-78), 73% were females, 65% were classic and 24% follicular variant of papillary thyroid cancer. 87% were AJCC stage I while the rest were stage II; 54% were ATA low risk, 31% intermediate risk and 15% high risk. Relaxin was strongly expressed in human DTC tissue (figure 1) and had a strong positive correlation with the abundance of CD163 (M2 macrophages) with an r2=0.55 (p< 0.0001) (figure 2) but did not colocalize with macrophages. In vitro experiments demonstrated variable expression of relaxin and its receptor RXFP1 in human thyroid cell lines (figure 3).
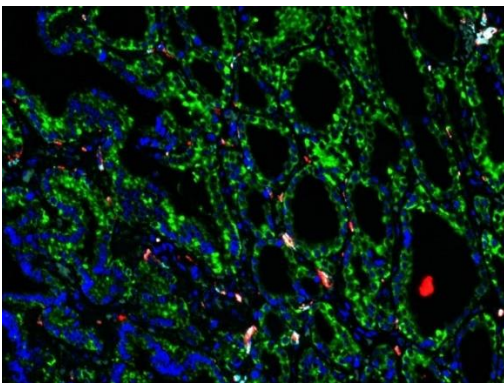
Abstract 63 Figure 1
Immunofluorescence image of experimental DTC core illustrating expression of RLN2, CD68, CD163, and nucleus.
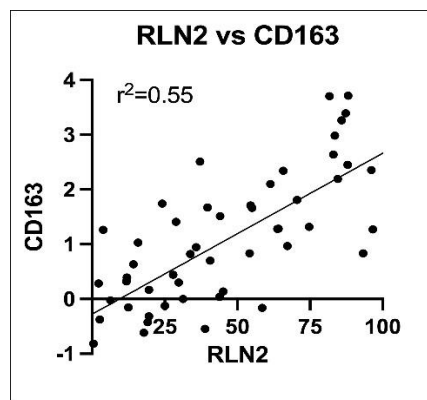
Abstract 63 Figure 2
Correlation of relative expression of RLN2 (experimental minus control) vs. relative expression of CD163 (experimental minus control). R2 value=0.55; p<0.0001

RLN2 and RXFP1 Expression in 7 Cell Lines
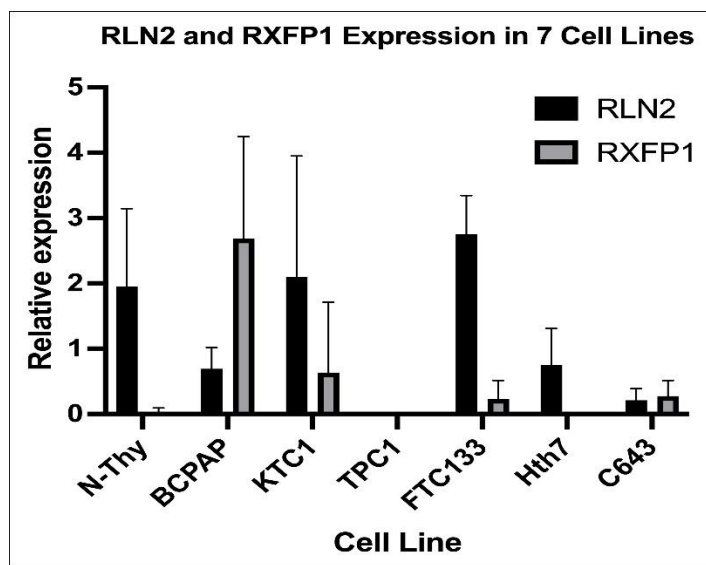
Abstract 63 Figure 3
qPCR analysis of gene expression in 7 thyroid cancer cell lines. Relative expression of RLN2 and RXFP1 calculated from mean of 3 qPCR trials compared to housekeeping TATA-box binding protein ($p<0.05$) (n=3).

Conclusion Our pilot study concluded that relaxin expression and its positive correlation with pro-tumoral M2 macrophage infiltration in the TME make it a potential biomarker for the occurrence and prognosis of DTC in humans. Thyroid cell lines' expression of relaxin and its receptor RXPF1 complement the TMA findings, hence may serve as a model for developing therapeutic options against advanced thyroid cancer.

64

UNDERSTANDING PHOSPHOLIPASE D2 ACTIVATION AND ITS ROLE IN VIRAL GENE EXPRESSION DURING DE NOVO KAPOSI SARCOMA-ASSOCIATED HERPESVIRUS (KSHV) INFECTION

Warren Nakazawa, Magdalena Dimitrova, Olivia Powrozek, Neelam Sharma-Walia. *Rosalind Franklin University*

Introduction/Background Kaposi's sarcoma-associated herpesvirus (KSHV), also known as human herpesvirus 8 (HHV8), is a double-stranded DNA virus implicated in the pathogenesis of Kaposi's sarcoma (KS), primary effusion lymphoma (PEL), and multicentric Castleman's disease (MCD). The induction of these cancers hinges on the replication of viral DNA in the host, as well as the latent and lytic cycles and associated proteins affecting viral gene expression. Phospholipase D2 (PLD2) is an enzyme that has been observed to play a role in neoplastic, proliferative cell growth and angiogenesis in various cell types. Generally, phospholipase D (PLD) hydrolyzes phosphatidylcholine to choline and phosphatidic acid. PLD2 specifically localizes to the plasma membrane of cells when overexpressed, whereas other PLD enzymes localize elsewhere. Knockout of PLD2 has been shown to inhibit hypoxic cellular responses, including the upregulation of hypoxia-inducible factor 1 alpha (HIF-1α) target genes and potentiation of VEGF-induced endothelial cell survival and angiogenesis. PLD inhibitors have been developed in hopes of decreasing the proliferative and angiogenic properties of multiple cancers, specifically showing promise in U87-MG glioblastoma cells. There is absence of research and literature on the implications of PLD2 inhibition in KSHV-induced cancers.
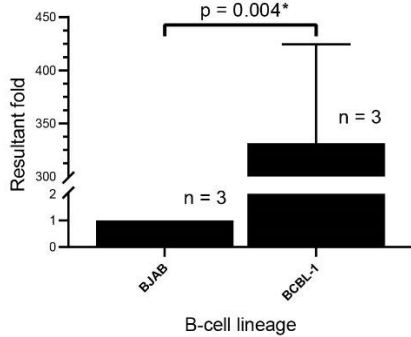
Objective(s) The primary objective of this study is to obtain novel information about the role of PLD2 during de novo KSHV infection, as well as about the effects of PLD2 inhibition in autophagic cell processes.

Methods BJAB (KSHV-negative B-cell lymphoma), BCBL-1 (KSHV-positive body cavity B-cell lymphoma), BC3 (KSHV-positive B-cell lymphoma), and HMVEC-d (human microvascular endothelial cells-dermal origin) cells were cultivated via feeding in their selective growth media and growth factors. HMVEC-d cells were infected with KSHV (10 MOI). RNA was extracted from BJAB, BCBL-1, BC-3, and BJAB-KSHV cells. RNA was extracted from HMVEC-d cells at different time points following KSHV infection. RNA from all cell types was converted to cDNA. RT-qPCR using SYBR Green was performed using GAPDH, a housekeeping gene, and PLD2 primers to quantify gene expression. PLD2 gene expression was normalized to GAPDH gene expression in all cell types.Cultivated BCBL-1 cells were treated with a PLD2 inhibitor for 48 hours. PLD2-inhibited BCBL-1 cells were incubated in RayBiotech human autophagy array 1. Densitometry data was collected and normalized to a solvent control in order to calculate relative protein expression. Relative fold gene expression of PLD2 for all cell lines was calculated and statistically analyzed using t-tests. Normalized values for relative autophagic protein expression were statistically analyzed via t-tests.

Results A statistically significant (p = 0.004) increase in gene expression was found in BCBL-1 cells compared to BJAB cells (figure 1). A statistically significant (p = 0.0144) increase in gene expression was found in HMVEC-d cells following two hours after initial infection compared to uninfected HMVEC-d cells (figure 2). Gene expression of various autophagic proteins was also quantified in PLD2 inhibitor treated BCBL-1 cells (Figures 3 and 4).

Abstract 64 Figure 1 Resultant fold of gene expression of PLD2 with respect to GAPDH in BJAB and BCBL-1 cell lines- RNA from BJAB, a KSHV-positive B-cell lymphoma, and BCBL-1, a KSHV-positive body cavity B-cell lymphoma, was extracted and converted to cDNA for analysis via RT-qPCR in order to quantify gene expression. GAPDH, a housekeeping gene, and PLD2 primers were utilized in the RT-qPCR. After normalization to gene expression of GAPDH, gene expression of PLD2 in BCBL-1 cells was 331.4-fold higher compared to BJAB cells (alpha = 0.05, p = 0.004).

Abstract 64 Figure 2 Resultant fold gene expression of PLD2 with respect to GAPDH in HMVEC-d cells infected with KSHV.
RNA from HMVEC-d (human microvascular endothelial cells-dermal origin) cells was extracted at different time points following de novo KSHV infection and again converted to cDNA for analysis via RT-qPCR. GAPDH, a housekeeping gene, and PLD2 primers were utilized in the RT-qPCR. After normalization to gene expression of GAPDH, gene expression of PLD2 in HMVEC-d cells two hours after de novo KSHV infection was 1.267-fold higher compared to uninfected HMVEC-d cells (alpha = 0.05, p = 0.0144).
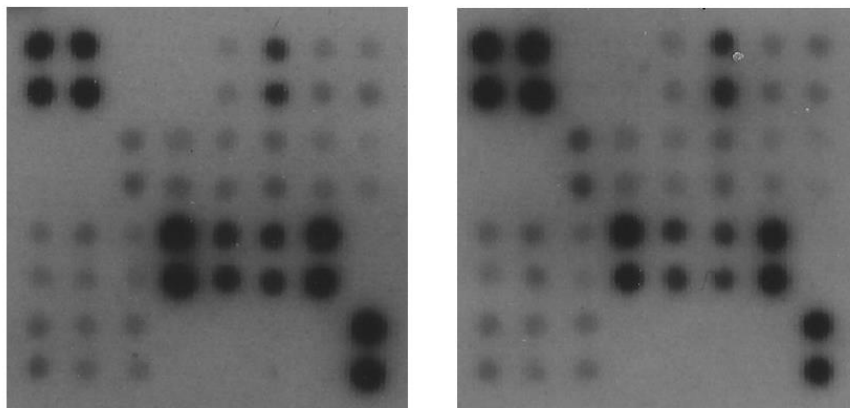
Abstract 64 Figure 3 Densitometry data from human autophagy protein array incubated with a solvent control (left) and with PLD2 inhibitor for 48 hours (right)

Conclusion In this study, PLD2 inhibition was shown to significantly affect regulation of a number of autophagic proteins The results of this study also demonstrate a significant increase in PLD2 gene expression in both previously infected KSHV B-cell lineages as well as B-cells infected de novo following two hours of infection. This may suggest an important role of PLD2 in KSHV infection of B cells. PLD2

should be investigated in this role with respect to expression of specifically latent and lytic genes in KSHV-infected cells to determine the potentiality of PLD2 inhibitors as a therapeutic agent.

REFERENCE(S)

1. Ganem, D. (2007). KSHV-induced oncogenesis. In A. Arvin, G. Campadelli-Fiume, E. Mocarski, P. S. Moore, B. Roizman, R. Whitley, & K. Yamanishi (Eds.), PubMed. Cambridge University Press. https://www.ncbi.nlm.nih.gov/books/NBK47373/Henkels, K. M., Short, S., Peng, H.-J., Fulvio, M. D., & Gomez-Cambronero, J. (2009).

2. PLD2 has both enzymatic and cell proliferation-inducing capabilities, that are differentially regulated by phosphorylation and dephosphorylation. Biochemical and Biophysical Research Communications, 389(2), 224–228. https://doi.org/10.1016/j.bbrc.2009.08.109Ghim, J., Moon, J.-S., Lee, C. S., Lee, J., Song, P., Lee, A., Jang, J.-H., Kim, D., Yoon, J. H., Koh, Y. J., Chelakkot, C., Kang, B. J., Kim, J.-M., Kim, K. L., Yang, Y. R., Kim, Y., Kim, S.-H., Hwang, D., Suh, P.-G., & Koh, G. Y. (2014).

3. Endothelial Deletion of Phospholipase D2 Reduces Hypoxic Response and Pathological Angiogenesis. Arteriosclerosis, Thrombosis, and Vascular Biology, 34(8), 1697–1703. https://doi.org/10.1161/atvbaha.114.303416Du, G., Huang, P., Liang, B. T., & Frohman, M. A. (2004).

4. Phospholipase D2 Localizes to the Plasma Membrane and Regulates Angiotensin II Receptor Endocytosis. Molecular Biology of the Cell, 15(3), 1024–1030. https://doi.org/10.1091/mbc.e03-09-0673Lee, C. S., Ghim, J., Song, P., Suh, P.-G., & Ryu, S. H. (2016).

5. Loss of phospholipase D2 impairs VEGF-induced angiogenesis. BMB Reports, 49(3), 191–196. https://doi.org/10.5483/bmbrep.2016.49.3.219Su, K.-Y., & Wu, Y.-J. (2020).

6. Updates on the diagnosis and management of multicentric Castleman disease. Tzu Chi Medical Journal, 0(0), 0. National Library of Medicine. https://doi.org/10.4103/tcmj.tcmj_15_20Nemunaitis, M. C., Schussler, J. M., Shiller, S. M., Sloan, L. M., & Mennel, R. G. (2009).

7. Primary effusion lymphoma diagnosed by pericardiocentesis. Proceedings (Baylor University. Medical Center), 22(1), 77–80. https://doi.org/https://doi.org/10.1080%2F08998280.2009.11928479Bishop, B. N., & Lynch, D. T. (2021).

8. Kaposi Sarcoma. PubMed; StatPearls Publishing. https://www.ncbi.nlm.nih.gov/books/NBK534839/Ganesan, R., Mahankali, M., Alter, G., & Gomez-Cambronero, J. (2015).

9. TWO SITES OF ACTION FOR PLD2 INHIBITORS: THE ENZYME CATALYTIC CENTER AND AN ALLOSTERIC, PHOSPHOINOSITIDE BINDING POCKET. Biochimica et Biophysica Acta, 1851(3), 261–272. https://doi.org/10.1016/j.bbalip.2014.12.007O'Reilly, M. C., Scott, S. A., Brown, K. A., Oguin, T. H., Thomas, P. G., Daniels, J. S., Morrison, R., Brown, H. A., & Lindsley, C. W. (2013).

10. Development of Dual PLD1/2 and PLD2 Selective Inhibitors From a Common 1,3,8-Triazaspiro[4.5]decane Core: Discovery of ML298 and ML299 that Decrease Invasive Migration in U87-MG Glioblastoma Cells. Journal of Medicinal Chemistry, 56(6), 2695–2699. https://doi.org/10.1021/jm301782e

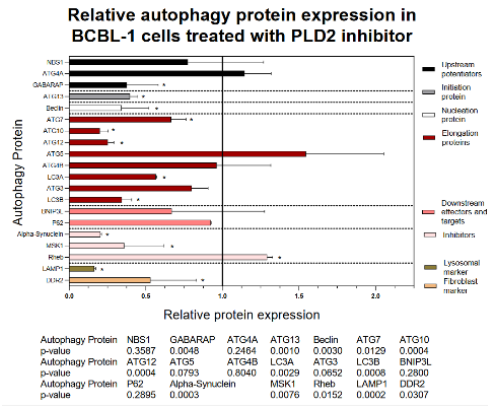**Abstract 64 Figure 4:** Relative autophagy protein expression in BCBL-1 cells treated with PLD2 inhibitor

Abstract 64 Figure 5: Resultant fold of gene expression of PLD2 with respect to GAPDH in untreated BJAB cells and BJAB cells infected de novo with KSHV

GATA2 SUPPRESSES CHROMOSOMAL INSTABILITY AND IS PREDICTIVE OF SURVIVAL IN ENDOMETRIAL SEROUS CARCINOMA

Apoorva Tarihalkar Patil, Tatiana Pavletich, Nicole Lacke, Demetra Pahopos, Stephanie McGregor, Daniel Matson. *University of Wisconsin School of Medicine and Public Health, Madison*

Introduction/Background Endometrial serous carcinoma (ESC) is an aggressive malignancy which occurs in elderly women and has a 5-year disease specific survival of 50%. Due to aggressive tumor behavior, all ESC patients are offered paclitaxel-carboplatin therapy and/or targeted radiation, resulting in significant morbidity. Currently, there are no robust disease markers predictive of ESC behavior or response to therapy. ESCs are characterized at the molecular level by p53 inactivation and high rates of chromosomal instability (CIN) which correlates with myometrial invasion and poor outcome. CIN occurs when cells loose or gain chromosomes or pieces of chromosomes during mitosis due to improper kinetochore (KT) attachments to the microtubule (MT) cytoskeleton. GATA-binding factor 2 (GATA2) is a transcription factor that binds genomic GATA motifs to promote transcriptional programs and enable development and function across multiple organs. GATA2 is expressed in the uterus where it functions with progesterone receptor to support embryo implantation.

Objective(s) 1. Evaluate GATA2 expression in patient ESCs using immunohistochemistry (IHC). 2. Compare GATA2 expression to clinicopathologic metrics. 3. Identify putative mechanism(s) through which GATA2 impacts ESC biology using patient-derived ESC cell lines.

Methods IHC: All work was approved by the UW-Madison IRB. IHC with custom rabbit anti-GATA2 polyclonal antibodies was performed on 70 patient derived ESCs and scored for percent positive nuclei, which was compared to clinicopathologic metrics.Tissue Culture: ARK-1 and ARK-2 ESC cell lines were provided by the Santin Laboratory (Yale) and grown in RPMI-1640 + 10% FBS and antibiotics. Depletion with anti-GATA2 siRNA or siScramble (Horizon Discovery) using Lipofectamine RNAiMAX (Life Technologies) was confirmed at 24 and 48 hr by western blot. CIN Assays: Aurora B signal strength was measured in 1 μM paclitaxel (Cayman) and 1 hr treatment with specific Aurora B inhibitor ZM447439 (ZM; Millipore). Monastrol (Enzo Life Sciences) washout experiments utilized 100 μM Monastrol for 5 hours followed by washout and incubation for 40 or 60 min. Multinucleation assays were performed post thymidine release for 24 hours in 12.5 nM paclitaxel.Immunofluorescence: Cells grown on lysine-coated coverslips were fixed in PHEM buffer + 2% paraformaldehyde (EMS) and 0.5% TX100 (Sigma). Primary antibodies: anti-Tubulin (DM1A, Cell Signaling), CREST sera (Antibodies Inc).Statistics: Statistical analyses were performed using GraphPad PRISM at $p < 0.05$.

Results 56% of ESCs are negative for GATA2 or contain only rare positive (low-GATA2), 20% of ESCs express GATA2 in 5-20% of nuclei (medium-GATA2), and 24% of ESCs express GATA2 in greater than 20% of nuclei (high-GATA2) (Fig. 1A-B). GATA2 expression did not correlate with patient age or tumor size (Fig. 1C-D), but high-GATA2 ESCs had less myometrial invasion (Fig. 1E), overall lower clinical stage, and had better disease-specific and overall survival compared to low-GATA2 ESCs (Fig. 1F-G). Depletion of GATA2 in patient-derived ESC cell lines (Fig. 2A) weakened the KT-MT error correction signal (Fig. 2B-C) resulting in elevated errors during mitosis compared to controls (Fig. 2D-F). Treatment of GATA2-depleted cells with paclitaxel resulted in elevated rates of multinucleation which was dependent on mitotic exit (Fig. 2G-I).

Conclusion We find that GATA2 is expressed in a subset of ESCs where it correlates with lower clinical stage at diagnosis and greatly improved patient outcome. In multiple patient-derived ESC cell lines, loss of GATA2 leads to a depleted KT-MT error correction signal, induction of CIN, and reduced capacity to faithfully segregate chromosomes upon paclitaxel treatment. Future studies aim to probe the factors

influencing GATA2 levels in patient ESCs and identify GATA2 transcriptional targets responsible for regulating CIN.

REFERENCE(S)

1. Siegel RL, Miller KD, Jemal A. Cancer statistics, 2020. CA: A Cancer Journal for Clinicians 2020;70:7–30.
2. McGunigal M, Liu J, Kalir T, et al. Survival Differences Among Uterine Papillary Serous, Clear Cell and Grade 3 Endometrioid Adenocarcinoma Endometrial Cancers: A National Cancer Database Analysis. Int J Gynecol Cancer 2017;27:85–92.
3. Tremblay M, Sanchez-Ferras O, Bouchard M. GATA transcription factors in development and disease. Development 2018;145.
4. Lentjes MHFM, Niessen HEC, Akiyama Y, et al. The emerging role of GATA transcription factors in development and disease. Expert Rev Mol Med 2016;18.
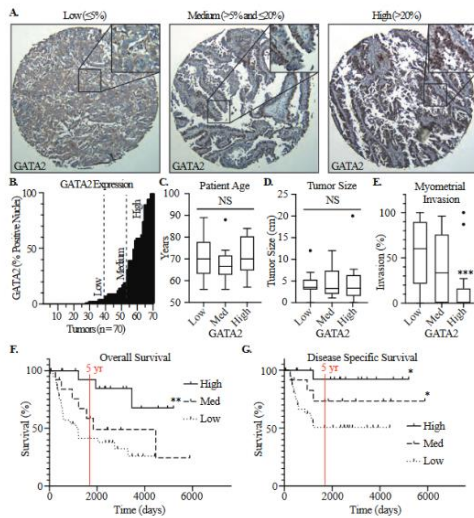
Abstract 65 Figure 1: High GATA2 expression in endometrial serous carcinoma (ESC) negatively correlates with myometrial invasion and is a positive predictor of survival.
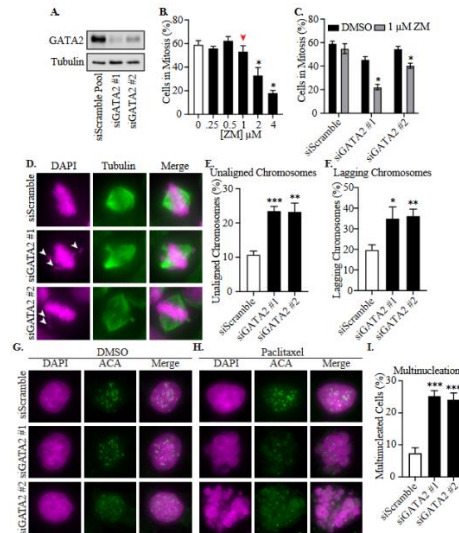
Abstract 65 Figure 2: GATA2 depletion in endometrial serous carcinoma (ESC) cells results in deficient kinetochore-microtubule (KT-MT) error correction and molecular hallmarks of chromosomal instability.

66

DELETION OF CCZ1 OR RMC1 ENHANCES ERYTHROID PROLIFERATION IN HUDEP2 CELLS

Masaki Ito, Greggory Myers, Rami Khoriaty. *University of Michigan Medical School*

Introduction/Background To prevent the development of anemia, the human body must produce ~2 million red blood cells (RBC) every second. Although the majority of the cell extrinsic factors that promote erythroid differentiation have been identified, the repertoire of erythroid genes that are required for erythroid differentiation remains poorly described.

Objective(s) The objective of this experiment is to identify genes that impair or enhance erythroid maturation and proliferation.

Methods We developed a genome-scale CRISPR knock-out screen to identify the repertoire of genes that are critical for erythroid differentiation, using the human erythroid cell line, HUDEP2. HUDEP-2 cells are maintained at the early proerythroblast cell stage but can be induced to differentiate to orthochromatic erythroblasts when cultured in 'differentiation media'. The abundance of sgRNAs for each gene was compared between orthochromatic erythroblasts and proerythroblasts.

Results This screen identified two candidate genes that had sgRNAs enriched in orthochromatic erythroblasts compared to proerythroblasts. These genes, CCZ1 (Vacuolar Protein Trafficking and Biogenesis Associated) and RMC1 (Regulator of MON1-CCZ1), are both associated with endosomal sorting of the low-density lipoprotein receptor (LDLR). To validate the role of these genes in erythroid proliferation and differentiation, we deleted each gene in HUDEP2 cells, using CRISPR-Cas9. We generated a lentiviral vector expressing Cas9, sgRNAs targeting one of the candidate genes, and a puromycin resistance cassette. Following transduction, HUDEP2 cells were selected with puromycin and subsequently subjected to synchronized differentiation. Deletion of CCZ1 or RMC1 did not result in impaired differentiation as determined by flow cytometry and cytospin evaluations. However, for both genes, a fitness advantage was observed for cells with indels for one of these genes compared to wild type cells. Consistent with this finding, deletion of either gene resulted in increased cell proliferation throughout erythroid differentiation.

Conclusion While we await validation of the findings in CD34+ hematopoietic stem and progenitor cells undergoing erythroid differentiation, our findings suggest that deletion of CCZ1 and RMC1 results in enhanced erythroid proliferation. As a result, it may be useful to investigate the mechanistic link between lipid trafficking and erythroid differentiation.

Abstract 66 Table 1 CCZ1 KO total cell counts. A graph representing total cell count by day of differentiation of CCZ1 KO cells and WT non-targeting cells.
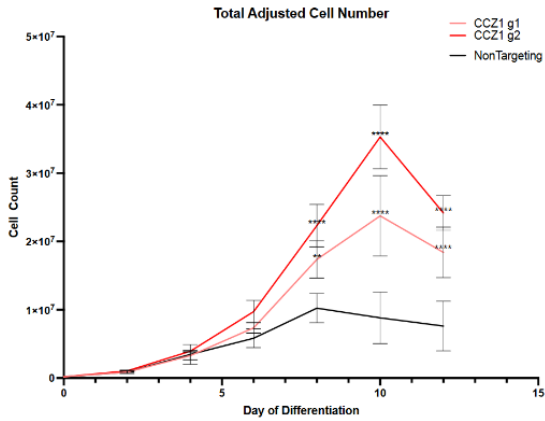
Abstract 66 Table 2 RMC1 KO total cell counts. A graph representing total cell count by day of differentiation of RMC1 KO cells and WT non-targeting cells.
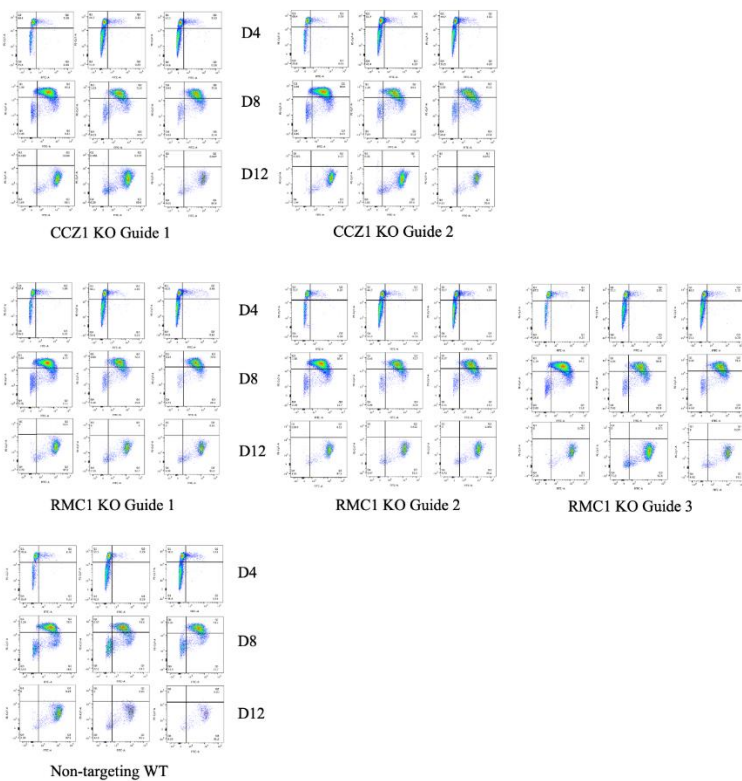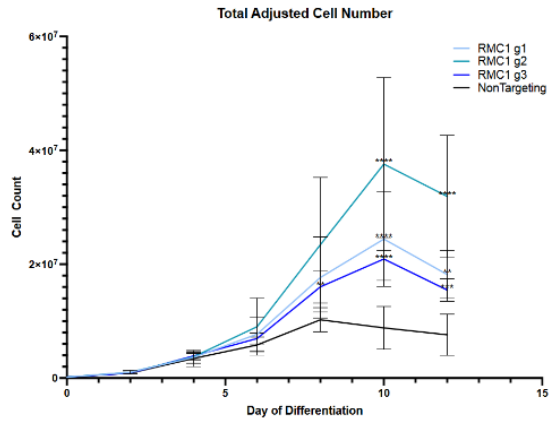
Abstract 66 Figure 1 Flow cytometry analysis of differentiation between CCZ1 and RMC1 KO cells compared to non-targeting WT at days 4, 8, and 12 of differentiation.
This image showcases the flow cytometry analysis of differentiation between knockout cells for CCZ1 and RMC1 compared to our non-targeting control. There is no difference in degrees of differentiation.

Abstract 66 Table 3 This data showcases the representative indel percentages of each guide at Day 0 and Day 12. The knockout cells utilizing each guide had indel percentages that increased from Day 0 to Day 12, indicating a possible advantage in fitness throughout differentiation.

D0 vs. D12 Indel Percentage by guide

Erythroid Essential Genes
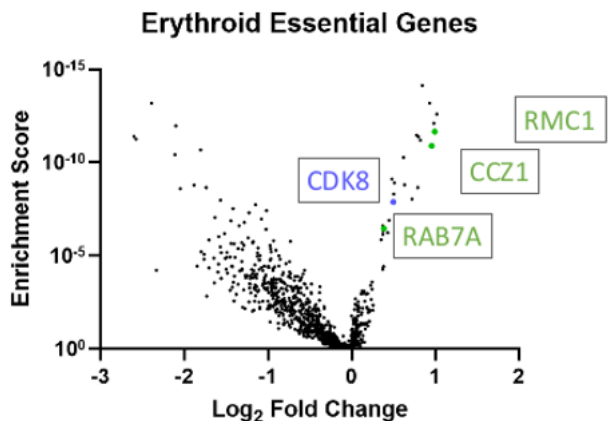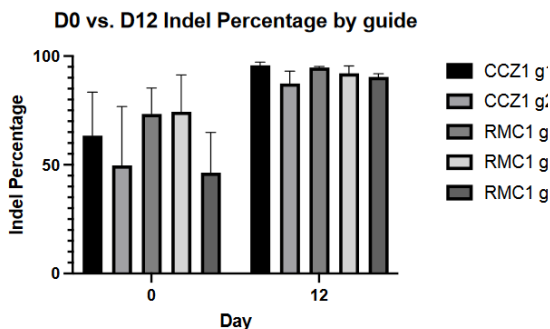
Abstract 66 Figure 2 Erythroid essential genes from genome-scale CRISPR KO screen
Shown here are genes that were highly enriched in the genome-scale screen. CDK8 is shown as a known regulator of cell cycle progression. The genes of interest - CCZ1 and RMC1 - were shown to be highly enriched, indicating increased guide abundance in terminally differentiated erythroid cells.

A USABILITY AND PARTICIPATORY DESIGN STUDY FOR GERI, AN OPEN-SOURCE, REMOTE CANCER TREATMENT TOXICITY AND FRAILTY MONITORING PLATFORM FOR OLDER ADULTS

Nabiel Mir, Gina Curry, Nita Lee, Russell Szmulewitz, Megan Huisingh-Scheetz. *The University of Chicago*

Introduction/Background Older adults are disproportionately affected by cancer, but there are significant barriers to studying cancer treatment tolerance in this population, including low enrollment in clinical trials and a lack of age-related outcome measures. Technology, such as wearable sensors and remote monitoring through tablets and smartphones, has the potential to overcome these barriers, but older adults may face challenges with adoption. Participatory design involves co-designing technology with end-users, is a promising strategy to enhance technology use among older adults. We present the usability results of GeRI, a technology-based platform for monitoring cancer treatment toxicity and aging metrics in the homes of older adults with cancer, which uses a simplified interface to collect activity, nutrition and symptom metrics.

Objective(s) To summarize usability scores and feedback of a customized platform, GeRI, connecting a tablet, wrist accelerometer, and scale that can be used to remotely collect frailty, activity, and nutrition markers from older adult cancer survivors and caregivers.

Methods In this participatory design study, n=7 older cancer survivors (OCS) and n=3 caregivers (CG) were recruited through the University of Chicago Cancer Center and Office of Community Engagement and Cancer Health Equity. They were given a GeRI prototype (Figure 1) to try at home for at least 2 weeks with access to technical support and a user manual. Semi-structured interviews were then conducted over videoconferencing. Participants were given a 10-item System Usability Scale (SUS) and a modified satisfaction and feature likeability survey (e.g., five-point Likert scales on their overall satisfaction with the platform as well as the touchscreen, user interface, font/notification size, wrist accelerometer). Based on their response, we probed further to identify ways to improve their experience with GeRI.
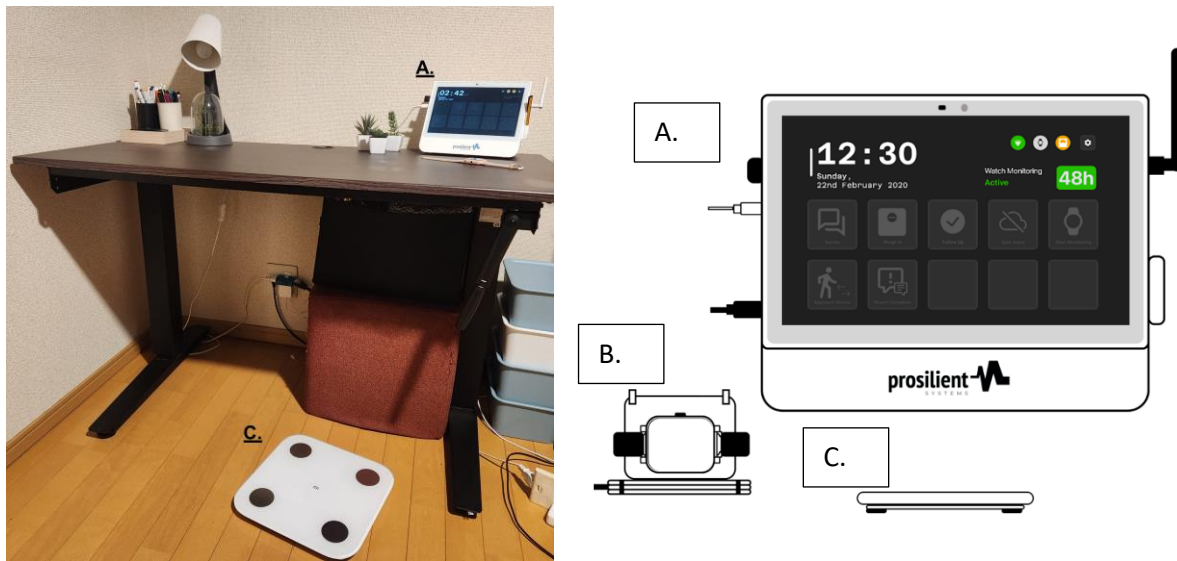
Abstract 67 Figure 1: The GeRI platform is composed of a A) WiFi-enabled tablet, B) bluetooth-enabled wrist accelerometer and magnetic charging dock, and C) bluetooth-enabled Body Composition Scale.
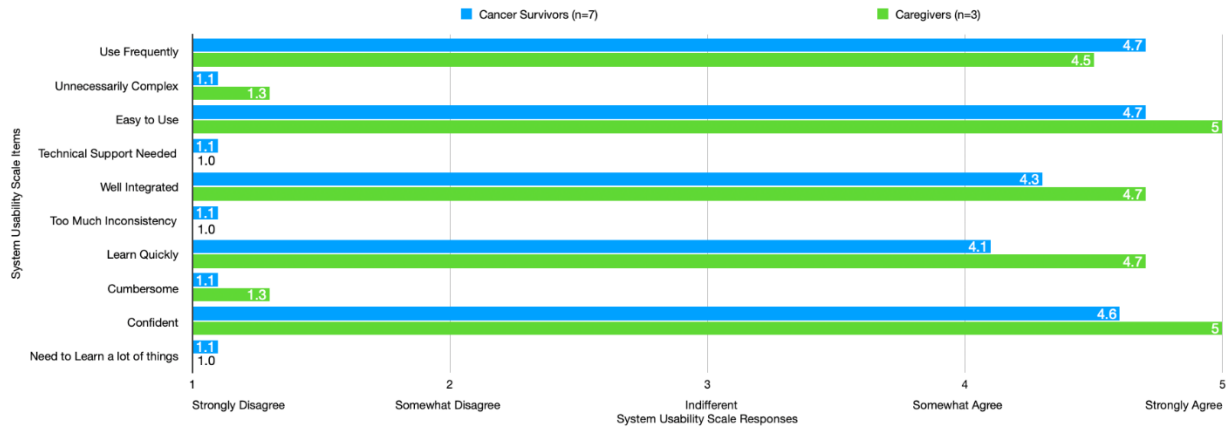
Abstract 67 Figure 2 GeRI System Usability Scale Scores Among Older Cancer Survivors (n=7) and their Caregivers (n=3)

Results The study's results on GeRI showed positive feedback from the predominantly minority older cancer survivors (mean age 74.9 [SD 6.6], Male, n=5 Black, n=6 Prostate Cancer) and caregivers (mean age 55, Female, n=2 Black) who consented and interviewed. The mean SUS score (0-100) was 92.8 (SD 8.7, range 72.5 - 100), and the mean overall satisfaction score (1-5) with the GeRI platform was 4.9 (SD 0.3) for all participants involved. Figure 2 depicts individual SUS item responses stratified by user type (OCS or CG). OCS mean SUS scores were 91.5 (SD 9.5), while the CG mean SUS was 95.8 (SD 7.2). 100% of participants rated the touchscreen, user interface, and wrist accelerometer as "Excellent" or "Very Good". 100% and 90% agreed that the size of notifications and font were sufficient, respectively, while only 70% believed that alerts and notifications were adequate enough to remind them to engage with the tablet. Condensed quick start guides or instructional pictures/videos on the tablet (n= 8), sound or voice notifications (n=7), improved task labeling (n=7), and symptom selection organization (n=7) were reported as features to enhance usability. The 2 highest-ranked enhancements by participants were "Messages from my Doctor" (n=4) and "My Smartwatch/Smart Scale Data" (n=4).

Conclusion The GeRI platform is the first open-source data collection platform targeting older adults with cancer and demonstrated high usability, with a mean SUS score of 92.8. However, more work is needed to optimize the user experience in a more diverse sample. The results of this study provide early design guidance for developers, including the most requested features, such as biometric data and provider communication, and recommendations for improved user materials, task notifications, and labeling/organization. Further participatory design studies with diverse older cancer cohorts are needed and planned to improve the user experience and maximize the adoption of the GeRI platform.

68

A NOVEL ROLE OF AQUAPORIN 3 IN REGULATING OXIDATIVE STRESS IN KAPOSI'S SARCOMA ASSOCIATED VIRUS-ASSOCIATED PRIMARY EFFUSION LYMPHOMA

Olivia Powrozek, Melanie Klemond, Neelam Sharma-Walia, Morgan Mroz. *Rosalind Franklin*

Introduction/Background Kaposi's sarcoma-associated herpesvirus (KSHV) is associated with Kaposi's sarcoma (KS), primary effusion lymphoma (PEL), multicentric Castleman's disease (MCD), and KSHV inflammatory cytokine syndrome (KICS). PEL is a highly aggressive B-cell non-Hodgkin's lymphoma presented as body cavity effusions called ascites. PEL patients have a poor prognosis and survival fewer than six months after diagnosis. PEL is treated with chemotherapy cyclophosphamide, doxorubicin, vincristine, prednisone (CHOP), and antiretroviral therapy for HIV coinfection. However, none of these therapeutics are targeted explicitly at KSHV and have side effects. Therefore, targeted antivirals and anticancer therapies for PEL are needed. KSHV has latent and lytic phases, which contribute to tumor formation and progression. Two essential KSHV proteins for its life cycle are latency-associated nuclear antigen-1 (LANA-1; ORF73) and regulator of transcription activator (RTA; ORF50). KSHV has evolved to reprogram several host factors to promote its latency, replication, and maintenance in the host cells and the survival and proliferation of the infected cells. Reactive oxygen species (ROS) mediated oxidative stress has been reported to regulate KSHV lytic cycle reactivation in latently infected PEL cells. Aquaporins (AQPs), integral membrane proteins, also known as water channel proteins, facilitate the uptake of hydrogen peroxide (H_2O_2) ROS into cells, thus mediating the downstream intracellular signaling involved in cancer cells. What has not been studied is the role of AQPs in the transmission of ROS within KSHV-infected PEL cells.

Objective(s) This study aims to identify aquaporins' role during KSHV infection and the potential of aquaporin 3 (AQP3) as a therapeutic target to treat PEL.

Methods This study utilized BJAB (KSHV-negative B-cell lymphoma), BCBL-1 (KSHV-positive body cavity B-cell lymphoma), and BC3 (KSHV-positive B-cell lymphoma) cells. These cells were cultivated via feeding in their selective growth media and growth factors. Here, we used DFP00173 as a specific AQP3 inhibitor. We also used AQP3 gene silencing to study the role of AQP3 in PEL cell death. We used quantitative, real-time-PCR, and Western blotting assays to evaluate AQP gene expression and protein levels in various PEL cell lines, respectively. In addition, we used DCFDA staining and Amplex red assays to measure ROS and peroxidase activity. All assays were performed according to standardized methods in the lab or following the manufacturer's protocols.

Results Screening for all AQPs within KSHV+ and KSHV- cells revealed that KSHV-infected PEL cells have higher expression of aquaporins 1, 3, 7, 10, 11, and 12. AQP3 was abundantly expressed at gene expression and protein levels in KSHV-infected BCBL-1 and BC-3 cells compared to non-infected BJAB cells. AQP3 maintains reactive oxygen species (ROS) in the infected cells. We found that inhibiting AQP3 by using its specific inhibitor or silencing its expression inhibited intercellular ROS. Interestingly, we observed increased expression of antioxidant enzymes in the AQP3-silenced KSHV-infected PEL cells. Our study establishes a critical role for AQP3-mediated ROS and oxidative stress in regulating KSHV reactivation and PEL cell death.

Conclusion We conclude that KSHV is utilizing AQP3 to promote its infection from the higher levels of ROS and expression of viral genes. Cells treated with either an AQP3-specific inhibitor or silenced for the protein had lower levels of ROS and the induction of antioxidant genes. In this study, we confirmed that KSHV-infected PEL cells express higher levels of AQP3 and a more significant reduction in shuttling ROS after treatment than non-infected. Since previous studies have determined the use of antioxidants to

reduce the lytic cycle for KSHV, we anticipate the therapeutic potential of targeting AQP3 to reduce the pathogenesis of KSHV in PEL based on our results.

REFERENCE(S)

1. Cesarman E, Chang Y, Moore PS, Said JW, Knowles DM. Kaposi's sarcoma-associated herpesvirus-like DNA sequences in AIDS-related body-cavity-based lymphomas. N Engl J Med. 1995;332(18):1186-91.
2. Soulier J, Grollet L, Oksenhendler E, Cacoub P, Cazals-Hatem D, Babinet P, et al. Kaposi's sarcoma-associated herpesvirus-like DNA sequences in multicentric Castleman's disease. Blood. 1995;86(4):1276-80.
3. Saini N, Hochberg EP, Linden EA, Jha S, Grohs HK, Sohani AR. HHV8-Negative Primary Effusion Lymphoma of B-Cell Lineage: Two Cases and a Comprehensive Review of the Literature. Case Rep Oncol Med. 2013;2013:292301.
4. Chen YB, Rahemtullah A, Hochberg E. Primary effusion lymphoma. Oncologist. 2007;12(5):569-76.
5. Ratner L, Lee J, Tang S, Redden D, Hamzeh F, Herndier B, et al. Chemotherapy for human immunodeficiency virus-associated non-Hodgkin's lymphoma in combination with highly active antiretroviral therapy. J Clin Oncol. 2001;19(8):2171-8.
6. Scott D, Cabral L, Harrington WJ, Jr. Treatment of HIV-associated multicentric Castleman's disease with oral etoposide. Am J Hematol. 2001;66(2):148-50.
7. Ablashi DV, Chatlynne LG, Whitman JE, Jr., Cesarman E. Spectrum of Kaposi's sarcoma-associated herpesvirus, or human herpesvirus 8, diseases. Clin Microbiol Rev. 2002;15(3):439-64.
8. Grundhoff A, Ganem D. Inefficient establishment of KSHV latency suggests an additional role for continued lytic replication in Kaposi sarcoma pathogenesis. J Clin Invest. 2004;113(1):124-36.
9. Moore PS, Gao SJ, Dominguez G, Cesarman E, Lungu O, Knowles DM, et al. Primary characterization of a herpesvirus agent associated with Kaposi's sarcomae. J Virol. 1996;70(1):549-58.
10. Schulz TF. Kaposi's sarcoma-associated herpesvirus (human herpesvirus-8). J Gen Virol. 1998;79 (Pt 7):1573-91.
11. Aneja KK, Yuan Y. Reactivation and Lytic Replication of Kaposi's Sarcoma-Associated Herpesvirus: An Update. Front Microbiol. 2017;8:613.
12. Wakeman BS, Izumiya Y, Speck SH. Identification of Novel Kaposi's Sarcoma-Associated Herpesvirus Orf50 Transcripts: Discovery of New RTA Isoforms with Variable Transactivation Potential. J Virol. 2017;91(1).
13. Cesarman E, Moore PS, Rao PH, Inghirami G, Knowles DM, Chang Y. In vitro establishment and characterization of two acquired immunodeficiency syndrome-related lymphoma cell lines (BC-1 and BC-2) containing Kaposi's sarcoma-associated herpesvirus-like (KSHV) DNA sequences. Blood. 1995;86(7):2708-14.
14. Chang Y, Cesarman E, Pessin MS, Lee F, Culpepper J, Knowles DM, et al. Identification of herpesvirus-like DNA sequences in AIDS-associated Kaposi's sarcoma. Science. 1994;266(5192):1865-9.
15. Gottwein E. Kaposi's Sarcoma-Associated Herpesvirus microRNAs. Front Microbiol. 2012;3:165.
16. Li W, Hu M, Wang C, Lu H, Chen F, Xu J, et al. A viral microRNA downregulates metastasis suppressor CD82 and induces cell invasion and angiogenesis by activating the c-Met signaling. Oncogene. 2017;36(38):5407-20.

17.   Chandrasekharan JA, Huang XM, Hwang AC, Sharma-Walia N. Altering the Anti-inflammatory Lipoxin Microenvironment: a New Insight into Kaposi's Sarcoma-Associated Herpesvirus Pathogenesis. J Virol. 2016;90(24):11020-31.

18.   Chandrasekharan JA, Sharma-Walia N. Lipoxins: nature's way to resolve inflammation. J Inflamm Res. 2015;8:181-92.

19.   Marginean A, Sharma-Walia N. Lipoxins exert antiangiogenic and anti-inflammatory effects on Kaposi's sarcoma cells. Transl Res. 2015.

20.   Sharma-Walia N, Chandran K, Patel K, Veettil MV, Marginean A. The Kaposi's sarcoma-associated herpesvirus (KSHV)-induced 5-lipoxygenase-leukotriene B4 cascade plays key roles in KSHV latency, monocyte recruitment, and lipogenesis. J Virol. 2014;88(4):2131-56.

21.   Paul AG, Chandran B, Sharma-Walia N. Cyclooxygenase-2-prostaglandin E2-eicosanoid receptor inflammatory axis: a key player in Kaposi's sarcoma-associated herpes virus associated malignancies. Transl Res. 2013;162(2):77-92.

22.   Paul AG, Chandran B, Sharma-Walia N. Concurrent targeting of eicosanoid receptor 1/eicosanoid receptor 4 receptors and COX-2 induces synergistic apoptosis in Kaposi's sarcoma-associated herpesvirus and Epstein-Barr virus associated non-Hodgkin lymphoma cell lines. Transl Res. 2013;161(6):447-68.

23.   Sharma-Walia N, Patel K, Chandran K, Marginean A, Bottero V, Kerur N, et al. COX-2/PGE2: molecular ambassadors of Kaposi's sarcoma-associated herpes virus oncoprotein-v-FLIP. Oncogenesis. 2012;1:e5.

24.   Paul AG, Sharma-Walia N, Chandran B. Targeting KSHV/HHV-8 latency with COX-2 selective inhibitor nimesulide: a potential chemotherapeutic modality for primary effusion lymphoma. PLoS One. 2011;6(9):e24379.

25.   George Paul A, Sharma-Walia N, Kerur N, White C, Chandran B. Piracy of prostaglandin E2/EP receptor-mediated signaling by Kaposi's sarcoma-associated herpes virus (HHV-8) for latency gene expression: strategy of a successful pathogen. Cancer Res. 2010;70(9):3697-708.

26.   Sharma-Walia N, Paul AG, Bottero V, Sadagopan S, Veettil MV, Kerur N, et al. Kaposi's sarcoma associated herpes virus (KSHV) induced COX-2: a key factor in latency, inflammation, angiogenesis, cell survival and invasion. PLoS Pathog. 2010;6(2):e1000777.

27.   Sharma-Walia N, Raghu H, Sadagopan S, Sivakumar R, Veettil MV, Naranatt PP, et al. Cyclooxygenase 2 induced by Kaposi's sarcoma-associated herpesvirus early during in vitro infection of target cells plays a role in the maintenance of latent viral gene expression. J Virol. 2006;80(13):6534-52.

28.   Mesri EA. Inflammatory reactivation and angiogenicity of Kaposi's sarcoma-associated herpesvirus/HHV8: a missing link in the pathogenesis of acquired immunodeficiency syndrome-associated Kaposi's sarcoma. Blood. 1999;93(12):4031-3.

29.   Naranatt PP, Krishnan HH, Svojanovsky SR, Bloomer C, Mathur S, Chandran B. Host gene induction and transcriptional reprogramming in Kaposi's sarcoma-associated herpesvirus (KSHV/HHV-8)-infected endothelial, fibroblast, and B cells: insights into modulation events early during infection. Cancer Res. 2004;64(1):72-84.

30.   Hara-Chikuma M, Verkman AS. Aquaporin-3 facilitates epidermal cell migration and proliferation during wound healing. J Mol Med (Berl). 2008;86(2):221-31.

31.   Hara-Chikuma M, Verkman AS. Prevention of skin tumorigenesis and impairment of epidermal cell proliferation by targeted aquaporin-3 gene disruption. Mol Cell Biol. 2008;28(1):326-32.

32.   Bollag WB, Aitkens L, White J, Hyndman KA. Aquaporin-3 in the epidermis: more than skin deep. Am J Physiol Cell Physiol. 2020;318(6):C1144-C53.

33.   Pimpao C, da Silva IV, Mosca AF, Pinho JO, Gaspar MM, Gumerova NI, et al. The Aquaporin-3-Inhibiting Potential of Polyoxotungstates. Int J Mol Sci. 2020;21(7).

34.   D'Agostino A, Pirozzi AVA, Finamore R, Grieco F, Minale M, Schiraldi C. Molecular Mechanisms at the Basis of Pharmaceutical Grade Triticum vulgare Extract Efficacy in Prompting Keratinocytes Healing. Molecules. 2020;25(3).

35.   Sharma-Walia N, George Paul A, Patel K, Chandran K, Ahmad W, Chandran B. NFAT and CREB regulate Kaposi's sarcoma-associated herpesvirus-induced cyclooxygenase 2 (COX-2). J Virol. 2010;84(24):12733-53.

36.   Kerur N, Veettil MV, Sharma-Walia N, Sadagopan S, Bottero V, Paul AG, et al. Characterization of entry and infection of monocytic THP-1 cells by Kaposi's sarcoma associated herpesvirus (KSHV): role of heparan sulfate, DC-SIGN, integrins and signaling. Virology. 2010;406(1):103-16.

37.   Bottero V, Sharma-Walia N, Kerur N, Paul AG, Sadagopan S, Cannon M, et al. Kaposi sarcoma-associated herpes virus (KSHV) G protein-coupled receptor (vGPCR) activates the ORF50 lytic switch promoter: a potential positive feedback loop for sustained ORF50 gene expression. Virology. 2009;392(1):34-51.

38.   Incani A, Marras L, Serreli G, Ingianni A, Pompei R, Deiana M, et al. Human Herpesvirus 8 infection may contribute to oxidative stress in diabetes type 2 patients. BMC Res Notes. 2020;13(1):75.

39.   Bottero V, Chakraborty S, Chandran B. Reactive oxygen species are induced by Kaposi's sarcoma-associated herpesvirus early during primary infection of endothelial cells to promote virus entry. J Virol. 2013;87(3):1733-49.

40.   Mesri EA, Cavallin LE, Ashlock BM, Leung HJ, Ma Q, Goldschmidt-Clermont PJ. Molecular studies and therapeutic targeting of Kaposi's sarcoma herpesvirus (KSHV/HHV-8) oncogenesis. Immunol Res. 2013;57(1-3):159-65.

41.   Ma Q, Cavallin LE, Leung HJ, Chiozzini C, Goldschmidt-Clermont PJ, Mesri EA. A role for virally induced reactive oxygen species in Kaposi's sarcoma herpesvirus tumorigenesis. Antioxid Redox Signal. 2013;18(1):80-90.

42.   Ma Q, Cavallin LE, Yan B, Zhu S, Duran EM, Wang H, et al. Antitumorigenesis of antioxidants in a transgenic Rac1 model of Kaposi's sarcoma. Proc Natl Acad Sci U S A. 2009;106(21):8683-8.

70

A PECULIAR CASE OF ANTI-G IN AN ALLOIMMUNIZED ANTENATAL MOTHER

[1]Ayesha Zaidi, [2]Christine Howard-Menk, [2]Aleta Nilson, [2]Cristine Clemente Dos Santos, [3]david Allison, [2]Jason Crane, [2]Mona papari, [2]Mingmar Sherpa, [3]Sally Campbell-Lee. [1]*University of Illinois at Chicago; [2]Vitalant; [3]UIC Pathology Department*

Introduction/Background The Rh system is the most important blood group system after ABO. The G antigen is a member of the Rh system of blood group antigens expressed on red blood cells (RBCs) possessing C, D or both C and D antigens. Antibodies against Rh antigens are notorious for causing hemolytic disease of the fetus and newborn (HDFN). Anti-D is the most common antibody responsible for severe HDFN, but other Rh antibodies, such as anti-C, anti-E, anti-e, and anti-G, can also cause HDFN. Anti-G has been reported as a possible cause of HDFN, either independently or in association with anti-D, anti-C or both. This antibody can be induced either by pregnancy or transfusion. Anti-G antibody mimics the pattern of anti-C and anti-D reactivity in the identification panel and is often present along with either or both antibodies, but cannot be serologically differentiated, since it is adsorbed by both C–D+ and C+D– red blood cells. The differentiation of anti-G with anti-D and anti-C in routine pretransfusion workup is especially significant in antenatal cases. The presence of anti-D in an expecting mother excludes the need for the administration of prophylactic anti-D immunoglobulin (RhIG). In contrast, D-negative mothers with anti-G are potential candidate for Rh prophylaxis to prevent possible formation of anti-D and subsequent HDFN.

Case Presentation We hereby present a case of a 29-year-old, gravida 3, para 2 woman at 15 weeks gestation age. Prenatal records indicate two previous pregnancies, both liveborn; no miscarriages, spontaneous abortions, or terminated pregnancies. She reportedly received RhIG with the previous pregnancies, and she denied history of blood transfusions. Prenatal type and screen was ordered. Blood group was O Rh (D) negative, and antibody screen was positive. Preliminary antibody identification was suspicious for Anti-C, Anti-D versus Anti-G, and so anti-G elution and adsorption were performed by the immunohematology reference laboratory. Anti-G determination is a complex procedure, involving challenging workups of double adsorption and elution techniques. In simpler words, the procedure first pulls one antibody out of the serum by using red cells with the corresponding antigen (adsorption), then isolates the anti-G by the use of a second adsorption procedure. This procedure is sometimes also known as "G-differentiation.

Discussion This case study highlights the importance of recognizing and differentiating anti-G from anti-D plus anti-C in a pregnant woman. Since anti-G may mask the presence of anti-D on standard antibody panels, antibody identification with extended cell panel and subsequent adsorption and elution studies are needed to distinguish anti-G from anti-D. If a D-negative mother has anti-G, she does still need RhIG. If, instead, she has anti-D plus anti-C, Rh immune globulin is not indicated, since she is already immunized.

Abstract 70 Table 1

Antibody	Titer
Anti-D	512
Anti-G	1
Anti-Fy[a]	2

REFERNECE(S)

1.   Daniels G. Rh and RHAG blood group system. In: Daniels G, editor. Human blood groups. 3. Oxford: Blackwell Scientific; 2013. pp. 182–258.
2.   Shirey R, Mirabella D, Ness P. Differentiation of anti-D, -C, and -G: clinical relevance in alloimmunized pregnancies. Transfusion. 1997;37(May):493–496. doi: 10.1046/j.1537-2995.1997.37597293879.
3.   www.bbguy.org4.Vos G. The evaluation of specific anti-G (CD) eluate obtained by a double absorption and elution procedure. Vox Sang. 1960;5:472–478. doi: 10.1111/j.1423-0410.1960.tb05226.

71

AN UNUSUAL ELEVATION IN INTERNATIONAL NORMALIZED RATIO IN THE SETTING OF APIXABAN USE

Grishma Pokharel, Hassan Alkhatatneh, Joseph Fleischer, Maxwell Janosky, Sofia Terner. *Englewood Health and Medical Center*

Introduction/Background Apixaban is a direct oral anticoagulant (DOAC) that works by directly inhibiting factor Xa of the coagulation cascade. Studies reveal an association between the use of DOACs and the prolongation of prothrombin time (PT) and the International Normalized Ratio (INR). In patients using Apixaban, INR elevations were observed with a median INR of 1.4 on day 1 and a median INR of 1.7 on day 7 of therapy. Extreme elevation in INR is rare with Apixaban. [1-3] Here, we report a case of a patient, who was found to have a critically elevated INR of 10.83 in the setting of Apixaban use.

Case Presentation A 67-Year-old man with a history of Atrial flutter, Heart failure, and Chronic kidney disease presented with acute, progressive, generalized swelling and shortness of breath with blood-tinged sputum. Of note, the patient had no history of liver disease and had never been on hemodialysis. On assessment, vital signs were stable and physical examination was unremarkable.Laboratory results revealed an INR of 10.83, PT of 84.9, and activated partial thromboplastin time (aPTT) of 109.6 with normal liver function test, Cr of 1.71, normal fibrinogen levels, and normal thrombin time. Mixing studies for PT 1:1 was 16.4 seconds, and for PTT was 37.4 seconds. Factor X activity was low at 5%, and Factor II activity was low at 12%. Dilute Russell Viper Venom Time (dRVVT) test was negative. Serum Immunoglobulins were normal.One month prior to presentation, the patient's INR was 1.4 prior to starting Apixaban and 1.8 one day after starting the drug. Patient denied use of warfarin and any herbal remedies.On admission, Apixaban was held, and the patient received 10 mg of Vitamin K. A repeat INR 12 hours later was unchanged (>9.4) and was 9.1 and 4.4 after 24 hours and 48 hours, respectively. A repeat dose of 5 mg of Vitamin K was given after 48 hours. On day 3 of admission (approximately 72 hours from last Apixaban dose), the patient's INR level improved to 4.4 and finally improved to 2.1 on day 4 of admission. The INR level remained stable for the rest of the hospitalization and the patient was eventually discharged.

Discussion Apixaban prolongs traditional clotting tests such as prothrombin time (PT), international normalized ratio (INR), and activated partial thromboplastin time (aPTT).[1] In a similar case report, an INR of 27 was seen in an 82-year-old male with End-Stage Renal Disease (ESRD) on hemodialysis, liver cirrhosis, and chronic hepatitis C infection. [2] Liver disease can disrupt the coagulation homeostasis due to a decrease in the production of clotting factors, which may result in an elevated INR. In our case, however, the patient did not have any obvious reasons for INR elevation such as history of liver disease or malnutrition. With a recently normal INR level, and mixing studies revealing lack of PT and PTT correction, Vitamin K deficiency did not appear to be the driving factor for the elevated INR but rather the presence of an inhibitor was more likely. Furthermore, large doses of Vitamin K usually normalize INR levels within 24 hours of administration, which was not the case with our patient. [5] While we cannot be certain which intervention was the main factor for normalizing the INR level in our patient, as Apixaban was stopped and Vitamin K was administered simultaneously, we believe that further workup as described best supports Apixaban as the main etiology for our patient's markedly elevated INR on presentation.Further studies are necessary to investigate these rare cases of elevated INR levels with Apixaban use in order to gain a deeper understanding of its pharmacokinetic and pharmacodynamic properties.

REFERENCE(S)

1. Byon, W., Garonzik, S., Boyd, R. A., & Frost, C. E. (2019). Apixaban: A Clinical Pharmacokinetic and Pharmacodynamic Review. Clinical pharmacokinetics, 58(10), 1265–1279. https://doi.org/10.1007/s40262-019-00775-z
2. Kahlon, N., Doddi, S., Ning, Y., Akpunonu, B., & Murphy, J. (2022). Elevated International Normalized Ratio Due to Apixaban in Patient With End-Stage Renal Disease on Hemodialysis. Cureus, 14(6), e25907. https://doi.org/10.7759/cureus.25907
3. Kovacevic, M. P., Lupi, K. E., Wong, A., Gilmore, J. F., & Malloy, R. (2019). Evaluation of the Effect of Apixaban on INR in the Inpatient Population. Journal of cardiovascular pharmacology and therapeutics, 24(4), 355–358. https://doi.org/10.1177/1074248419838502
4. Harrison M. F. (2018). The Misunderstood Coagulopathy of Liver Disease: A Review for the Acute Setting. The western journal of emergency medicine, 19(5), 863–871. https://doi.org/10.5811/westjem.2018.7.37893
5. Thigpen, J. L., & Limdi, N. A. (2013). Reversal of oral anticoagulation. Pharmacotherapy, 33(11), 1199–1213. https://doi.org/10.1002/phar.1270

72

COMPLEMENT MEDIATED TMA AND SPLENIC RUPTURE ASSOCIATED WITH CMV INFECTION

Sadia Shabir, Wasef Sayeh, Shahab Ud Din. *University of Toledo Medical Center*

Introduction/Background Complement-mediated thrombotic microangiopathy (TMA) is characterized by a triad of microangiopathic hemolytic anemia (MAHA), thrombocytopenia, and acute renal failure.[1,2] It sometimes presents following an event causing activation of complement cascade in a predisposed individual with genetic abnormalitiesinvolving complement factors or autoantibodies against complement regulators. Spontaneous splenic rupture is a rare complication of CMV infection and potentially life threatening event. The goal is to resuscitate the patient with conservative management. Cytomegalovirus (CMV) is a DNA virus with high seroprevalence. Although it is well known for causing serious infections in immunocompromised and transplant patients, CMV has been reported with serious complications in previously healthy immunocompetent patients. Here we are reporting a case of a previously healthy female patient with complement-mediated TMA and splenic rupture caused by a systemic CMV infection that wassuccessfully treated with plasmapheresis, steroids, and parenteral valganciclovir.

Case Presentation A 35 year old female patient presented with 1 week history of nausea, vomiting, diarrhea, and malaise.Her medical history was significant for postpartum hemorrhage 1 week after delivery that occurred 7 months before her current presentation. Initially the patient was hemodynamically stable. Labs showed hemoglobin 9.1 g/dL (normal 11.7-15.5), platelets 24 x 109/L (normal 150-450 x 109), creatinine 1.6 mg/dL (normal 0.40-1.00), LDH 1095 U/L (normal 100-235), haptoglobin Coomb's test was negative, C3 53 mg/dL (normal 86-184), C4 was normal, and schistocytes were seen on peripheral smear. While evaluation of hemolytic uremic syndrome (HUS) and thrombotic thrombocytopenic purpura (TTP) was ongoing, the patient's clinical condition deteriorated with shock with systolic pressures in the 70s mmHg, worsening abdominal pain, and drop in hemoglobin to 3.4 g/dL. The patient was transferred to ICU and given 3 L intravenous fluids. Emergent computed tomography (CT) angiogram of the abdomen and pelvis showed splenic rupture with active bleeding. Massive transfusion protocol was activated with 8 units packed red blood cells, 3 units platelets, and 3 units fresh frozen plasma (FFP) given. She underwent an emergent splenic artery embolization for hemostasis by interventional radiology. Transfusion of such high volume of blood products in the setting of poor kidney function led to massive pulmonary edema with acute respiratory failure requiring intubation. Continuous renal replacement therapy (CRRT) with ultrafiltration was started for volume overload. CRRT was discontinued before 24 hours, and the patient was extubated the next day. The patient received three sessions of plasmapheresis while the ADAMTS-13 test was pending and ultimately came back normal.ADAMTS-13 inhibitor was also negative. Prednisone 60 mg was started empirically. CMV IgM and IgG were positive and later confirmed by PCR as well. Valganciclovir 900 mg twice daily was started and planned for 3 weeks for treatment of systemic CMV infection. The patient responded well to the treatmentas evidenced by cell count and renal function improving quickly to normal range 10 days after her deterioration. Repeat CMV titer 3 weeks after presentation was negative.

Discussion Complement Mediated TMA is the result of dysregulation of the alternative complement pathway on the endothelial lining of vessels leading to endothelial damage. It is rare but frequently results in end stage renal disease (ESRD). These patients have poor outcomes after kidney transplant due to recurrence of complement-mediated TMA leading to high rate of transplant failure.[3] As such, early identification and treatment are important.In our patient, complement-mediated TMA was suggested by combination of MAHA (direct Coomb's test negative, schistocytes on peripheral smear,

elevated LDH, low haptoglobin), thrombocytopenia (platelets 24000/microliter), ARF (Cr 1.4, BUN 47 mg/dl), low C3 with normal C4 and normal ADAMTS-13 level.,The trigger was thought to be CMV systemic infection with CMV IgM >4.0, CMV IgG 3.0, and CMV DNA detected on PCR. Moreover, treatment with valganciclovir led to rapid recovery and return to normal cell count and renal functions. The patient did not require Eculizumab, a humanized antiC5 monoclonal antibody, which blocks the terminal complement pathway and is approved in many countries to treat complement mediated TMA.4,5 Our case highlight the fact that some secondary TMAs could be improved by treatment of triggering factors as this patient improved once the trigger for complement activation i.e. CMV infection was treated.Patient also received Prednisone 60 mg once daily. Steroids inhibit activation of the Alternative Pathway of complement. High dose glucocorticoids have been shown to inhibit complement activation by both classical and the alternative pathways 6,7,8 These steroids act both to prevent the assembly of effective convertase and to stabilize membranes against the lytic action of complement.6,7,8CMV is a DNA virus belonging to the Herpesviridae family. About 50% of the population in developed countries is seropositive. This percentage is even higher in developing countries ranging from 40-100%.10,11 CMV infection is well studied in kidney transplant patients, frequently triggering complement mediated TMA and leading to transplant failure. This patient was otherwise healthy, and treating CMV infection with valganciclovir led to early recovery with complete resolution of complement mediated TMA. CMV increases the expression of endothelial adhesion molecules and von Willebrand factor.9 Our patient had no other known risk factors for complement mediated TMA such as common bacterial or viral infections, HIV, autoimmune disease, malignancy, organ transplant, irradiation, or certain drug exposure (e.g., tacrolimus).1,2,12,13Complement-mediated TMA is described in association with various mutations in genes of complement factors or with autoantibodies against complement regulators. Around 60% of patients with complementmediated TMA have an identified complement abnormality14. Although 30%-50% are diagnosed without an identified mutation, it is hard to rule out genetic mutation in those patients as there are several heterogeneous mutations involved, and not all of them are known and tested for.Furthermore, spontaneous splenic rupture is another rare complication of CMV infection. Typical signs of splenic rupture include left upper quadrant abdominal pain with guarding due to peritonitis and hemorrhagic shock. The absence of trauma or other well known risk factors, such as EBV infection, expose these patients to delayed diagnosis and management. Our patient was resuscitated with blood product transfusion and prompt embolization. Splenectomy is reserved for patients who don't respond to conservative management and are hemodynamically unstable.

REFERENCE(S)
1. Noris M,Remuzzi G. Atypical hemolytic-uremic syndrome.N Eng J Med 2009;361:1676-87.
2. Loirat C,Fremeaux-Bacchi V.Atypical hemolytic uremic syndrome. Orphanet J Rare Dis 2011:6:60
3. Romanan P Razonable RR. Cytomegalovirus infections in solid organ transplantation:a review. Infect Chemother 2013;45:260-71.
4. Zuber J, Fakhouri F, Roumenina LT,et al. French study Group for aHUS/C3G.Use of eculizumab for atypical hemolytic uremic syndrome and C3 glomerulopathies..Nat Rev Nephrol 2012;8:643-57.
5. Legendre CM, Licht C, Muus P, et al.Terminal complement inhibitor eculizumab in atypical hemolytic-uremic syndrome. N Eng J Med 2013;368:2169-81.
6. Gewurz, H.P.R.Wernick, P.G Quie, and R.A.Good.1965. Effects of hydrocortisone succinate on the complement system. Nature (London) 208:755-757
7. Jennings,J.F.,and G.Taylor.1964.Effects of hydrocortisone hemi-succinate on immune lysis of sheep erythrocytes. Nature (London) 203:661.

8.   Weller, J.M., and B.D. Packard. 1982.Methylprednisolone inhibits the alternative and amplification pathways of complement. Infect. Immun. 38:122-126.

9.   Jeejeebhoy FM, Zaltzman JS: Thrombotic microangiopathy in association with cytomegalovirus infection in a renal transplant patient: A new treatment strategy. Transplantation 65:1645-1648, 1998

10.   Hecker M, Qui D, Marquardt K, Bein G, Hackstein H (2004) continuous cytomegalovirus seroconversion in a large group of healthy blood donors. Vox Sang 86:41-44

11.   Yilmazer M, AltindisM, Cevizoglu S (2004) Afyon Bolgesinde Yasayan Gebe Kadinlarda Toksoplazma, Sitomegalovirus, Rubella, Hepatit B, Hepatit C, Seropozitiflik, Oranlari Kocatepe Tip Dergisi. Med J Kocatepe 5:49-53.

12.   Loirat C, Girma JP Desconclois C, Coppo P, Veyradier A (2009) Thrombotic thrombocytopenic purpura related to severe ADAMTS13 deficiency in children. Pediatr Nephrol 24: 19-29

13.   Copelovitch L, Kaplan BS (2008) Streptococcus pneumoniae-associated hemolytic uremic syndrome. Pediatr Nephrol 23:1951-1956.

14.   Fremeaux-Bacchi V, Fakhouri F, Garnier A, et al. Genetics and outcome of atypical hemolytic uremic syndrome: a nationwide french series comparing children and adults.Clin J Am Soc Nephrol 2013;8:554-62.

73

OH, WHAT A STORM: A CASE OF BLINATUMOMAB-INDUCED CYTOKINE RELEASE SYNDROME

Chadane Thompson, Kemar Barrett, Devon Scott, Jason Lofters, Natasha Rastogi. *Englewood Hospital and Medical Center*

Introduction/Background Acute lymphoblastic leukemia (ALL) is a rare malignant proliferation of immature lymphoid precursors and is uncommon in adulthood. Blinatumomab is a bispecific T-cell engaging drug used in patients with Philadelphia chromosome-positive (Ph+) or -negative (Ph-) relapsed/refractory (R/R) ALL, prior tyrosine kinase inhibitor (TKI) exposure and T315I mutation [1-5]. T315I mutation is a defect in the BCR-ABL fusion protein that limits therapeutic options in Ph+ ALL by conferring resistance to TKIs except for ponatinib. Blinatumomab can be used as a single agent or in combination with ponatinib to further improve outcomes. Despite the potential benefits of blinatumomab, cytokine release syndrome (CRS) is a potentially life-threatening complication [2,6]. As the use of novel immunotherapy agents expands, it is vital that physicians promptly recognize and manage their associated toxicities [1,6]. We present a case of relapsed Ph+ B-cell ALL due to T315I mutation requiring treatment with blinatumomab and ponatinib in which initial infusion of blinatumomab incited Grade 1 CRS.

Case Presentation A 72-year-old female with a past medical history of Ph+ B-cell ALL presented with a one-week history of bilateral calf pain and swelling associated with fatigue and weight loss. She was maintained on nilotinib, prednisone and allopurinol. She denied cough, dyspnea or chest pain. Vital signs were normal. Physical exam revealed mucosal pallor and bilateral lower extremity edema. She had anemia (10.3g/dL), thrombocytopenia (106K/uL), leukocytosis (217K/uL) with 95% blasts and an absolute neutrophil count of 0.34K/uL. Venous Doppler of the lower limbs showed bilateral acute soleal vein thromboses and enoxaparin was started. She had re-induction chemotherapy with vincristine for relapsed Ph+ B-cell ALL. BCR-ABL kinase mutation analysis was positive for T315I mutation with nilotinib resistance. Therefore, blinatumomab was initiated but despite dexamethasone premedication, she developed sudden-onset generalized rigors, fever (101.7F) and tachycardia (101 beats/min). Exam revealed intact orientation and no rash or urticaria. She was given intravenous fluids, acetaminophen and meperidine with resolution of symptoms. Tumor lysis syndrome (TLS) was ruled out. Empiric antibiotics were also started but infectious workup later returned negative. A diagnosis of Grade 1 CRS was made. She received two weeks of blinatumomab with appropriate premedication and leukocytes normalized to 8K/uL (Fig. 1). She was discharged on ponatinib to follow up in the hematology clinic.

Discussion CRS is a systemic inflammatory response mediated by an increase in circulating cytokines and other inflammatory markers [1]. It occurrs in ~15% of patients with R/R ALL on blinatumomab and is most common during the first treatment cycle, due to higher disease burden at immunotherapy initiation [2,4,5]. It presents with varying severity ranging from fever and constitutional symptoms (Grade 1) to organ dysfunction, hypoxia and shock, requiring mechanical ventilation and vasopressors (Grade 4) [6]. Severe clinical and laboratory features include coagulopathy, elevated c-reactive protein, multi-organ failure, shock and hemophagocytic lymphohistiocytosis [6]. CRS is a challenging diagnosis as it presents similarly to other inflammatory conditions such as TLS, sepsis and allergic reactions [6]. Low-grade CRS requires vigilant supportive care [6]. High-grade CRS is life-threatening and requires cytoreduction, dose titration, prophylactic dexamethasone, tocilizumab, or permanent drug discontinuation [1-3,6]. Our case showcases that blinatumomab is effective in R/R ALL and T315I mutation but can be complicated by CRS. Early recognition and treatment of CRS are crucial steps in preventing progression to life-threatening toxicity.
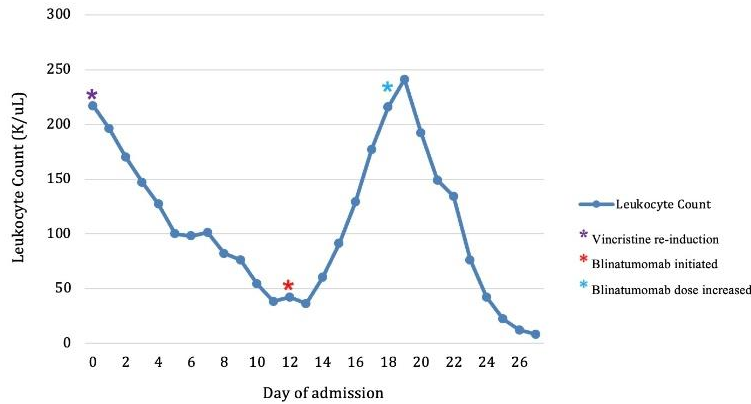
Abstract 73 Figure. 1: Line graph showing the leukocyte counts over the course of hospital admission while on treatment with blinatumomab (following vincristine re-induction).

REFERENCE(S)

1. Jain T, Litzow M. Management of toxicities associated with novel immunotherapy agents in acute lymphoblastic leukemia. Ther Adv Hematol. 2020;11:1-13. doi:10.1177/2040620719899897
2. Frey N. Cytokine release syndrome: Who is at risk and how to treat. Best Pract Res Clin Haematol. 2017;30(4):336-340. doi:10.1016/j.beha.2017.09.002
3. Benjamin J, Stein A. The role of blinatumomab in patients with relapsed/refractory acute lymphoblastic leukemia. Ther Adv Hematol 2016;7(3):142-156. doi:10.1177/2040620716640422
4. Martinelli G, Boissel N, Chevallier P, et al. Complete Hematologic and Molecular Response in Adult Patients With Relapsed/Refractory Philadelphia Chromosome-Positive B-Precursor Acute Lymphoblastic Leukemia Following Treatment With Blinatumomab: Results From a Phase II, Single-Arm, Multicenter Study. J Clin Oncol. 2017;35(16):1795-1802. doi:10.1200/JCO.2016.69.3531
5. Topp MS, Gökbuget N, Stein AS, et al. Safety and activity of blinatumomab for adult patients with relapsed or refractory B-precursor acute lymphoblastic leukaemia: a multicentre, single-arm, phase 2 study. Lancet Oncol. 2015;16(4):e158. doi:10.1016/S1470-2045(14)71170-2
6. Shimabukuro-Vornhagen A, Gödel P, Subklewe M, et al. Cytokine release syndrome. J Immunother Cancer. 2018;6(1):56. doi:10.1186/s40425-018-0343-9

74

DELAYED ONCONEURONAL ANTIBODY DEVELOPMENT IN IMMUNE CHECKPOINT INHIBITOR INDUCED PARANEOPLASTIMC SYNDROME

[1]Doo Woong Choi, [1]Angila Bag, [1]Shalva Eilava, [1]Smitha Agadi, [2]Maxwell Janosky, [1]Dipal Patel. [1]*Englewood Hospital and Medical Center;* [2]*Hematology Oncology Physicians of Englewood*

Introduction/Background With wider use of immune checkpoint inhibitors (ICI) in treatment of various solid organ cancers, an increasing number of neurologic paraneoplastic syndromes from ICIs are reported[1, 3, 5]. Onconeuronal antibodies are used to support the diagnosis of paraneoplastic syndrome but there are limited studies regarding timing of antibody development in ICI-induced paraneoplastic syndromes. We present a unique case of delayed development of onconeuronal antibodies in ICI-induced paraneoplastic syndrome, the diagnosis of which was strongly supported by the presence of rare onconeural antibodies in the absence of progression of cancer. Also, we will discuss the use of western blot in ICI induced paraneoplastic syndrome.

Case Presentation A 64-year-old non-smoker male with Stage IV tonsillar squamous cell carcinoma presented to the hospital with vertigo, dysarthria and gait instability. Patient had received six cycles of chemotherapy with carboplatin/pembrolizumab/5-fluorouracil, with maintenance pembrolizumab for 3 months prior to presentation. CSF analysis revealed mildly elevated white count of 12/mm3, lymphocyte 93% with elevated protein of 90mg/dl. Other work-up including MRI, paraneoplastic antibody and viral encephalitis panels were initially unremarkable with stable cancer. He was treated empirically with high-dose methylprednisolone, IVIG and plasmapheresis for presumed paraneoplastic syndrome, with slight improvement. Patient was then readmitted in 3 months for progressive worsening of gait instability with dysphagia. Examination revealed a dysarthric patient with bilateral non-fatigable nystagmus in all directions, dysmetria and dysdiadochokinesia. CT and MRI head showed cerebellar atrophy but no metastasis or encephalitis. CT chest/abdomen/pelvis and neck showed only unilateral necrotic, mildly enlarging cervical lymph nodes. Lumbar puncture revealed inflammatory CSF findings with lymphocytic pleocytosis with WBCs 120/mm3, lymphocytes 88% and elevated protein of 63mg/dl. Paraneoplastic antibody panel now noted fluorescence for Anti-Hu, Anti-Yo and Anti-Ri antibodies, with borderline results for GM-1 antibody, however Western blots were negative. Progressive cerebellar degeneration secondary to ICI-use was suspected given exaggerated immune response with 4 rare antibodies and relatively stable tumor burden, and he was treated again with pulse steroids, followed by mycophenolate and cyclophosphamide. The patient showed improvement in motor function and speech but remained ataxic and dysarthric.

Discussion While many cases of ICI-induced paraneoplastic syndrome have been reported[1, 3, 5], 11 cases of ICI-induced cerebellar degeneration were identified, of which 7 cases had positive onconeural antibodies including Hu, CRMP5, Striational, Amphiphysin, VFCC[1, 2, 3, 4, 5, 6]. However, none documented conversion of antibody testing from an initial negative to positive by fluorescence. Our patient showed delayed development of Anti-Hu, Anti-Yo, and Anti-Ri onconeural antibodies which are known to be related to paraneoplastic cerebellar degeneration[5, 7], 3 months after symptom development. In this case, the use of repeat antibody screening in ICI-induced paraneoplastic syndrome can be justified. Additionally, our case revealed negative western blot for paraneoplastic antibodies, which suggests that western blot utility is sometimes limited in ICI-induced paraneoplastic syndrome.

REFERENCE(S)

1.   Sechi E, Markovic SN, McKeon A, et al. Neurologic autoimmunity and immune checkpoint inhibitors: Autoantibody profiles and outcomes. Neurology. 2020;95(17):e2442-e2452. doi:10.1212/WNL.0000000000010632
2.   Abbadessa G, Miele G, Fratta M, Bonavita S. Paraneoplastic syndrome or immune-related adverse event? A case of rhomboencephalitis in a patient treated with Pembrolizumab. Acta Neurol Belg. 2021;121(5):1341-1342. doi:10.1007/s13760-020-01564-3
3.   Vogrig A, Muñiz-Castrillo S, Joubert B, et al. Central nervous system complications associated with immune checkpoint inhibitors. J Neurol Neurosurg Psychiatry. 2020;91(7):772-778. doi:10.1136/jnnp-2020-323055
4.   Kawamura R, Nagata E, Mukai M, et al. Acute Cerebellar Ataxia Induced by Nivolumab. Intern Med. 2017;56(24):3357-3359. doi:10.2169/internalmedicine.8895-17
5.   Duong SL, Prüss H. Paraneoplastic Autoimmune Neurological Syndromes and the Role of Immune Checkpoint Inhibitors. Neurotherapeutics. 2022;19(3):848-863. doi:10.1007/s13311-022-01184-0
6.   Zurko J, Mehta A. Association of Immune-Mediated Cerebellitis With Immune Checkpoint Inhibitor Therapy. Mayo Clin Proc Innov Qual Outcomes. 2018;2(1):74-77. Published 2018 Feb 1. doi:10.1016/j.mayocpiqo.2017.12.001
7.   Loehrer PA, Zieger L, Simon OJ. Update on Paraneoplastic Cerebellar Degeneration. Brain Sci. 2021;11(11):1414. Published 2021 Oct 26. doi:10.3390/brainsci11111414

A CD1A NEGATIVE BIOPSY AND A CD1A POSITIVE BIOPSY: AN EXTREMELY RARE PRESENTATION OF ROSAI-DORFMAN DISEASE WITH LANGERHANS CELL HISTIOCYTOSIS

Ayman Salih, Rayna Patel. *University of Toledo*

Introduction/Background Rosai-Dorfman disease (RDD), also known as sinus histiocytosis with massive lymphadenopathy, is a systemic proliferation of cells that resemble the sinus histiocytes of lymph nodes and is often characterized by painless, massive cervical lymphadenopathy.(1) It has been reported that about 43% of cases have extra-nodal involvement, most commonly involving skin and subcutaneous tissues. (2,3) RDD is a rare subtype of histiocytic disorders, which also includes Langerhans cell histiocytosis (LCH). LCH is characterized by an abnormal reactive process that involves the proliferation of abnormal Langerhans cells. While it may initially present as a rash it can involve several organs including the lungs, bone marrow, lymph nodes, and pituitary gland.(4) Here, we shed the light on a unique case of a 24-year-old female who originally presented at the age of 14 and was diagnosed with RDD involving the CNS, and had a skin rash that was originally thought to be secondary to RDD but was, in fact, cutaneous LCH.

Case Presentation A previously healthy 14-year-old female presented to the hospital with increased weight gain and fatigue. She was diagnosed with hypothyroidism and treated accordingly. Despite this, her symptoms worsened, and she developed an intractable headache. Further workup led to an MRI revealing a 2x2 cm lesion in the hypothalamic region. Biopsy of the mass revealed histiocytic proliferation with negative CD1a and positive S100, consistent with RDD. Initial treatment included unsuccessful focal radiation and clofarabine mono-therapy, which she was unable to tolerate. She then presented with a vulvar and ulcerative perirectal rash that was originally thought to be a reaction from clofarabine or RDD cutaneous metastasis. The biopsy, surprisingly, revealed positive CD1a histiocytic proliferation consistent with LCH. She began vinblastine monotherapy, which was poorly tolerated. Due to intolerance of cytotoxic chemotherapy, she started oral trametinib. Surprisingly, Follow-up brain MRI revealed resolution of the hypothalamic mass. But unfortunately, The patient was readmitted to the hospital due to medication side effects, and trametinib was discontinued. She began on cobimetinib and has since been on that medication with no recurrence of the mass.

Discussion The co-occurrence of LCH and RDD is extremely rare with only 18 cases reported in the English literature since the first report in 2002 by Wang et al. (5,6) In fact, our patient is the only case among all reported cases to have a metachronous combination of RDD involving the CNS with LCH presenting secondarily in a different organ. Although the histiocytic precursors of both LCH and RDD originate in the bone marrow, a definitive mechanism linking these two processes has not been described. The LCH diagnosis relies on electron microscopic demonstration of Birbeck granules or the characteristic immunophenotype (CD1a+). On the other hand, in RDD a (CD1a-) and emperipolesis found in histiocytes are crucial for a definite diagnosis. (7,8) In our case, RDD related hypothalamic mass completely resolved after trials of unsuccessful therapies that favored the use of trametinib due her poor tolerance of cytotoxic chemotherapy. Future studies should focus on gathering larger case series with long-term follow-up to better understand the prognosis and develop evidence-based guidelines for diagnosis and targeted treatment.

Abstract 75 Table 1

Table 1

Reported cases of combined RDD-LCH

Authors	Year	No. of cases	Age (years)	Sex	Site
Wang KH et al. [5]	2002	1	45	F	Skin
Kong YY et al. [9]	2007	1	52	F	Skin
Sachdev R et al. [10]	2008	1	3	M	LN
O'Malley DP et al. [11]	2010	9	25[a]	2 M/7 F	LN : 8 Abdominal mass/SC : 1
Llamas-Velasco M et al. [12]	2012	1	68	M	Skin
Cohen-Barak. E et al. [13]	2014	1	10	M	Skin-Bone
Jin W et al. [14]	2014	1	20	F	Skin
Kutty SA et al. [15]	2015	1	31	M	Bone-dura mater
Litzner BR et al. [16]	2015	1	48	F	Skin
Boubacar Efared. [6]	2016	1	30	F	Bone
Our case	2022	1	14	F	Hypothalamic mass / Skin

[a]the average age of the 9 reported cases; F female sex, M male sex, LN lymph node, SC subcutaneous

REFERENCE(S)

1. McClain, K.L., Bigenwald, C., Collin, M. et al. Histiocytic disorders. Nat Rev Dis Primers 7, 73 (2021).

2. Abla O, Jacobsen E, Picarsic J, Krenova Z, Jaffe R, Emile JF, Durham BH, Braier J, Charlotte F, Donadieu J, Cohen-Aubart F, Rodriguez-Galindo C, Allen C, Whitlock JA, Weitzman S, McClain KL, Haroche J, Diamond EL. Consensus recommendations for the diagnosis and clinical management of Rosai-Dorfman-Destombes disease. Blood. 2018 Jun 28;131(26):2877-2890. doi: 10.1182/blood-2018-03-839753. Epub 2018 May 2. PMID: 29720485; PMCID: PMC6024636.

3. Goyal G, Ravindran A, Young JR, Shah MV, Bennani NN, Patnaik MM, Nowakowski GS, Thanarajasingam G, Habermann TM, Vassallo R, Sher T, Parikh SA, Rech KL, Go RS; Mayo Clinic Histiocytosis Working Group. Clinicopathological features, treatment approaches, and outcomes in Rosai-Dorfman disease. Haematologica. 2020 Jan 31;105(2):348-357. doi: 10.3324/haematol.2019.219626. PMID: 31004029; PMCID: PMC7012468.

4. Tillotson CV, Anjum F, Patel BC. Langerhans Cell Histiocytosis. 2022 Jul 18. In: StatPearls [Internet]. Treasure Island (FL): StatPearls Publishing; 2022 Jan–. PMID: 28613635.

5. Wang KH, Cheng CJ, Hu CH, Lee WR. Coexistence of localized Langerhans cell histiocytosis and cutaneous Rosai-Dorfman disease. Br J Dermatol. 2002 Oct;147(4):770-4. doi: 10.1046/j.1365-2133.2002.04879.x. PMID: 12366428.

6. Efared B, Mazti A, Chaibou B, Atsame-Ebang G, Sidibé IS, Tahiri L, Erregad F, Hammas N, El Mrini A, El Fatemi H, Chbani L. Bone pathologic fracture revealing an unusual association: coexistence of Langerhans cell histiocytosis with Rosai-Dorfman disease. BMC Clin Pathol. 2017 Apr 7;17:5. doi: 10.1186/s12907-017-0044-1. PMID: 28396615; PMCID: PMC5383940.

7. Pérez A, Rodríguez M, Febrer I, Aliaga A. Sinus histiocytosis confined to the skin: case report and review of the literature. Am J Dermatopathol 1995; 17: 384–8.

8. Foucar E, Rosai J, Dorfman RF. Sinus histiocytosis with massive lymphadenopathy (Rosai–Dorfman disease): review of the entity. Semin Diagn Pathol 1990; 7: 19–73.

9. Kong YY, Kong JC, Shi DR, Lu HF, Zhu XZ, et al. Cutaneous rosai-dorfman disease: a clinical and histopathologic study of 25 cases in China. Am J Surg Pathol. 2007;31(3):341–350. doi: 10.1097/01.pas.0000213387.70783.b6.

10. Sachdev R, Shyama J. Co-existent Langerhans cell histiocytosis and Rosai-Dorfman disease: a diagnostic rarity. Cytopathology. 2008;19(1):55–58.
11. O'Malley DP, Duong A, Barry TS, Chen S, Hibbard MK, Ferry JA, et al. Co-occurrence of Langerhans cell histiocytosis and Rosai-Dorfman disease: possible relationship of two histiocytic disorders in rare cases. Mod Pathol. 2010;23(12):1616–1623. doi: 10.1038/modpathol.2010.157.
12. Llamas-Velasco M, Cannata J, Dominguez I, García-Noblejas A, Aragües M, et al. Coexistence of Langerhans cell histiocytosis, Rosai-Dorfman disease and splenic lymphoma with fatal outcome after rapid development of histiocytic sarcoma of the liver. J Cutan Pathol. 2012;39(12):1125–1130. doi: 10.1111/cup.12013.
13. Cohen-Barak E, Rozenman D, Schafer J, Krausz J, Dodiuk-Gad R, et al. An unusual co-occurrence of Langerhans cell histiocytosis and Rosai-Dorfman disease: report of a case and review of the literature. Int J Dermatol. 2014;53(5):558–563. doi: 10.1111/ijd.12051.
14. Wei J, Zhang Y, Jin J, Zhang J. Cutaneous Rosai-Dorfman disease accompanied by Langerhans cell hyperplasia responsive to combined treatment. Chin Med J (Engl) 2014;127(17):3200.
15. Kutty SA, Sreehari S. Co-occurrence of intracranial Rosai-Dorfman disease and Langerhans histiocytosis of the skull : case report and review of literature. Turk Neurosurg. 2015;25(3):496–499.
16. Litzner BR, Subtil A, Vidal CI. Combined cutaneous Rosai-Dorfman disease and localized cutaneous Langerhans cell histiocytosis within a single subcutaneous nodule. Am J Dermatopathol. 2015;37(12):936–939. doi: 10.1097/DAD.0000000000000347.

A CASE OF PLEXIFORM NEUROFIBROMA OF THE APPENDIX: A RARE ENTITY IN NEUROFIBROMATOSIS

Hassan Alkhatatneh, Tanganyika Barnes, Jason Lofters, Danielle Pope. *Englewood Hospital and Medical Center*

Introduction/Background Neurofibromatosis one (NF1), or Von Recklinghausen's disease, is an autosomal dominant disorder with a prevalence of about 1 in 3000.[8] It is a multi-system disorder that affects any organ in the body. However, patients typically present with cutaneous neurofibromas , café-au-lait spots, Lisch nodules, or inguinal/axillary freckling.[2,8] Gastrointestinal (GI) involvement is reported in 10-25% of cases, most frequently involving the jejunum, stomach, ileum, duodenum, and colon.[2] Appendiceal neurofibromas (ANF) are extremely rare with less than 10 cases previously reported.[2] Here, we describe a case of an ANF in a patient with NF1.

Case Preentation A 51-year-old female previously diagnosed with NF1 with diffuse cutaneous neurofibromas. She presented with a burning epigastric pain, nausea, and episodes of vomiting. Physical exam was significant for generalized abdominal tenderness but no rebound or guarding. Circumferential mural thickening of a tubular loop of the bowel was seen on abdominal CT suggestive of an appendiceal mucocele (figure 1). Emergent laparoscopic appendectomy showed a severely dilated, non-inflamed, and non-perforated appendix measuring three by eight centimeters. She was transfused postoperatively due to anemia. She was discharged on postoperative day 5 but returned 9 days later with abdominal pain, diarrhea, and leukocytosis. CT abdomen revealed a rim-enhancing collection contiguous with the ileocolic anastomosis (figure 2) and underwent CT-guided aspiration that showed dark, foul-smelling fluid. She was started on ceftriaxone, metronidazole and analgesics. The collection resolved by day 6, and she was discharged after 8 days.The pathology report was consistent with plexiform neurofibroma diffusely involving the appendix, with positive S-100 staining. The appendiceal mucosa showed hyperplastic changes. The small bowel and colonic margins of resection were negative for malignancy.
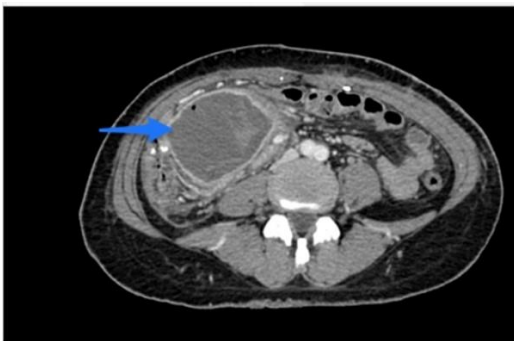
Abstract 76 Figure 1 CT showing circumferential mural thickening of a tubular bowel loop within the right lower quadrant extending to the base of the cecum as well as a focally dilated loop of bowel extending to the expected location of the ileocecal valve (arrow)

Abstract 76 Figure 2 CT showing a rim enhancing collection measuring 6.1x 7.4x 9.3cm contiguous with the ileocolic anastomosis with features concerning for an infected hematoma or abscess (arrow).

Discussion Plexiform neurofibromas are tumors that present as infiltrative lesions growing and expanding within peripheral nerves,[1] which are considered pathognomonic of NF1. Microscopically, they

are characterized by the presence of Schwann cells, fibroblasts and inflammatory cells surrounded by a loose myxoid background. They tend to present as cutaneous lesions, but a study using whole-body MR reported that 56% of the patients had internal, clinically asymptomatic plexiform neurofibromas.[2] Internal plexiform neurofibromas rarely develop in the gastrointestinal tract (GIT) and are reported at a frequency of 5%-25%. They occur at any site along the GIT and can arise from peritoneal and mesenteric soft tissues.[3] Yet, they mostly involve the upper GIT and less than 5% of patients report symptoms. When symptomatic, patients present with obstruction, intussusception, ulceration, or bleeding.[4] Based on our patient's presentation and history of NF1, one would expect an upper GI manifestation of the disorder. Case reports[5,6] previously published described ANFs, with the majority presenting with abdominal pain and imaging findings suspicious for appendicitis or appendiceal masses. As in our patient, surgical removal is recommended given the risk of rupture as well as the possibility of the presence of a malignant nerve sheath tumor. Our case showcases the need for considering lower GI lesions in NF1 patients with atypical presentations. The GIT is an uncommon site of NF1 involvement. The presence of an ANF is particularly rare and may present in an unconventional manner. Characteristic histologic findings confirm the diagnosis and complete removal of the tumor is recommended given the small risk of malignancy.

REFERENCE(S)
1. Abbas, A. K., & Aster, J. C. (2015). Robbins and Cotran pathologic basis of disease. Elsevier/ Saunders
2. Mautner, V. F., Asuagbor, F. A., Dombi, E., Fünsterer, C., Kluwe, L., Wenzel, R., ... & Friedman, J. M. (2008). Assessment of benign tumor burden by whole-body MRI in patients with neurofibromatosis 1. Neuro-oncology, 10(4), 593-598.
3. Ferner, R. E., & Gutmann, D. H. (2013). Neurofibromatosis type 1 (NF1): diagnosis and management. In Handbook of clinical neurology (Vol. 115, pp. 939-955). Elsevier.
4. Agaimy, A., Vassos, N., & Croner, R. S. (2012). Gastrointestinal manifestations of neurofibromatosis type 1 (Recklinghausen's disease): clinicopathological spectrum with pathogenetic considerations. International journal of clinical and experimental pathology, 5(9), 852.
5. Komo T, Oishi K, Kohashi T, et al. Appendiceal neurofibroma with low-grade appendiceal mucinous neoplasm in neurofibromatosis type 1 patient: A case report. Int J Surg Case Rep. 2018;53:377-380. doi:10.1016/j.ijscr.2018.11.005
6. Jeong, G. A. (2014). Neurofibroma of the appendix and multiple gastrointestinal stromal tumors of small bowel in neurofibromatosis type 1 patient. Korean Journal of Clinical Oncology, 10(2), 116-121.
7. Levy, A, Patel, N, Dow, N, Abbot, R, Miettinen, M, & Sobin, L. (2005). Abdominal Neoplasms in patients with Neurofibromatosis Type 1: radiologic pathologic correlation. Radiographics, 25:455-480

77

MALIGNANT TRITON TUMOR IN AN OTHERWISE ASYMPTOMATIC NEUROFIBROMATOSIS TYPE 1 PATIENT: AN ATYPICAL CASE

Chadane Thompson, Amer Hammad, Hassan Alkhatatneh, Maxwell Janosky, Alyssa Foster. *Englewood Hospital and Medical Center*

Introduction/Background Neurofibromatosis (NF) is an autosomal dominant tumor-predisposition syndrome primarily affecting the skin and nervous system and typically presenting in childhood.[1] Malignant peripheral nerve sheath tumors (MPNSTs) are a group of rare, aggressive spindle cell neoplasms of peripheral nerves or plexiform neurofibromas in NF type 1 (NF-1).[2] MPNSTs represent only 3-5% of all soft tissue sarcomas but are the leading cause of mortality and most common malignant neoplasm seen in NF-1, where the lifetime risk is ~8-13%.[1-3]. Malignant Triton tumor (MTT) is a rare subset of MPNSTs with heterologous skeletal muscle (rhabdomyoblastic) differentiation and is scarcely reported in literature.[2] Here, we report a case of NF-1 with the atypical presentation of an isolated retroperitoneal MTT in the fifth decade of life.

Case Presentation A 47-year-old male with a history of nephrolithiasis presented to the ED with right flank pain radiating to the pelvis with associated nausea. On examination, vital signs were within normal limits and right costovertebral tenderness was noted. Labs revealed no abnormalities other than microscopic hematuria. Abdominal computed tomography (CT) scan was requested to rule out nephrolithiasis. CT showed a retroperitoneal right lower pelvic soft tissue mass (9.7 x 6.3 x 7.5 cm) arising from the right obturator internus muscle, which was suspicious for a sarcoma. CT-guided core biopsy revealed a bland spindle cell lesion in a collagenous stroma with non-specific initial immunohistochemical findings. Repeat immunostaining showed focal positivity for S-100 protein and desmin, consistent with Schwannian differentiation and rhabdomyoblastic components respectively. There was also evidence of somatic and germline mutations of the neurofibromin 1 (NF1) gene. Histopathology revealed a high-grade MPNST with heterologous rhabdomyosarcomatous differentiation, which is diagnostic of a malignant Triton tumor. The lesion was surgically resected. However, it later recurred with peritoneal metastasis and radiologic progression despite chemoradiation. The patient is currently enrolled in a clinical trial.

Discussion NF-1 typically presents in the childhood with distinct cutaneous (café au lait spots, intertriginous freckling) and ophthalmic findings (Lisch nodules, optic gliomas), with both benign and malignant tumors arising later in adolescence and adulthood.[1] MPNSTs commonly arise in pre-existing plexiform neurofibromas and often present as persistent pain or a rapid increase in size of a previously known tumor.[1-2] MPNSTs may be NF-1-associated (most common), sporadic, or radiation-induced [2]. They are particularly aggressive tumors with a predilection for local recurrence and blood-borne metastasis.[1] Therefore, prognosis is poor, particularly with truncal location, tumor size > 5cm, high-grade morphology, metastasis and presence of NF-1, as seen in this case.[2,4] This atypical presentation raises several questions as it is unusual for NF-1 to first present in the fifth decade of life, let alone with MTT in an otherwise asymptomatic patient with no family history of NF-1. However, NF has variable expression and rare, atypical forms. Given our patient's characteristic presentation, this case may represent the late-onset form of NF—a very rare variant with absence of usual cutaneous findings and development of neurofibromas or malignant tumors, classically after age 30.[5] Moreover, there may be no known family history of NF. To our knowledge, there are few reported cases of late-onset NF presenting with MPNSTs.Based on this, we recommend that patients diagnosed with sporadic MPNST/MTT be considered for NF1 gene mutation screening. Furthermore, the role of risk stratification and monitoring for MPNSTs in late-onset NF must be emphasized.

REFERENCE(S)

1. Friedman J. Neurofibromatosis 1. In: GeneReviews ® [Internet]. University of Washington, Seattle; 1998 Oct 2 [updated 2022 Apr 21].
2. WHO Classification of Tumours Editorial Board. Soft tissue and bone tumours. 5th ed. vol 3. WHO classification of tumours series. International Agency for Research on Cancer; 2020.
3. Evans D, Baser M, McGaughran J, et al. Malignant peripheral nerve sheath tumours in neurofibromatosis 1. J Med Genet. 2002;39(5):311–314.
4. Cai Z, Tang X, Liang H, et al. Prognosis and risk factors for malignant peripheral nerve sheath tumor: a systematic review and meta-analysis. World J Surg Oncol. 2020;18(1):257. doi:10.1186/s12957-020-02036-x
5. Ideshita Y, Harada Y, Yasaki S, et al. A Case of late-onset neurofibromatosis speculated as type 7. J Case Rep Stud. 2016;4(5):503. doi:10.15744/2348-9820.4.503

DOUBLE WHAMMY!: NEW DIAGNOSIS OF GLUCOSE 6-PHOSPHATE DEHYDROGENASE DEFICIENCY WITH HEMOLYTIC ANEMIA AND METHEMOGLOBINEMIA

[1]Zachary Banbury, [2]Joel Wright, [3]Adam Zayac, [2]Sofia Terner. [1]*Englewood Health;* [2]*Englewood Hospital;* [3]*Westchester Medical Center/ New York Medical College*

Introduction/Background Glucose 6-phosphate dehydrogenase (G6PD) deficiency is the most common enzymatic deficiency affecting upward of 400 million people worldwide. It affects men more than women due to its X-linked inheritance with prevalence in African, Asian and Mediterranean ethnicities. It is often diagnosed after exposure to oxidative stresses including medications (e.g. Isoniazid, Methylene blue, Primaquine, Trimethoprim) which induce hemolytic anemia. Methemoglobinemia (MetHb) can be congenital or acquired with acquired Methb accounting for the majority of cases seen, often occurring after exposure to direct oxidizing agents (e.g. benzocaine, prilocaine), indirect oxidizing agents (e.g. nitrates) or metabolic activation (e.g. aniline, dapsone). The co-occurence of G6PD deficiency and MetHb is seldom seen in literature. We present a rare case of a 30 year old male presenting after a urinary tract infection diagnosed with concurrent G6PD deficiency and MetHb.

Case Presentation A 30 year old Cuban man presented with three days of urinary frequency, dysuria, dark urine, malaise, right flank pain and lower abdominal pain radiating to the testes for three days and one day of fever. He had no known family history of blood disorders, toxin or dye exposure, over the counter or herbal medication use. On exam, vital signs were normal other than pulse oximetry of 83% for which he was placed on oxygen. The rest of the exam was normal. Laboratory investigations revealed arterial blood gas showing a partial pressure of oxygen of 130.2mmHg (80-100mmHg) with co-oximeter testing revealing a methemoglobin level of 12.5% (0.4-1.5%). Further labs showed Hemoglobin of 11.3 K/UL on admission, which precipitously fell to 5.9 K/UL; on day 3 (requiring two units of red blood cell transfusion), indirect hyperbilirubinemia (Total bilirubin 6.3 mg/dL, Direct bilirubin 0.5mg/dL), elevated CRP (93.6 mg/dL) and elevated ferritin (6071 ng/mL). Urinalysis confirmed a urinary tract infection. He had a hyperproliferative anemia (Retic % 4.2) with evidence of intravascular hemolysis suggested by low haptoglobin and elevated LDH levels. Peripheral blood smear demonstrated macrospherocytosis with rouleaux formation. He was empirically started on prednisone. Further hemolytic workup with Coombs test, cold agglutinin testing and complement levels were all negative, however G6PD levels returned low (6.4 U/g), confirming the diagnosis of G6PD deficiency. The methemoglobinemia was treated with intravenous ascorbic acid rather than methylene blue due to concern for worsening hemolysis. With stabilization of hemoglobin, improvement of hyperbilirubinemia and resolution of presenting symptoms, he was discharged with outpatient Hematology follow up.

Discussion This case highlights the occurrence of two distinct hematologic processes occurring simultaneously, namely G6PD deficiency, in which there is an acute hemolytic anemia, and MetHb in which there is a functional anemia due to the loss of the oxygen carrying capacity from the conversion of reduced ferrous iron to the oxidized ferric state. It is postulated that patients with G6PD deficiency have decreased NADPH (nicotinamide adenine dinucleotide phosphate) production which is a cofactor required by the NADPH-MetHb reductase pathway to keep MetHb levels less than 1%- thus providing a link between these two hematologic conditions. While some case reports describe an association between G6PD deficiency and MetHb in the setting of classic precipitants such as fava beans and hydroxychloroquine use, this association is quite rare (1,2) As seen in our case, only ascorbic acid should be used for treatment of MetHb in patients with G6PD deficiency since methylene blue can lead to worsening hemolysis. In clinical practice, the presence of both acute hemolytic anemia and MetHb

should lead physicians to consider underlying G6PD deficiency and thus avoid use of methylene blue as it can worsen hemolysis and increase risk of deterioration.

REFERENCE(S)
1.   Al-Dubai, Husam MD; Al-Mashdali, Abdulrahman MD; Hailan, Yousef MD. Acute hemolysis and methemoglobinemia secondary to fava beans ingestion in a patient with G6PD deficiency: A case report of a rare co-occurrence. Medicine: November 24, 2021 - Volume 100 - Issue 47 - p e27904doi: 10.1097/MD.0000000000027904
2.   Laslett N, Hibbs J, Hallett M, et al. (May 25, 2021) Glucose-6-Phosphate Dehydrogenase Deficiency-Associated Hemolytic Anemia and Methemoglobinemia in a Patient Treated With Hydroxychloroquine in the Era of COVID-19. Cureus 13(5): e15232. doi:10.7759/cureus.15232

MALIGNANT RECTAL LIPOSARCOMA: A RARE CAUSE OF A COMMON PRESENTING COMPLAINT

[1]Hassan Alkhatatneh,[1]Jason Lofters, [1]Mahmoud Abdelhadi, [2]Meghan Kaumaya, [1]Tanganyika Barnes.
[1]*Englewood Hospital and Medical Center;* [2]*Hematology/Oncology Physicians of Englewood*

Introduction/Background Sarcomas are malignant tumors arising from connective tissue. One of the more common histologies is the liposarcoma which may present as a painless, gradually enlarging mass, usually of the extremities and retroperitoneum. Unusual origins have however, been known to occur. Here we present a rare case of a metastatic dedifferentiated liposarcoma of rectal origin.

Case Presentation Patient is an 80-year-old male with a medical history of coronary artery disease, atrial fibrillation, and prostate cancer post radiotherapy in 2019. He presented with one week of constipation and intermittent rectal bleeding. Colonoscopy revealed non-bleeding diverticulosis, multiple polyps in the colon and rectum including a 2cm pedunculated polyp in the transverse colon which was the source of bleeding and an 8mm rectal polyp (figure 1). Polypectomy was performed on all visible lesions. On biopsy, the colonic polyps were found to be hyperplastic and tubulovillous adenomas. The rectal polyp however, consisted of pleomorphic, discohesive sheets of neoplastic cells with infiltration of the lamina propria. Immunohistochemistry (IHC) was positive for vimentin and negative for Melan A, S-100, AE1/AE3, Cam 5.2, SMA, CD30, CD45 and CD34. These findings were consistent with a high-grade sarcomatoid malignant neoplasm with differentials of a true sarcoma or a sarcomatoid carcinoma with loss of epithelial marker expression considered. Staging investigations revealed widespread lytic lesions one of which was biopsied. Pleomorphic discohesive sheets of sarcomatoid neoplastic cells similar to those of the rectal lesion were noted. IHC was positive for MDM2, CDK4 and SMA while negative for Desmin, STAT6 and EMA. These findings were felt to be most consistent with that of a metastatic high grade spindle cell sarcoma, specifically a dedifferentiated liposarcoma. Treatment with Pazopanib was subsequently initiated.
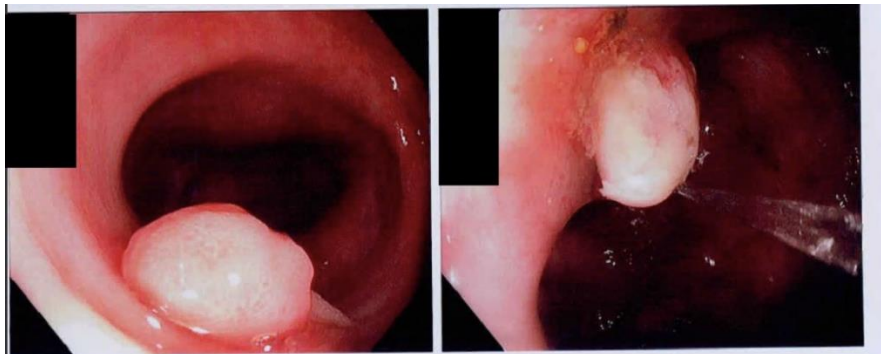
Abstract 79 Figure 1 Polyps seen at Colonoscopy

Discussion DDLPs exhibit a wide morphologic spectrum and often present with histologic features of undifferentiated pleomorphic or spindle cell sarcomas.[1] They frequently arise from the retroperitoneum and are diagnosed in late adulthood. Risk factors are varied, but include prior radiation which portends poorer prognosis. Liposarcomas arising from the gastrointestinal tract (GIT) are rare with incidence ranging from 0.1-5.8%.[2] The incidence of DDLPs specifically is even lower. In one study examining 155 cases of DDLPs, none arose from the GIT.[3] Lesions often achieve considerable size before being symptomatic, and patients with GIT involvement often present with abdominal pain, constipation, weight loss and GI bleeding with resulting anemia.[2] DDLPs behave as high-grade sarcomas with rates of

local recurrence of 41% and metastasis of 15-30%.[1] In one study of 148 cases of metastatic DDLPs, the most common sites were the lung, subcutaneous tissue, lymph node and liver; bone was the site of metastasis in 4.7% of cases.[4]   The fact that our patient's lesion arose from the rectum and appeared to have metastasised early makes this case particularly rare. Management of this malignancy is difficult, particularly when advanced and includes chemotherapeutic agents such as doxorubicin as well as targeted therapies as in our case.[5,6] In summary, thorough work-up and pathologic analysis of rectal polyps, particularly in the setting of prior radiation therapy, is crucial for proper determination of diagnosis, prognosis and treatment.

REFERENCE(S)
1.   Thway, K. (2019, March). Well-differentiated liposarcoma and dedifferentiated liposarcoma: an updated review. In Seminars in diagnostic pathology (Vol. 36, No. 2, pp. 112-121). WB Saunders.
2.   Gajzer, D. C., Fletcher, C. D., Agaimy, A., Brcic, I., Khanlari, M., & Rosenberg, A. E. (2020). Primary gastrointestinal liposarcoma—a clinicopathological study of 8 cases of a rare entity. Human pathology, 97, 80-93.
3.   Henricks, W. H., Chu, Y. C., Goldblum, J. R., & Weiss, S. W. (1997). Dedifferentiated liposarcoma: a clinicopathological analysis of 155 cases with a proposal for an expanded definition of dedifferentiation. The American journal of surgical pathology, 21(3), 271-281.
4.   Tirumani, S. H., Tirumani, H., Jagannathan, J. P., Shinagare, A. B., Hornick, J. L., Ramaiya, N. H., & Wagner, A. J. (2015). Metastasis in dedifferentiated liposarcoma: Predictors and outcome in 148 patients. European Journal of Surgical Oncology (EJSO), 41(7), 899-904.
5.   Chamberlain, F. E., Wilding, C., Jones, R. L., & Huang, P. (2019). Pazopanib in patients with advanced intermediate-grade or high-grade liposarcoma. Expert opinion on investigational drugs, 28(6), 505-511.
6.   Ratan, R., & Patel, S. R. (2016). Chemotherapy for soft tissue sarcoma. Cancer, 122(19), 2952-2960.

IRINOTECAN INDUCED TRANSIENT DYSARTHRIA: A CASE SERIES

[1]Caleb Spencer, [2]Abid Miah, [1]Prajwal Hegde, [1]Abdul Miah, [1]David Macari, [1]Ahmed Elsayed, [1]Danae Hamouda. [1]*University of Toledo;* [2]*Texas Tech University*

Introduction/Background Irinotecan, a topoisomerase inhibitor also known as CPT-11, is an anti-tumor agent against a variety of cancers. It acts to prevent DNA replication of cancer cells by inhibiting DNA stability and replication. Irinotecan in combination with leucovorin calcium and fluorouracil (FOLFIRI) with the addition of oxaliplatin (FOLFIRINOX) has proven to be an effective treatment against advanced cases of colorectal and pancreatic cancers. It is also an alternative treatment in metastatic gastric cancer if cisplatin is not tolerated. The most common adverse events with irinotecan use are diarrhea and neutropenia, with roughly a third of patients experiencing these symptoms. Here we describe two patients that developed transient dysarthria after infusion of irinotecan. There have been approximately 50 cases described in the literature to date. The goal of this article is to add to the growing volume of similar cases and call to attention the importance of shared decision making with patients.

Case Presentation PATIENT AA 61-year-old female initially presented to her primary care physician (PCP) in July 2022 with a two-month duration of persistent watery diarrhea up to six times daily along with epigastric abdominal pain radiating to the back, nausea, vomiting, early satiety, worsening nocturnal heartburn, and 3.6-kilogram weight loss. Her medical history included atrial fibrillation, acid reflux, and rheumatoid arthritis. Besides an elevated lipase at 438 U/L (normal 23-300), labs including Complete Metabolic Panel (CMP), Complete Blood Count (CBC), amylase, GI Pathogen Panel, and C. difficile PCR were negative. Her PCP referred her to Gastroenterology after an abdominal ultrasound revealed a dilated pancreatic duct at 1.5 cm and common bile duct at 0.9 cm. Cancer antigen (CA) 19-9 was obtained and found to be 272.0 U/mL (normal 0.0-35.0). Magnetic resonance cholangiopancreatography (MRCP) showed dilation of the main pancreatic and common bile duct (known as the "double duct sign"). She then underwent endoscopic ultrasound (EUS) with fine needle aspirate (FNA) taken from the pancreatic head, of which the pathology was consistent with adenocarcinoma. Additional imaging was negative for any signs of metastasis, so the patient underwent total pancreatectomy, splenectomy, and cholecystectomy with diagnostic laparoscopic wedge liver biopsy, lymph node resection, and superior mesenteric vasculature biopsy in September 2022. Pathology showed moderately differentiated adenocarcinoma invading through duodenum muscularis propria into the mucosa, the superior mesenteric artery showed neoplasm, and one of eight portal lymph nodes was positive for malignancy. She was staged at III pT4pN1 and initiated on adjuvant FOLFIRINOX in November 2022.Approximately an hour after her first infusion of irinotecan 150 mg/m2 (288 mg total) at a rate of 176 mL/hr over 90 minutes, the patient began experiencing slowing and thickening of her speech. Prior to this, oxaliplatin 85 mg/m2 (total 163.2 mg) was initiated in dextrose 5% in water (D5W) 250 mL at a rate of 141 mL/hr over 2 hours followed by atropine 0.4 mg and famotidine 20 mg. She was also administered leucovorin 400 mg/m2 (total 769 mg) in D5W 500 mL at a rate of 269 mL/hr over 2 hours during the irinotecan infusion. At the time of her onset of dysarthria, she was hemodynamically stable and afebrile with no signs of additional neurological deficits. She was alert and oriented with no confusion or headache. Irinotecan was held for 30 minutes with slight improvement to her symptoms, so resumed at half rate of 88 mL/hr. 10 minutes after resuming infusion, her dysarthria returned, and irinotecan was stopped. Leucovorin infusion was resumed and completed. No rescue medications were required, and her symptoms resolved completely after an hour. No imaging of the brain was obtained.The patient agreed to continue with irinotecan, and although her symptoms recurred during subsequent infusions, they were much less severe. The infusion time was increased to 180 minutes instead of 90. To date, the

patient is doing well. She is regaining weight, has ample energy levels, and has minimal side effects to her regimen. PATIENT BA 58-year-old female presented to the hospital in August 2022 with a 2-day duration of sharp epigastric pain with associated nausea. There were no other symptoms reported. Her medical history included hyperthyroidism and asthma. The patient had elevated white blood cell count of 13.3 x 109/L (normal 4.0-11.0 x 109/L) and lipase 518 U/L, but otherwise labs were unremarkable. Computed tomography (CT) of the abdomen and pelvis with intravenous contrast showed distal body and tail induration with some stranding of adjacent peripancreatic fat, consistent with pancreatitis. No masses were noted. An US was obtained that did not show evidence for gallstones or ductal dilatation. She was treated for pancreatitis and discharged with follow up with gastroenterology 2 months after. In that timeframe, her symptoms were intermittent and began to include diarrhea and progressive acid reflux. She underwent MRCP that showed dilatation of the distal pancreatic duct with heterogeneity. CA 19-9 was normal at 28.1 U/mL; regardless, EUS was performed with FNA of a lesion found on the pancreatic body that was consistent with pancreatic adenocarcinoma. CT angiogram of the abdomen showed contact of the 1.5 cm pancreatic mass with the splenic vein without evidence of tumor vascular involvement, and no enlarged lymph nodes were noted. CT chest with contrast with unremarkable. She was staged at IA cT1cN0. It was opted to pursue neoadjuvant therapy instead of immediate surgery due to the tumor proximity to the portosplenic confluence. It was agreed to initiate FOLFIRINOX for 3-6 months that was initiated January 2023. At her first infusion, oxaliplatin 85 mg/m2 (total 136.85 mg) in D5W 250 mL was given at 139 mL/hr over 2 hours. Leucovorin 400 mg/m2 (total 644 mg) in D5W 500 mL was initiated at 266 mL/hr over 2 hours with atropine 0.4 mg and famotidine 20 mg given 30 minutes after infusion started. Irinotecan 150 mg/m2 (total 242 mg) in D5W 250 mL was then initiated at 175 mL/hr over 90 minutes, but 30 minutes into the infusion, the patient reported headache, shortness of breath, dizziness, feelings of irregular heart rhythm, and feelings of "tongue thickness". The infusion was stopped and normal saline, solumedrol, and diphenhydramine were administered. She experienced some improvement of symptoms but endorsed continued dizziness and residual feelings of "thick tongue". Symptoms resolved after an hour, and infusions were restarted at half rate of 87.5 mL/hr over 180 minutes. Patient did not experience any further complications and was discharged in stable condition. At her following infusion, irinotecan was again administered at the half rate of 87.5 mL/hr over 180 minutes; however, she again experienced tongue thickness and dysarthria. She ultimately opted to discontinue the irinotecan due to these side effects. Magnetic resonance imaging (MRI) of the brain with and without contrast was obtained to evaluate for metastasis, which was negative for masses or other abnormalities.

Discussion The exact mechanism of irinotecan induced dysarthria is unclear. It is postulated that acetylcholinesterase inhibition could be the etiology as evidenced by the gastrointestinal manifestations that commonly arise with its use. One might expect, though, that atropine administration would then alleviate or prevent the dysarthria, yet so far this has been described in only one case. The authors of that case, though, propose that oxaliplatin could augment the cholinergic effects of irinotecan. Patients with UGT1A1*28 or UGT1A1*6 locus mutations tend to have an increased incidence of blood and gastrointestinal adverse events compared to wildtype patients. Such patients are recommended to have an irinotecan-dose reduction; however, no difference in clinical response or prognosis were found. This could perhaps elucidate the etiology for dysarthria as well, but currently it remains unknown. As uncertain as the reason for the dysarthria is, it is equally reassuring that symptoms spontaneously and quickly resolve without lasting impact. The efficacy of irinotecan in advanced cancers should encourage oncologists to recommend continuation of irinotecan despite the worrisome adverse effect of dysarthria. Nonetheless, it is important to consider the patient's willingness to proceed with further treatment, as in the case of our second patient who decided not to continue with irinotecan. Shared decision making is vital to reinforcing patient trust. Hopefully with more evidence and continued reports, patients can feel more reassured should they develop irinotecan induced dysarthria.

REFERENCE(S)

1. Champoux JJ. DNA topoisomerases: structure, function, and mechanism. Annu Rev Biochem 2001; 70: 369-413.
2. Douillard JY, Cunningham D, Roth AD et al. Irinotecan combined with fluorouracil compared with fluorouracil alone as first-line treatment for metastatic colorectal cancer: a multicentre randomised trial. Lancet 2000; 355 (9209): 1041-1047.
3. Conroy T, Desseigne F, Ychou M et al. FOLFIRINOX versus gemcitabine for metastatic pancreatic cancer. N Engl J Med 2011; 364 (19): 1817-1825.
4. Dank M, Zaluski J, Barone C et al. Randomized phase III study comparing irinotecan combined with 5-fluorouracil and folinic acid to cisplatin combined with 5-fluorouracil in chemotherapy naive patients with advanced adenocarcinoma of the stomach or esophagogastric junction. Ann Oncol 2008; 19 (8): 1450-1457.
5. Riera P, Paez D. Elucidating the role of pharmacogenetics in irinotecan efficacy and adverse events in metastatic colorectal cancer patients. Expert Opin Drug Metab Toxicol 2021; 17 (10): 1157-1163.
6. Sevilla Garcia I, Rueda A, Alba E. Irinotecan-induced central nervous system toxicity: a case report. J Natl Cancer Inst 1999; 91 (7): 647.
7. Baz DV, Bofill JS, Nogueira JA. Irinotecan-induced dysarthria. J Natl Cancer Inst 2001; 93 (18): 1419-1420.
8. Ceccaldi B, Kara F, Mommeja-Marin H et al. [Dysarthria during irinotecan administration]. Rev Med Interne 2002; 23 (11): 950-951.
9. De Marco S, Squilloni E, Vigna L et al. Irinotecan chemotherapy associated with transient dysarthria and aphasia. Ann Oncol 2004; 15 (7): 1147-1148.
10. Gomez JA, Sanchez I, Ramirez JA. Irinotecan-induced dysarthria: an insight into its pathogenesis? Gastrointest Cancer Res 2008; 2 (4): 209-210.
11. Hamberg P, De Jong FA, Brandsma D et al. Irinotecan-induced central nervous system toxicity. Report on two cases and review of the literature. Acta Oncol 2008; 47 (5): 974-978.
12. Dressel AJ, van der Mijn JC, Aalders IJ et al. Irinotecan-induced dysarthria. Case Rep Oncol 2012; 5 (1): 47-51.
13. Lee KA, Kang HW, Ahn JH et al. Dysarthria induced by irinotecan in a patient with colorectal cancer. Am J Health Syst Pharm 2013; 70 (13): 1140-1143.
14. Chandar M, de Wilton Marsh R. Severe Generalized Weakness, Paralysis, and Aphasia following Administration of Irinotecan and Oxaliplatin during FOLFIRINOX Chemotherapy. Case Rep Oncol 2015; 8 (1): 138-141.
15. Matsuoka A, Maeda O, Inada-Inoue M et al. FOLFIRINOX-induced reversible dysarthria: A case report and review of previous cases. Oncol Lett 2015; 10 (4): 2662-2664.
16. Gunturu KS, Yao X, Cong X et al. FOLFIRINOX for locally advanced and metastatic pancreatic cancer: single institution retrospective review of efficacy and toxicity. Med Oncol 2013; 30 (1): 361.
17. Ramirez KG, Koch MD, Edenfield WJ. Irinotecan-induced dysarthria: A case report and review of the literature. J Oncol Pharm Pract 2017; 23 (3): 226-230.
18. Elbeddini A, Hooda N, Gazarin M et al. Irinotecan-Associated Dysarthria in Patients with Pancreatic Cancer: A Single Site Experience. Am J Case Rep 2020; 21: e924058.
19. Zhen DB, McDevitt RL, Zalupski MM et al. Irinotecan-associated dysarthria: A single institution case series with management implications in patients with gastrointestinal malignancies. J Oncol Pharm Pract 2019; 25 (4): 980-986.
20. Sogabe S, Yuki S, Takano H et al. [A case of sigmoid colon cancer with temporary dysarthria associated with irinotecan]. Gan To Kagaku Ryoho 2011; 38 (8): 1375-1377.

21. De Lisa M, Ballatore Z, Marcantognini G et al. Irinotecan-Induced Transient Dysarthria: Case Series and Updated Literature Review. Oncol Ther 2020; 8 (1): 147-160.
22. .Li M, Wang Z, Guo J et al. Clinical significance of UGT1A1 gene polymorphisms on irinotecan-based regimens as the treatment in metastatic colorectal cancer. Onco Targets Ther 2014; 7: 1653-1661.

81

A MYSTERIOUS CASE OF RECURRENT SINUSITIS

[1]Nicoy Downie, [1]Abigiail Phelps, [2]Nakhle Saba. *[1]Tulane University; [2]Tulane Cancer Center*

Introduction/Background Extranodal NK/T cell lymphoma (ENKL) is a rare subtype of peripheral T cell lymphoma. ENKL, nasal type commonly occurs in the nasal and upper aerodigestive region. Patients typically present initially with nonspecific localized symptoms including nasal obstruction, nasal discharge, and epistaxis, typically treated as sinusitis. Given the overlapping features in recurrent infections and underlying lymphomas, persistent sinusitis should prompt additional workup for lymphoma including imaging, assessment of EBV viral load, and LDH levels due to the difference in overall survival when diagnosed as early stage. Adequate staging is also a concern, thus early use of PET imaging even prior to oncology referral is recommended to not delay treatment.

Case Presentation A 47-year-old man presented with cervical lymphadenopathy, persistent rhinorrhea, and night sweats. He failed two antibiotic courses, and nasal cavity and maxillary sinus biopsies were inconclusive, showing necrotic debris without organisms.   At three months, a 2.5 cm necrotic, ulcerating lesion developed on the soft palate and erythematous, pruritic papules and plaques on face and neck. Qualitative serum Epstein-Barr Virus (EBV) PCR was positive. Biopsies revealed atypical lymphocytic infiltrate. Flow cytometry was positive for CD3, CD7, CD30, CD56 and EBV (EBER-ISH), diagnostic of Extranodal NK/T-cell Lymphoma (ENKL), nasal type.   He received two cycles of modified SMILE regimen and initiated radiation before succumbing. Despite responding to chemotherapy initially, the patient progressed while receiving radiation therapy to involved sites after two cycles of mSMILE. He passed from liver failure. Pre-mortem biopsy confirmed extensive ENKL liver involvement.

Discussion ENKL, nasal type is a rare subtype of peripheral T cell lymphoma associated with EBV. Patients typically present initially with nonspecific localized symptoms including nasal obstruction, nasal discharge, and epistaxis. Internists should have high suspicion in patients with persistent sinusitis and/or epistaxis that fails antibiotics, as early detection is paramount for survival. Workup should include PET/CT scan given its superior detection of nodal and extranodal lesions and its use in evaluating clinical response/progression-free survival. PET imaging may have revealed liver involvement in our patient without abnormal liver enzymes or focal lesions on CT. Any soft tissue abnormalities on imaging should be evaluated with biopsy. Notably, as in our case, histologic diagnosis is challenging due to prominent necrosis and vascular damage. EBV infection should be assessed by EBV-encoded RNA in situ hybridization (EBER-ISH) as viral load correlates with clinical stage, tumor burden, response to therapy, and survival (NCCN 20-22).In patients with persistent sinusitis that fails antibiotics, internists should consider workup for ENKL, including imaging, biopsy, and EBV viral load while awaiting Oncology referral given significant difference in overall survival in early stage ENKL vs advanced stage.

REFERENCE(S)
1. Kim WY, Montes-Mojarro IA, Fend F, Quintanilla-Martinez L. Epstein-Barr Virus-Associated T and NK-Cell Lymphoproliferative Diseases. Front Pediatr. 2019 Mar 15;7:71. doi: 10.3389/fped.2019.00071. PMID: 30931288; PMCID: PMC6428722.
2. Fox CP, Civallero M, Ko YH. Survival outcomes of patients with extranodal natural-killer T-cell lymphoma: a prospective cohort study from the international T-cell Project. Lancet Haematol.2020 Apr;7(4):e284-e294.doi: 10.1016/S2352-3026(19)30283-2. Epub 2020 Feb 24. PMID: 32105608.
3. Moon, S. H., Cho, S. K., & Kim, W.-S. (2013, July). The Role of 18F-FDG PET/CT for Initial Staging of Nasal Type Natural Killer/T-Cell Lymphoma: A Comparison with Conventional Staging Methods. Journal of Nuclear Medicine. https://jnm.snmjournals.org/content/54/7/1039

Implementation Science

82

A HYBRID 2 TRIAL OF PHAT LIFE EFFECTIVENESS AND IMPLEMENTATION FOR ADOLESCENTS ON PROBATION: DELIVERY BY YOUTH LEADERS VS. PROBATION STAFF

[1]Geri Donenberg, [1]Erin Emerson, [1]Ashley Kendall, [2]Nyssa Snow-Hill. [1]*University of Illinois Chicago;* [2]*Depaul University*

Introduction/Background Juvenile justice involvement is implicated in long-term health disparities in Black communities, including poor sexual and reproductive health and substance use. Justice-involved youth report high rates of marijuana and alcohol use and risky sexual activity and are more likely to test positive for sexually transmitted infections than their peers. One evidence-based intervention for youth on probation, Preventing HIV/AIDS among Teens (PHAT) Life, has been shown to reduce sexual risk taking among youth who report the highest risk behavior when research assistants delivered PHAT Life. Research assistants, however, are not sustainable within the justice system. To increase feasibility, acceptability, and sustainability, this hybrid 2 trial compared two implementation strategies, youth-led (YL) versus probation staff-led (PS) PHAT Life and examined effectiveness and implementation outcomes.

Objective(s) To compare two implementation strategies, youth-led (YL) versus probation staff-led (PS) PHAT Life and examine effectiveness and implementation outcomes.

Methods Adolescents 13-17 years old (M=16.15) recently arrested and placed on probation were group randomized to YL-led (n=90) versus PS-led (n=80) PHAT Life. Participants were 91% male, and 87% African American. Teens self-reported their condom use at baseline and six months, and key informant interviews (n=12) with PS and juvenile justice administrators evaluated implementation outcomes. Retention efforts were curbed due to COVID, but retention at 6-months reached 69%.

Results Groups did not differ on any study variables at baseline. Across conditions, youth reported a significant decrease in the number of vaginal/anal sex partners in the past 6-months from pre-intervention to post-intervention (p=.01) and significant decreases in marijuana use from pre-intervention to post-intervention (p=.02). T-tests comparing the means of the two conditions (YL vs. PS) at follow-up, controlling for baseline reports, showed teens in the PS group reported more condom use at 6-months than teens in the YL group. Key informant interviews revealed extensive support for the PHAT Life program. PS reported appreciating the opportunity to learn to deliver PHAT Life, but challenges with carving out time given competing job responsibilities. Justice administrators expressed a desire to sustain the program, but expressed concern about funding.

Conclusion Findings re-confirm the effectiveness of PHAT Life on sexual risk for adolescents on probation and support new evidence for decreased marijuana use. Surprisingly, findings favored the PS group on condom use. Future analyses will explore other behavioral effects between conditions, including potential mediators and moderators, and additional implementation factors. Of note, almost all of the post-intervention data were collected pre-COVID, and thus, cannot be attributed to pandemic-related effects.

REFERENCE(S)
1. Donenberg, G., Emerson, E., & Kendall, A. (2018). HIV-Risk Reduction Intervention for Juvenile Offenders on Probation: The PHAT Life Group Randomized Controlled Trial. Health Psychology, 37(4), 364-374.

PATIENT AND PROVIDER PERCEIVED BARRIERS AND FACILITATORS TO OPHTHALMOLOGY VISIT ADHERENCE: IDENTIFYING THE ROLE OF MOTIVATION VERSUS ABILITY

Archit Potharazu, R. McKinley Sherrod, Diana Nguyen, Cameron Beversluis, R. V. Paul Chan, Sage Kim, Jerry Krishnan, Hugh Musick, Angelica Scanzera. *University of Illinois Chicago*

Introduction/Background Adherence to eye care visits is associated with improved visual outcomes for those with eye disease.[1] However, less than 60% of adults at high risk of vision loss reported receiving eye care in 2017.[2] Social vulnerability is associated with reduced healthcare access and may represent a contributing barrier to visit adherence.[3] Understanding influencing factors is essential for the design of effective interventions aimed at increasing visit adherence for patients living in neighborhoods with high social vulnerability.

Objective(s) To engage patients from neighborhoods with high social vulnerability and providers to identify perceived barriers and facilitators to eye visit adherence at a diverse urban hospital-based ophthalmology department to inform future interventions.

Methods Potential participants were stratified via neighborhood social vulnerability index (SVI), a composite measure ranging from 0 to 1, with 1 representing the 100th percentile for extreme social vulnerability. A classification tree using binary recursive partitioning was used to determine a minimum cutoff SVI of 0.61. Semi-structured interviews were conducted with individuals 18 years and older with a neighborhood SVI greater than 0.61 and providers delivering care in the General Eye Clinic of the University of Illinois Chicago. We conducted rapid qualitative analysis informed by human-centered design – an approach that emphasizes end-user viewpoints to unearth insights – to identify barriers and facilitators to eye visit adherence. Identified factors were then situated within the Consolidated Framework for Implementation Research (CFIR) framework. Upon identification of additional factors that did not fit within CFIR, factors were further characterized via the Fogg Behavior model, which posits that behaviors occur when sufficient motivation, ability, and triggers are present.

Results A total of 17 of 85 patients and 8 of 12 providers agreed to participate (table 1). Participants identified four themes situated primarily in the outer setting of CFIR: transportation, time burden, economic situation, and social support. Providers tended to identify insufficient motivation – stemming from patients' lack of understanding of diagnosis or disease – as the main challenge to overcoming these barriers. In contrast, most patients reported feeling well-educated about their diagnosis or disease, expressed a high motivation to attend appointments, expressed strong self-advocacy, and reported vision health as a priority. Therefore, while patients and providers aligned on the role of ability-related barriers as categorized by the Fogg Behavior Model, they had divergent perspectives on motivation-related barriers.

Abstact 83 Table 1 Demographic characteristics of eligible and recruited study participants.

TABLE 1: Demographic characteristics of eligible and recruited study participants

	Participants
Status	Non-adherent: 11 Adherent: 6
Mean Age (years ± SD)	52 ±13 (Range 25-66)
Social Vulnerability Index (mean ± SD)	0.79 (Range 0.62-0.95)
	N (%)
Gender	
Female	11 (64.7)
Male	6 (35.3)
New Patient	4 (23.5)
Race/Ethnicity	
Non-Hispanic Black	12 (70.6)
Hispanic	1 (5.9)
Non-Hispanic White	2 (11.8)
Other/Unknown	2 (11.8)
Insurance Type	
Medicaid	14 (82.3)
Medicare	1 (5.9)
Private	2 (11.8)

Conclusion Visit non-adherence is often attributed to a lack of patient education or motivation. Our findings indicate that lack of ability and resources present more significant barriers for patients from neighborhoods with high social vulnerability versus a lack of motivation or education. Understanding barriers and facilitators within CFIR can provide useful guidance for where within the health system future interventions should be located, while the Fogg Behavior Model can help further refine the purpose of such interventions by introducing considerations of motivation, ability, and triggers. Such interventions may reside outside the four walls of the clinic; hence, healthcare institutions interested in health equity may need to broaden the scope of assistance provided.

REFERENCE(S)
1. Ramakrishnan MS, Yu Y, VanderBeek BL. Visit adherence and visual acuity outcomes in patients with diabetic macular edema: a secondary analysis of DRCRnet Protocol T. Graefes Arch Clin Exp Ophthalmol. Jun 2021;259(6):1419-1425. doi:10.1007/s00417-020-04944-w
2. Benoit SR, Swenor B, Geiss LS, Gregg EW, Saaddine JB. Eye Care Utilization Among Insured People With Diabetes in the U.S., 2010–2014. Diabetes Care. 2019;42(3):427-433. doi:10.2337/dc18-0828
3. Al Rifai M, Jain V, Khan SU, Bk A, Mahar JH, Krittanawong C, Mishra SR, Dani SS, Petersen LA, Virani SS. State-Level Social Vulnerability Index and Healthcare Access: The Behavioral Risk Factor Surveillance System Survey. Am J Prev Med. 2022 Sep;63(3):403-409. doi:10.1016/j.amepre.2022.03.008.

EFFECTS OF COVID-19 ON STOCK INHALER IMPLEMNTATION: A QUALITATIVE ANALYSIS

Paige Hardy, Andrea Pappalardo. *University of Illinois Chicago*

Introduction/Background In 2018, Illinois passed Public Act 100-0726, which allows schools to stock inhaler medication for asthma symptoms.[1] While this program has the potential to ensure critical medication access to individuals without an asthma rescue inhaler, the uptake of stock inhaler programming in Illinois has been slow.[2,3] One potential reason for delays is the COVID-19 pandemic, which has changed school-based health significantly.

Objective(s) This analysis aims to describe barriers and facilitators to stock inhalers resulting from the COVID-19 pandemic and to propose potential solutions.

Methods Key stakeholders in stock inhaler programming from a variety of occupations were targeted for semi-structured interviews. Employees of rural, urban, and suburban school districts across Illinois, especially those located in counties with a high burden of asthma, were recruited. Representatives of national and statewide advocacy groups and public health officials were also asked to participate. Semi-structured interviews were transcribed and uploaded into Atlast.ti for qualitative data analysis. Upon completion of initial coding, another thematic data analysis was performed exclusively on passages designated as "Impact of COVID-19."

Results Overall, the code "COVID-19" was mentioned 32 times in 14 of the 18 interviews (78%). Thematic data analysis of these passages revealed subthemes of: "Too Overwhelmed" (11/14), "Nebulizers not Recommended" (5/14), "Other Safety Concerns" (4/14) and "Potential Positive Impact (5/14) (Table 1). Now that the pandemic has lessened its effect on schools, at least three are revisiting their stock inhaler programs, and the trend is expected to continue. "Nebulizers not Recommended" and "Other Safety Concerns" were also mentioned. These perceived barriers have been addressed by the uniform recommendation to utilize MDIs with disposable spacers and to ready companies with these supplies for statewide distribution. Cleaning instructions and clear protocols have been iteratively constructed with school districts to ensure safe use of stock inhalers between students. "Other Safety Concerns" also include post-COVID conditions which are poorly understood and will warrant further study, which may complicate stock inhaler emergency protocols. Unexpectedly, some stakeholders believed additional public health attention and funding related to the COVID-19 pandemic actually increased recruitment of school nurses in some districts and may have inadvertently facilitated a greater focus on childhood respiratory symptoms and interest in stock inhaler programming. Since four stakeholders in the wider study did mention financial barriers to stock inhalers, and COVID-19 funds will not be sustainable, statewide funding obtained cooperatively with our newly formed stock inhaler coalition can be used as a long-term solution.

Abstract 84 Table 1 Frequency and Illustrative Quotations of Themes and Subthemes. N* - number of unique interviews containing at least one instance of the code

Codes	N*	Subtheme	Illustrative Quotes
Interruption in planning/using inhalers	3	Too Overwhelmed	*"So, you know, just to be honest with you know after looking at commentaries and hearing from school health nurses, you know, so many of them are stressed and burnt-out … with COVID … and everything that's going on."*
Refocus on inhalers	3		
No time	3		
Stress and burnout	2		

New programs choose inhalers	3	Nebulizers not Preferred	*"Shortly after I came on COVID really got started. And so one of the early questions I started asking school nurses and allergists and principals and various school folks was well, "how is this going to work with nebulizers, right, because they produce a mist. And then, of course as you know, CDC came in and said, if you can avoid using a nebulizer please do so."*
Replace nebulizers in use	3		
Fear of spreading COVID-19 through shared inhaler	2	Other Safety Concerns	*"So our worry with using our undesignated albuterol inhaler was that, what if this kid has COVID. And we use our undesignated one even with a spacer and somehow get it infected with COVID and then use it for somebody else."*
COVID-related chronic disease	2		
More resources	3	Potential Positive Impacts	*"I think we have some initiatives and ... recent conversations about health initiatives and educational models. You know, much of it stemming from the pandemic."*
Focus on health	1		

Conclusion While COVID-19 has likely delayed the widespread uptake of stock inhaler programs, it has also led to the allocation of unexpected funds, resources, and attention to the respiratory health of students. Policy implementation efforts should focus on simplifying and reducing the cost of stock inhaler programs and simplifying the processes when possible. These efforts will collectively facilitate the greater dissemination of this evidence-based policy.

REFERENCE(S)
1. Public Act 100-0726.; 2019. https://www.ilga.gov/legislation/publicacts/fulltext.asp?Name=100-0726
2. Volerman A, Lowe AA, Pappalardo AA, et al. Ensuring Access to Albuterol in Schools: From Policy to Implementation. An Official ATS/AANMA/ALA/NASN Policy Statement. Am J Respir Crit Care Med. 2021;204(5):508-522. doi:10.1164/rccm.202106-1550ST
3. Ayala C. The Administration of Undesignated Asthma Medication, School Year 2021-22. Illinois State Board of Education; 2022.

85

INTRODUCING A REAL-TIME METHOD FOR IDENTIFYING THE PREDICTORS OF NON-COMPLIANCE WITH EVENT-BASED REPORTING OF TOBACCO USE IN ECOLOGICAL MOMENTARY ASSESSMENT

[1]Ashley Kendall, [2]Charles Robinson, [1]Kathleen Diviak, [2]Donald Hedeker, [1]Robin Mermelstein.
[1]*University of Illinois Chicago;* [2]*University of Chicago*

Introduction/Background The use of ecological momentary assessment (EMA) or "real-time data capture"—in which data are collected from people in real time as they go about their daily lives—has surged over recent decades as a method of studying a broad range of health outcomes.[1,2] Importantly, certain people may be less likely to complete EMA reports than other people, and some circumstances may be less conducive to reporting than others. To the extent that undetected person- or moment-level factors systematically drive missing reports, the findings from EMA studies will be biased, and the effectiveness of interventions built on these data will be compromised. Noncompliance with reporting thus represents a central threat to realizing the full clinical translational potential of this method. A small body of work has begun to examine the predictors of noncompliance with time-based reporting (i.e., reporting that is prompted by the EMA device).[3-5] Many EMA studies, however, rely on event-based reporting (i.e., reporting that is self-initiated by participants) to capture key health outcomes ranging from pain to heart symptoms in real time. Due to the difficulty inherent to tracking failures to self-initiate event reports, very little is known about noncompliance with event-based reporting.

Objective(s) The present study aimed to introduce a real-time method for identifying the predictors of noncompliance with event-based reporting of tobacco use in EMA and for enhancing the capture of event reports. Tobacco use served as an ideal event type for illustrating the method—which has implications for a broad spectrum of health behaviors—because it represented a high frequency yet meaningful health behavior that has been linked with both person-level characteristics and momentary circumstances.[6]

Methods N=410 adults who used both cigarettes and e-cigarettes (59% male, mean age = 34.70 years (SD=12.70), 48% White and 34% Black/African African) completed a 1-week EMA protocol that combined randomly-prompted reporting of current subjective and objective contexts with event-based reporting of tobacco use. Each random assessment first asked if participants were currently using tobacco and, if so, the assessment converted (i.e., branched) into a "randomly captured" event report—indicating failure to self-initiate that report. Multilevel modeling tested hypotheses regarding the predictors of failing to complete random reports and failing to self-initiate event reports. Person-level results reflected mean differences between people, uncovering subgroups of participants who were more likely to be noncompliant with reporting. Moment-level results indicated participants' report-level deviations from their own means, pointing to the within-subject, momentary circumstances associated with noncompliance.

Results On the person level, male sex (OR=1.41, p < .05), higher average cigarette rate (OR=1.03, p < .01), and higher average cigarette urge (OR=1.10, p < .05) each predicted missing random reports. The person-level predictors of failing to self-initiate event reports (i.e., disclosing current tobacco use at the start of random reports versus indicating no use on those reports) were older age (OR=1.02, p < .01), higher average cigarette rate (OR=1.05, p < .001), higher average e-cigarette rate (OR=1.04, p < .001), higher average urge for cigarettes (OR=1.42, p < .001), and being alone more on average (OR=2.96, p < .01). The moment-level predictors of failing to self-initiate event reports were higher momentary urge for cigarettes (OR=1.43, p < .001), lower positive affect (OR=0.89, p < .001), alcohol use within the past hour (OR=1.60, p < .001), and cannabis use within the past hour (OR=2.36, p < .001). Strikingly, the randomly captured events comprised more of the total EMA reports (28%) than did the self-initiated

event reports (24%). These report types were similar across most variables, with some exceptions, such as momentary cannabis use predicting the random capture of tobacco events (OR=1.31, p < .01). **Conclusion** The present study introduced a method for identifying predictors of noncompliance with event-based reporting in EMA and for enhancing the capture of event reports. The analyses produced a conceptually meaningful pattern of results regarding tobacco use events and potential bias from nonresponse. At the same time, it is worth emphasizing that the salient predictors of noncompliance are likely to vary across areas of behavioral health research as a function of sample and event type. In that light, the most powerful contribution of the study was not necessarily the specific results it returned, but rather the methodological blueprint it provided for future research. These methods have implications for improving the implementation of remote monitoring of various health conditions and improving its translational intervention potential.

REFERENCE(S)
1. Shiffman S, Stone AA, Hufford MR. Ecological momentary assessment. Annu Rev Clin Psychol. 2008;4:1-32.
2. Trull TJ, Ebner-Priemer, UW. Ambulatory assessment in psychopathology research: A review of recommended reporting guidelines and current practices. J Abnorm Psychol. 2020;129:56-63.
3. Sokolovsky AW, Mermelstein RJ, Hedeker D. Factors predicting compliance to ecological momentary assessment among adolescent smokers. Nicotine Tob Res. 2014;16:351-358.
4. Rintala A, Wampers M, Myin-Germeys I, Viechtbauer W. Momentary predictors of compliance in studies using the experience sampling method. Psychiatry Res. 2020;286:112896.
5. Williams-Kerver Ga, Schaefer LM, Hazzard VM, et al. Baseline and momentary predictors of ecological momentary assessment adherence in a sample of adults with binge-eating disorder. Eat Behav. 2021;41:101509.
6. Hedeker D, Mermelstein RJ, Berbaum ML, Campbell RT. Modeling mood variation associated with smoking: An application of a heterogeneous mixed-effects model for analysis of ecological momentary assessment (EMA) data. Addiction. 2009;104:297-307.

86

HELPING STUDIES FIT PEOPLE: USING HUMAN-CENTERED DESIGN METHODS TO BRIDGE THE IMPLEMENTATION GAP IN CLINICAL TRIALS

[1]Jennifer Sculley, [1]R. McKinley Sherrod, [1]Lynn Gerald, [1]Jerry Krishnan, [2]Kim Erwin. [1]*University of Illinois Chicago;* [2]*Institute of Design at Illinois Tech*

Introduction/Background Clinical trials are a critical part of the translational research process. Over 90% of clinical trials report delays in enrollment and 20% terminate early or have lower than expected sample size due to insufficient enrollment or retention. Implementation science offers theories, frameworks, and models that may be helpful in the conduct of clinical trials to increase the likelihood of successful completion. Human-centered design (HCD, sometimes called user-centered design or design thinking) is an approach to developing products, services, and systems that are tailored to the people who use them and the contexts in which they are used. HCD methods are well-recognized in industries outside of healthcare as critical to meeting the needs of people they serve. HCD may offer complementary methods to implementation science and help researchers plan trials that are more contextually appropriate, acceptable to stakeholders, and feasible to implement.

Objective(s) To describe how to integrate HCD methods with implementation science frameworks adapted for application to clinical trials.

Methods HCD methods include contextual inquiry (observation of work processes), stakeholder mapping (visually representing key users and their unique roles and needs), experience modeling (visually representing the end-to-end user experience of a service or product), rapid prototyping and evaluation (quickly assembling a sample solution and evolving it with stakeholder input), and pilot testing (a small-scale test of a larger effort).

Results Table 1 lists HCD methods to prospectively create study implementation strategies to improve performance against five implementation outcomes: acceptability, appropriateness, feasibility, adoption, fidelity. Table 2 lists HCD methods that could help researchers align clinical trials to participants, clinicians, and other stakeholders as well as the organizational, local community, and national contexts in which the trial will unfold.

Abstract 86 Table 1 Implementation outcomes framework applied to the clinical trial context and relevant HCD methods adapted to the clinical trial context.

Proctor's implementation outcome[16]	Examples in the clinical trial context[3]	Example HCD methods[7]	Example HCD areas of inquiry[7] adapted to the clinical trial context
Acceptability	Perceived existence of equipoise between intervention arms Anticipated or possible benefit to a participant over existing options Acceptable anticipated side effect profile Reasonable participant logistics (e.g., number of clinic visits, distance traveled to the trial site) Reasonable additional clinical burden (e.g., minimal additional biopsies or other invasive procedures) Additional direct time and financial cost to participants is acceptable to participants	Provotypes Projectives Stakeholder maps Card sorting	Does the trial and supporting content align with stakeholder beliefs, values and goals? What is the gap between current practice and trial procedures? And what would it take to cross it? What features are required for acceptability? Is there common ground across stakeholders that we can leverage?
Adoption	Proportion of providers offering clinical trials to patients	Prototype review Simulation and assessment Immersive communication and engagement	What experiences do stakeholders need to build belief, conviction that this trial and its results are important? Who are the local and organizational thought leaders who need to be on board? What are impediments to offering the trial to patients?
Appropriateness	Question is amenable to a clinical trial Trial design is appropriate for the trial question	Contextual Inquiry Multi-level design requirements gathering Iterative prototyping + refinement	What are all the specific requirements of each stakeholder group to take part in the trial? How might we optimize the intervention and trial itself to fit stakeholders needs?
Feasibility	Possible to meet enrollment goals Timeline for enrollment and completion is reasonable Anticipated effect size is reasonable	Contextual Inquiry Multi-level design requirements gathering Iterative prototyping + refinement Visual modeling of workflows/practices	Who are all the actors involved in current care delivery related to the trial? What are all the real-world factors that shape current behaviors + practices? How might we optimize the intervention, trial protocol, and local procedures to fit real-world settings?
Fidelity	Amount of intervention group crossover Adherence to trial protocol including follow-up	Contextual Inquiry Experience modeling	What is the experience model of the trial--is it desirable? Are there unexpected consequences of the intervention or trial implementation that need attention? Have the enablers (IT, HR, training, etc) been properly engaged across sites to ensure fidelity?

Abstract 86 Table 2 Adaptation of the CFIR domains and constructs to the clinical trial context and relevant HCD methods adapted to the clinical trial context

Domain[17]	Summarized domain description	Summarized domain-level focus adapted to a clinical trial context[a]	Example objectives[7] adapted to the clinical trial context	Example HCD methods[7]
Outer Setting	Policies, payments, guidelines, external professional networks and peers, patient needs	Relationships between individual providers, other institutions, clinical trial networks, and industry groups that influence the success of trial design and implementation.	Build and align a coalition to champion the trial and mitigate system-level barriers	Systems modeling Alignment workshops Immersion rooms
Inner Setting	Institutional culture + structure; implementation climate + readiness; communication channels	Characteristics within institutions (culture + structure, implementation climate + readiness, communication channels) that influence or can be adapted to promote the successful design and implementation of trials	Identify site-level barriers, facilitators and requirements Define stakeholder needs, knowledge, goals, expectations related to the trial Define a process to guide trial planning and execution Build organizational capacity to implement the trial	Contextual inquiry In-situ observation Provotyping Co-design Stakeholder mapping
Implementation Process	Activities such as engaging teams and change agents, and planning, executing, evaluation	Activities such as engaging teams to inform the planning, engagement, execution, and evaluating of trial implementation		
Characteristics of Individuals	All people involved in the implementation and their knowledge, belief, self-efficacy, readiness	All people involved in a trial (potential trial participants, trialists, their teams, and individual providers) and their knowledge, belief, self-efficacy, readiness		
Intervention Characteristics	Attributes of the intervention related to the success of its implementation	Attributes of both the interventions tested in the trial (e.g., trial medication) and the trial protocol itself related to the success of its implementation	Adapt intervention or trial attributes to local conditions (but maintain fidelity)	Service blueprints Prototyping User testing/RITE

Conclusion Implementation of clinical trials should be considered a priority in tandem with the trial science to improve completion rates. Anecdotal evidence suggests HCD methods may help describe trial contexts, identify stakeholder requirements, and develop interventions that fit people, however, empirical evidence to support the broader use of these methods in clinical trial planning and conduct is lacking. To evaluate the impact of HCD methods on clinical trial implementation, the degree to which clinical trials have been successfully implemented should be more routinely assessed. Using survey instruments, qualitative observations or interviews with study staff and participants, or randomized studies-within-a-trial (SWATs) to measure implementation outcomes should be considered.

REFERENCE(S)
1. Institute of Medicine (US) Forum on Drug Discovery, Development, and Translation. Transforming Clinical Research in the United States: Challenges and Opportunities: Workshop Summary. Washington (DC): National Academies Press (US); 2010.
2. The State of Clinical Research in the United States: An Overview. Available from: https://www.ncbi.nlm.nih.gov/books/NBK50886/2. Carlisle B, Kimmelman J, Ramsay T, MacKinnon N. Unsuccessful trial accrual and human subjects protections: an empirical analysis of recently closed trials. Clin Trials. 2015 Feb;12(1):77-83. doi: 10.1177/1740774514558307. Epub 2014 Dec 4. PMID: 25475878; PMCID: PMC4516407.

3. Stensland KD, Sales AE, Damschroder LJ, Skolarus TA. Applying implementation frameworks to the clinical trial context. Implement Sci Commun. 2022 Oct 10;3(1):109. doi: 10.1186/s43058-022-00355-6. PMID: 36217172; PMCID: PMC9552519.

4. International Organization for Standardization. (2019). Ergonomics of human-system interaction — Part 210: Human-centred design for interactive systems (ISO Standard No. 9241-210:2019). https://www.iso.org/obp/ui/#iso:std:iso:9241:-210:ed-2:v1:en

5. Erwin K, Krishnan JA. Redesigning healthcare to fit with people. BMJ. 2016 Aug 23;354:i4536. doi: 10.1136/bmj.i4536. PMID: 27553644.

6. Chen E, Neta G, Roberts MC. Complementary approaches to problem solving in healthcare and public health: implementation science and human-centered design, Translational Behavioral Medicine, Volume 11, Issue 5, May 2021, Pages 1115–1121, https://doi.org/10.1093/tbm/ibaa079

7. Erwin K "Human-centered design + Implementation Science for Human-centered healthcare." EPI 243 - Human Centered Design, Fall 2021, University of San Francisco California, Lecture.

8. Beyer H, Holtzblatt K. Contextual Design. Interactions, a publication of the ACM. 1999 Jan/Feb (1):32-42.

9. Suchman L. Plans and Situated Actions: The Problem of Human-Machine Communication. 1987, Cambridge University Press. Cambridge, UK.

10. Hanington B, Martin B. Universal methods of design expanded and revised: 125 Ways to research complex problems, develop innovative ideas, and design effective solutions. Rockport publishers, 2019.

11. Medlock, M.C., Wixon, D.R., Terrano, M., & Romero, R.L. Using the RITE method to improve products; a definition and a case study. 2007

12. Erwin K, Norell S, Martin MA, Paik SM, Press VG, Thompson TM, & Krishnan JA. Applying design methods to care delivery science: Improving the care of minority children with uncontrolled asthma and their caregivers who present to six Emergency Departments in Chicago through a stakeholder-optimized discharge tool. Information Design Journal, 2018;23(3), 248-267.

13. "Evaluation Design—Qualitative Data." The Consolidated Framework for Implementation Research, https://cfirguide.org/evaluation-design/qualitative-data/. Accessed February 13, 2023.

14. Lewis, C.C., Fischer, S., Weiner, B.J. et al. Outcomes for implementation science: an enhanced systematic review of instruments using evidence-based rating criteria. Implementation Sci 10, 155 (2015). https://doi.org/10.1186/s13012-015-0342-x

15. Treweek S, Bevan S, Bower P, Campbell M, Christie J, Clarke M, et al. Trial Forge Guidance 1: what is a Study Within A Trial (SWAT)? Trials. 2018;19:139. doi: 10.1186/s13063-018-2535-5.

16. Proctor E, Silmere H, Raghavan R, Hovmand P, Aarons G, Bunger A, et al. Outcomes for implementation research: conceptual distinctions, measurement challenges, and research agenda. Adm Policy Ment Health. 2011;38:65–76. doi: 10.1007/s10488-010-0319-7.

17. Damschroder LJ, Aron DC, Keith RE, Kirsh SR, Alexander JA, Lowery JC. Fostering implementation of health services research findings into practice: a consolidated framework for advancing implementation science. Implement Sci. 2009;4:50. doi: 10.1186/1748-5908-4-50.

87

OPTIMIZING TWO PATIENT-FACING IMPLEMENTATION STRATEGIES TO INCREASE FAMILY SCREENING IN PARTERNSHIP WITH THE FAMILY HEART FOUNDATION

[1]Nkiru Ogbuefi, [1]Christina Johnson, [1]Rinad Beidas, [2]Sri Adusumalli, [3]Catherine Ahmed, [2]Jinbo Chen, [2]Tamar Klaiman, [2]Adina Lieberman, [3]Diane MacDougall, [3]Mary McGowan, [2]Maeve Moran, [3]Kelly Myers, [2]Laurie Norton, [2]Jennifer Orr, [4]Amy Pettit, [2]Daniel Rader, [2]Krystin Sinclair, [3]Eric Tricou, [2]Kevin Volpp, [3]Katherine wilemon. [1]*Feinberg School of Medicine;* [2]*Perelman School of Medicine, University of Pennsylvania;* [3]*Family Heart Foundation;* [4]*Independent Consultant*

Introduction/Background Over 1 million Americans with familial hypercholesterolemia (FH) are undiagnosed; inequities exist with regard to race, ethnicity, and gender.Cascade screening – an evidence-based practice of contacting and screening first-degree biological relatives of individuals diagnosed with FH ("probands") – improves timely FH diagnosis and reduces morbidity. Despite success in other countries, cascade screening has been challenging in the US. Applying insights from behavioral economics to design implementation strategies to address barriers can help improve equitable implementation of cascade screening.Our team includes investigators from Penn Medicine and the Family Heart Foundation (FHF), a research and advocacy nonprofit with the mission to save generations of families from heart disease through timely and improved care for FH. Our team has co-designed, and will pilot test, two patient-facing implementation strategies to increase cascade screening to plan for a fully powered RCT. The first strategy will involve direct outreach via Penn Medicine using automated text messages; the second strategy will involve direct outreach via the FHF using a navigator.

Objective(s) We have co-designed two patient-facing implementation strategies based upon insights gleaned from interviews and behavioral economics that will be piloted and tested in a fully powered trial.

Methods We conducted semi-structured qualitative interviews with 15 probands and 17 clinicians.We met with Penn Medicine leadership and key partners to assess capacity and motivation to deploy the proposed implementation strategies. We co-designed the implementation strategies based on these inputs and leveraging insights from behavioral economics.

Results We recruited a diverse sample of probands with FH to interview by gender (9 female), race (5 Black/African American, 5 Asian, and 1 multiple races), and age (range = 19-77).Rapid qualitative interview analysis and meetings with Penn Medicine leadership and stakeholders elucidated several barriers and facilitators to cascade screening. Our team designed behavioral economics-informed implementation strategies to address barriers. In the Penn Medicine condition, automated text messages will be delivered by Way to Health to probands and family members. In the FHF condition, after initial text outreach via Way to Health, a genetic counselor will engage in direct outreach to probands and relatives. Both conditions will incorporate insights from behavioral economics to boost reach.

Conclusion Our process of gathering a variety of inputs and leveraging behavioral economic principles to inform the design of our implementation strategies sought to develop an effective and equitable approach. Next, we will conduct mini-pilots with 20 probands and their family members to assess the feasibility, acceptability, and appropriateness of our implementation strategies.Then, we will conduct a three-arm hybrid effectiveness-implementation trial with 300 probands to compare the (a) Penn Medicine-mediated strategy, (b) Family Heart Foundation-mediated strategy, and (c) usual care.By testing sustainable and scalable implementation approaches, our study results will be poised to guide future wide-scale implementation of cascade screening for FH and other genetic conditions within and

outside large health systems while also answering important questions related to equitable implementation.
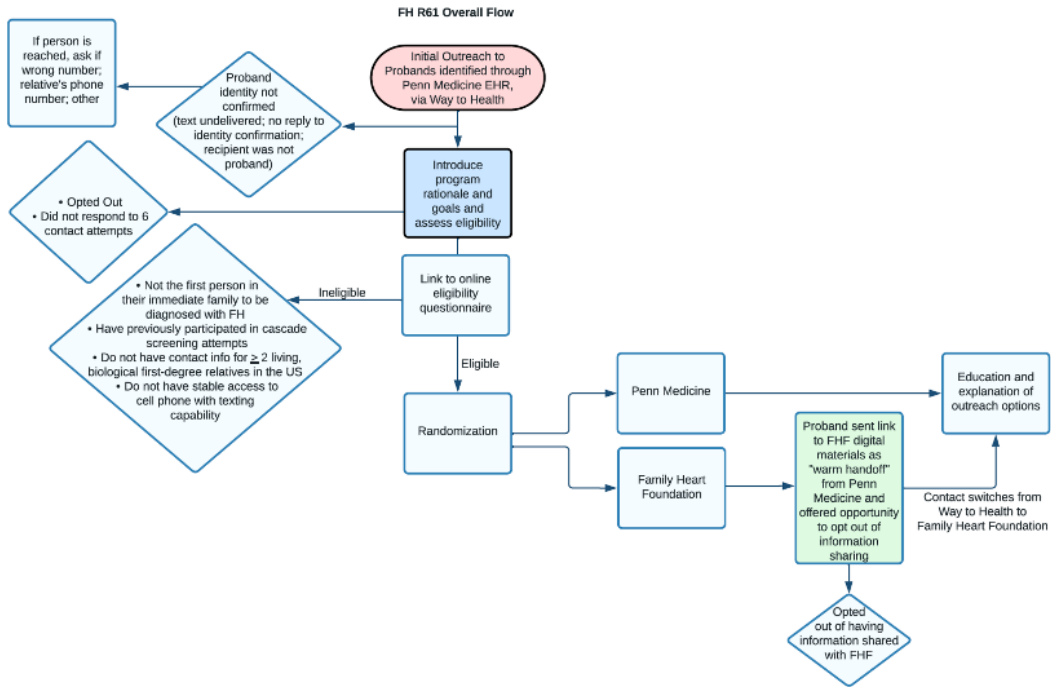
Abstract 87 Figure 1. R61 Overall Flow

88

PROCESS EVALUATION OF THE COMMUNITY ASTHMA PROGRAM ON THE NAVAJO NATION USING THE RE-AIM FRAMEWORK

[1]Priyanka Ravi, [1]Ashley Lowe, [2]Bryan Simmons, [1]Elvira Begay, [2]Peter Nez, [2]Andrew Liu, [2]Bruce Bender, [3]Lynn Gerald, [4]Diane King. *[1]University of Arizona Health Sciences, Tucson, AZ; [2]National Jewish Health, Denver, CO; [3]University of Illinois at Chicago; [4]University of Alaska Anchorage, Anchorage, AK.*

Introduction/Background Children living on the Navajo Nation have high rates of asthma prevalence and severity. The Community Asthma Program (CAP) is an evidenced-based program that is being implemented in partnership with the Navajo Nation across 3 communities: Tuba City, Chinle, and Fort Defiance, Arizona. CAP's purpose is to reduce asthma exacerbations by implementing evidence-based preventive practices within healthcare and school settings. We report the preliminary findings of a robust implementation process evaluation of CAP.
Objective(s) To describe community and setting-level variation in program implementation and report on key indicators of implementation success, we used the RE-AIM (Reach, Effectiveness, Adoption, Implementation, Maintenance) framework.
Methods The CAP program is a multi-component, evidenced-based program aimed at reducing pediatric asthma disparities. CAP components include collaborating with: (1) Diné (Navajo) schools to implement the Open Airways for Schools Program®, an evidence-based curriculum of the American Lung Association, Asthma 101 training, and a Stock Albuterol Inhaler Program; and (2) healthcare teams to implement an evidenced-based asthma toolkit to promote adoption of guidelines-concordant asthma practices. Process data were collected during implementation activities (2017-2022) and included communications with tribal leadership, parents, school and healthcare staff (phone, e-mail correspondence) and field and meeting notes from CAP team members. We also conducted and transcribed interviews with 3 CAP research staff to document their perceptions and experiences working directly with communities. Data were compiled in Excel. Two research staff independently coded the data and transcripts for themes using constructs from the implementation science framework, RE-AIM. Coding discrepancies were resolved by a senior researcher. The program is funded by the National Heart, Lung, and Blood Institute (NHLBI U01HL138689) and approved by the National Jewish Health Institutional Review Board and Navajo Nation Human Research Review Board (#NNR-16.247).
Results Thematic analysis of process data identified factors that facilitated and/or challenged CAP implementation. Factors that supported CAP acceptance included engagement with tribal leadership and maintaining a local, visible presence within communities. The existence of "champions", i.e., parents, tribal leaders, school and health system leaders within the community, schools and healthcare settings was an indicator of buy-in for CAP adoption and implementation. Potential barriers to adoption included external environment factors such as federal policies that impeded implementation of stock albuterol programs in some Diné schools. Factors influencing implementation quality and potential for long-term maintenance included organizational requirements for participating in training and access to equipment and resources that support program delivery. A theme of partnerships and connections emerged, reflecting the importance of social relationships and inter-agency networks that both promoted and challenged CAP implementation.
Conclusion Sustaining engagement with Navajo stakeholders and tribal leadership, promoting access to resources that build community capacity, and policies that support program implementation are important facilitators of CAP implementation.

89

COVID-19 INTERVENTION IMPLEMENTATION: DISRUPTIONS AND BARRIERS FOR ELEMENTARY CLASSROOM TEACHERS, SCHOOL HEALTH STAFF, AND SCHOOL CLEANING STAFF

[1]Amanda Wilson, [1]Ashley Lowe, [1]Priyanka Ravi, [1]Olusola Ogunseye, [1]Olivia DiGioia, [1]Sydney Mooneyham, [1]Ivana Klymko, [1]Josie Eck, [1]Carlos Romo, [2]Vineeth Vaidyula, [1]Sam Sneed, [3]Lynn Gerald, [1]Paloma Beamer.
[1]*University of Arizona;* [2]*Virginia Commonwealth University;* [3]*University of Illinois at Chicago*

Introduction/Background The COVID-19 pandemic brought many changes including interventions meant to reduce COVID-19 spread in schools. The Centers for Disease Control and Prevention issued school specific guidance for K-12 schools. Lack of adherence to these guidelines could result in outbreaks and increased transmission at schools.

Objective(s) We conducted two projects during COVID-19 to elucidate barriers regarding the implementation of the CDC school specific guidance. We aimed to examine the three major groups involved in implementation of these interventions including elementary classroom teachers, school health staff, and janitors.

Methods An online survey was sent to K-5 elementary school teachers in Tucson, AZ in Winter 2022, and they were invited to participate in one-on-one interviews. The survey and interviews inquired about barriers to the implementation of physical distancing, mask use, increased natural ventilation, and cleaning and disinfection. School health staff from two school districts in Tucson, AZ were invited to participate in two focus groups conducted in Spring 2022. The moderator asked participants to share their experiences regarding challenges in taking on new work duties (e.g., vaccination, contact tracing, developing and sharing intervention guidance) and personal and professional burdens as a result of increased work demands. In Summer of 2022, janitors from the largest school district in AZ were invited to participate in English and Spanish mailed surveys regarding asthma-related respiratory symptoms, changes in symptoms and cleaning protocols during the pandemic. Cleaning staff were also invited to participate in one-on-one interviews, with follow-up questions regarding cleaning protocol changes, respiratory health impacts, and use of personal protective equipment.

Results One hundred eleven teachers participated in the survey, and six participated in the interviews. Elucidated barriers included not having proper furniture for social distancing (e.g., tables instead of desks), large student to teacher ratios, health concerns for special education students regarding the use of masks (choking hazard) and hand sanitizer (ingestion hazard), and damage to commonly disinfected equipment. Forty-eight school health staff participated in the focus groups. These focus groups revealed that new duties because of the pandemic often meant lower prioritization for managing students' acute and chronic illnesses. Increased job demands resulted in longer hours and strain on personal and family relationships, affecting their mental health. Fifty-one cleaning staff participated in the survey, and 10 participated in the interviews. Eighty-four percent indicated that cleaning protocols had changed during the pandemic, and of those who indicated a change, 92% said that cleaning and disinfection was more frequent. The second most commonly reported (57%) change was application type (e.g., fog, spray, wipe). Interviews demonstrated that the fogging devices caused itching of the skin and difficulty breathing for some staff. Staff also shared challenges with heat when using masks (e.g., janitors lifting ~50lb bags of garbage).

Conclusion While COVID-19 interventions were designed to decrease transmission, these changes resulted in unintended barriers and disruptions. Reducing barriers for key interventions or prioritizing future interventions that have the greatest transmission reduction potential but minimize barriers or disruptions for occupational groups on the frontlines will likely increase their successful implementation.

90

MY ILLINET RECOVER RETURN OF INDIVIDUAL RESEARCH RESULTS (MIRROR): A PILOT STUDY ABOUT PARTICIPANT PREFRENCES IN A LONGITUDIAL COVID STUDY

Denise Kent, Crystal Patil, Beth Calhouhn, Michael Freedman, Cynthia Fritischi, Nathan Tintle, Jerry Krishnan. *University of Illinois at Chicago*

Introduction/Background Disclosing individual research results with participants is not standard practice. In 2018 the National Academy of Sciences, Engineering, and Medicine (NASEM) published a recommendation for researchers to return individual research results which has created a paradigm shift. With the call for increased transparency in healthcare, it is apparent that the return of individual research results (ROIRRs) is likely to increase public engagement and trust in the research enterprise, improving the efficiency, generalizability, and lead to research that is more participant-centered.
Objective(s) The University of Illinois Chicago-ILLInet Hub is an active research site for the NIH funded long-COVID-RECOVER study (OT2HL16184701). The purpose of this pilot study was to identify participant preferences and expectations related to ROIRRs for the active parent study RECOVER.
Methods The ILLInet RECOVER study collects biospecimens, questionnaires and physical exam data totaling more than 1500 individual results on more than 900 research participants. We consented and interviewed 58 RECOVER participants to explore their experiences and preferences related to the ROIRRs. Interviews were conducted in English and Spanish. Inclusion criteria were completion of the baseline RECOVER visit and the release of individual results. The interviews were recorded, transcribed and analyzed to produce an understanding of RECOVER participants preferences and experiences with ROIRRs. Using descriptive analyses, we compared qualitative and quantitative responses.
Results Twenty-seven of 45 English-speaking participants were female. English speakers were middle-aged (mean age= 50.6 +/-13.2). Nine of 13 Spanish speakers were female with a mean age of 49.9+/-12.4 (n=13). The ethnic and racial make-up of our sample was representative of the community we serve at the University of Illinois Chicago-ILLInet Hub (27% White, 30% Black, 34% Hispanic, and 5% Asian). Participants expressed the desire to review all their research results. Additionally, participants communicated an altruistic intention to help humanity combat COVID due to the recent experience of living through a global pandemic, having so many questions still unanswered, and in some cases, experiencing the death of family members (n=36). MIRROR participants also emphasized the benefits of participating in RECOVER, such as the frequency of biospecimens, questionnaire and physical data that is available to them through the electronic medical record (EMR). Most participants reported that this was information that they shared or plan to share with their primary care providers to help them improve their health. Some participants did report anxiety and worry associated with learning about their research results. Nonetheless, most (n=49) want to continue to receive their research results when they become available.
Conclusion Through MIRROR's access to a diverse participant population enrolled by the ILLInet Hub of the NIH RECOVER study, we learned that research participants want their individual research results returned to them. Despite the existing population-level inequities among minority races and ethnicities, both English and Spanish speakers want their health results from participating in research disclosed to them to improve their overall health. As we obtain more complex research results, RECOVER researchers will be ready to share those results with participants in a way that is meaningful to them. The information gathered from this study will improve the way in which research results are returned to participants.

REFERENCE(S)

1. Institute of Medicine (US) Forum on Drug Discovery, Development. The state of clinical research in the united states: An overview. National Academies Press (US); 2010. https://www.ncbi.nlm.nih.gov/books/NBK50886/. Accessed Jul 5, 2022.

2. Long CR, Stewart MK, McElfish PA. Health research participants are not receiving research results: A collaborative solution is needed. Trials; Trials. 2017;18(1):449. doi: 10.1186/s13063-017-2200-4.

3. National Academies of Sciences, Engineering, and Medicine, Health and Medicine Division, Board on Health Sciences Policy, Committee on the Return of Individual-Specific Research Results Generated in Research Laboratories. No title. . 2018. doi: NBK513173 [bookaccession].

4. Sobel ME, Dreyfus JC, Dillehay McKillip K, et al. Return of individual research results: A guide for biomedical researchers utilizing human biospecimens. Am J Pathol. 2020;190(5):918-933. doi: 10.1016/j.ajpath.2020.01.014.

91

USING IMPLEMENTATION SCIENCE TO INFORM THE PREPARATION PHASE OF THE MULTIPHASE OPTIMIZATION STRATEGY (MOST) FRAMEWORK

[1]Katherine Merrill, [1]Jacqueline Silva, [2]Angela Sedeno, [3]Susana Salgado, [2]Sara Vargas, [3]Jennifer Cano, [1]Jamison Merrill, [4]Jeff DeCelles, [5]Kate Guastaferro, [1]Geri Donenberg. [1]*University of Illinois Chicago;* [2]*The Kedzie Center;* [3]*Centro Romero;* [4]*Grassroot Soccer;* [5]*NYU*

Introduction/Background The multiphase optimization strategy (MOST) framework is an innovative approach to intervention science, facilitating an assessment of the effectiveness of individual components of an intervention prior to testing the effectiveness of the full intervention package. There is growing recognition of the critical role that implementation factors play in the success of an intervention, but gaps in the literature remain on how implementation science can and should inform use of the MOST framework.

Objective(s) We sought to assess the potential implementation of a sexual and reproductive health program—called Informed, Motivated, Aware, and Responsible Adolescents and Adults (IMARA), originally designed for African American teens and their mothers—which we are adapting for Latina teens and their mothers/female caregivers in partnership with two community-based organizations in Chicago. Our goal was to integrate our findings on implementation into the preparation phase of MOST, which centers on selecting and refining the intervention components to be tested in an optimization trial.

Methods We conducted seven focus group discussions, including two with Latina teens, two with mothers/female caregivers of Latina teens, and three with staff from the CBOs. We also conducted key informant interviews with individuals with expertise in designing and implementing SRH programs for teens. Our research was carried out under the guidance of a community advisory council composed of CBO representatives, teens and mothers/female caregivers, researchers, and other experts. We thematically coded the transcripts using MAXQDA. We primarily used a deductive coding approach to align our analysis with implementation determinants specified in the Exploration, Preparation, Implementation, and Sustainment (EPIS) implementation science framework.

Results Findings revealed potential barriers and facilitators to implementation in relation to the intervention itself (i.e., "innovation factors"), the organizational context (i.e., "inner context"), and the broader setting (i.e., "outer context"). A key topic centered on the logistics of when to schedule the program amidst competing commitments of teens and mothers/female caregivers. Focus group participants discussed the qualities that facilitators of the program should have and where the program should be delivered. Staff shared their views on what it will take for their organizations to adopt the program and implement it sustainably over time. Key informants added valuable insight into challenges they have faced with implementing similar programs in the past and how they sought to overcome these challenges.

Conclusion Our findings directly informed the refinement of our intervention components, which will be tested in a pilot optimization trial. This work highlights the invaluable role that implementation science can play in the first phase of the MOST framework and should be considered by future researchers interested in using MOST.

EVALUATION OF THE EFFECTIVENESS OF A STOCK ALBUTEROL PROGRAM IN MARICOPA (PHOENIX) ARIZONA

[1]Ashley Lowe, [1]Olivia DiGioia, [2]Kimberly Ivich, [3]Lynn Gerald. [1]*University of Arizona;* [2]*Maricopa County Department of Public Health;* [3]*University of Illinois*

Introduction/Background Acute respiratory symptoms often prevent students with asthma from participating in school activities and frequently lead to unplanned absences. To relieve symptoms and avert severe exacerbations, the National Asthma Education Prevention Program recommends that all students have access to rescue medication (albuterol sulfate) at school, and, when developmentally appropriate, self-carry and administer it. Despite these recommendations, most students lack an inhaler when needed. Parents may not provide one; students may forget or misplace it; or the inhaler might be expired, empty, or difficult to access. Furthermore, some children lack an Asthma Action Plan (AAP) on file with their school or a completed medication administration form authorizing the school to administer the medication. Schools can overcome these challenges by maintaining a single, stock albuterol inhaler (stock inhaler) for use among multiple students via disposable holding chambers.
Objective(s) After a county-wide stock inhaler program was implemented and evaluated in Pima County Arizona, the program was subsequently expanded to Arizona's largest and most populous county (Maricopa County). We seek to describe and evaluate the effectiveness of a stock albuterol program in Maricopa County between 2018-2021.
Methods One-hundred thirty-eight schools (12%) of schools located in Maricopa County enrolled in the stock inhaler program. As described in Table 1, 76% of the 138 participating schools were public schools. Approximately 56% of participating schools were multi-grade schools, and 55.8% of participating schools had an enrollment of over 250 students. Of the non-participating schools, 61.1% were public schools. 67.2% of were multi-grade serving, and 29.7% of them had an enrollment of 251-500 students. Schools documented information involving each stock albuterol inhaler event including the student's final disposition (sent back to class, sent home, called 9-1-1, and/or transported ambulance transport). These data were collected over the course of three school years. Descriptive methods were used to summarize the data and outcomes were compared to a similar program implemented in Pima County.

Abstract 92 Table 1 Stock Albuterol Inhaler Events reported by Maricopa County schools, 2018-2021.

Characteristic	N (%)
Schools reporting use	70 (43.2)
Events reported	329
Student gender	
Male	214 (65.1)
Female	115 (35.0)
Student National School Lunch Program	93,128 (62.0)
Student health status; asthma	
Yes	259 (78.7)
No	56 (17.0)
Do not Know	14 (4.3)
Puffs administered, mean (SD)	3.6 (1.6)
Student disposition	
Returned to class	256 (77.8)
Sent home	67 (20.4)
Called 9-1-1 only	4 (1.2)
Called 9-1-1 + ambulance transport	2 (0.6)

Results Seventy-six percent of the 138 participating schools were public schools, 56% were multi-grade schools, and 55.8% had an enrollment of over 250 students. Of the non-participating schools, 61.1%

were public schools. 67.2% of were multi-grade serving, and 29.7% of them had an enrollment of 251-500 students. As described in table 1, 43.2% of participating schools reported at least one stock albuterol inhaler event during 2018-2021 academic years. 329 total stock albuterol inhaler events were reported. Of these 329 events, 65.1% of the events occurred in males. Approximately 79% of students who used the stock albuterol inhaler were known to have asthma. During the events, a mean of 3.6 puffs were administered to the student. Approximately 77.8% of these events resulted in the student being sent back to the classroom rather than being sent home or calling emergency medical services. Out of the 329 total stock albuterol inhaler events that occurred, 217 (66%) of them took place in elementary schools.

Conclusion Stock inhaler programs effectively increase access to rescue medication among school children, but especially among children with previously known asthma. Such programs can decrease EMS utilization for mild events and effectively keep children learning in their classroom.

Infectious Disease

93

A SYSTEMATIC REVIEW OF METHODOLOGY AND REPORTING OF DIAGNOSTIC PREDICTION MODELS FOR HEALTHCARE FACILITY-ONSET CLOSTRIDIOIDES DIFFICILE INFECTION

[1]Jesse Fajnzylber, [1]William Patterson, [2]Adrian Hernandez-diaz, [3]Abhishek Deshpande. [1]*Cleveland Clinic Lerner College of Medicine of Case Western Reserve University;* [2]*University of Connecticut School of Pharmacy;* [3]*Cleveland Clinic Foundation*

Introduction/Background Clostridioides difficile infection (CDI) is the most common cause of healthcare-associated diarrhea and is associated with significant morbidity and mortality. Previous studies developed diagnostic models to identify inpatients at risk for developing healthcare facility-onset CDI (HO-CDI); however, the quality and the clinical utility of these models remains uncertain. Therefore, the uptake of these diagnostic models has been limited and increasing physician's confidence in these tools is paramount to implementation and improved patient outcomes.

Objective(s) The objective of this study was to systematically review and appraise the methodology, performance, reporting, and generalizability of the diagnostic models for HO-CDI.

Methods We systematically searched PubMed and three other databases to identify studies published before January 21, 2022 describing the development and/or validation of multivariable diagnostic models for HO-CDI in an inpatient setting. HO-CDI was defined as having a positive CDI assay (toxin or PCR) with an onset of diarrhea >48 hours after admission or with the onset of symptoms < 48 hours, with hospitalization in the prior 90 days. All publication dates, languages, and study designs with adult inpatients (≥18y) were considered. We excluded studies that included patients with community-acquired CDI or when all patients in the control group had diarrhea. For each of the included studies, we extracted information relating to study design, sample size, outcome variable definition, model development, validation strategies, and performance.

Results Of 2,361 studies initially evaluated, 10 developed their own diagnostic models and were selected for final analysis. One study (10%) performed sample size calculations, but was underpowered. Three studies (30%) limited predictors to those present at admission (static), while seven studies (70%) included clinical values that change during hospital admission (dynamic). Only one of the dynamic models created a daily risk-assessment of developing HO-CDI, and therefore, the other six dynamic models use their data in a static fashion, and may have failed to capture trends. Most models (70%) used a stepwise approach to variable selection and model calibration, while one used L2 shrinkage, one used hierarchical clustering, and one utilized prior literature review and expert consensus. The number of model coefficients ranged from 2-20 and the number of CDI events ranged from 25-2,141 (Table 1). Nine studies (90%) reported area under the receiver operating characteristic curve (AUROC) as a measure of discriminatory ability of the models, ranging from 0.68 to 0.95. Five studies (50%) used retrospective data for model development and validation, one validated their study by performing 1,000 bootstrapped simulations, and one used ambispective data (trained on a historical cohort and evaluated prospectively). Three studies (30%) did not include a validation step on independent data, making overfitting difficult to evaluate. No study reported how missing data was handled.

Abstract 93 Table 1 Number of coefficients, sample size, and number of CDI events per model

	Model coefficients	Sample size		Events (CDI)	
		Derivation	Total	Derivation	Total
Chandra et al. (2012)	6	21,541	32,334	121	179
Cooper et al. (2013)	4	29,453	44,236	274	488
Davis et al. (2018)	11	75,545	97,130	1,172	1,481
Garey et al. (2008)	5	41,224	54,226	288	392
Hornbuckle et al. (1998)	3	78	152	29	87
Tabak et al. (2015)	12		78,080		323
Oh et al. (2018)[a]					
MGH	20	33,477	65,718	315	552
UM	20	155,009	191,014	1,781	2,141
Tilton et al.[b]					
Index model (2019)	2		200		100
Validation model (2021)	3		322		161
Voicu et al. (2021)					
Model 1	4		367		25
Model 2	4		367		25

Bolded studies included multiple models
[a] Created institution specific models.
[b] Validated prior model on external population.

Conclusion Diagnostic models varied considerably in their ability to estimate the risk of HO-CDI. Many models had methodological shortcomings. Poor methodology can impact the reliability of the diagnostic models and compromise their diagnostic accuracy. Future studies should use consistent definitions for reporting HO-CDI and be validated on a prospective external cohort, ensuring external validity and generalizability. A robust diagnostic model will allow high risk patients to be flagged for increased risk of HO-CDI allowing for effective triage and improving outcomes.

94

A SCOPING REVIEW OF TRENDS IN ANTIMICROBIAL RESISTANCE AMIDST THE COVID-19 PANDEMIC

[1]Meggie Griffin, [1]Noora Reffat, [1]Rebecca Schwei, [1]Aurora Pop Vicas,[2]Lucas Schulz, [1]MIchael Pulia.
[1]University of Wisconsin School of Medicine and Public Health; [2]University of Wisconsin Madison School of Pharmacy

Introduction/Background The introduction of a new respiratory pathogen that mimics bacterial pneumonia along with disruptions to normal antimicrobial stewardship and infection prevention operations have been predicted to accelerate the emergence and spread of antimicrobial resistance (AMR) amidst the COVID-19 pandemic. While some studies have been done to suggest that rates of AMR have increased throughout the pandemic, no reviews have comprehensively characterized the available literature.
Objective(s) The objective of this scoping review is to characterize the scope and results of available literature comparing AMR in clinical cultures before and after the start of the COVID-19 pandemic.
Methods This scoping review follows the Preferred Reporting Items. Web of Science, PubMed, and Scopus databases were searched on August 2, 2022 for articles describing AMR trends before and after the start of the COVID-19 pandemic. Articles were included if they 1.) were written in English, 2.) presented primary evidence, 3.) were published in peer-reviewed journals, 4.) included clinical culture data from humans, 5.) reported AMR for at least one specific organism type, and 6.) included and compared data from a time period before and after the start of the COVID-19 pandemic. The pre-data timeframe was defined as data before November 2019 and the post timeframe was data March 2020 or later. Two reviewers assessed all articles, extracted data, and resolved discrepancies through consensus meetings. During data extraction, the following fields were extracted: publication year, country, study design, type of analysis, study period, setting and population, # of positive cultures or isolates, culture type(s), method of AMR analysis, organisms studied, AMR results, and funding for study. For each study that had AMR results with statistical comparisons, we organized study results by organism and antimicrobial class. AMR results were grouped into 3 categories for each organism and antimicrobial class that was studied: increase (yes/no), decrease (yes/no) or no change (yes/no). Finally, we created a global summary measure by aggregating the AMR results within studies to determine an overall increase, decrease, no change, or mixed change in resistance per study.
Results In total, 3,047 articles were identified for title and abstract screening. Of those, 96 studies were moved onto full-text screening with 48 papers meeting inclusion criteria. Included studies came from 25 different countries with Italy (n=12) and China (n=6) being the only two countries with more than 2 articles. Thirty-two of the studies had formal statistical comparisons in their analysis and 16 had descriptive results. When analyzing the global summary AMR measure, 41% (n=13) had increasing results; 19% (n=6) had decreasing results, 22% (n=7) had mixed results and19% (n=6) had results that only showed no change in AMR resistance. Ninety four percent (n=30) of studies evaluated Gram negative organisms, 59% (n=19) evaluated Gram positive and 6% (n=2) evaluated fungus. The organisms with the most AMR results included: Klebsiella pneumoniae (n=60), Pseudomonas aeruginosa (n=59), Acinetobacter baumannii (n=53), Escherichia coli (n=50), and Staphylococcus aureus (n=40).
Conclusion The literature examining the impact of COVD-19 is heterogenous. The number of studies demonstrating an increase in AMR seems to indicate a potential reversal of pre-COVID trends of declining AMR globally. There is a need for further inquiry into the impact of the pandemic related disruptions to infection control practices and antimicrobial prescribing patterns on AMR at the regional/local level.

95

INPATIENT ANTIBIOTIC PRESCRIBING BEFORE AND DURING THE COVID-19 PANDEMIC IN A LARGE SAMPLE OF U.S. HOSPITALS

[1]Meggie Griffin, [1]Michael Pulia, [1]Daniel Hekman, [1]Rebecca Schwei, [1]Aurora Pop-Vicas, [2]Lucas Schulz, [3]Meng-Shiou Shieh, [3]Penelope Pekow, [3]Peter Lindenauer. [1]*University of Wisconsin - Madison School of Medicine and Public Health;* [2]*University of Wisconsin Hospital and Clinics;* [3]*University of Massachusetts Chan Medical School-Baystate*

Introduction/Background Because of disruptions in hospital infection control and antibiotic stewardship operations caused by the COVID-19 pandemic, there is concern about the short and long-term effects of these changes on antibiotic resistance trends.

Objective(s) This study aims to assess changes in inpatient antibiotic prescribing before and during the COVID-19 pandemic.

Methods Using the Premier Healthcare Database (PHD), all non-elective hospital admissions and observations from 1/2019-2/2020 (pre-COVID) and 3/2020-3/2022 (during COVID) from 746 hospitals (over 20 million encounters), were analyzed for antibiotic prescribing. We conducted an interrupted time series analysis of the monthly percentage of patients receiving at least one dose of a systemic antibiotic in aggregate and at the individual hospital level. Additionally, we conducted an interrupted time series analysis of the mean days of antibiotic treatment per hospital for encounters involving at least one systemic antibiotic prescription.

Results At least one antibiotic was prescribed in 53.1.0% of hospital encounters pre-COVID and 54.5% of hospital encounters during COVID (p < 0.001). From 1/2019-2/2020, there was a statistically significant increase in antibiotic prescribing of 0.067% per month (p = 0.006). There was a significant immediate increase in antibiotic prescribing of 0.76% from 2/2020 to 3/2020 (p = 0.002). From 3/2020-3/2022, there was a sustained negative trend in antibiotic prescribing of -0.12 percentage points per month (p < 0.001). Amongst encounters where at least one antibiotic was prescribed, patients received an average of 4.40 days of antibiotic treatment pre-COVID and 4.65 days of antibiotic treatment during COVID (p < 0.001). Before 3/2020, there was a significant negative trend of -0.016 days per month in mean days of antibiotic treatment. The COVID-19 pandemic had no immediate effect on the mean days of antibiotic treatment but between 3/2020-3/2022 there was a sustained positive trend of 0.023 in mean days of antibiotic treatment.

Conclusion In a national sample of U.S. hospitals, antibiotic prescribing rates for inpatient and observation encounters had a significant initial but non-sustained increase at the start of the COVID-19 pandemic. Trends in overall antibiotic prescribing both before and after the pandemic are statistically significant but of a very small magnitude that is of uncertain significance for antibiotic resistance trends. Future work should focus on hospital-level changes in antibiotic spectrum and prescribing appropriateness during the pandemic.

96

EFFECT OF MONOVALENT COVID-19 BOOSTER AMONG HOSPITALIZED PATIENTS WITH BREAKTHROUGH INFECTION

Megan Corn, Austin Nickell, Thomas Baker, Sean Keup, Abe Sahmoun, Dubert Guerrero. *University of North Dakota*

Introduction/Background The virus that causes severe acute respiratory syndrome coronavirus 2 (SARS-CoV-2) infection has changed over time. In 2021, the Omicron variant of SARS_CoV-2 led to increased Coronavirus 2019 infections (COVID-19) prompting recommendations for patients to receive a booster (monovalent) dose of the vaccine.
Objective(s) In this study, we evaluated the outcomes of patients who were fully vaccinated against those who received the original COVID-19 booster.
Methods We conducted a retrospective review of adults either fully vaccinated or who have received the initial monovalent booster admitted with breakthrough COVID-19 infection in January 2022.
Results Of 208 patients, 129 (62%) were fully vaccinated while 79 (38%) received a booster. There were more males who received a booster, 48 (61%) versus females, 31 (39%), $p < 0.04$. Mean age patients who received a booster was 74 years versus 67 of those without. ($p < .0001$). The time to breakthrough infection requiring hospitalization among the fully vaccinated patients were significantly higher at 287 days (Interquartile range 245-323 days) compared to those who received a booster 88 days (IQR 66-113 days), $p < .001$. There were no significant differences among the two groups in proportion of need for mechanical ventilation or severity of illness. There were 18 deaths among those who received the booster dose and 12 in the fully vaccinated. Multivariate regression did not show any significant differences with $p=0.69$. However, those who received the booster had a significant lower mean length of stay of 8.6 days versus 13.6 days among those who did not, $p < .001$.
Conclusion Among patients fully vaccinated or received an additional monovalent COVID-19 booster who were hospitalized with a breakthrough infection, those who received the additional vaccine had the infection sooner than those who did not. There were no significant benefits in mortality, mechanical ventilation, or severity. However, the length of stay is decreased. This study shows the short comings of the monovalent vaccine in the real world setting. It justifies the current updated recommendations for the available bivalent booster vaccinations.

97

TYPICAL HEMOLYTIC UREMIC SYNDROME IN AN ADULT: A CASE REPORT

[1]Zayd Ahmed, [2]Taqi Khaja, [3]Mustafa Farooqi. [1]*University of Illinois College of Medicine;* [2]*Midwestern University;* [3]*Rosalind Franklin University*

Introduction/Background Hemolytic Uremic Syndrome (HUS) involves the clinical triad of thrombocytopenia, microangiopathic hemolytic anemia with schistocytosis, and acute kidney injury. It can also be associated with fever and neurologic symptoms. Typical HUS is more commonly associated with Shiga-toxin producing Escherichia coli (STEC) or less frequently Streptococcus pneumoniae, while atypical HUS (aHUS) is not related to an infection but is rather driven by complement activation and dysregulation. While HUS associated with E. Coli O157:H7 is a recognized yet rare cause of acute kidney injury in children, the incidence in adults is exceedingly uncommon. Due to the rarity of the condition in adults, it is likely that the diagnosis will often be delayed, which can defer treatment and negatively impact outcomes. This report demonstrates a case of a previously healthy 68-year-old female inflicted with STEC-HUS, with the hope of aiding in early diagnosis and differentiation from other thrombotic microangiopathies, ultimately decreasing the time in which an adequate treatment plan can be formulated.

Case Presentation A 68-year-old female with no reported past medical history presented to the emergency department (ED) with crampy abdominal pain, nausea, vomiting, and diarrhea for the past 3 days. Her diarrhea initially was watery, but she noticed bright red blood in her stool the morning of presentation. Her symptoms began after eating some home-cooked schnitzel with beef and some sausage at a family gathering. She denied any fever, chills, recent travel or antibiotic use, weight loss, or sick contacts. On arrival to the ED, she was hypertensive and tachypneic but was otherwise stable and resting comfortably. On physical examination, she had abdominal tenderness in the right lower quadrant. A CT abdomen and pelvis showed findings consistent with inflammatory or infectious colitis. An enteric pathogen panel returned positive for Escherichia coli (O157), Shiga-like toxin-producing E. coli (STEC), and Giardia lamblia. She was initially started on ceftriaxone and metronidazole and admitted for supportive care. Her blood pressure was managed with carvedilol. Infectious disease was consulted for antibiotic management, and per their recommendation ceftriaxone was discontinued as antibiotics have the potential to increase the risk of developing HUS, and metronidazole was discontinued as Giardia was clinically insignificant. The patient had already received 1 dose of each. Although her bloody diarrhea and abdominal pain resolved a few days in, on day 3 of admission, her platelet count dropped, followed by a gradual decline in her hemoglobin over the next few days. (Figure 1) The patient was given one dose of eculizumab per a hematology consult and azithromycin for meningitis prophylaxis. She received a total of 5 units of platelet transfusions over the course of her admission, and 2 units of packed RBCs. She never required plasma exchange. The patient was discharged on day 20 with a WBC count of 5.6 K/mcL, a hemoglobin of 7.1 g/dL, and a platelet count of 276 K/mcL.

Component	WBC	HGB	PLT	BUN	Creatinine	RETIC COUNT	LDH	Trans-fusions
Latest Ref Rng & Units	4.2 - 11.0 K/mcL	12.0 - 15.5 g/dL	140 - 450 K/mcL	6 - 20 mg/dL	0.51 - 0.95 mg/dL	0.3 - 2.5 %	82 - 240 Units/L	
Day 1, PM	29.1 (H)	15.2	217	15	0.73			
Day 2	25.8 (H)	14.3	163	15	0.68			
Day 3, AM	20.4 (H)	12.9	63 (L)	15	0.77	2.1	643 (H)	
Day 3, PM	21.9 (H)	12.4	38 (L)	20	0.89			
Day 4, AM	22.1 (H)	11.8 (L)	9 (LL)	26 (H)	1.06 (H)		1,245 (H)	Platelets
Day 4, PM	25.0 (H)	11.3 (L)	32 (L)	30 (H)	1.19 (H)			
Day 5, AM	22.8 (H)	10.1 (L)	10 (LL)	36 (H)	1.53 (H)		1,444 (H)	Platelets
Day 5, PM	22.0 (H)	9.7 (L)	28 (LL)					
Day 6, AM	17.5 (H)	9.2 (L)	19 (LL)	41 (H)	2.11 (H)		1,483 (H)	Platelets
Day 6, PM	18.6 (H)	8.2 (L)	43 (L)					
Day 7, AM	17.4 (H)	7.8 (L)	28 (LL)	46 (H)	2.48 (H)		1,522 (H)	
Day 7, PM	18.1 (H)	7.5 (L)	22 (LL)			6.3 (H)		
Day 8, AM	16.0 (H)	6.9 (LL)	19 (LL)	51 (H)	2.62 (H)		2,016 (H)	RBCs, Platelets
Day 8, PM	23.0 (H)	8.6 (L)	19 (LL)					
Day 9, AM	23.4 (H)	7.3 (L)	18 (LL)	56 (H)	2.79 (H)	7.6 (H)	2,378 (H)	Platelets
Day 9, PM	21.7 (H)	7.3 (L)	48 (L)					
Day 10, AM	13.4 (H)	6.3 (LL)	38 (L)	58 (H)	2.93 (H)	11.5 (H)	1,644 (H)	
Day 10, PM	12.6 (H)	6.3 (LL)	43 (L)					
Day 11, AM	12.1 (H)	6.1 (LL)	55 (L)	58 (H)	2.85 (H)	13.7 (H)	1,689 (H)	
Day 11, PM	11.8 (H)	6.2 (LL)	67 (L)					
Day 12, AM	10.8	5.8 (LL)	74 (L)	49 (H)	2.62 (H)	17.2 (H)	1,488 (H)	RBCs
Day 12, PM	11.2 (H)	6.9 (LL)	78 (L)					
Day 13, AM	9.9	7.0 (L)	88 (L)	46 (H)	2.46 (H)	15.1 (H)	1,408 (H)	
Day 13, PM	10.2	7.1 (L)	107 (L)					
Day 14	8.7	6.6 (LL)	116 (L)	46 (H)	2.49 (H)	15.4 (H)	1,190 (H)	
Day 15, AM	7.3	6.2 (LL)	156	43 (H)	2.47 (H)	15.2 (H)	982 (H)	
Day 15, PM	7.9	6.6 (LL)	195					
Day 16	6.2	6.2 (LL)	189	37 (H)	2.24 (H)	13.0 (H)	857 (H)	
Day 17	6.3	6.7 (LL)	226	32 (H)	2.07 (H)		822 (H)	
Day 18	5.3	6.7 (LL)	246	31 (H)	1.99 (H)		658 (H)	
Day 19	6.9	6.5 (LL)	257	31 (H)	1.80 (H)	8.4 (H)	591 (H)	
Day 20	5.6	7.1 (L)	276	28 (H)	1.63 (H)	7.8 (H)	521 (H)	

Abstract 97 Figure 1: Patient's Lab Values- A summary of the patient's lab values from Day 1 (admission) to Day 20 (discharge), including White Blood Cell count, Hemoglobin, Platelet count, BUN, Creatinine, Reticulocyte count, LDH, and Transfusions.

Discussion While typical HUS in a previously healthy adult is an uncommon diagnosis, this case demonstrates the importance of recognizing the condition early to provide adequate supportive care. A

patient presenting with an acute diarrheal illness should have STEC excluded before initiating antibiotics, as a suggested relationship exists between antibiotic management and the development of HUS, which was reinforced by this case report. Further research with randomized controlled trials are necessary to determine the true association, as well as to formulate guidelines on the recommended modality of care for STEC-HUS in adults.

REFERENCE(S)
1. Ko H, Maymani H, Rojas-Hernandez C. Hemolytic uremic syndrome associated with Escherichia coli O157:H7 infection in older adults: a case report and review of the literature. J Med Case Rep. 2016;10:175. Published 2016 Jun 15. doi:10.1186/s13256-016-0970-z
2. Feng, J., Xu, K., Shi, X. et al. Incidence and cost of haemolytic uraemic syndrome in urban China: a national population-based analysis. BMC Nephrol 23, 122 (2022). https://doi.org/10.1186/s12882-022-02746-2
3. Kielstein JT, Beutel G, Fleig S, et al. Best supportive care and therapeutic plasma exchange with or without eculizumab in Shiga-toxin-producing E. coli O104:H4 induced haemolytic-uraemic syndrome: an analysis of the German STEC-HUS registry. Nephrol Dial Transplant. 2012;27(10):3807-3815. doi:10.1093/ndt/gfs394
4. Pandey Y, Atwal D, Sasapu A (April 11, 2019) Diarrhea-associated Hemolytic Uremic Syndrome in Adults: Two Case Reports and Review of the Literature. Cureus 11(4): e4435. doi:10.7759/cureus.4435
5. Kouzy R, Alawieh R, Sukhon F, Temraz S. A Case of Typical Hemolytic Uremic Syndrome in an Adult. Cureus. 2018;10(9):e3289. Published 2018 Sep 11. doi:10.7759/cureus.3289
6. Ko H, Maymani H, Rojas-Hernandez C. Hemolytic uremic syndrome associated with Escherichia coli O157:H7 infection in older adults: a case report and review of the literature. J Med Case Rep. 2016;10:175. Published 2016 Jun 15. doi:10.1186/s13256-016-0970-z
7. Grisaru S, Xie J, Samuel S, et al. Associations Between Hydration Status, Intravenous Fluid Administration, and Outcomes of Patients Infected With Shiga Toxin-Producing Escherichia coli: A Systematic Review and Meta-analysis. JAMA Pediatr. 2017;171(1):68-76. doi:10.1001/jamapediatrics.2016.2952
8. Joseph A, Rafat C, Zafrani L, et al. Early Differentiation of Shiga Toxin-Associated Hemolytic Uremic Syndrome in Critically Ill Adults With Thrombotic Microangiopathy Syndromes. Crit Care Med. 2018;46(9):e904-e911.
9. Frank C, Werber D, Cramer JP, et al. Epidemic profile of Shiga-toxin-producing Escherichia coli O104:H4 outbreak in Germany. N Engl J Med. 2011;365(19):1771-1780.
10. STARRT-AKI Investigators; Canadian Critical Care Trials Group; Australian and New Zealand Intensive Care Society Clinical Trials Group; Timing of Initiation of Renal-Replacement Therapy in Acute Kidney Injury [published correction appears in N Engl J Med. 2020 Jul 15;:]. N Engl J Med. 2020;383(3):240-251.
11. Pérez-Cruz FG, Villa-Díaz P, Pintado-Delgado MC, Fernández Rodríguez ML, Blasco-Martínez A, Pérez-Fernández M. Hemolytic uremic syndrome in adults: A case report. World J Crit Care Med. 2017;6(2):135-139. Published 2017 May 4. doi:10.5492/wjccm.v6.i2.135
12. Tarr PI, Freedman SB. Why antibiotics should not be used to treat Shiga toxin-producing Escherichia coli infections. Curr Opin Gastroenterol. 2022;38(1):30-38. doi:10.1097/MOG.0000000000000798

Nephrology

98

LONGITUDINAL CHARACTERIZATION OF METABOLIC CHANGES IN ADPKD

Cassandra Trask, Yahya Alsawaf, Ali Tug, Eirin Alfonso, Maria Irazabal. *Mayo Clinic PKD Center*

Introduction/Background Metabolic dysregulations and mitochondrial abnormalities are implicated in the pathogenesis of autosomal dominant polycystic kidney disease (ADPKD), but reports differ between studies, and there are no longitudinal studies that determine the timing of these alterations through the disease.

Objective(s) This study aimed to determine the longitudinal metabolic changes in a slowly progressive Pkd1 mouse model (Pkd1RC/RC) of ADPKD.

Methods We analyzed the kidney metabolome of Pkd1RC/RC mice and WT controls (n=5 males and 5 females/group) at 1, 2, 4, 6, 8, 12, and 16 months (m, renal failure) using 1HNMR and mitochondrial characteristics in kidneys and urine from the same animals at 1, 6, and 16m using electron microscopy, RNAseq, and qPCR. Disease severity and progression were evaluated by kidney weight/body weight (KW/BW), cystic index (CI), fibrotic index (FI), and BUN.

Results KW/BW and CI were higher in Pkd1RC/RC from 1m and FI from 4m, but BUN was similar until 8m. Metabolic changes were present throughout the disease, but the metabolic profile varied at different stages. At 1m, kidney mitochondria resembled the typical appearance of WT controls, but the mitochondria number was lower in Pkd1RC/RC. Changes in mitochondria area and matrix density became apparent as the disease progressed. The mitochondrial genetic profile in Pkd1RC/RC versus WT differed at 1, 6, and 16m. However, functional analysis revealed distinct changes at different stages of the disease. In urine, the mtDNA copy number was lower at 1m, but unexpectedly, it increased with disease progression.

Conclusion ADPKD is associated with metabolic dysregulations and mitochondria abnormalities throughout the disease. However, the abnormalities observed differed in the disease's early, middle, and late stages. These findings have significant implications for treating patients with ADPKD and suggest that different therapeutic strategies might be beneficial throughout the disease.

99

SEX-BASED DIFFERENCES IN IMMUNE-MEDIATED KIDNEY DISEASE

Valerie Garcia, Esther Liu, Matthew Wright, Jennie Lin. *Northwestern University*

Introduction/Background Chronic kidney disease (CKD) affects approximately 850 million people worldwide. While CKD is more prevalent among women, men with CKD are more likely to progress to kidney failure. Despite this observation, the underlying mechanisms driving this difference remain unknown.

Objective(s) To delineate sex-based differences in an immune-mediated model of kidney injury and fibrosis.

Methods Female and male C57BL/6 mice were ordered from Jackson Labs and used for experiments. Mice were either eight- to twelve-weeks-old or 18-months-old to represent different stages of fertility. To induce kidney injury, the nephrotoxic serum (NTS) nephritis model was used for its ability to model the progression of disease. All mice were injected with sheep IgG (250 µg/20 g) emulsified with Complete Freund's Adjuvant (100 µl/20 g) on day 0. On day 5, mice received an injection of sheep anti-rat GBM serum or PBS as a control (100 µl/20 g). Weight, urine, and serum were collected throughout the study. On day 15, endpoint samples for urine, blood, and kidney tissue were collected.

Results Young mice tended to maintain their weight throughout the study, and aged mice had a slight decrease in weight overall with no significant difference between males and females. Aged male mice treated with NTS had higher blood urea nitrogen (BUN) levels compared to controls at day 15 (24.48 mg/dL vs 17.36 mg/dL, p = 0.0466). There were no significant differences among female BUN levels. However, all NTS treated groups had significantly higher urinary albumin to creatinine ratios (ACR) than controls at day 7 and later. Between NTS treated groups, young males had higher ACR levels than young females at day 9 (2076 mg/g vs 521.8 mg/g, p = 0.0173). At early time points, aged females had higher ACR levels than aged males, such as at day 6 (717.8 mg/g vs 153.4 mg/g, p = 0.0205). Meanwhile, young males also had higher ACR values than aged males at day 9 (2076 mg/g vs 420.7 mg/g, p = 0.0075).

Conclusion The results found in this study indicate that sex-based differences occur during immune-mediated kidney injury, with young male mice experiencing worse injury than both their female counterparts and aged male mice. While female mice tended to have similar or higher ACR levels compared to male counterparts early on, male mice tended to experience a more dramatic increase in ACR levels throughout the study, recapitulating CKD progression as observed in humans. While these findings indicate potential sex-based differences in the progression of kidney disease, additional research is needed to further understand underlying mechanisms driving these responses.

100

AN IMPROVED MODEL OF CHRONIC KIDNEY DISEASE: ADENINE DIET IN THE SKH1 MOUSE

Benjamin French, Joshua Breidenbach, Shereen Yassine, Sara Kazmi, Bella Khatib-Shahidi, Humza Bashir, Shivani Patel, Irum Syed, Shungang Zhang, Apurva Lad, Prabhatchandra Dube, David Kennedy, Steven Haller. *The University of Toledo*

Introduction/Background Chronic kidney disease (CKD) is often complicated by wound healing and other dermatologic disorders. Experimental models of the skin disorders which often accompany CKD are lacking. Low protein diets high in the purine derivative adenine have been utilized to model CKD in both rats and mice and mimic several key phenotypes including reduced glomerular filtration rate, kidney fibrosis, proteinuria and polyuria, and elevated plasma levels of cystatin-C. These occur in the adenine diet model largely through tubular atrophy and glomerular damage (glomerulosclerosis and hypertrophy). The C57BL/6 mouse is highly resistant to many features of experimentally induced CKD, including kidney fibrosis, polyuria, proteinuria, and various cardio-renal pathologies. Additionally, for dermatologic studies, C57BL/6 mice require depilatory or shaving procedures which can introduce confounding effects on the skin. The SKH1 mouse strain is an immunocompetent hairless strain of mice which is ideal for dermatological studies, including wound-healing models, and in some skin cancer research. Adenine-induced CKD has not been investigated in the SKH1 strain and represents an important need in order to model and investigate the dermatological disorders which often complicate CKD.

Objective(s) The objective of this study was to establish a reliable model of CKD in the SKH1 mouse strain based on a low protein adenine diet.

Methods Five-week-old male SKH1 mice were fed normal chow (n=5) or a low-protein (2.5%) adenine-supplemented (0.15%) diet (n=5) for 6 weeks to induce CKD. The mice were then placed in metabolic cages for 24 hours to collect urine, followed by euthanasia and collection of blood and organs. Quantitative PCR analysis was performed on kidney tissues to assess markers of renal injury.
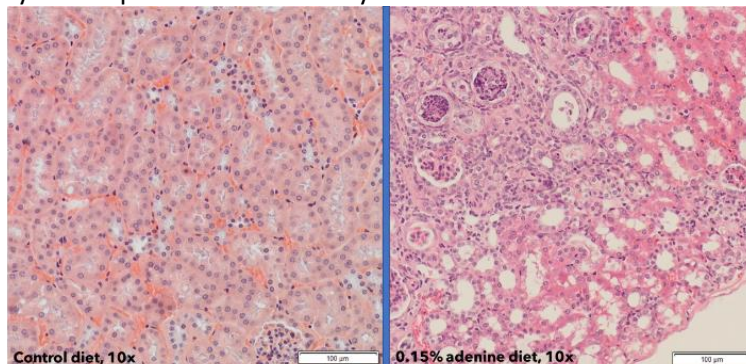
Abstact 100 Figure 1: Histopathological Changes: Hematoxylin and eosin staining from the renal cortex of control diet-fed mice (left) and adenine diet-fed mice (right). Images at 10x magnification.

Results SKH1 mice on an adenine diet demonstrated excessive polyuria (8.2 ± 2.2 mL/24 hrs vs 0.61 ± 0.31 mL/24 hours, p=0.0004), increased proteinuria (7.77 ± 1.97 mg/24 hrs vs 2.27 ± 1.63 mg/24 hrs, p=0.0159), reduction in bodyweight (21.28 ± 1.05 g vs 33.04 ± 2.17 g, p=0.0002), and strong histopathological changes consistent with CKD (including interstitial inflammation and fibrosis; figure). Common markers of renal injury including transforming growth factor-β (TGFβ; a key mediator of renal fibrosis, 3x increase, p=0.0159), tumor necrosis factor α (TNFα; a potent mediator of inflammation, 26x increase, p=0.0159), and interleukin-1β (IL-1β; a key factor in CKD progression and anaemia, 10x

increase, p=0.0079) were all significantly upregulated in mice on the adenine-supplemented diet compared to controls. Additionally, mice on the adenine-supplemented diet show significantly increased levels of circulating cystatin-C (3x increase, p≤0.0001), which is an early and reliable biomarker for the onset of CKD.

Conclusion Our results demonstrate that a low-protein (2.5%) adenine-supplemented (0.15%) diet induces significant renal inflammation and injury in SKH1 mice indicating that adenine diet is a suitable model of CKD in this mouse strain. Characterization of this model provides an important tool in the study of the dermatologic disorders which often accompany CKD.

101

CHARACTERIZING MEDIAL AMYGDALA RESPONSE TO SOCIAL STRESSORS

Alexandra Ritger, Nimah Rasheed, Maxine Loh, Courtney Stickling, Mallika Padival, Nicole Ferrara, Jeremy Rosenkranz. *Rosalind Franklin University*

Introduction/Background Depression is characterized by social withdrawal and avoidance and can emerge after exposure to a social stressor. The medial amygdala (MeA) regulates social behaviors and responds to social cues, and there is evidence of reduced MeA volume and connectivity in people with depression. Repeated social defeat is a natural stressor in rats that results in negative long-term outcomes, including social avoidance and anhedonia, and increases MeA immediate early gene expression, an indirect marker of neuronal activity. x

Objective(s) A clearer understanding of how and when MeA neuronal activity is engaged during social investigation following social stress would help delineate a role of the MeA in stress-induced changes in social behavior.

Methods To induce social stress, we used 5 days of repeated social defeat stress with an aggressive Long Evans rat using the resident-intruder paradigm, or a transport cage control in adult male Sprague-Dawley rats. In Experiment 1 we used in vivo electrophysiology in anesthetized rats to measure the firing rate of spontaneously active neurons in the MeA and identified whether they projected to the bed nucleus of the stria terminalis (BNST) or the ventromedial hypothalamus (VMH), two behaviorally relevant brain areas. In Experiment 2 we used fiber photometry in freely moving, awake rats to measure MeA population activity during two trials of a social preference task. In Trial 1, a novel conspecific (Sprague-Dawley) rat and novel object were placed in cages in opposite corners of the apparatus, and we measured the time spent investigating each cage. In Trial 2, another novel conspecific and a novel aggressor rat were used instead.

Results In Experiment 1, we found that MeA neurons fired faster in socially defeated rats than controls, and this effect was directly associated with the intensity of the stressor. This increase in MeA activity was driven by neurons in the posterodorsal subnucleus (MeApd), while posteroventral (MeApv) activity was similar between groups. We also found that MeA-BNST neurons fired faster in socially defeated rats than controls, while MeA-VMH activity was not affected by stress. This indicates that the MeA, especially the MeApd, is hyperactive following social stress, and identifies heightened MeA-BNST activity as one potential route for the expression of social stress-related behaviors.In Experiment 2, we found that MeA activity was preferentially activated during close social contact in both groups. In Trial 1, the pattern of MeA activity was similar between groups. However, in Trial 2 we observed that stressed rats showed a higher MeA response to the novel aggressor than controls, while exhibiting a slightly diminished MeA response to the novel conspecific. This context-dependent response of the MeA in stressed rats may assist with threat discrimination. The change in MeA activity was paralleled by a change in behavior. While both stressed and control rats showed equal preference for the novel conspecific over the object in Trial 1, in Trial 2 the stressed rats spent most of their time near the aggressor throughout the session, while control rats rapidly habituated to the presence of the aggressor and began to spend more time with the conspecific.

Conclusion We attribute these results to increased vigilance in the stressed rats and suggest that heighted baseline MeA and MeA-BNST activity may drive rats to selectively attend to threats rather than harmless stimuli. This response may be adaptive if it leads to selective avoidance of a novel threat, however it may become maladaptive if it generalizes to non-threatening peers. These results are useful

for understanding more complex mechanisms that may underlie social withdrawal and the response to novel social contexts in individuals with depression.

REFERENCE(S)

1. Brown, S.S.G., J.W. Rutland, G. Verma, R.E. Feldman, M. Schneider, B.N. Delman, J.M. Murrough, and P. Balchandani. 2020. Ultra-High-Resolution Imaging of Amygdala Subnuclei Structural Connectivity in Major Depressive Disorder. Biol. Psychiatry Cogn. Neurosci. Neuroimaging. 5:184–193. doi:10.1016/j.bpsc.2019.07.010.

2. Fekete, É.M., Y. Zhao, C. Li, V. Sabino, W.W. Vale, and E.P. Zorrilla. 2009. Social defeat stress activates medial amygdala cells that express type 2 corticotropin-releasing factor receptor mRNA. Neuroscience. 162:5–13. doi:10.1016/j.neuroscience.2009.03.078.

3. Hollis, F., and M. Kabbaj. 2014. Social defeat as an animal model for depression. ILAR J. 55:221–232. doi:10.1093/ilar/ilu002.

4. Luo, Q., J. Chen, Y. Li, Z. Wu, X. Lin, J. Yao, H. Yu, H. Wu, and H. Peng. 2022. Aberrant static and dynamic functional connectivity of amygdala subregions in patients with major depressive disorder and childhood maltreatment. NeuroImage Clin. 36:103270. doi:10.1016/j.nicl.2022.103270.

5. Newman, S.W. 1999. The medial extended amygdala in male reproductive behavior. A node in the mammalian social behavior network. Ann. N. Y. Acad. Sci. 877:242–257. doi:10.1111/j.1749-6632.1999.tb09271.x.

6. Pezawas, L., A. Meyer-Lindenberg, E.M. Drabant, B.A. Verchinski, K.E. Munoz, B.S. Kolachana, M.F. Egan, V.S. Mattay, A.R. Hariri, and D.R. Weinberger. 2005. 5-HTTLPR polymorphism impacts human cingulate-amygdala interactions: A genetic susceptibility mechanism for depression. Nat. Neurosci. 8:828–834. doi:10.1038/nn1463.

102

ANALYSIS OF TREM2 INTERACTIONS WITH ALZHEIMER'S DISEASE LIGANDS APOE AND OLIGOMERIC AMYLOID BETA REVEALS THE TREM2 HYDROPHOBIC SITE AS A POTENTIAL THERAPEUTIC TARGET

Jessica Greven, Tom Brett. *Washington University in St. Louis*

Introduction/Background The development of new innovative treatments to prevent and ameliorate AD requires knowledge of molecular mechanisms that are critical to neuronal health. The triggering receptor expressed on myeloid cells 2 (TREM2) receptor is part of a signaling complex that modulates inflammatory responses, phagocytosis and cell survival in microglia, resident immune cells in the brain that play a critical role in clearing misfolded aggregates. Examples include neurotoxic aggregates consisting largely of amyloid beta (Aβ) and apoliproteinE (apoE). Both molecules have emerged as important signaling ligands for TREM2. Although TREM2 signaling in microglia is generally associated with beneficial outcomes, intense or prolonged signaling may produce overactivated microglia leading to neuronal damage. Such events may also contribute to other diseases such as Parkinson's or cancers. Furthermore, rare TREM2 variants, most notably R47H and R62H, have been identified that are associated with a significantly increased risk of developing AD. Given these significant roles, TREM2 has emerged as an important yet challenging therapeutic target for AD.
Objective(s) Although a number of ligands for TREM2 with relevance to AD have been identified, little is known regarding the molecular details of how TREM2 engages them. Detailed knowledge of the molecular mechanisms underlying TREM2 signaling in microglia is urgently needed to facilitate the development of specific, potent, safe and efficacious therapies for AD that target the TREM2 signaling pathway. The objective of this study was to identify the critical surfaces on TREM2 that mediate interactions with both apolipoproteinE (apoE) and oligomeric amyloid β1-42 (oAβ42) using rigorous structural and biophysical methods.
Methods We used a mass spectrometry footprinting method (fast photochemical oxidation of proteins), structure-based mutations, and biolayer interferometry (BLI) to investigate TREM2 interactions with apoE and oAβ42.
Results We found that TREM2 utilizes a distal hydrophobic site to engage apoE. We found that N-terminal peptide region of oAβ42 engages both the hydrophobic and basics sites on TREM2.
Conclusion Our results indicate that the hydrophobic site on TREM2 (consisting of the CDR1, CDR2, and CDR3 loops) is a critical ligand-engaging surface on TREM2. They also indicate that therapeutics that either directly bind or allosterically alter the hydrophobic site on TREM2 should modulate TREM2 signaling as potential AD treatments.

REVIVIFY GEL ATTENUATES HUMAN BRAIN MICROVASCULAR ENDOTHELIAL CELLS (HBMEC) FROM HYPOXIA INDUCED DISRUPTION OF BLOOD BRAIN BARRIER (BBB) PERMEABILITY IN A IN VITRO MODEL

[1]Syeda Afroze, [1]ahmed Pantho, [1]Thomas Kuehl, [2]Liaquat Hossain, [3]Mohammad Uddin. [1]*Orion Institute for Translational Medicine;* [2]*Advance Pharmaceutical Inc;* [3]*Texas A&M University School of Medicine*

Introduction/Background Accumulating data suggests that oxidative stress and mitochondrial damage are involved in the pathogenesis of neurodegenerative disorders including Parkinson Disease [PD], Multiple Sclerosis[MS], Alzheimer' s Disease[AD], and many others. Brain uses about 20% of oxygen consumption, thus high producer of reactive oxygen species [ROS]. Also brain cell membrane composed of more unsaturated fatty acids [M UFA and PUFA], thus more prone to lipid auto-oxidation due to ROS. REVIVIFY GEL, addresses instant reduction of oxidative stress from multi-dimensional pathways and resulted an immediate effect induced by the disease symptoms. The purpose of the study is to evaluate whether revivify gel attenuates human brain microvascular endothelial cells (HBMEC) from oxidative damage.

Objective(s) To evaluate whether Revivify gel attenuates the hypoxia induced disruption of HBMEC Monolayer Permeability.

Methods Human brain microvascular endothelial cells (HBMEC) were seeded on 6 well plates in hypoxia condition. Prior to treatment, cells were incubated in serum free media for 24 hours. Cells will be treated with following agents: 1. Superoxide Dismutase only; 2. Prebiotic fiber only; 3.   Fruit juice only; 4. superoxide Dismutase + Prebiotic fiber + Fruit juice (Combination); 5. Negative Control: Cell culture media for 48 hours. The monolayer permeability study was performed by a method described previously in hypoxia condition and pretreatment with revivify. HBMEC were grown on poly-L-lysine glass chamber slides. The cells were treated with the treatment conditions mentioned above. After hypoxia condition, cells were washed in PBS and fixed in 4% paraformaldehyde. After repeated washing steps, Triton X-100 treatment, and blocking for nonspecific binding, cells were incubated with a primary antibody for ZO-1, Occludin, Claudin-1 or E-Cadherin (Invitrogen) at 4°C overnight. Cells were washed in PBS and exposed to an FITC-conjugated secondary antibody for 1 h. After repeated washing steps, the cells were mounted in an antifade mounting medium that contained the nuclear stain DAPI (Invitrogen, Eugene, OR). Cells were observed under an Olympus FluoView FV 300 confocal laser-scanning microscope with appropriate filters for visualizing FITC and DAPI.

Results HBMEC monolayer permeability was significantly increased in hypoxic condition. Revivify significantly attenuated the hyperpermeability induced by hypoxia. Revivify Finished Product Attenuated the Hypoxia-induced monolayer hypermeability in Human Brain Microvascular Endothelial Cells (HBMEC) In Vitro BBB. Immunofluorescence images of endothelial cell tight junction proteins: ZO-1, Occludin and E-Cadherin in HBMEC. CONTROL (No treatment) cells show intact tight junctions evidenced by the strong and continuous presence of ZO-1, Occludin and E-Cadherin at the junctions. HOPOXIA: Disruption of the tight junction proteins; HYPOXIA + FIBERSOL: No Attenuation of tight junction proteins; HYPOXIA + SOD: Partial Attenuation of tight junction proteins; HYPOXIA + POLYPHENOL: Attenuation of tight junction proteins; HYPOXIA + FINISHED PRODUCT: Attenuation of tight junction proteins.

Conclusion REVIVIFY GEL; Pertaining to PD, it can improve motor activity, muscle stiffness, and overall body response with less exhaustion. For AD, it may improve the memory response, coordination with surrounding atmosphere. As others, it can improve focus, concentration, and alertness, which may be beneficial to people with learning disability, people with autistic problem, people with mental

exhaustion, and can benefit to the people who needs study focus, or job associated with high concentration. The pre-biotic soluble corn fiber encompasses the healthy gut-echo-system where the modulation of beneficiary microbes influences various positive neurological effect. The gut-brain bi-directional axis can relate instant neuro-responses. Thus, REVIVIFY PRO-VITALITY GEL is unique and exert prompt responses towards neuro disease induced symptoms in PD, MS, AD and other conditions.

POSTERIOR REVERSIBLE ENCEPHALOPATHY SYNDROME IN A TRAUMA PATIENT WITH MULTIPLE GUNSHOT WOUNDS

Vijay Dimri, Shruti Mishra, Mauli Patel, Binod Wagle. *University of Missouri Kansas City*

Introduction/Background Posterior Reversible Encephalopathy Syndrome (PRES) is a neurological condition with variable manifestations confirmed by radiological findings of vasogenic edema. While the exact pathophysiology of the condition is unknown, the leading endothelial dysfunction theory posits that damage to the blood-brain-barrier due to hypertension, acute fluctuations in blood pressures, or toxin-mediated endothelial damage causes leak of vessel contents into the interstitial space.1 Clinicians may not be aware of trauma as an inciting factor for PRES given the scarcity of such cases in the literature. As such, we aim to increase recognition of these cases in clinical practice. Here we delineate the first reported case of PRES occurring in a trauma patient with multiple gunshot wounds (GSW).

Case Presentation A 24-year-old male with a history of colostomy after GSW to the abdomen and without history of hypertension presented to the trauma bay with multiple GSW to the abdomen, chest, and left thigh. On evaluation, the patient was tachycardic but normotensive, and the FAST exam was positive for a right pleural effusion. An exploratory laparotomy was performed with diaphragm and liver laceration repair, pericardial window, and chest tube placement bilaterally. He received 4 units of packed red blood cells, 4 units of fresh frozen plasma, and 1 unit of platelets during the case. An ABThera was placed, and the patient was taken back to the OR the next day for reexploration, abdominal washout, and abdominal fascial closure. He was extubated on hospital day 2, at which point the primary medicine team noted the patient was agitated and confused. He was initially managed on haloperidol, and later quetiapine was added. On hospital day 9, a non-contrast CT of the head was obtained for persistent altered mental status which was suggestive of multifocal acute infarcts. Follow-up magnetic resonance imaging (MRI) was performed and demonstrated small acute infarcts in the right frontal and left posterior occipital lobe, as well as T1 hypointensity, and T2 hyperintensity with associated FLAIR signal in the bilateral posterior horns of the occipital lobes consistent with PRES (Fig. 1). Neurology was consulted regarding the infarcts on imaging and for new onset memory deficits, somnolence, and agitation. On the initial neurological exam, the patient was alert and oriented, and the only defects found were difficulty with concentration and calculation. On hospital day 11, the patient was no longer oriented to the month and did not know the current or first president. He registered 3/3 words but recalled 0/3 words, and his language was mildly slowed compared to the previous day. The patient also demonstrated cognitive impairment in concentration and calculation. On hospital day 12, he was drowsy but once again oriented to the month. New deficits found included decreased confrontation in upper visual fields bilaterally. The remainder of the neurological examination was normal. Repeat imaging reconfirmed suspicions for PRES, and a lumbar puncture was performed to rule out infection and was normal. Throughout his hospital course, the patient did not have seizures or headaches. He was started on aspirin and worked with PT/OT to regain strength throughout his hospital stay. Other postoperative complications included a postoperative fever on hospital day 4. Blood cultures were obtained and grew Bacteroides vulgatus and a Clostridium species, for which he was treated with IV piperacillin-tazobactam. He also had an infected biloma, found on CT angiogram of the abdomen and pelvis that was obtained for abdominal pain with new tachycardia on hospital day 8. A drain was placed and ERCP with stent placement was performed. Culture from the drain grew Pseudomonas aeruginosa and Enterococcus faecalis, which was treated with outpatient antibiotics.The patient was discharged on hospital day 16 with an appropriate pain regimen, amoxicillin-clavulanate and levofloxacin for his infections, and instructions to return for stent removal in 8 weeks and repeat MRI in 1-2 months to

evaluate for resolution of PRES. At the time of discharge, his mental status remained altered as described above. The patient was lost to follow-up, thus no MRI was performed after discharge and there were no outpatient appointments made.

Discussion The clinical manifestations of PRES are variable. While the most common presentation is seizures; encephalopathy, altered mental status, headache, and changes in vision can also occur.[2] The etiology of PRES is multifaceted. Hypertension and blood pressure fluctuations are the most commonly reported precipitating cause of the condition, with immune-suppressing medication, infection, and preeclampsia being reported less commonly.[2] In the majority of the cases implicating blood pressure, the mechanism of PRES is hyperperfusion overwhelming the capacity of cerebral autoregulation leading to extravasation of fluid and vasogenic edema.[1] In cases without hypertension as a precipitating factor, a cytotoxic theory has been proposed with endogenous and/or exogenous toxins damaging endothelial cells of the blood-brain-barrier. This leads to release of vasoactive compounds from endothelium causing vascular leakage.[1] Common etiologies of PRES that likely arise from the cytotoxic mechanism include immunosuppressant use, infection, (pre)eclampsia, and renal failure. Blood transfusion has been reported in previous case studies as a rare cause of PRES, with recent literature reviews identifying less than 30 reported cases.[3] The posited mechanism of this etiology is a sudden increase in blood viscosity due to rising hematocrit levels, causing injury to endothelium, similar to the cytotoxic theory of PRES.[4] The significance of the above etiologies of PRES is that these phenomena (blood pressure changes with hypertension, infection leading to sepsis, and blood transfusions) are complications which may arise in the course of treatment in patients with acute trauma from external injury. However, this concept has been poorly defined. In order to further explore the possible link between acute trauma and its complications with PRES, we aim to provide a brief overview of the current literature regarding PRES following acute trauma from external injury. The general demographics of our final population of twelve patients are listed in Table 1 below. The most common trauma type related to eventual development of PRES was motor vehicle accidents (MVAs), accounting for eight of the twelve cases.[5, 6, 9, 12,-14] MVAs included collisions of a motor vehicle with another object or vehicle, or collision with a motor vehicle as a pedestrian. The remainder of causes in other cases were composed of falls (2) or other blunt trauma (2).[7, 8, 10, 11] Blood pressure abnormalities were present in all but one case of PRES related to external traumas.[5-10, 12-14] Hypertension and blood pressure fluctuations are well established causes of PRES, making up the most commonly reported precipitating cause of the condition; this aligns with our findings. Three of the twelve cases also involved transfusions in the acute setting after a trauma, and two of the twelve cases developed sepsis during the course of their hospital stay, which may have contributed to the development of PRES.[5, 6, 8, 10] Other potential factors known to be related to PRES that were found within the literature review included renal dysfunction and cytotoxic medications.[5, 8, 12] Perhaps equally important are the symptomatic manifestations of PRES in patients in acute-trauma settings. Seven of the twelve cases mentioned seizures as a notable clinical occurrence, including both single generalized seizures and status epilepticus.[5, 7-9, 12-14] Six patients experienced headaches and three experienced vision changes, although it is unclear if these are symptomatic manifestations of hypertension or related to development of PRES.[6-9, 14] In terms of diagnostic imaging, MRIs (identified as the standard of care for PRES) were ordered on all patients, and the distribution of PRES-related imaging findings uniformly implicated the posterior circulation.[2, 5-14] Some cases (5) had anterior circulation involvement in addition; however, in no cases was only the anterior circulation involved.[5, 9, 10, 13, 14] Notably, all articles were written in the last decade, with the exception of one.[5-8, 10-14] In the case study above, the patient's hospitalization included multiple potential causes of PRES. These included the large volume blood transfusion upon admission, blood pressure fluctuations, and infection. Recorded systolic blood pressures ranged from 94-163 mmHg, diastolic blood pressures ranged from 42-124 mmHg, and mean arterial pressure ranged from 70-137 mmHg. These same factors were found across the cases in the literature review, supporting the

correlation between these complications of trauma and the future development of PRES. There is a scarcity of cases regarding the correlation between trauma and PRES in the literature, and there are none regarding gunshot wounds as the source of trauma preceding PRES. The cases discussed in the literature review all were precipitated by trauma; however, the case report we present above is the first reported case of PRES incited by a gunshot wound specifically. This case report aims to increase awareness of PRES as a possible complication of traumatic injuries and associated resuscitation measures. While rare, it is important to keep this diagnosis in mind as trauma patients frequently experience several inciting factors such as hemodynamic instability, blood transfusions, and infections.
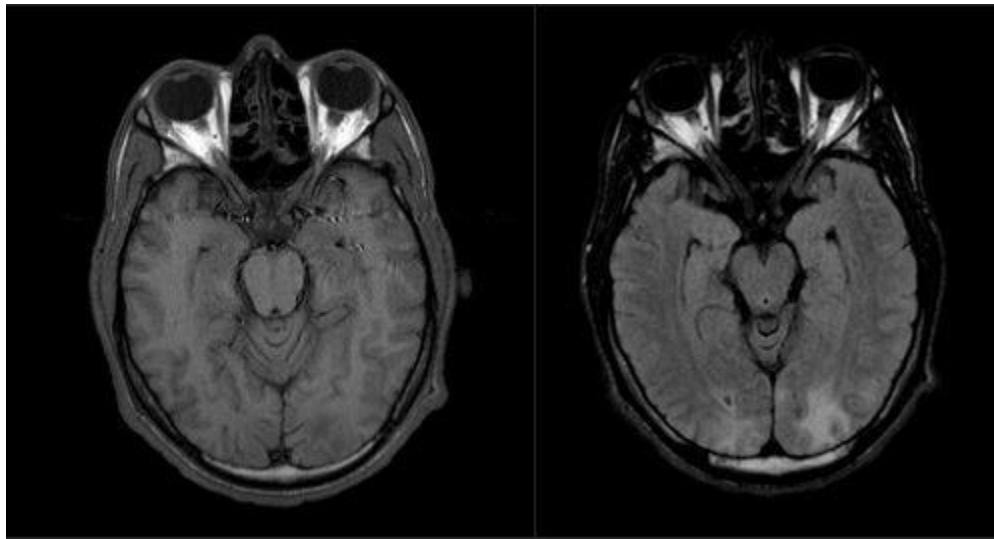
Abstract 104 Figure 1 MRI Results- MRI showing T1 hypointensity and T2 hyperintensity of the bilateral posterior horns of the occipital lobes with associated FLAIR signal and sulcal effacement.

REFERENCE(S)
1. Fischer M, Schmutzhard E. Posterior reversible encephalopathy syndrome. J Neurol. 2017;264(8):1608-1616. doi:10.1007/s00415-016-8377-8
2. Fugate JE, Claassen DO, Cloft HJ, Kallmes DF, Kozak OS, Rabinstein AA. Posterior reversible encephalopathy syndrome: associated clinical and radiologic findings. Mayo Clin Proc. 2010;85(5):427-432. doi:10.4065/mcp.2009.0590
3. Gurumukhani JK, Patel HD, Patel DM, et al. Posterior reversible encephalopathy syndrome following blood transfusion: A rare case report with literature review. The Open Neurology Journal. 2021;15(1):31-36. doi:10.2174/1874205x02115010031
4. Nakamura, Y., Sugino, M., Tsukahara, A. et al. Posterior reversible encephalopathy syndrome with extensive cytotoxic edema after blood transfusion: a case report and literature review. BMC Neurol 18, 190 (2018). https://doi.org/10.1186/s12883-018-1194-1
5. Aggarwal R, Saxena A, Soni K. Posterior reversible encephalopathy syndrome during recovery from hypovolemic acute kidney injury after trauma; case report and literature review. Bull Emerg Trauma. 2017;5(3):215-218.
6. Braganza J, Pratt A. Posterior reversible encephalopathy syndrome in the setting of trauma: A case report. International Journal of Surgery Case Reports. 2020;72:528-532. doi:10.1016/j.ijscr.2020.06.061
7. Chen H, Xu Z, Yuan Y. Posterior reversible encephalopathy syndrome and reversible cerebral vasoconstriction syndrome associated spinal subdural hematoma: A case report. Medicine. 2020;99(31):e21522. doi:10.1097/MD.0000000000021522

8. Daly WC, Reynolds T, Tanzer M, Chalmers DJ. Posterior reversible encephalopathy syndrome following failure of conservative management in renal trauma: case report. Urology. 2020;145:247-249. doi:10.1016/j.urology.2020.05.059

9. El Rachkidi R, Soubeyrand M, Vincent C, Molina V, Court C. Posterior reversible encephalopathy syndrome in a context of isolated cervical spine fracture: CT angiogram as an early detector of blunt carotid artery trauma. Orthopaedics & Traumatology: Surgery & Research. 2011;97(4):454-458. doi:10.1016/j.otsr.2011.02.011

10. Sigurtà A, Terzi V, Regna-Gladin C, Fumagalli R. Posterior reversible encephalopathy syndrome complicating traumatic pancreatitis: a pediatric case report. Medicine. 2016;95(22):e3758. doi:10.1097/MD.0000000000003758

11. Yonekura S, Anno T, Kobayashi N. Posterior reversible encephalopathy syndrome and guillain-barré syndrome after head injury: case report. Neurol Med Chir(Tokyo). 2018;58(10):453-458. doi:10.2176/nmc.cr.2018-0049

12. Zimering JH, Mesfin A. Posterior reversible encephalopathy syndrome following elevated mean arterial pressures for cervical spinal cord injury. The Journal of Spinal Cord Medicine. 2018;41(1):111-114. doi:10.1080/10790268.2016.1250030

13. Yoon JE, Lee CY, Kim HW. Posterior reversible encephalopathy syndrome after head trauma surgery in pediatric patient without any underlying disease. Korean J Neurotrauma. 2017;13(2):167. doi:10.13004/kjnt.2017.13.2.167

14. Hubbard ME, Phillips AA, Charbonneau R, Squair JW, Parr AM, Krassioukov A. PRES secondary to autonomic dysreflexia: A case series and review of the literature. The Journal of Spinal Cord Medicine. 2021;44(4):606-612. doi:10.1080/10790268.2019.1616146

Abstract 104 Table 1 Literature Review Results- AC: anterior circulation- circulation fed by the internal carotid arteries PC: posterior circulation- circulation fed by the vertebral arteries.

Article	external trauma with resulting injury	Surgery preceding PRES	Patient age	Sex	Possible factors contributing to PRES	Clinical findings	MRI findings distribution	Year
Posterior Reversible Encephalopathy Syndrome during Recovery from Hypovolemic Acute Kidney Injury after Trauma; Case Report and Literature Review	Road traffic accident leading to above knee amputation	Above knee amputation	6	F	Acute kidney injury Blood pressure fluctuation Hypertension Transfusion (5U pRBCs, 3U FFP, 3U platelets, and 3U cryoprecipitate)	Epileptic seizures	AC, PC	2017
Posterior reversible encephalopathy syndrome in the setting of trauma: A case report	Motor vehicle collision resulting in small bowel perforation and knee laceration	Exploratory laparotomy Debridement and irrigation of lower extremity Open reduction and internal fixation	40	F	Blood pressure fluctuations	Headache Vision changes (central blurriness, right hemianopsia)	PC	2020
Posterior reversible encephalopathy syndrome in the setting of trauma: A case report	Assault with a motor vehicle causing TBI, hydrocephalus, bilateral pneumothorax, pulmonary contusion, multiple fractures, and pancreatic laceration	Tracheostomy Bilateral chest tube placement External ventricular drain placement Percutaneous cholecystectomy	56	M	Transfusion Sepsis Hypertension	None reported	PC	2020

Posterior reversible encephalopathy syndrome and reversible cerebral vasoconstriction syndrome associated spinal subdural hematoma	Unspecified minor neck trauma resulting in spinal subdural hematoma	N/A	40	F	Hypertension	Epileptic seizure Headache Altered mental status Vision changes (blurred vision)	PC	2020
Posterior Reversible Encephalopathy Syndrome Following Failure of Conservative Management in Renal Trauma: Case Report	Fall onto right abdomen resulting in renal trauma	Coil embolization of renal artery branches with stent placement	4	M	Hypertension Renal disease Transfusion with pRBCs	Altered mental status Headache Epileptic seizure	PC	2020
Posterior reversible encephalopathy syndrome in a context of isolated cervical spine fracture: CT angiogram as an early detector of blunt carotid artery trauma	Motor vehicle collision resulting in cervical spine fracture with blunt carotid artery injury	N/A	36	M	Hypertension	Altered mental status Headache Epileptic seizure	AC, PC	2011
Posterior Reversible Encephalopathy Syndrome Complicating Traumatic Pancreatitis	Blunt abdominal trauma with resulting acute pancreatitis complicated by pseudocyst	Two exploratory laparotomies Small bowel resection	15	M	Hypertension Sepsis	Altered mental status	AC, PC	2016

	Mechanism	Procedure	Age	Sex	Risk factors/Trigger	Symptoms	Circulation	Year
Posterior Reversible Encephalopathy Syndrome and Guillain-Barré Syndrome after Head Injury: Case Report	Fall causing head injury with resulting subarachnoid hemorrhage and subdural hematoma	N/A	74	M	None reported	None reported	PC	2018
Posterior reversible encephalopathy syndrome following elevated mean arterial pressures for cervical spinal cord injury	Motor vehicle collision resulting in cervical spine subluxation with spinal cord injury	Anterior and posterior cervical spine fusion and decompression	68	F	Cytotoxic medication (methotrexate) Blood pressure fluctuation	Status epilepticus Altered mental status	PC	2018
Posterior Reversible Encephalopathy Syndrome after Head Trauma Surgery in Pediatric Patient without Any Underlying Disease	Head trauma secondary to motorcycle accident causing depressed frontal fracture	Dura repair, frontal sinus sealing, bony reconstruction and galeal reposition on skull base	16	F	Hypertension	Epileptic seizure	AC, PC	2017
PRES secondary to autonomic dysreflexia: A case series and review of the literature	Motor vehicle collision resulting in T4 spinal cord injury	N/A	36	M	Autonomic dysreflexia: blood pressure fluctuations	Generalized seizures Headache	PC	2021
	Motor vehicle collision with C2 spinal cord injury	N/A	18	F	Autonomic dysreflexia: hypertension	Altered mental status Headache Vision changes (visual field loss and light sensitivity)	AC, PC	2021

105

RESPIRATORY FAILURE AS THE SOLE MANIFESTATION OF ANTI-MUSK MYASTHENIA GRAVIS

Mustafa AW. Mohammed, Shelby Macrae, Jesus F. Lovera, Rima N. El-Abassi, Bennett P. deBoisblanc, Edward C. Mader, Jr. *LSUHSC Department of Neurology and University Medical Center*

Introduction/Background Approximately 80% of patients with myasthenia gravis (MG) have antibodies to the acetylcholine receptor (AChR) and 8% have antibodies to muscle-specific kinase (MuSK)1. Younger females are more likely to be affected than males2; and blacks are more likely to have these antibodies compared to whites. The incidence of MuSK antibody-positive MG considerably varies depending on the geographic location3-5. Patients with Anti-MuSK antibodies have HLA-DRB1, DQB1, DQ5, and DR14 alleles,6-8. Anti-MuSK MG typically presents with acute onset of bulbar symptoms followed by rapid progression to respiratory failure within a few weeks. Occasionally, anti-MuSK MG may resemble anti-AChR MG and present with generalized weakness and fatigue. Anti-MuSK MG presenting with isolated ocular findings, vocal cord paralysis, or head drop have been reported. We report a case of anti-MuSK MG with chronic respiratory failure as the only manifestation.

Case Presentation A 50-year-old woman with a BMI 35 kg/m2 and 15 years of chronic hypercapnia (paCO2 72 mmHg) was on home BIPAP for presumed obesity-hypoventilation syndrome. During vacation air travel, she became unarousable, necessitating emergency landing. On arrival to the hospital, she was intubated and mechanically ventilated for worsening hypercapnia. Although her peripheral muscle strength was completely normal, an occult neuromuscular disorder was suspected because her syndrome seemed out of proportion to her obesity. Her pulmonary function tests suggested extrapulmonary restriction. Negative inspiratory force (NIF) was -10 cmH2O (normal -100 +/- 20 cmH2O). Myasthenia gravis autoimmune antibody panel showed an elevated anti-MuSK antibody titer (48 nmol/L; reference ≤ 0.02 nmol/L). Other tests for myopathy and autoimmunity were normal and chest CT did not show thymoma. She was treated with intravenous immunoglobulin (IVIG) 400 mg/kg/day IV for 5 days with improvement in both her NIF to -45 cmH2O and her paCO2 to 44 mmHg. She has remained asymptomatic with monthly IVIG infusion.

Discussion Unexplained acute on chronic respiratory failure prompted a search for a neuromuscular disorder leading to the diagnosis of anti-MuSK MG. This case shows that anti-MuSK MG can manifest exclusively as chronic respiratory failure and that IVIG can be a treatment option for this disorder.

REFERENCE(S)
1. Lindstrom JM, Seybold ME, Lennon VA, Whittingham S, Duane DD. Antibody to acetylcholine receptor in myasthenia gravis: prevalence, clinical correlates, and diagnostic value. Neurology. 1976;26(11):1054-1059.
2. Stickler DE, Massey JM, Sanders DB. MuSK-antibody positive myasthenia gravis: clinical and electrodiagnostic patterns. Clinical neurophysiology : official journal of the International Federation of Clinical Neurophysiology. 2005;116(9):2065–2068
3. Huang YC, Yeh JH, Chiu HC, Chen WH. Clinical characteristics of MuSK antibody-positive myasthenia gravis in Taiwan. J Formos Med Assoc. 2008;107(7):572–575.
4. Yeh JH, Chen WH, Chiu HC, Vincent A. Low frequency of MuSK antibody in generalized seronegative myasthenia gravis among Chinese. Neurology. 2004;62(11):2131–2132.
5. Kostera-Pruszczyk A, Kaminska A, Dutkiewicz M, et al. MuSK-positive myasthenia gravis is rare in the Polish population. European journal of neurology : the official journal of the European Federation of Neurological Societies. 2008;15(7):720–724.

6. Bartoccioni E, Scuderi F, Augugliaro A, et al. HLA class II allele analysis in MuSK-positive myasthenia gravis suggests a role for DQ5. Neurology. 2009;72(2):195–197.

7. Alahgholi-Hajibehzad M, Yilmaz V, Gulsen-Parman Y, et al. Association of HLA-DRB1 *14, -DRB1 *16 and -DQB1 *05 with MuSK-myasthenia gravis in patients from Turkey. Hum Immunol. 2013;74(12):1633–1635.

8. Kanai T, Uzawa A, Kawaguchi N, et al. HLA-DRB1*14 and DQB1*05 are associated with Japanese anti-MuSK antibody-positive myasthenia gravis patients. Journal of the neurological sciences. 2016;363:116–118.

106

POST LUMBAR PUNCTURE (LP) SUBDURAL HEMATOMA: A CASE REPORT.

Omar Sajdeya, Nezam Altorok, Ragheb Assaly, Saif-Eddin Malhas, Fadi Safi, Wasef Sayeh. *University of Toledo*

Introduction/Background Lumbar puncture is considered an important minimally invasive tool that can be used for diagnostic and therapeutic purposes. One of the most important indications for performing LP is to confirm or rule out an infectious pathology affecting the central nervous system. Complications of the procedure include post-LP headache, back pain, radicular pain or numbness, and less likely cerebral herniation and bleeding1. Serious bleeding is usually rare in the absence of thrombocytopenia or coagulopathy and presents mainly in the form of spinal hematoma. We are presenting a rare case of post-LP subdural hematoma

Case Presentation A 64-year-old female patient with a known past medical history significant for end-stage renal disease (ESRD) on hemodialysis, heart failure with reduced ejection fraction, diabetes mellitus, and hypertension was admitted to the hospital due to alteration in the mental status of one-day duration prior to admission. Upon admission, she was found to be confused and awakened only to verbal stimuli. Her vital signs were within normal limits except for a temperature of 100.8 F. Physical examination was unremarkable except for neck paraspinal tenderness with negative meningeal signs. CBC was mainly remarkable for a WBC count of 12x103 (normal range: 4-10 X103). A Head CT scan was done upon admission and was not suggestive of any acute pathology (figure 1). A brain MRI was also done and was unremarkable. The patient was started empirically on Vancomycin, Ampicillin, Cefepime, and Acyclovir for empiric coverage of meningitis immediately with an intent to proceed with performing a diagnostic LP. Before doing the procedure, PT/INR, aPTT and platelets count were all checked and were completely within normal limits. The patient was off anticoagulation. Bedside LP was attempted once but failed due to the patient's anxiety and pain. On the next day, LP was performed under fluoroscopy guidance where 16 cc of clear fluids were collected using an L3-L4 right oblique sublaminar approach. The procedure was well tolerated by the patient without immediate complications and the fluids were sent for analysis, gram stain and cultures which came back all unremarkable for any acute pathology. Therefore, antibiotics were discontinued later that day and the patient's mental status was noted to be improving. Almost 12 hours after performing the LP, the patient's mental status deteriorated significantly. She became obtunded with slurred speech. A stroked alert was called and the immediate neurological assessment was significant for an NIH stroke scale of 34. An immediate head CT scan was done and showed the development of left frontoparietal and temporal subdural hematoma with complete effacement of the left lateral ventricle and midline shift to the opposite direction (figure 2). The patient had to be intubated urgently and transferred to the ICU.
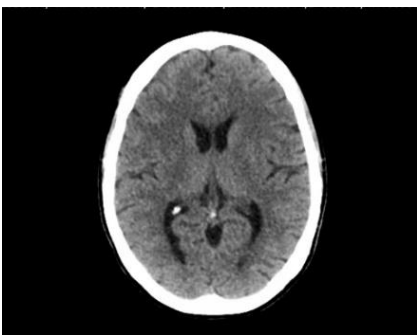
Abstract 106 Figure 1 CT on Admission
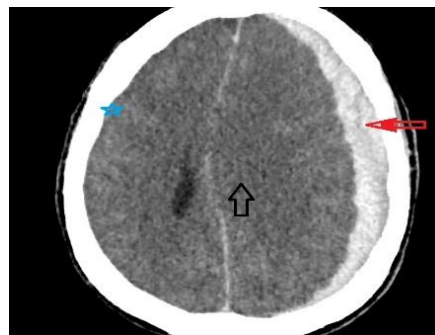
Abstract 106 Figure 2 CT after LP

Discussion Subdural bleeding is usually associated with traumatic events, especially in patients with advanced age, brain atrophy, or coagulopathy. There are very few cases where patients develop subdural hematoma after performing LP2. The presumed pathophysiology behind it is that cerebrospinal fluid (CSF) leakage causes a reduction in the intraspinal and intracranial pressure which can cause caudal displacement of the brain and stretching of the bridging vein leading to subdural bleeding. Risk increases in patients with advanced age and brain atrophy, coagulopathy, and in cases where large spinal needles are used to do a spinal tap or when multiple attempts are tried. Our patient developed post-LP subdural hematoma without having known risk factors. Therefore, we believe that this is a rare case of post-LP subdural hematoma formation.

REFERENCE(S)
1. Benesch MGK, Mathieson A. Epidemiology of Signet Ring Cell Adenocarcinomas. Cancers (Basel). Jun 11 2020;12(6)doi:10.3390/cancers12061544
2. Layton KF, Kallmes DF, Horlocker TT. Recommendations for anticoagulated patients undergoing image-guided spinal procedures. AJNR Am J Neuroradiol. Mar 2006;27(3):468-70.

107

WARFARIN INDUCED NEW-ONSET HEADACHE IN A PATIENT WITH MIGRAINE AND ANTIPHOSPHOLIPID SYNDROME

Mustafa AW. Mohammed, Edward Mader, Jr. *LSUHSC Department of Neurology and University Medical Center*

Introduction/Background There are several published reports of serendipitous improvement in migraine among patients treated with the anticoagulant warfarin. In one case series, the authors proposed that warfarin ameliorates migraine headaches by inhibiting platelet aggregation and serotonin secretion resulting in a drop in serotonin levels below the threshold necessary for triggering vasoconstriction. However, we are not aware of any reports of warfarin triggering a new type of headache or aggravating the headache of patients who happen to have migraine.

Case Presentation A 41-year-old lady with a history of systemic lupus erythematosus (in remission for many years) and chronic migraine (well-controlled for many years) presented with a basal ganglia stroke. Serology was positive for lupus anticoagulant but negative for signs of lupus activity. Warfarin was started and titrated towards an INR of 2 to 3. One day after the initiation of warfarin, she started having severe bioccipital headache that lasted 10 to 14 hours and occurred almost everyday. She feels her new-onset headache was different from her usual migraine headache. She described her typical migraine as a left frontal throbbing pain with nausea and vomiting that occurs once a month on average and readily responds to acetaminophen. Her new headache was bioccipital, intense (10/10), constant, pressure-like, and exacerbated by bending forward. Neurological and ophthalmological examinations, as well as brain MRI, were all unremarkable. The patient was motivated to stop warfarin 3 months after it was started. Five days later, the headache resolved completely. Rheumatology decided to start enoxaparin. She remained headache-free on this treatment.

Discussion We believe the patient's new-onset headache was triggered by warfarin because it resolved completely when this drug was discontinued. Her new headache was different from her usual migraine in terms of distribution, frequency, and other characteristics. To our knowledge, this is the only case report where warfarin made the patient's headache worse; all other reports described improvement of headache with warfarin.

Pathophysiology

108

INCREASED EXPRESSION OF (PRO)RENIN RECEPTOR DURING PREGNANCY IS ASSOCIATED WITH PREECLAMPSIA

[1]Waverly Kundysek, ,[2]Syeda Afroze, [3]Niraj Vora, [1]David Zawieja, [3]Mohammad Nasir Uddin. [1]*Texas A&M School of Medicine;* [2]*Orion Institute for Translational Medicine;* [3]*Baylor Scott and White Health*

Introduction/Background Preeclampsia (preE), a complex syndrome of hypertension and proteinuria, is a leading cause of maternal and fetal morbidity and mortality. Methods for early diagnosis and treatment are not yet available, yet the renin-angiotensin system (RAS) has been implicated in preeclampsia pathogenesis.

Objective(s) In this study, placental expression of (P)RR and serum soluble (P)RR were evaluated in patients with and without preE and in animal models.

Methods Human placenta and blood samples were collected from 40 normal pregnant (NP) and 30 patients with preE who consented to participation. Samples from 10 normal rats with normal pregnancy and 10 with induced preE were evaluated for the expression of (P)RR in placenta and amount of soluble (P)RR. (P)RR expression was measured by western blotting and immunohistochemistry was used visualize (P)RR expression. Soluble (P)RR was detected using a commercially available ELISA Kit.

Results Placental expression of (P)RR was greater ($p< 0.05$) in patients with preE compared to normally pregnant women. Soluble (P)RR was significantly higher in both human patients and rat with induced preE. The preterm placenta of the owl monkey expressed higher ($p< 0.05$) levels of (P)RR compared to term placentas. Placental expression was localized in the fetal villus cells.

Conclusion This study provides new information about the role of (pro)renin and (P)RR associated novel RAS in PreE pathogenesis by suggesting that (pro)renin binding to its receptor may not only facilitate angiotensin generation locally, but also activate second messenger pathways within the vascular cells. This research can open possibilities to advance drug design for specific blocking agents (for example, (P)RR blockers) with greater benefit in gestational hypertension and preE. Elevations in soluble (P)RR also may serve as an early biomarker for diagnosis of preE, as early as the second trimester.
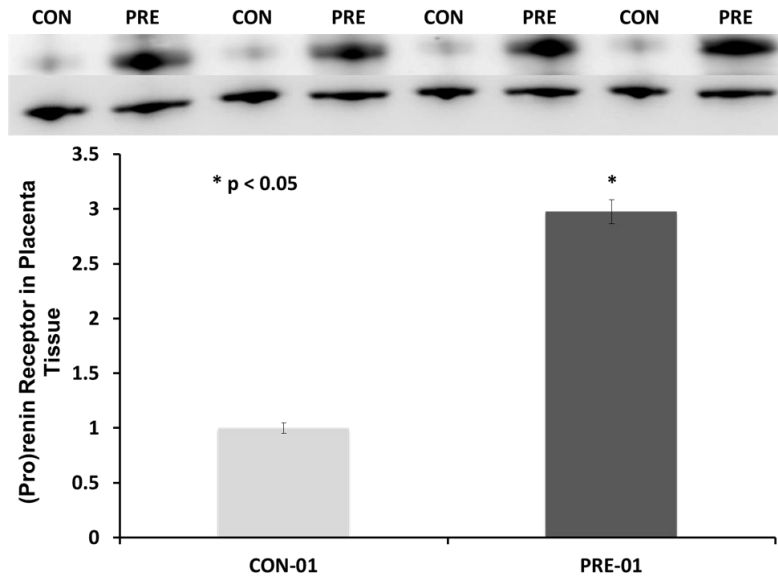
Abstract 108 Figure 1A The (P)RR expression was measured in placental tissue of 2 groups of pregnant patients by gel electrophoresis of the placental homogenate followed by detection with Western blotting using anti-ATP6IP2 antibody. The subjects were: NP (n=40) and preE pregnant (n=30). The placental (pro)renin receptor was significantly upregulated in preE human patients compared to normal (p<0.05). The results presented are mean +/- SE. Figure shows a representative blot.
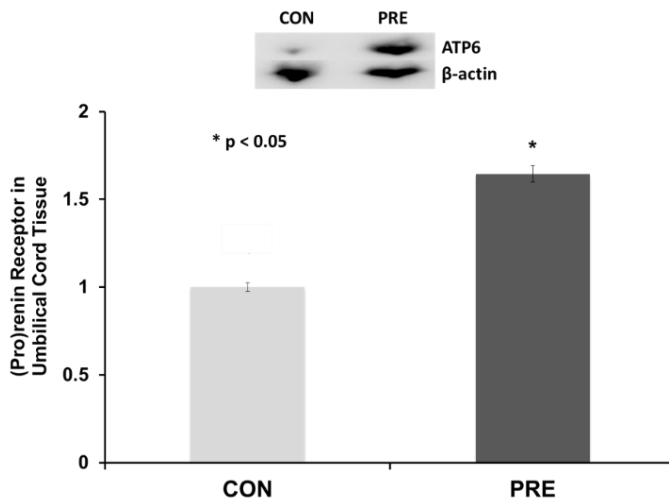
Abstract 108 Figure 1B The (P)RR expression was measured in umbilical cord of 2 groups of pregnant patients by gel electrophoresis of the placental homogenate followed by detection with Western blotting using anti-ATP6IP2 antibody. The subjects were: NP (n=40) and preE pregnant (n=30). The placental (pro)renin receptor was significantly upregulated in preE human patients compared to normal (p<0.05). The results presented are mean +/- SE. Figure shows a representative blot.
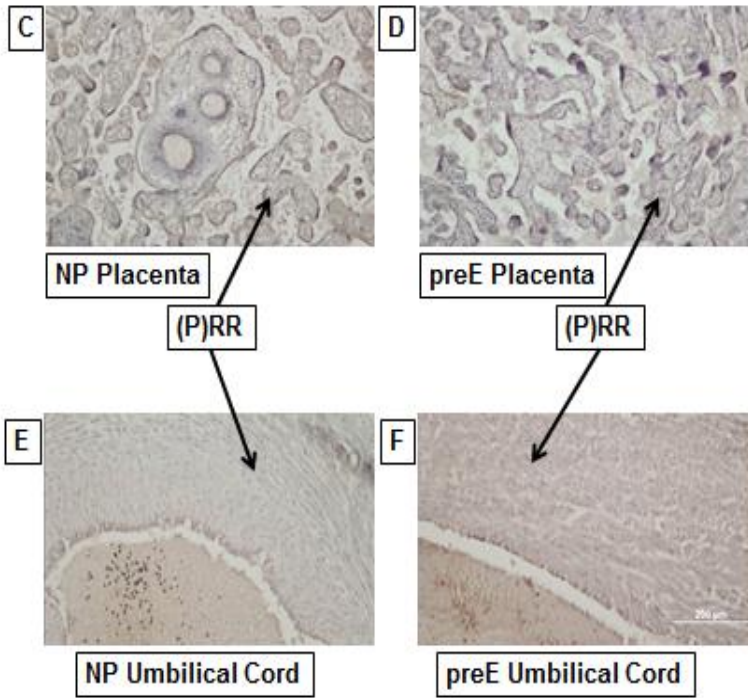
Abstract 108 Figure 1 C – F The immunuhistochemistry images shown in Figs. 2 C – F ; (C) NP placenta; (D) preE Placenta; (E) NP Umbilical Cord; (F) preE Umbilical Cord. Both placental and umbilical cord expression (P)RR are higher in preE patients compared to NP.
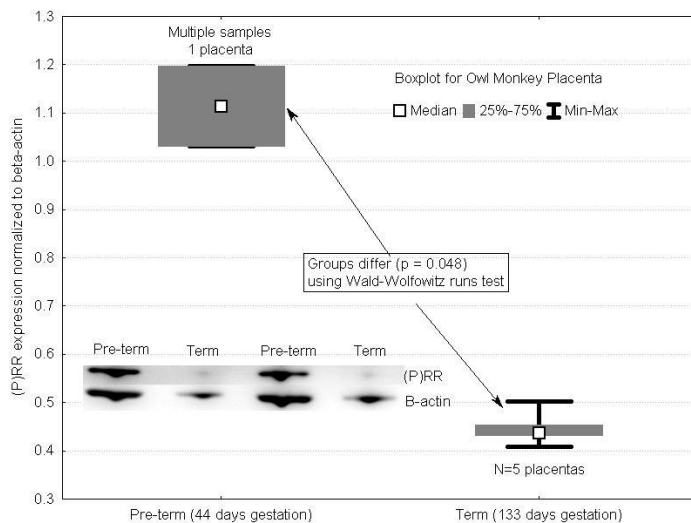
Abstract 108 Figure 2 A The (P)RR expression was measured in owl monkey placenta from one animal delivering at 44 days and 5 animals delivering at term (133 days). (P)RR measurements expressed as the mean of five measurements from each placenta using gel electrophoresis of the placental homogenates followed by detection with Western blotting using anti-ATP6IP2 antibody. Levels in the early placenta (n=1) were greater ($p < 0.05$) that in the term placentas (n = 5).

OWL MONKEY PLACENTAL (PRO)RENIN RECEPTOR ((P)RR) EXPRESSION

(a) Early Placenta   **(b) Term Placenta**

100X   100X

Negative Control →
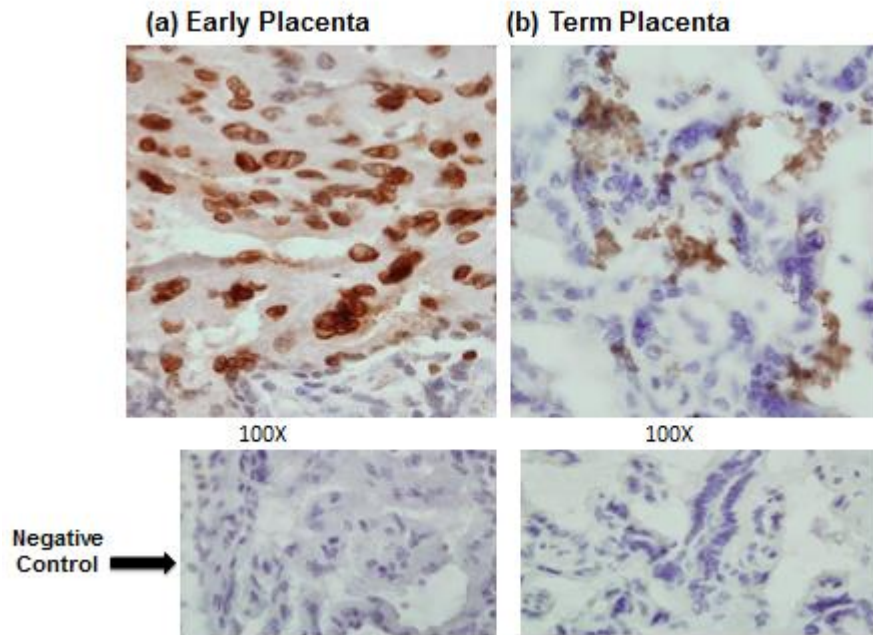
Abstract 108 Figure 2B The immunuhistochemistry using anti-ATP6IP2 antibody demonstrates (P)RR expression localized to fetal cells throughout the chorinoic vili of the preterm placenta. Fewer fetal cells are labelled in the term placenta.
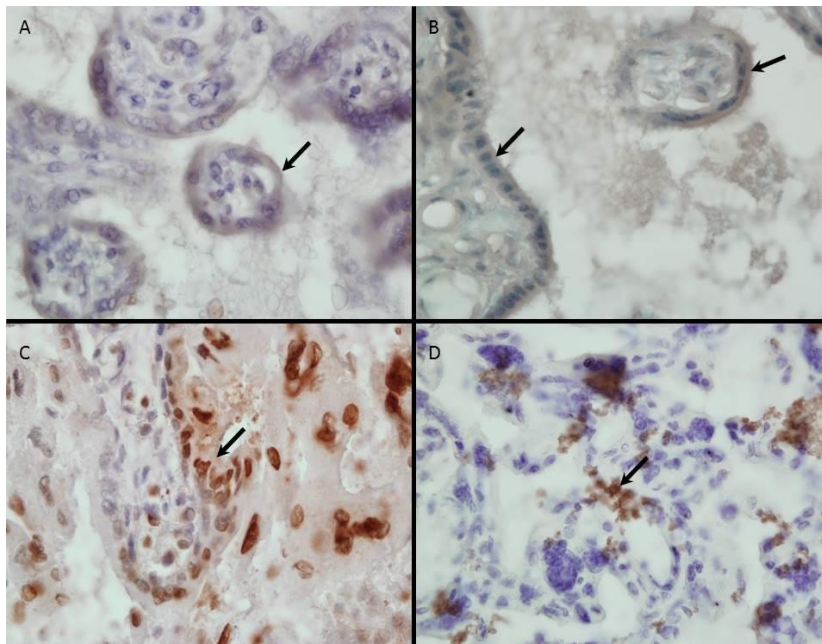
Abstract 108 Figure 3 A-D Higher magnification (100x) and localization of (P)RR. (A) is term human placenta from normal pregnancy, (B) is term human placenta from pregnancy with preeclampsia, (C) is preterm owl monkey placenta (44 days gestation), and (D) is term owl monkey placenta form normal pregnancy. The arrows in all 4 panels point to fetal cells with (P)RR staining are cytotrophoblasts or syncytiotrophoblasts of fetal origin.
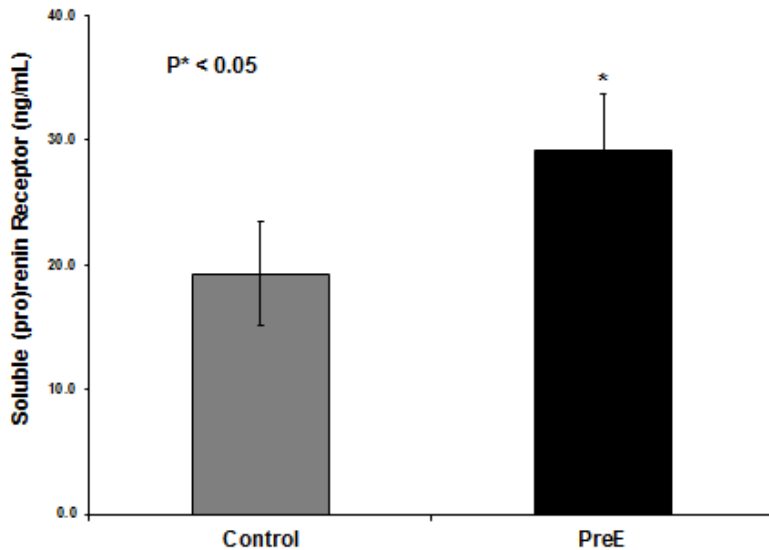
Abstract 108 Figure 4 A. The soluble (P)RR expression was measured in plasma samples from both NP and preE patients by a commercially available kit. The subjects were: NP (n=40) and preE pregnant (n=30). The soluble (P)RR was significantly higher in preE human patients compared to normal (p<0.05). The results presented are mean +/- SE.
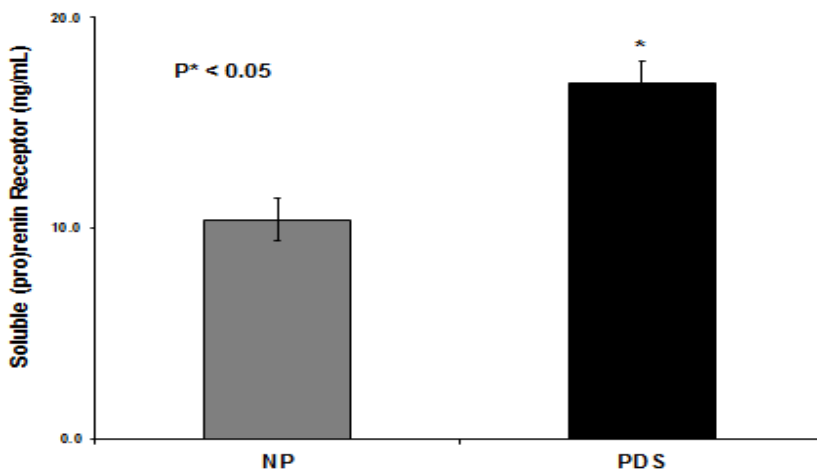
Figure 4 B. The soluble (P)RR expression was measured in plasma samples from both NP and preE rats by a commercially available kit. The animals were: NP (n=10) and pregnant+desocorticosterone acetate +saline (preE) (n=10). The soluble (P)RR was significantly higher in preE rats compared to NP (p<0.05).

Pediatrics

109

CHEMOKINE CHANGES DURING PREECLAMPTIC PREGNANCY AND ITS EFFECTS ON FETOPLACENTAL STRESS

Sara Mohamed, Niraj Vora, Ram R Kalagiri, Waverly B Kundysek, Muppala Raju, Vinayak Govande, Raza Bajwa, Madhava Beeram, Mohammad N Uddin. *Baylor Scott White McLane Children's Medical Center*

Introduction/Background Preeclampsia (PreE) is the de novo development of hypertension and proteinuria after 20 weeks of gestation and has a link to alterations of feto-placental stress that pass to the offspring causing detrimental effects.
Objective(s) To evaluate clinical outcomes and chemokines from maternal and cord blood in women with and without PreE.
Methods Ten normal (NP) and Ten PreE pregnancies who delivered an infant at Scott & White Memorial hospital from November 2015 to November 2016 were recruited in a prospective cohort study. Serum levels of six chemokines in maternal-fetal paired samples were measured using commercially available ELISA. The markers are: Human CCL4/MIP-1beta, Human CXCL10/IP-10, Eotaxin/CCL11, RANTES (CCL5), Human MCP1, Human M-CSF. Chi square and paired t-tests were used to compare PreE patients to those with NP.

Abstract 109 Table 1 Pregnancy characteristics (means with SD or proportions) of 10 subjects with pre-eclampsia and 10 subjects with normal pregnancies
Note that as expected women with preE had high blood pressures, shorter gestations, and smaller babies. However, in this cohort the women were of similar age, size, and parity prior to pregnancy.

Characteristic	Pre-eclampsia pregnancies (n=10)	Normal pregnancies (n=10)	P-values for comparison
Age in years	27.6 (5.4)	29.4 (3.7)	0.40A
Weight in pounds	244 (74)	212 (30)	0.36B
Height in inches	64 (3)	63 (2)	0.64A
BMI in kg/m^2	41.8 (10.8)	36.8 (4.2)	0.09B
Number previous pregnancies	1.4 (1.3)	1.8 (1.3)	0.51A
Gestational age at preE diagnosis in weeks	33.9 (5.9)	-	-
Gestational age at delivery in weeks	35.1 (3.8)	39.2 (0.3)	< 0.001B
Highest systolic blood pressure in mmHg	162 (17)	121(3)	< 0.001A
Highest diastolic blood pressure in mmHg	97 (12)	75 (9)	< 0.001A
Birth weight in grams	2556 (977)	3385 (328)	0.011B
Baby length in cm	45 (5)	48 (3)	0.03A
Head circumference in cm	32 (4)	35 (1)	0.015B
PI in kg/cm^3	2.63 (0.39)	3.05 (0.37)	0.025A

Abstract 109 Table 2 Paired analysis of maternal-fetal pairs for markers (means with SD) Note for each of the marker's fetuses had values greater than maternal which might be expected if placental cells are the source.

Variable	Pre-eclampsia pregnancies (n=10)		Normal pregnancies (n=10)		p-value for PreE pairs	p-value for normal pairs
	Maternal	Fetal	Maternal	Fetal		
Human CCL4/MIP-1beta (ng/mL)	566 (93)	730 (105)	258 (48)	346 (74)	< 0.001A	< 0.001A
Human CXCL10/IP-10 (pg/mL)	725 (133)	1024 (124)	276 (79)	440 (77)	< 0.001A	< 0.001A
Eotaxin/CCL11 (pg/mL)	120 (13)	233 (34)	48 (8)	101 (13)	< 0.001A	< 0.001A
RANTES (CCL5) (pg/mL)	9856 (1527)	11,390 (1621)	7653 (618)	7486 (2283)	< 0.001A	< 0.001A
Human MCP1 (pg/mL)	202 (45)	275 (63)	80 (15)	132 (28)	< 0.001A	< 0.001A
Human M-CSF (pg/mL)	1862 (188)	2295 (229)	992 (149)	1318 (85)	< 0.001A	< 0.001A

Results Maternal systolic and diastolic blood pressure and maternal BMI were significantly higher in PreE women compared to NP. Infant gestational age and birth weight at delivery were lower in PreE compared to NP indicating a link to intrauterine growth restriction (IUGR). Maternal and fetal cord serum of six chemokines levels in mothers and their offspring differed in those with and without PreE (p< 0.001). A significant difference was detected between the maternal and fetal levels for the six chemokines (p< 0.01).

Conclusion PreE increases the risk of fetal preterm deliveries and fetal IUGR. All six chemokines had significantly higher values in neonates compared to their mothers, which identifies the placental cell as the source, therefore, affirming the link between PreE and the altered intrauterine environment.

110

TRANSCRIPTOME BASED DRUG REPURPOSING IN GROUP 3 MEDULLOBLASTOMA

[1]David Doss, [2]Ranjana Kanchan, [2]Naveenkumar Perumal, [2]Surinder Batra, [3]Sidharth Mahapatra.
[1]*Creighton University;* [2]*University of Nebraska Medical Center;* [3]*Children's Hospital and Medical Center*

Introduction/Background Medulloblastoma (MB) is the most common malignant brain tumor of childhood, accounting for 20% of pediatric brain tumors. With the advent of high throughput sequencing, international consensus has identified four molecular subgroups of MB: WNT, SHH, group 3 (G3), and group 4 (G4). Each subgroup is characterized by unique methylomic and transcriptomic signatures, cytogenetic aberrations, histology, and prognosis. Mainstay of therapy consists of surgical resection followed by craniospinal irradiation (CSI) and chemotherapy. Based primarily on clinical features, treatment regimens fail to capitalize on unique subgroup-specific molecular signatures. However, subgroup-specific prognoses vary widely, from >95% five-year survival in WNT MB to < 50% five-year survival in G3MB. As such, there is a great need to address these outcome disparities, specifically in G3MB, with more selective therapies.

Objective(s) We aimed to identify FDA-approved compounds that may be repurposed to effectively target G3MB by comparing patient-derived G3MB transcriptomes against drug signature databases.

Methods Differential expression analysis was performed using two cohorts of RNA-seq data: a local cohort of pediatric MB samples and an external validation cohort. These data were analyzed against the LINCS database, which has gene expression data for various cancer cell lines treated with >42,000 compounds. Our analysis identified putative drug candidates with a potential to reverse the G3MB gene signature to a more normal cerebellar state. These compounds were further filtered to identify only FDA-approved drugs (using the DrugBank database) that were blood-brain permeable (using Lipinski's Rules of 5). Functional assays were then used to quantify each drug's anti-neoplastic impact in a classic group 3 MB cell line, HDMB03. Effects on cytotoxicity, clonogenicity, wound healing, cell cycle progression, and apoptosis were recorded in vitro. Finally, RNA sequencing was performed on treated cells to identify differentially expressed genes and cancer-associated molecular pathways that were inhibited by drug treatments.

Results 81 candidates passed filtering thresholds to qualify for further testing. 13 were selected for in vitro testing based on good safety profiles in pediatric patients. We measured the IC50 of these compounds via an MTT assay in HDMB03 cells and identified three classes of drugs with effective cytotoxicity: selective serotonin reuptake inhibitors (SSRIs), tricyclic antidepressants (TCAs), and statins. Specifically, these compounds included fluoxetine (48h IC50 ~11uM), sertraline (48h IC50 ~7uM), nortriptyline (48h IC50 ~7uM), and simvastatin (48h IC50 ~8uM). With each compound of interest, we observed a clear inhibitory effect on wound healing and clonogenicity in HDMB03 cells. Each compound also induced a dose-dependent increase in apoptosis by flow cytometry. Western blotting confirmed dose- and time-dependent increases in apoptotic markers, including cleaved caspases 3 and 9, cleaved PARP, and Bcl-2. NT-treated HDMB03 cells underwent RNA sequencing and revealed a significant inhibitory effect on the E2F pathway, which is purported to play a key role in cancer cell proliferation. Notably, five of the six E2F transcription factors as well as a panel of E2F target genes (HN1, KIF4A, CDC3A, CDCA8, and SSRP1) are specifically enriched in G3MB tumors.

Conclusion In all, we have successfully identified compounds that are actively cytotoxic against G3MB in vitro using our in silico drug discovery pipeline. Their anti-neoplastic effects have been corroborated in other cancers. Our pipeline can serve as a relatively accessible method to identify repurposable FDA-approved candidates against high-risk tumors, like G3MB.

111

AN EVALUATION OF OUTPATIENT PEDIATRIC ASTHMA PRESCRIBING PATTERNS IN THE UNITED STATES

Noopur Walia, *Rosalind Franklin University*

Introduction/Background Pediatric asthma is often underdiagnosed and under-treated, resulting in a lack of concentration, difficulty sleeping, and tiredness. The GINA guidelines recommended that children should be prescribed maintenance inhalers along with rescue inhalers. If both were prescribed concurrently, it was considered appropriate, otherwise deemed inappropriate for this study. The global prevalence, morbidity and mortality of childhood asthma has increased significantly over the last 40 years with inappropriate prescribing of inhalers as one of the major contributing factors.

Objective(s) The aim of the study was to determine the prevalence of inappropriate prescribing patterns against various patient and prescriber demographic factors.

Methods A total of 2,264 patients meeting the inclusion criteria for ICD 10 codes, J45.20 - J45.52, and age less than 18 were extracted from the 2018 National Ambulatory Medical Care (NAMCS) survey, which captures ambulatory services offered in physicians' offices directly engaged in patient care. This data is collected by the National Center of Health Statistics (NCHS), a division of the CDC. The data was checked for integrity and exported into the Statistical Package for Social Sciences software (SPSS®). The data were analyzed using descriptive analysis, two-tailed t-tests, and ANOVA with an alpha significance level of 0.05.

Results The majority of the pediatric patient population was in the age range of 17-18 years old with the next highest majority being the 13–16-year-old range. The majority of the pediatric patient population was of the white race (44.2%) and majority of the patients were male (55.4%). Patient's saw family practice physicians the most (34.5%) followed by nurse practitioners next (23.5%). There was a significant percentage of inappropriate prescribing in the south (48.6%). Overall, more patients were prescribed inappropriately (68.3%) as compared to appropriate prescribing (31.7%). There was a significant difference among different types of patient payments with regard to appropriate prescribing. Inappropriate prescribing was seen more for patients with Medicaid (24.8%) and self-payment (38.2%) as compared to other types of payment (p= 0.052). There was a significant difference among various prescribers in terms of appropriateness of prescribing. General practice/ family physicians (35.1%) and nurse practitioners (20.9%) prescribed more inappropriately as compared to other prescribers. (p= 0.001). Patients from the Southern region of the U.S. were prescribed more inappropriately compared to the other regions in the U.S. (p= 0.205).

Conclusion This study concluded that a significant number of pediatric asthma patients across all demographics were not appropriately prescribed inhalers, thus not following GINA guidelines indicating the necessity for proactive interventions by prescribers and policymakers. The primary care prescribers appear to prescribe more inappropriately as compared to other prescriber groups. Efforts should be made to promote appropriate prescribing amongst this group. Patients from the southern region of the US were prescribed more inappropriately, which could be due to socioeconomic disparities. Appropriate prescribing and adhering to guidelines would prevent morbidity, mortality and improve the patient's quality of life, thereby saving healthcare costs.

112

NEONATAL HYPOGLYCEMIA IS NOT ASSOCIATED WITH NEURODEVELOPMENTAL DELAY IN CHILDREN UP TO 2 YEARS OF AGE

Manisha Singh, Vinayak Govande, Martha Hemingway, Muppala Raju, Mohammad Uddin, Niraj Vora.
Baylor Scott and White

Introduction/Background Neonatal hypoglycemia is linked to poor neurological outcomes. In newborns with hypoglycemia, long-term neurologic consequences, such as epilepsy and cognitive impairments, have been documented. There is currently no agreement among doctors as to what constitutes neonatal hypoglycemia, what the treatment threshold should be, or how long low blood sugar levels are safe for infants.

Objective(s) To determine if hypoglycemia is associated with neurodevelopmental outcomes in neonates.

Methods Retrospective matched cohort analysis of neonates admitted to the Baylor Scott & White neonatal intensive care unit between January 2014 and December 2016. Infants who were born ≥ 32 weeks gestation were included, if they had a diagnosis of hypoglycemia—defined as blood glucose below 40 mg/dl. Based on gestational age, birthweight, sex, and year of birth, controls were matched. Major congenital anomalies, births outside of hospitals, readmissions after birth, and infants who died before age 2 yrs were excluded. Data from the clinical charts, laboratory values, and demographic variables were examined. As available, follow-up data were gathered starting at 2 to 3 years of age. The main findings were the identification of developmental delay in children using ICD-9 and ICD-10 codes. The preschool language scale-5 was used to objectively quantify speech delay. Logistic regression was used to determine the effect of hypoglycemia on developmental outcomes.

Results 404 infants met inclusion criteria. Median birthweight was 2.76 kg (range, 1.52-4.79) and median gestational age was 36.2 weeks (range, 32.0-41.2) in the hypoglycemia group. Infants with hypoglycemia had longer length of stay (8 days vs. 6 days, p=0.06). Of those infants with hypoglycemia, 15% were small for gestational age and 31% born to mothers with diabetes during pregnancy. The median blood glucose at 12 hours of life was 29 mg/dl (range, 10-70) (p< 0.0001) and at 48 hrs. of life was 57 mg/dl vs 68 mg/dl (p< 0.0001) in the non-hypoglycemia group. In logistic regression, infants with hypoglycemia were more likely to be diagnosed with neurodevelopmental delays in childhood but were not statistically significant compared to those without hypoglycemia.

Conclusion Late preterm and term neonates diagnosed with neonatal hypoglycemia are at a higher risk of being diagnosed with a developmental delay 2-3 years of age compared to neonates without hypoglycemia.

113

INDUCING IRON IMBALANCE BY TARGETING THE ABCB7/GPX4 AXIS ACCELERATES FERROPTOSIS IN MEDULLOBLASTOMA

[1]Ranjana Kanchan, [1]Surindra Batra, [1]Ramakanth Chirravuri, [2]David Doss, [1]Jyoti Kaushal, [1]Parvez Khan, [1]Sidharth Mahapatra, [1]Mohd Wasim Nasser, [3]Naveenkumar Perumal, [1]Jawed Siddiqui, [1]Ishwor Thapa, [1]Raghupathy Vengoji. [1]*University of Nebraska Medical Center;* [2]*Creighton University;* [3]*Vellore Institute of Technology*

Introduction/Background Medulloblastoma (MB), the most common malignant pediatric brain tumor and a leading cause of childhood mortality, is stratified into four primary subgroups, i.e. WNT (wingless), SHH (sonic hedgehog), group 3, and group 4, the latter two representing high-risk MB. Improvements in targeted therapies for WNT and SHH MB have improved overall survival, while chemotherapy toxicity limits effective treatment of high-risk tumors, fueling recurrence and mortality rates. Deletions within chromosomal locus 17p13.3, which houses multiple tumor suppressor genes including miR-1253, characterize high-risk tumors. Leveraging the tumor-suppressive properties of miRNAs as adjuncts to chemotherapy may provide a promising alternative to current therapeutic strategies.

Objective(s) Group 3 tumors enrich iron transport genes to satisfy their high proliferative need. MiR-1253 targets iron transport by inhibiting the mitochondrial Fe-S transporter, ABCB7. Iron imbalance can lead to cell death by ferroptosis, characterized by iron overload leading to oxidative stress and inducing lipid peroxidation. This study elucidated the impact of targeting ABCB7 on cisplatin cytotoxicity in group 3 MB and whether these effects were mediated by ferroptosis.

Methods Bioinformatics analyses were first utilized to identify deregulated oncoproteins that were targets of miR-1253 in group 3 MB, identifying the mitochondrial iron-sulfer transporter ABCB7. Dual luciferase reporter assay and Western blotting confirmed direct binding of miR-1253 to ABCB7. The effect of miR-1253 overexpression (miR-1253OE) or ABCB7 knockout (ABCB7KO) on cellular and mitochondrial iron levels, oxidative stress, lipid peroxidation, and glutathione levels was studied via confocal microscopy, immunostaining, and Western blotting. The effect of miR-1253OE and ABCB7KO on cancer cell survival and proliferation was assessed via FACS, clonogenicity, and medullosphere assays. Impact of ABCB7 repression on cancer cell capacity for glycolysis and oxidative phosphorylation was assessed by Seahorse assays. ABCB7 inhibition on cisplatin cytotoxicity was assessed with and without a ferroptosis inhibitor, ferrostatin-1. Ultimately, an orthotopic mouse model was generated to illustrate that cisplatin cytotoxicity can be potentiated in group 3 tumors by repressing ABCB7.
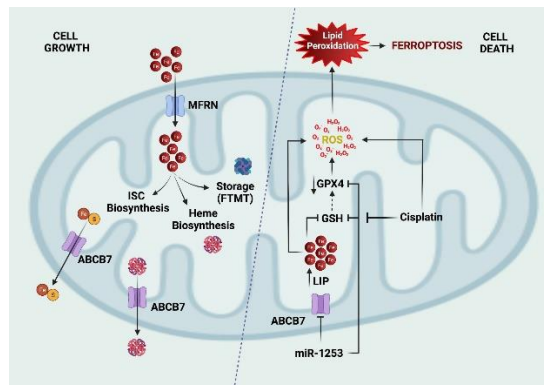
Abstract 113 Figure 1: Schematic representation of miR-1253-induced ferroptosis.

Results In silico and in vitro analyses revealed specific enrichment of ABCB7 and GPX4, a critical regulator of ferroptosis, in group 3 MB cell lines and tumors. Restoration of miR-1253 resulted in downregulation of both ABCB7 and GPX4, concurrently increasing mitochondrial and cytoplasmic iron pools and, in turn, mitochondrial oxidative stress and lipid peroxidation, leading to cell death and abrogation of medullosphere formation; ABCB7 knockdown recapitulated these effects but also abrogated GPX4 expression. Fractionation studies confirmed that miR-1253OE or ABCB7KO led to downregulation of GPX4 in the cytosol and mitochondria. Seahorse studies showed that the bulk of ATP generation was occurring in the cytoplasm by glycolysis and not oxidative phosphorylation, suggesting mitochondrial toxicity with ABCB7 inhibition. Cisplatin, a chemotherapeutic agent used in group 3 MB treatment, induces cell death by DNA crosslinking; it has also been shown to reduce GPX4 levels and lead to ferroptosis. In miR-1253OE cancer cells, cisplatin IC50 was reduced 2-fold. Resultantly, in miR-1253OE or ABCB7KO group 3 cells, concurrent treatment with cisplatin augmented oxidative stress and lipid peroxidation, depleted glutathione stores, and culminated in a higher index of ferroptosis. In a mouse model of group 3 tumors, ABCB7KO dramatically prolonged survival and potentiated cisplatin effects.

Conclusion The current study illustrates how targeting iron transport by a tumor suppressive miRNA can augment ferroptosis to potentiate cisplatin in group 3 MB tumors. For better understanding we have summarized the study through graphical representation in Figure1.

PUTATIVE B7-H3 INHIBITORS MITIGATE GROUP 3 MEDULLOBLASTOMA AGGRESSIVENESS

Prakadeeswari Gopala Krishnan, Prachi Agrawal, Hamdan Alrefaei, Yashpal Chhonker, David Doss, Ranjana Kanchan, Sidharth Mahapatra, DJ Murry, Paul Trippier. *University of Nebraska Medical Center*

Introduction/Background Medulloblastoma (MB) is a primary childhood malignancy of the central nervous system (CNS). Clinically heterogeneous, MBs are sub-grouped into four molecular subgroups, i.e., Wingless (WNT), Sonic Hedgehog (SHH), Group 3, and Group 4. Among all, Group 3 MBs (G3MB) are known to be the most aggressive form, with less than 50% five-year survival. G3MBs are associated with large cell/anaplastic (LCA) histology, a distinctive methylation profile, amplification of c-MYC, and isochromosome 17q (i17q). Targeting these high-risk molecular features unique to G3MB has been challenging, necessitating alternative approaches to therapy for G3MB. One innovative approach is targeting immune checkpoint molecules involved in tumor evasion. B7 homolog 3 (B7-H3/CD276) is an example of an immunosuppressive checkpoint protein and member of the B7 superfamily that is significantly enriched in G3MB. The enhanced expression of B7-H3/CD276 has been associated with an elevated aggressive and metastatic potential for G3MB. B7-H3/CD276 is also a primary target of miR-1253, a novel tumor suppressor gene silenced in G3MB.

Objective(s) Our primary goal is to target B7-H3/CD276 by using potential B7-H3 inhibitors with the dual ability to reinstate immune activation within the tumor suppressive microenvironment and to target aggressiveness of G3MB.

Methods Homology modelling was used to virtually screen 100,000 diverse compounds to rank potential B7-H3 small-molecule inhibitors based on binding score and brain penetration. We used B7-H3 inhibitors Ni1 and Ni4, which were resynthesized and confirmed for their structure and purity. In vitro cytotoxicity of these inhibitors against G3MB HDMB03 cells was determined by MTT assay. Effects of these inhibitors on proliferation was determined by a colony formation assay. Wound healing assay was performed to understand the anti-migratory potential of these inhibitors in the same cell line. A rapid, selective, and sensitive LC-MS/MS method was developed and validated for the quantitation of Ni1 in mouse plasma. The validated method was successfully applied to assess the solubility, in vitro metabolism, in vivo pharmacokinetics (PK) and bio-distribution of Ni1. Following an intraperitoneal dose of 10 mg/kg in healthy mice, maximum concentration, time to achieve maximum concentration, elimination half-life, and clearance were estimated.

Results Potential B7-H3 inhibitors Ni1 and Ni4 exhibited strong binding scores, CNS penetrance, and oral bioavailability. In vitro, both compounds had appreciably low IC50 values of 3 µM (Ni1) and 0.75 µM (Ni4). Further, both compounds inhibited wound healing and colony formation. Ni1 shifted the thermostability of B7-H3 by approximately 2.5 degrees, suggesting in vitro binding. After PK/PD and MTD studies, Ni1 showed stability in plasma, good blood-brain barrier permeability, and a half-life of 8 hours. We are now elucidating B7-H3-activated downstream signaling through JAK2/STAT3 signaling and testing the in vivo efficacy for Ni1 against G3MB tumors in a murine model.

Conclusion This study has provided 2 potential inhibitors of B7-H3, which may hold promise as targeted therapies to mitigate the aggressiveness of G3MB tumors. Inhibition of B7-H3 with small molecule inhibitors may be translated into viable immunotherapy for high-risk patients.

Pulmonary / Critical Care

115

YAP1 DEFICIENCY PROTECTS HYPOXIA-MEDIATED PULMONARY HYPERTENSION IN MICE

[1]Ali Imran Sarwar, [2]Maricela Castellon, [2]Jiwang Chen, [3]Dustin Fraidenburg, [2]Longshuang Huang, [2]Ayman Isbatan, [4]Roberto Machado, [2]Viswanathan Natarajan. [1]*Cardiovascular Research Core;* [2]*University of Illinois at Chicago;* [3]*UI Health;* [4]*Indian University Health*

Introduction/Background Pulmonary hypertension(PH) is a chronic vascular disease characterized by pulmonary vasoconstriction and pulmonary arterial remodeling (PVR). PVR is mainly due to the uncontrolled pulmonary artery smooth muscle cell proliferation. It is known that activation of YAP1 (an oncogene) promotes cell proliferation and inhibits apoptosis.
Objective(s) We examined whether inhibiting the YAP1 gene expression protect from experimental PH.
Methods We employed genetic and pharmaceutical approaches to silence YAP1 gene expression. We generated endothelial cell-specific YAP1 conditional knockout (YAP1 ECKO) mice. 8-week-old YAP1 ECKO and their wild-type (WT) mice were exposed to hypoxia (10% O2) for 4 weeks. A Millar catheter was used to measure right ventricular systolic pressure (RVSP) and Fulton Index (RV/[LV+S]), Aperio Imaging system was employed to measure pulmonary artery (PA) wall thickness.For the pharmaceutical approach, verteporfin (a YAP1 specific inhibitor) was administrated (4.5 mg/kg bw, IP, every other day for 2 weeks) in male C57Bl6 WT mice after 2-week hypoxia exposure (10% O2).
Results We showed that there is no difference in RVSP, Fulton Index, PA wall thickness, TAPSE, and PAT/PET ratio between YAP1 ECKO and their WT mice under normoxia conditions. After 4-week hypoxia exposure (10% O2), YAP1 ECKO mice had significantly lower RVSP, Fulton Index and PA wall thickness compared to their WT siblings. The standard of error was calculated to be less than 5% for RVSP, RVH and PA wall thickness (±3%, ±4.26% and ±2.96%, respectively).
Conclusion Our data showed that the therapy with verteporfin significantly attenuated hypoxia mediated PH in mice. We conclude that YAP1 inhibition may have therapeutical benefit for patients with PH.

116

AUGMENTATION OF KINDLIN-2 EXPRESSION ATTENUATES ENDOTHELIAL CELL PERMEABILITY AND MURINE ACUTE LUNG INJURY

[1]Weiguo Chen, [2]Anne Cress, [1]Yulia Epshtein, [1]Jeffrey Jacobson. [1]*University of Illinois at Chicago;* [2]*University of Arizona*

Introduction/Background We previously reported lung endothelial cell (EC) inflammation attenuated by simvastatin, an HMG CoA-reductase inhibitor, is mediated by integrin β4 (ITGB4). The unique cytoplasmic domain of ITGB4 contains amino acid sequences that would be predicted to bind integrin adapters of the kindlin-2 family. Further, kindlin-2 expression is mediated by SMURF1 (Smad ubiquitination regulatory factor-1), an E3 ubiquitin ligase that promotes kindlin-2 ubiquitination and degradation.

Objective(s) we hypothesized that increased kindlin-2 expression via the inhibition of SMURF1 mediates ITGB4 and EC inflammatory responses relevant to acute lung injury (ALI).

Methods To investigate the role of kindlin-2 in EC ITGB4 expression and barrier regulation human pulmonary artery ECs were treated with simvastatin (5 μM, 16 h) prior to immunoprecipitation of kindlin-2 and Western blotting for ITGB4. In separate assays of EC barrier function, kindlin-2 was silenced (siRNA) in EC prior to thrombin treatment (1 U/ml) and measurements of transendothelial resistance (TER) and FITC-dextran transwell monolayer flux. Next, ECs were treated with a SMURF1 inhibitor, A01, followed by Western blotting to confirm decreased kindlin-2 expression. ECs were then treated with A01 prior to repeating assessments of EC barrier function in response to thrombin as measured by both TER and FITC-dextran flux. Finally, to study the effects of SMURF1 inhibition in ALI in vivo, mice were pretreated with A01 (0.1 mg/kg, intraperitoneal injection) or vehicle for 48 h prior to repeating treatments of the same, with LPS (1.25 mg/kg) given by intratracheal administration 1 h later. At 24 h, bronchoalveolar lavage (BAL) fluid was collected to measure protein, cell counts, and cytokines (IL-6 and KC) with lungs harvested for histology.

Results These experiments confirmed increased ITGB4:kindlin-2 association induced by simvastatin while silencing of kindlin-2 was associated with a significant increase in thrombin-induced EC barrier disruption. Further, treatment with A01 resulted in increased EC kindlin-2 expression as well as a decrease in thrombin-induced EC barrier disruption. Finally, A01 treatment was associated with a significant attenuation of LPS-induced murine ALI.

Conclusion Our data support the idea that kindlin-2 via effects on ITGB4 is an important mediator of EC inflammatory responses relevant to ALI. Moreover, inhibition of SMURF1 augments EC kindlin-2 expression and is associated with an attenuation of EC barrier disruption in vitro and ALI in vivo. Our findings suggest targeting kindlin-2 may serve as a novel and effective therapeutic strategy in ALI and other syndromes characterized by increased lung vascular permeability.

117

UCHL1, A DEUBIQUITINATING ENZYME, AUGMENTS ENDOTHELIAL CELL BARRIER FUNCTION IN RADIATION- INDUCED LUNG INJURY

Yulia Epshtein, Weiguo Chen, Jeffrey Jacobson. *UIC*

Introduction/Background Radiation-induced lung injury (RILI) is a common complication in patients administered thoracic radiotherapy that is characterized by increased lung endothelial cell (EC) inflammation and permeability and is associated with significant morbidity and mortality. Although the molecular etiology is poorly understood, we previously identified dysregulation of sphingolipids as an important mediator of RILI in a murine model and confirmed radiation-induced increases in lung expression of sphingosine kinase (SphK) isoforms 1 and 2. Moreover, mice with a targeted deletion of SphK1 (SphK1-/-) exhibited marked RILI susceptibility and we confirmed significant RILI protection conferred by the sphingosine-1 phosphate (S1P) analog, (S)-FTY720-phosphonate (Tysiponate, Tys). Separately, we have also identified differential RILI responses mediated by the deubiquitinating enzyme, UCHL1 (ubiquitin carboxyl terminal esterase L1) and we have confirmed SphK1 ubiquitination is regulated by UCHL1.

Objective(s) Thus, we hypothesized that UCHL1, via effects on SphK1, mediates lung EC barrier function relevant to RILI.

Methods In initial studies, human pulmonary artery EC were subjected to radiation (10 or 20 Gy, 4 or 24 h) prior to Western blotting for UCHL1 and SphK1. To study the role of UCHL1 in EC barrier function after radiation, UCHL1-silenced EC and control cells were irradiated and transendothelial barrier resistance (TER) measured in response to the barrier augmenting and barrier disrupting agonists, Tys (1 M) and thrombin (1 U/ml), respectively. Next, EC were treated with LDN-57444L (LDN), an inhibitor of UCHL1, prior to treatment with either Tys or thrombin and measurements of TER. Finally, a UCHL1 potentiator, C19H28N2O5S, was used to augment UCHL1 activity in EC prior to treatment with S1P followed by measurements of TER and FITC-dextran transwell monolayer flux.

Results These experiments confirmed dose- and time-dependent increases in EC UCHL1 and SphK1 expression after radiation. In irradiated EC, barrier enhancement by Tys was reduced in UCHL1-silenced cells while barrier disruption by thrombin was augmented. In addition, inhibition of UCHL1 was associated with decreased barrier enhancement by S1P and increased barrier disruption by thrombin. Treatment with a UCHL1 potentiator demonstrated the opposite effect with augmented barrier enhancement after S1P.

Conclusion Collectively, our results yield new insights into mechanisms of sphingolipid signaling induced by radiation and support lung vascular-protective effects mediated by UCHL1. These findings may ultimately identify effective modulators of EC radiation responses that could also serve as effective therapeutic targets for RILI.

118

INCREASED RISK OF POST-LIVER TRANSPLANT PULMONARY COMPLICATIONS IN PATIENTS WITH ABNORMAL NON-INVASIVE HEMODYNAMICS, EVEN WITHOUT SIGNIFICANT PULMONARY HYPERTENSION

Anne Osuji, Dustin Fraidenburg. *University of Illinois at Chicago*

Introduction/Background Portopulmonary hypertension (PoPH) as a complication of liver cirrhosis is a significant risk factor for perioperative complications and mortality with liver transplant, particularly in patients with moderate to severe disease, and screening is an important part of the pre-transplant evaluation. Right heart catheterization (RHC) is used to diagnose PoPH when the echocardiogram is significantly abnormal, yet it is unclear if non-invasive hemodynamic measurements are sufficient to identify risk factors for complications and poor outcomes of liver transplant in patients both with and without confirmed PoPH.

Objective(s) To associate non-invasive and invasive hemodynamic findings with post-operative outcomes, specifically pulmonary complications, among patients who received an orthotopic liver transplant (OLT) at University of Illinois Health.

Methods We conducted a retrospective study of patients who underwent OLT at UI Health between January 1, 2019 to July 31, 2022. Adult patients with pre-OLT echocardiographic data were included in the study. Primary outcomes were pulmonary complications, including but not limited to pneumonia, pleural effusion, atelectasis and prolonged postoperative ventilation. Demographic and clinical characteristics were also collected. Statistical testing included t-test, ANOVA, and Spearman correlation where appropriate.

Results 106 patients met inclusion criteria with a median age of 54 years old and 43% were women. Pulmonary complications occurred in 53% of patients while 49% were readmitted to the hospital during the study period and overall mortality was 11%. When stratified into three groups, pre-transplant echocardiogram showing tricuspid regurgitant velocity (TRV) of 2.8 m/s; the incidence of postoperative pulmonary complications were 48%, 44%, and 87%, respectively (p 3 Wood units. There was a trend toward increased pulmonary complications with right atrial pressure > 8 mm Hg (44% vs 78%), mean pulmonary artery pressure ≥ 25 mm Hg (33% vs 75%), or PA wedge pressure ≥ 15 mm Hg (46% vs 86%). There was also a significant correlation between decreasing cardiac output associated with increasing risk of post-transplant pulmonary complications (p < 0.05).

Conclusion Elevated TRV and decreasing cardiac output were associated with increased pulmonary complications post-liver transplantation even in the absence of significant pulmonary hypertension on RHC. Expanding our current dataset and a comprehensive evaluation of echocardiographic parameters in this population will strengthen the clinical utility of this testing for risk assessment prior to liver transplantation.

119

MURINE MODEL OF PHENYLHYDRAZINE-INDUCED CHRONIC HEMOLYSIS COMBINED WITH HYPOXIA LEADS TO DEVELOPMENT OF SEVERE PULMONARY HYPERTENSION

Janae Gonzales, Jiwang Chen, Weiguo Chen, Yulia Epshtein, Dustin Fraidenburg, Cat Humpal. *University of Illinois at Chicago*

Introduction/Background Pulmonary hypertension (PH) is a severe complication of sickle cell disease associated with high morbidity and early mortality. The pathogenesis remains incompletely understood and PH specific therapies have limited supportive evidence. We previously implicated the in vitro toxicity of extracellular hemoglobin on the pulmonary artery endothelium as a contributing mechanism for the vascular remodeling seen in PH related to chronic hemolytic states.

Objective(s) We sought to support our findings with an in vivo model, and hypothesize that a murine model of chronic hemolysis will show development of PH.

Methods C57BL/6J mice were treated with 40 mg/kg of phenylhydrazine (PHZ), a toxin known to induce hemolysis, or saline control, twice a week for three weeks in normoxia. An additional group of mice were exposed to hypoxia (10% 02 in a ventilated chamber) for four weeks and concurrently received PHZ 40 mg/kg or saline, twice a week for the latter two weeks of hypoxia exposure. Blood and lung tissues were utilized for experiments. Hemodynamic pressure assessments evaluated right ventricular systolic pressure (RVSP) as well as measurements of RV hypertrophy.

Results PHZ-normoxia treatment causes significant anemia (9.1 vs 11.4 g/dL in vehicle mice) with an accentuated difference when combined with hypoxia (7.1 vs 14.7 g/dL). Plasma cytokine levels were higher after PHZ treatment compared to control in normoxia: IL-6 levels increased 4 fold and KC levels increased 1.5 fold. Whole lung lysates from PHZ-normoxia mice also show an increase in endothelial to mesenchymal transition (EndMT) transcription factors SNAI1 and SLUG. Invasive hemodynamics show a non-significant increase in RVSP and RV hypertrophy, yet PHZ treatment combined with hypoxia mice show a considerable increase in RVSP compared to hypoxia alone (52.8 vs 37.9 mm Hg). Fulton index in PHZ-hypoxia also shows a robust increase (0.42 vs 0.33) compared to hypoxia alone.

Conclusion PHZ-treated mice under normoxic conditions show increased inflammatory cytokines and signs of EndMT in lung tissues, yet there is little evidence for PH at 3 weeks. When combined with hypoxia, PHZ-treated mice show development of severe PH. The pro-inflammatory and EndMT changes likely contribute to the severe PH phenotype observed when this model is combined with hypoxia. These findings support the important role of chronic extracellular hemoglobin exposure in PH pathogenesis. The double hit of PHZ and hypoxia is a novel murine model for PH due to chronic hemolysis and may assist in therapeutic discovery for this devastating complication of sickle cell disease.

120

MRSA INDUCES LUNG ENDOTHELIAL DYSFUNCTION VIA EPIGENETIC MECHANISMS AND CYP1A1 UPREGULATION

Lucille Meliton, Eleftheria Letsiou, Lichun Wang, Steven Dudek. *University of Illinois Chicago*

Introduction/Background Lung endothelial injury is a hallmark of Acute Respiratory Distress Syndrome (ARDS), which is commonly triggered by bacterial infections [e.g. Methicillin-resistant Staphylococcus aureus (MRSA)]. Epigenetic mechanisms, including histone modifications that regulate gene expression, play an important role in endothelial cell (EC) dysfunction and contribute to the pathophysiology of ARDS.

Objective(s) Our studies aimed to 1) investigate histone acetylation modifications in lung EC after stimulation with MRSA, and 2) identify differentially acetylated target genes that are involved in lung EC barrier disruption in ARDS.

Methods For all experiments, we employed human lung microvascular (HLMVEC) or macrovascular (HPAEC) endothelial cells treated with heat-killed MRSA ($2-2.5 \times 10^8$/ml). ChIP-seq analysis was used to evaluate the differential acetylation status of histone 3 at lysine 9 (H3K9ac), a modification associated with upregulation of gene expression. Expression of CYP1A1 (Cytochrome P450 1A1), a top target of MRSA-induced H3K9ac in lung EC, was determined by immunoblotting and qPCR. The role of CYP1A1 in regulating lung EC barrier function was assessed in cells transfected with siRNA prior to MRSA treatment. CYP1A1 expression and EC function were characterized in EC pre-treated with the epigenetic modulators, RVX-208 (BET inhibitor) or C646 (histone acetyltransferase-HAT inhibitor). Endothelial barrier function was assessed by ECIS and measurement of pro-inflammatory markers (IL-6, IL-8, VCAM-1).

Results ChIP-seq analysis revealed 1605 H3K9 acetylation sites that were significantly altered by MRSA, of which 68% were increased after MRSA treatment. H3K9ac is highly correlated with active promoters, and therefore we next analyzed sites located in the promoter proximity region. H3K9ac peaks were annotated to the nearest transcription start site to identify 148 potential genes of interest differentially regulated by MRSA. CYP1A1 was among the most significant of these genes. MRSA increased H3K9ac levels in the CYP1A1 promoter in association with upregulation of CYP1A1 mRNA and protein levels in lung EC. Down-regulation of CYP1A1 expression reduced MRSA-induced EC permeability and IL-6 levels. BET or HAT inhibition suppressed CYP1A1 expression and inflammatory EC markers (cytokines and VCAM-1 expression) induced by MRSA.

Conclusion The main findings of our study are: 1) MRSA causes significant alterations in the histone acetylation status of lung endothelium; 2) CYP1A1, a target of H3K9ac, is upregulated in MRSA-treated lung EC and mediates EC barrier disruption; 3) BET or HAT inhibition reduces CYP1A1 expression and protects against EC pro-inflammatory signaling. These data identify CYP1A1 as an epigenetically-regulated and novel mediator of MRSA-induced injury in lung EC.

121

ENDOTHELIAL SPECIFIC CARMIL1 KNOCKDOWN EXACERBATES IN VIVO LUNG INJURY

[1]Cat Humpal, [1]Patrick Belvitch, [1]Weiguo Chen, [1]Steven Dudek, [2]Joe G.N. Garcia. [1]*University of Illinois at Chicago;* [2]*University of Arizona Tucson*

Introduction/Background The acute respiratory distress syndrome (ARDS) secondary to systemic or lung inflammation causes significant morbidity and mortality. Vascular leak and alveolar flooding are hallmarks of ARDS pathology. Regulation of the pulmonary endothelial barrier by the actin cytoskeleton is an intriguing area of research to identify risk factors and develop therapies for lung injury. Variations in the gene encoding the cytoskeletal regulator capping protein Arp2/3 complex myosin-I linker (CARMIL1) have been implicated in human ARDS outcomes through preservation of platelet count (Wei, et al. AJRCCM 2017 and Wei, et al, CHEST 2015) but also identified differences in CARMIL1 expression. We have previously demonstrated that CARMIL1 is expressed in pulmonary endothelial cells and contributes to barrier regulation.

Objective(s) In the current study we investigate the effects of endothelial specific CARMIL1 silencing in a clinically relevant murine model of inflammatory lung injury.

Methods Control and CARMIL1 siRNA were packaged in ACE-tagged liposomes to specifically target the lung endothelium. Wild-type C57/BL6 mice were injected intravenously with control or siCARMIL1 liposomes and allowed to recover x 48 hours. To induce lung injury animals were intubated and treated with intratracheal lipopolysaccharide (LPS 1.25 mg/kg). After 18 hrs bronchoalveolar lavage (BAL) was performed and lung tissue harvested. BAL cell counts and protein level were determined. Lung tissue was processed for immunohistochemistry (IHC) to assess CARMIL1 expression and histologic analysis. Inflammatory cytokines were measured by ELISA. Soluble VCAM-1 in the BAL was measured by western blot.

Results Animals treated with siCARMIL1 liposomes demonstrate significantly reduced CARMIL1 staining in the endothelium compared to siControl liposomes. Following LPS siCARMIL1 animals had increased septal thickening, neutrophil infiltration and alveolar flooding compared to control. CARMIL1 silencing was associated with an 84% increase in BAL cell count (4.94 +/- 0.69 vs 9.15 +/- 1.83 x10^6) and 35% increase in BAL protein (1.02 +/- 0.05 vs 1.37 +/- 0.17 mg/dl) compared to control. BAL IL-6 level was higher (210.4 +/- 46.7 vs 156.3 +/- 15.5) and endothelial specific soluble VCAM-1 was significantly increased (1.78 fold; $p < 0.05$) in siCARMIL1 vs siControl treated animals.

Conclusion Reduced endothelial CARMIL1 expression exacerbates murine lung injury after LPS. Changes in lung endothelial CARMIL1 may explain its role as a genetic biomarker in ARDS.

122

DISTINCT TRANSCRIPTIONAL PROGRAMS DEFINE IMMUNOTYPE SPECIFIC CD4+ T-CELL SUBTYPES IN SARCOIDOSIS

[1]Christian Ascoli, [1]Yue Huang, [1]Christen Vagts, [1]Dustin Fraidenburg, [1]Seung-jae Kim, [1]Min Joo, [1]Steven Dudek, [1]Nadera Sweiss, [2]Kenneth Oestreich, [1]Gye Young Park. [1]*University of Illinois at Chicago;* [2]*Ohio State University*

Introduction/Background In sarcoidosis, paradoxical peripheral CD4+ T-cell lymphopenia accompanied by exhaustion and anergy are thought to impair immune surveillance and elicit a state of persistent maladaptive inflammatory activity that predisposes to chronic and progressive disease. Our prior transcriptomic analysis of peripheral blood mononuclear cells (PBMCs) utilizing bulk RNA-sequencing suggests that aberrant crosstalk between hyperactive monocytes and CD4+ T-cells results in dysregulated transcriptional programming that may incite the lymphopenic immunotype. We hypothesize that CD4+ T-cell subtypes exhibit unique gene regulatory networks (GRNs) that are associated with decreased cell survival and function in the lymphopenic immunotype.
Objective(s) To characterize specific CD4+ T-cell GRNs and determine biologic pathways associated with the lymphopenic immunotype in sarcoidosis.
Methods Transcriptomic libraries were prepared from PBMCs isolated from subjects with sarcoidosis utilizing the 10X Chromium Single-Cell Gene Expression v3 kit and sequenced on a NovaSeq 6000 S4 lane with 2x150nt reads. Utilizing CellRanger (v.6.0.2), raw reads were demultiplexed and annotated against the Ensembl 104 reference database and sequencing quality was ascertained. Cells with ≤1 or ≥20,000 UMI counts and with ≥20% mitochondrial reads as well as genes present in < 20 cells were filtered out with the Seurat R-package. Gene expression data was SCT normalized, and cell types were predicted using the Monaco reference dataset on the celldex R-package. Then, utilizing the SCORPION, ALPACA, and CRANE R-packages, weighted bipartite GRNs for specific CD4+ T-cell subtypes were constructed, and differential modularity-based scoring and random alteration of network edges were used to determine lymphopenia associated gene modules and individual gene module membership. Finally, to gain insight into lymphopenia associated biologic pathways, gene set enrichment analysis (GSEA) was performed using gene ontology (GO) terms on genes with significant module membership (p-value < 0.05) within modules with ≥100 features utilizing the fgsea R-package.

Results Three male and two female subjects (4 African American and 1 Hispanic) with pulmonary sarcoidosis ranging in age from 26-50 years were included. Three were lymphopenic with absolute lymphocyte counts < 1.25 kcells/μL. A total of 17,430 PBMCs were obtained from all subjects and gene expression of terminal effector memory (TEM) and naïve CD4+ T-cells was explored further given their association with the immune paradox and with cell death markers. TEM cell proportions were comparable between lymphopenic and non-lymphopenic subjects (10.15% vs. 9.87% from 10,295 and 7,135 total PBMCs) whereas the proportion of naïve cells was greater in lymphopenic subjects (17.8% vs 10.69%). GRNs from cell subtypes were found to have differential topology based on immunotype (Figure 1A-B). Specifically, the TEM cell GRN contained 20 lymphopenia associated modules while the naïve cell GRN contained 22. Among these, 7 TEM cell and 4 naïve cell modules had ≥100 genes and GSEA was performed on genes with significant module membership in these modules. Notably, 1 TEM cell and 1 naïve cell module were found significantly enriched with GO terms associated with cell "responses," "differentiation," "proliferation," "cell cycle," and "apoptosis" (Figure 1C-D).

Figure 1.
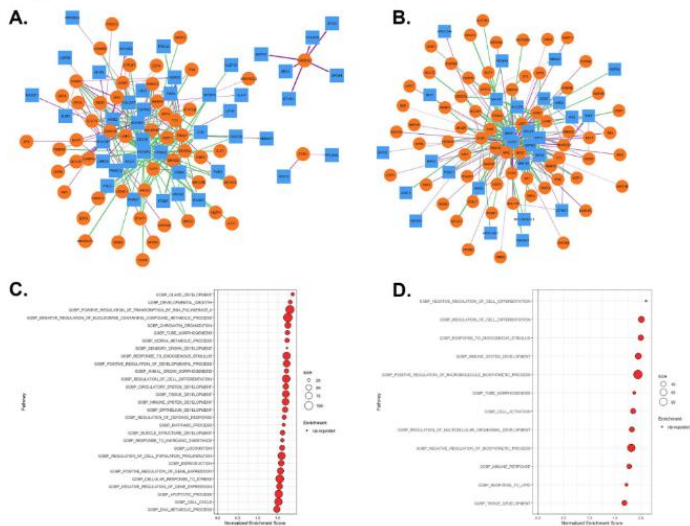
Abstract 122 Figure 1: Gene Regulatory Networks of CD4+ T-Cell Subtypes and Biologic Process Enrichment

Conclusion Within GRNs of specific CD4+ T-cell subtypes we identified distinct gene modules enriched with biologic processes associated with cell function and survival which suggests that inherent dysregulation of cell programs underlies differences between sarcoidosis immunotypes. Further depiction of genes and their interactions within these GRNs is warranted and may reveal novel therapeutic targets capable of mitigating CD4+T-cell dysfunction.

REFERENCE(S)

1. Ascoli C, Schott CA, Huang Y, et al. Altered transcription factor targeting is associated with differential peripheral blood mononuclear cell proportions in sarcoidosis. Front Immunol. 2022;13:848759. Published 2022 Oct 13. doi:10.3389/fimmu.2022.848759

2. Vagts C*, Ascoli C*, Fraidenburg DR, et al. Unsupervised Clustering Reveals Sarcoidosis Phenotypes Marked by a Reduction in Lymphocytes Relate to Increased Inflammatory Activity on 18FDG-PET/CT. Front Med (Lausanne). 2021;8:595077. Published 2021 Feb 24. doi:10.3389/fmed.2021.595077

3. Garman L, Pelikan RC, Rasmussen A, et al. Single Cell Transcriptomics Implicate Novel Monocyte and T Cell Immune Dysregulation in Sarcoidosis. Front Immunol. 2020;11:567342. Published 2020 Dec 8. doi:10.3389/fimmu.2020.567342

4. Hawkins C, Shaginurova G, Shelton DA, et al. Local and Systemic CD4+ T Cell Exhaustion Reverses with Clinical Resolution of Pulmonary Sarcoidosis. J Immunol Res. 2017;2017:3642832. doi:10.1155/2017/3642832

123

RIG-I AGONIST SLR10 PROMOTES MACROPHAGE M1 POLARIZATION DURING INFLUENZA VIRUS INFECTION

[1]Jordan Metcalf, [1]Wei Zhang, [1]Jeremy Alexander, [1]J. Leland Booth, [2]Craig Miller, [1]Chao Xu, [1]Wenxin wu. *[1]University of Oklahoma Health Sciences Center; [2]Oklahoma State University*

Introduction/Background Retinoic-acid-inducible gene I (RIG-I) is a cytosolic pattern recognition receptor (PRR) that recognizes viral nucleic acids and induces innate immune responses. A family of short synthetic, triphosphorylated stem-loop RNAs (SLRs) have been designed to activate the RIG-I pathway and induce a potent interferon (IFN) response, which may have therapeutic potential **Objective(s)** We investigated immune response modulation by SLR10. We addressed whether RIG-I pathway activation with SLR10 leads to protection of nonsmoking (NS) and cigarette smoke (CS)-exposed mice after influenza A virus (IAV) infection.
Methods Mice were given 25 μg of SLR10 1 day before IAV infection. We compared the mortality and host immune responses of NS and CS-exposed mice following challenge with IAV.
Results SLR10 significantly reduced weight loss and improved survival in both NS and CS-exposed mice during IAV infection. SLR10 administration repaired the impaired proinflammatory response in CS-exposed mice without increasing lung injury in NS mice as assessed by physiologic measurements. Although histopathologic scoring of the cardinal features of IAV infection revealed that SLR10 appeared to result in higher overall pathological scores than untreated groups in both NS and CS mice, this change was not enough to increase lung injury by lung weight/body weight. Both qRT-PCR on lung tissues and multiplex immunoassay on bronchoalveolar lavage fluids (BALFs) showed that most IFNs and proinflammatory cytokines were expressed at lower levels in SLR10-treated NS mice than control-treaded NS mice at day 5 post infection (p.i.). As we showed in our prior publications, CS-exposed mice had a suppressed innate cytokine response profile in the lung compared to NS mice during IAV infection. Remarkably, proinflammatory cytokines IL-6, IL-12 and GM-CSF were increased in CS-exposed mice by SLR10 at day 5 p.i. Significantly, SLR10 elevated the ratio of the two chemokines (CXCL9: CCL17) in BALFs, suggesting macrophages were polarized to classically activated (M1) status. In vitro testing also found that SLR10 not only stimulated human alveolar macrophage polarization to an M1 phenotype but also reversed cigarette smoke extract (CSE)-induced M2 to M1 polarization.
Conclusion Our results demonstrate that SLR10 administration in mice is protective in both NS and CS-exposed IAV-infected mice. Mechanistically, SLR10 treatment promoted M1 macrophage polarization in the lung early during influenza infection. The protective effects of administration of SLR10 suggest this may be a promising intervention for infections with viruses, particularly those with CS-enhanced susceptibility to adverse outcomes.

124

NON-CANONICAL AUTOPHAGY BY LYSOSOME-MUCIN GRANULE FUSION REGULATES THE ELIMINATION OF EXCESS MUCIN GRANULES

[1]Erik Sillaste, [2]Katrina Kudrna, [2]Paul Thomes, [2]John Dickinson. [1]*Purdue University; [2]UNMC*

Introduction/Background Introduction: Muco-obstructive airway diseases (e.g., COPD and asthma) are associated with mucous cell metaplasia and mucin hypersecretion, leading to airway obstruction and symptoms such as shortness of breath and cough. How mucous cells regulate excess mucin granules is poorly understood. Previous paradigms suggested that mucous cells only secrete mucin granules to the external airway. However, our recent data indicates that mucin granules can be degraded through the autophagy-lysosomal pathway. In this highly orchestrated process, cells eliminate excess organelles or proteins through double-membraned autophagosomes fusing with lysosomes for degradation by acid hydrolases.

Objective(s) We hypothesized that the elimination of excess mucin granules is dependent on lysosome-mediated degradation in airway secretory cells.

Methods Calu-3 cells, an airway epithelial cell line containing abundant mucin granules, were treated with inhibitors of lysosomal acidification (Bafilomycin A1) and lysosomal enzyme activity (Pepstatin-E64d).

Results We found that both Pepstatin-E64d (PE) and Bafilomycin A1 (Baf) significantly increased the levels of cytoplasmic mucin, MUC5AC, by immunoblotting and immunostaining. This demonstrates that the lysosome is the ultimate fate of certain mucin granules, rather than secretion. We then performed immunostaining of Calu-3 cells treated with either PE or Baf to detect autophagosome marker, Lc3 and lysosome marker, Lamp1. With these lysosomal inhibitors, we found increased fusion of the MUC5AC mucin granule with Lamp1-labeled lysosomes. However, there was no corresponding increase in LC3-labeled autophagosomes engulfing MUC5AC granules.

Conclusion Our data suggests that mucin granules rely on direct fusion with degradative lysosomes, independent of the double-membraned autophagosomes.

125

LUNG EPITHELIAL CELL-DERIVED EXTRACELLULAR VESICLES CAUSE MICROVASCULAR ENDOTHELIAL DYSFUNCTION

Eleftheria Letsiou, Lucille Meliton, Weiguo Chen, Jeffrey Jacobson, Steven Dudek. *University of Illinois Chicago*

Introduction/Background Pulmonary infection by Streptococcus pneumoniae can cause acute lung injury (ALI), which is characterized by disruption of lung epithelial and endothelial normal functioning. We previously demonstrated that pneumolysin (PLY), a pneumococcal pore-forming toxin, stimulates lung epithelial cells (Epi) to release large extracellular vesicles (EVs) that carry mitochondrial cargo. EVs are important mediators of intercellular communication, and extracellular mitochondria encapsulated within EVs have pro-inflammatory properties.

Objective(s) Our study investigated whether lung epithelial EVs regulate endothelial barrier function by transferring mitochondrial cargo to adjacent microvascular endothelial cells (EC).

Methods In vitro, human lung Epi (A549 or primary HBEC) were treated with PLY (100 ng/ml, 4 hrs), and EVs (EV-PLY) were isolated from conditioned media. EV mitochondrial cargo was assessed by labeling with MitoTracker dyes and by immunoblotting (Tom20 expression). For some experiments, EVs were isolated from Epi pre-treated with MitoTempo, a specific mitochondrial ROS (mtROS) scavenger. Isolated EVs were then added to naïve or TNF-α treated human lung microvascular EC. Uptake of EVs by EC was measured by FACS, EC permeability was assessed by transendothelial electrical resistance (TER), and IL-8 levels were measured in cell supernatants. In vivo, naïve mice were injected intratracheally with EVs isolated from PLY-treated MLE-12 (mouse lung alveolar Epi), and bronchoalveolar lavage (BAL) was collected 18 hours later.

Results To determine if EVs can transfer their mitochondrial cargo to lung EC, ECs were incubated with MitoTracker-labeled EV-PLY and analyzed by FACS. 70% of these lung EC were MitoTracker positive by 2 hours after exposure to EVs, demonstrating transfer of mitochondrial cargo. In TER studies to assess the effects of EVs on EC barrier function, EV-PLY from both A549 and HBEC significantly decreased TER over time, indicative of increased endothelial permeability. Moreover, TNF-α-induced lung EC barrier disruption and IL-8 release were exacerbated in the presence of EV-PLY. EVs from control cells had no effect. Importantly, EV-PLY derived from MitoTempo-pretreated Epi contain less mitochondrial cargo and cause less EC barrier disruption and IL-8 release after TNF-α. In vivo, EV-PLY induced a significant recruitment of neutrophils into alveoli.

Conclusion Our studies demonstrate that EVs from PLY-treated lung Epi cause endothelial injury in vitro and inflammation in vivo, and that the pro-inflammatory potential of EVs is dependent on their mitochondrial cargo. These new findings expand our understanding of the mechanisms underlying lung endothelial dysfunction in ALI.

126

THE ASSOCIATION OF NEIGHBORHOOD TRAFFIC AND PHYSICAL ACTIVITY LEVELS IN ADULTS WITH ASTHMA DURING COVID-19 PANDEMIC

[1]Caroline Youssef, [2]Sharmilee Nyenhuis, [3]Barbara Polivka, [4]Luz Huntington-Moskos, [1]Kamal Eldeirawi.
[1]*University of Illinois Chicago;* [2]*University of Chicago;* [3]*University of Kansas;* [4]*University of Louisville*

Introduction/Background Higher rates of physical inactivity occur among adults with asthma, and this is associated with worse asthma outcomes. Specific barriers to physical activity in adults with asthma may include fear of exercise due to exercise-induced bronchoconstriction and lack of social support however additional environmental factors may contribute.

Objective(s) The aim of this study is to explore the association of self-reported neighborhood traffic on physical activity levels among adults living with asthma.

Methods A cross-sectional study using an online survey was conducted in US adults with asthma starting May-December 2020. Survey questions included perceptions of neighborhood traffic, financial problems created by the pandemic and self-reported physical activity of adults with asthma. Participants' exercise frequency was dichotomized into meeting or not meeting US physical activity guidelines (exercise ≥30 minutes per day ≥5 days/week). Perception of heavy car and truck traffic in the neighborhood since the pandemic was also dichotomized into agreement (strongly agree, somewhat agree, neither agree or disagree) or disagreement (strongly disagree, somewhat disagree). A logistic regression model was used to examine the associations of self-reported perceived neighborhood traffic and physical activity. In the analysis, the covariates included age, body mass index (BMI), gender, education, race, and an assessment of financial problems experienced. The regression analysis was also adjusted for COVID-19 status and exposure. We analyzed the data using Statistical Analysis System (SAS).

Results A total of 877 respondents had a mean age of 44 +/-15, with 82% being female and 18% being male. The majority of the participants were White (80%) and had a mean body mass index of 30 +/- 8. The sample was highly educated, with 70% holding a college degree or higher. Of the participants, 61% reported financial difficulties due to the COVID-19 pandemic. Nearly half of the participants (48%) agreed that their neighborhood had heavy car and truck traffic. Results showed that individuals who reported less heavy traffic in their neighborhood were 1.6 times more likely to meet physical activity guidelines after adjusting for covariates. Further adjustment for COVID-19 status or exposure did not significantly alter the association.

Conclusion Perceived neighborhood traffic was associated with physical activity levels in adults with asthma. This and other neighborhood factors should be further explored to understand and address low levels of physical inactivity among adults living with asthma.

127

SARCOIDOSIS RELATED SYMPTOM SEVERITY CORRELATES WITH INFLAMMATORY GENE SIGNATURES

[1]Christen Vagts, [1]Christian Ascoli, [1]Kai Huang, [1]Yue Huang, [1]Jessica Lee, [2]Montserrat Hernandez, [1]Nadera Sweiss, [2]David Perkins, [2]Patricia Finn. [1]*University of Illinois at Chicago; [2]University of New Mexico*

Introduction/Background Sarcoidosis is an immune mediated systemic disease of unknown etiology that results in granulomatous inflammation and multiorgan dysfunction. While there is no universal biomarker to guide sarcoidosis management, the presence of systemic symptoms is a major consideration to treatment initiation and titration. The Sarcoidosis Health Questionnaire (SHQ) is a validated tool that assesses sarcoidosis related morbidity with three domains: physical functioning (PF), daily functioning, and emotional functioning.[1] We hypothesize that sarcoidosis related symptom severity, as measured by the PF domain, is associated with alteration in gene expression profiles and that the assessment of gene networks will yield further insight into drivers of disease.

Objective(s) To characterize the relationship between sarcoidosis related symptom severity and gene expression in individuals with pulmonary sarcoidosis to determine gene signatures associated with disease activity.

Methods Peripheral blood mononuclear cells (PBMCs) were isolated from individuals with sarcoidosis followed at the University of Illinois for bulk RNA sequencing. The Sarcoidosis Health Questionnaire (SHQ) was concurrently administered, from which the PF domain score was extracted. Gene-wise negative binomial generalized linear modelling was used to correlate differential gene expression with PF domain scores with consideration of age, sex, body mass index, and treatment as covariates.[2] Weighted gene co-expression network analysis (WCGNA) was employed to group communities of likely-expressed genes into modules.[3] Modules that significantly correlated to symptom severity were assessed for relevant biological pathways. Finally, immune cell subtype abundance was estimated using gene expression profiles to evaluate how immune cell proportions vary with sarcoidosis symptom severity.[4]

Results Thirty-three subjects with sarcoidosis were included. Subjects were predominantly black (n=23) and women (n=26). All subjects had pulmonary manifestations while 30 had extra pulmonary manifestations. Thirteen were not on any sarcoidosis therapy, while 20 subjects required therapy with systemic corticosteroids, hydroxychloroquine, and/or antimetabolites. The mean PF domain score was 3.9 (2.3 to 5.3, st dev 0.7) on a scale of 1 (less symptomatic) to 7 (more symptomatic). Linear modelling revealed that PF domain scores significantly predicted gene expression as higher symptom scores were associated with 1076 upregulated and 1059 downregulated genes. WCGNA clustered co-expressed genes into 20 modules, of which 9 modules significantly correlated to symptom severity scores. One positively correlated module of interest contained genes related to NK cell related immunity and cytotoxicity as well as genes involved in the negative regulation of T cell differentiation. Analysis of various immune cell subtypes revealed that higher symptom severity scores were significantly associated with higher natural killer CD56+ bright cell and lower CD14+ monocyte proportions.

Conclusion Symptom severity, as measured by the PF domain of the SHQ, is not only predictive of differential gene expression but is significantly correlated to gene regulatory networks of subjects with sarcoidosis. Higher symptom scores are significantly related to NK cell gene expression and abundance, suggesting that NK cell activity may be a driver of sarcoidosis related symptoms and inflammation. Further study is needed to assess the relationship between symptom severity and cell specific gene expression on a single cell level.

REFERENCE(S)

1. Cox CE, Donohue JF, Brown CD, Kataria YP, Judson MA. The Sarcoidosis Health Questionnaire: a new measure of health-related quality of life. Am J Respir Crit Care Med. 2003;168(3):323-329. doi:10.1164/rccm.200211-1343OC

2. Robinson MD, McCarthy DJ, Smyth GK. "edgeR: a Bioconductor package for differential expression analysis of digital gene expression data." Bioinformatics. 2010; 26(1), 139-140. doi: 10.1093/bioinformatics/btp616.

3. Langfelder P, Horvath S. "WGCNA: an R package for weighted correlation network analysis." BMC Bioinformatics. 2008; 559. https://bmcbioinformatics.biomedcentral.com/articles/10.1186/1471-2105-9-559.

4. Steen CB, Liu CL, Alizadeh AA, Newman AM. Profiling Cell Type Abundance and Expression in Bulk Tissues with CIBERSORTx. Methods Mol Biol. 2020; 2117:135-157. doi:10.1007/978-1-0716-0301-7_7

128

CLINICAL RESEARCH PARTICIPANT AS CUSTOMER: FIVE PRINCIPLES FOR DESIGNING HUMAN-CENTERED RESEARCH STUDIES

R. McKinley Sherrod, Jenny Sculley, Aditi Jha, Lauren Castro, Hugh Musick, Jerry Krishnan, Lynn Gerald.
University of Illinois Chicago

Introduction/Background Over 90% of clinical research studies report delays in enrollment; 20% terminate early or have lower than expected sample size due to insufficient enrollment or retention. While many factors affect recruitment and enrollment, the research community has not yet paid sufficient attention to the participant experience. Human-centered design is a practice used to create products, systems and services. It can be employed to identify and understand factors affecting enrollment and retention as a basis for improving the participant experience. As with any service,, the recruitment and retention of clinical study participants necessitates responding to their motivations, needs, and challenges.The RE-CONNECTS study enrolled participants from nine CONNECTS parent studies of potential treatments for SARS CoV2. The goals of RE-CONNECTS were to understand if recontacting participants from previous, related studies was a viable recruitment method and, if so, what qualities a future COVID-focused study would need to possess for participants to join a registry in which they would be contacted several times a year to answer surveys about their health and provide biospecimens (blood, stool, etc).. The study employed human-centered design to explore these questions.

Objective(s) To outline key principles for developing human-centered-informed clinical research studies, toward the goal of increasing recruitment and retention.

Methods Human-centered design has six defining principles. It 1) places stakeholder needs at the center of the problem to solve, 2) understands the real-world context of stakeholders, 3) creates models that describe stakeholder experiences as a basis for identifying factors that drive behavior and motivation, 4) reframes understanding of the context based on interviews and direct observation as a basis for defining solution criteria, 5) conducts iterative prototyping with feedback from stakeholders, and 6) produce testable solutions. These principles were used to interview participants in the RE-CONNECTS study to identify desirable qualities of a future study.

Results 69% (n=105/152) of participants were successfully recontacted and 85% of these participated in the RE-CONNECTS interviews. A subset of these participants (n=18) also participated in a focus group. Data from these conversations yielded five principles for developing human-centered clinical studies that are meaningful to participants: 1) make benefits to participation clear and relevant to participants; 2) set expectations about study activities upfront and reinforce them often; 3) maximize optionality; 4) promote data transparency and ownership; 5) cultivate personal relationships. Table 1 offers an operational definition and examples for each principle.

Conclusion The RE-CONNECTS study yielded five principles for developing human-centered clinical research studies that emphasize the need for a mindset shift among researchers toward acknowledging participants as people engaged in a service. Future research should aim to use the principles in designing clinical research to determine if they improve recruitment and retention.

REFERENCE(S)
1. International Organization for Standardization. (2019). Ergonomics of human-system interaction — Part 210: Human-centred design for interactive systems (ISO Standard No. 9241-210:2019). https://www.iso.org/obp/ui/#iso:std:iso:9241:-210:ed-2:v1:enHanington, Bruce, and Bella Martin. 2.Universal methods of design: 100 ways to research complex problems, develop

innovative ideas, and design effective solutions. Rockport Publishers, 2012.Kumar, Vijay. 101 Design Methods: A structured approach for driving innovation in your organization. John Wiley & Sons, 2012.

Abstract 128 Table 1 Principles for a human-centered clinical research studies

| Principle	Operational definition	Operational example
1. Make benefits to participation clear and relevant to participants	Connect study activities and participant priorities and motivations (e.g., helping others, scientific progress, desire to improve own health)	Return individual and aggregate results at periodic intervals Give participants a "behind the scenes" look at what goes into a research study Cultivate channels for bi-directional communication Offer opportunities to inform the protocol or suggest topics for future research
2. Set expectations about study activities upfront and reinforce them often	Share as much information as possible about what will be expected of the participant upon enrollment. If it is likely that the study protocol or procedures will change, be honest and upfront with participants.	Share information about study activities: • Duration of the study • Frequency of data collection • Method of contact • Level of effort required Share information about compensation: • Amount of compensation • Method of compensation (eg, preloaded debit cards, e-codes) • Frequency of compensation (eg, all at study conclusion, per completed activity, other?)
3. Maximize optionality	Allow participants as much flexibility as possible to choose how they participate without compromising the quality of data collected	Schedule visit appointments outside business hours Offer surveys online or by phone Conduct consent process via phone, e-consent, or in person Allow modalities for sharing data, thoughts, and feelings (e.g., text, audio, video fields)
4. Promote data transparency and ownership	Create multiple, regular opportunities for participants to understand how their participation connects to the study objectives, as well as their motivations for joining.	Inform participants about how researchers will use their data and what they can learn from it Keep participants informed about study progress Give participants a way to view their own data and participation (e.g., survey responses, test results) Share aggregate trends or results at periodic intervals Flag abnormal test results and help participants understand necessary next steps
5. Cultivate personal relationships	Leverage relationships between participants and study staff as a tool for retention and engagement.	Collect information on participants' motivations for joining the study upon enrollment Connect participants with the same coordinator and/or call center agent whenever possible Allow for casual conversation and general check-ins during the study visit Train coordinators and call center agents in trauma-informed, motivational interviewing techniques Prepare coordinators and call center agents to refer participants to additional resources or escalate their questions/concerns

129

REVISTING PROPOFOL INFUSION SYNDROME: EARLY DIAGNOSIS LEADING TO BETTER SURVIVAL AND OUTCOME

[1]Sasmit Roy, [2]Sunil Rajan. [1]*Centra Lynchburg General Hospital;* [2]*Centra Southside Community Hospital*

Introduction/Background Propofol related infusion syndrome (PRIS) is a dreaded complication that can happen to critically ill patients initiated on propofol, as an infusion agent for sedation. PRIS is mostly seen in patients receiving high dose (> 67 microgram/kilogram/minute[mcg/kg/min]) and/or prolonged infusion of > 48 hours (hrs) along with associated clinical features of high anion gap metabolic acidosis, renal failure, cardiogenic shock, hypertriglyceridemia, lactic acidosis.[1] Most patients with reported PRIS succumb to their illness because of its high mortality i.e., 30-70%.[2]

Case Presentation 49-year-old Hispanic female with history of hypertension presented with complains of dyspnea and hemoptysis for last 3 days. Vitals in emergency department revealed low oxygen saturation at 90%, tachypnea of 22/min, tachycardia of 104 beats/min and fever of 39 degree Celsius. Chest Xray on admission revealed left sided wedge like consolidation. (figure1)Labs revealed elevated WBC of 36000/microliter while creatinine was slightly elevated at 1.8 milligram/deciliter(mg/dl). Rest of electrolytes including potassium, anion gap and CO2 were normal. She was initiated on azithromycin and ceftriaxone. Covid-19 and pulmonary embolism were ruled out. She tested positive for Influenza A and was started on Tamiflu. Her condition deteriorated rapidly in next 24 hrs with severe hypoxia thought to be secondary to aspiration. She was subsequently intubated and started on broad spectrum antibiotics with vancomycin and cefepime. Cefepime was later changed to Meropenem, given persisting fevers. Vasopressor support and stress dose steroids were also added. For sedation, she was initiated on propofol and fentanyl infusions. Initially propofol was started at 40 mcg/kg/min, but by 24 hrs it was increased to 70mcg/kg/min, due to difficulties with sedating the patient. Labs drawn simultaneously revealed low CO2 of 19, anion gap of 16, sodium of 146 mg/dl, creatinine of 5.3 mg/dl with serum triglyceride of 1372 mg/dl and blood glucose of 558 mg/dl. Creatinine kinase level was normal. Immediately propofol was discontinued and sedation changed to midazolam. She was started on insulin infusion along with iv sodium bicarbonate infusion. Sputum culture demonstrated streptococcus pyogenes and antibiotics were de-escalated to meropenem alone. Over the course of next 5 days, her condition improved significantly; her acidosis, hypertriglyceridemia, and renal function all improved. She required bronchoscopy three times for recurrent mucus plugging and resultant atelectasis. (figure 2) She remained non oliguric throughout, without needing renal replacement therapy. She was successfully extubated and weaned off pressors. After 14 days of ICU stay her condition improved substantially and she was discharged with normal creatinine, normal CO2 level and normal triglycerides.
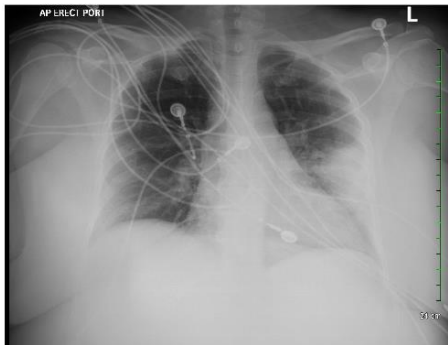
Abstract 129 Figure 1: Initial Chest Xray on admission
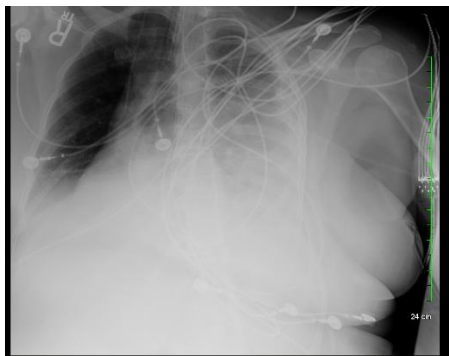
Abstract 129 Figure 2: Xray demonstrating atelectasis and consolidation

Discussion Due to its rapid onset of action along with sedative, anxiolytic and anticonvulsant properties propofol is a popular agent of choice in selected critically ill patients.[3] The incidence of this complication can be seen in 4.7 % of patients receiving this agent[2] The pathophysiology of this condition is from interruption of the electron transport chain, impeding the beta-adrenoreceptors and cardiac calcium channels and destruction of beta-oxidation of fatty acids in mitochondria.[1] Treatment options are mainly conservative with stopping the propofol and other supportive means like iv fluids, bicarbonate, renal replacement therapy, extra corporal membrane oxygenation. In our case, despite the severe electrolyte imbalances, her condition improved remarkably upon timely identification of this complication. Our case highlights the importance of this disease and portrays hope that early diagnosis and appropriate therapy can improve outcome in this otherwise life-threatening condition.

REFERENCE(S)
1. Mirrakhimov AE, Voore P, Halytskyy O, Khan M, Ali AM. Propofol infusion syndrome in adults: a clinical update. Crit Care Res Pract. 2015;2015:260385. doi:10.1155/2015/260385
2. Krajčová A, Waldauf P, Anděl M, Duška F. Propofol infusion syndrome: a structured review of experimental studies and 153 published case reports. Crit Care. 2015;19:398. Published 2015 Nov 12. doi:10.1186/s13054-015-1112-5
3. Kotani Y., Shimazawa M., Yoshimura S., Iwama T., Hara H. The experimental and clinical pharmacology of propofol, an anesthetic agent with neuroprotective properties. CNS Neuroscience and Therapeutics. 2008;14(2):95–106.

130

SUBCLINICAL CARDIAC DYSFUNCTION DETECTED BY SPECKLE TRACKING ECHOCARDIOGRAPHY IN DERMATOMYOSITIS/POLYMYOSITIS: A META-ANALYSIS

[1]Faria Sami, [2]Shahzad Ahmed Sami, [3]Thomas Minik, [4]Hania Sami, [1]Muhammad Khawar Sana, [5]Ata Ul Haiy. [1]*John H. Stroger Hospital of Cook County;* [2]*Trinity Health Oakland Campus;* [3]*Midwestern University Chicago College of Osteopathic Medicine;* [4]*Shalamar Medical and Dental College;* [5]*King Edward Medical University*

Introduction/Background Dermatomyositis and Polymyositis (DM/PM) are connective tissue disorders characterized by autoimmune-mediated inflammatory myopathy along with other multisystem manifestations. Cardiac abnormalities are also frequent in these patients, and often subclinical. In comparison to standard echocardiography, speckle tracking echocardiography (STE) has become a more useful ultrasound technique to estimate myocardial function. We report the STE parameters in DM/PM patients in our study to estimate the degree of cardiac dysfunction.

Objective(s) The main objective of this study was to assess cardiac involvement in dermatomyositis/polymyositis patients. We also aim to determine the utility of speckle tracking echocardiology (two-dimensional) in investigating ventricular deformation for early detection of cardiac dysfunction.

Methods A literature search using PubMed, Embase, and cochrane library was performed. The medical subject headings (MeSH) were used to obtain and combine the results of dermatomyositis, polymyositis, and echocardiography. The initial search yielded 107 articles but final meta-analysis was performed using 5 studies. For each included study mean age, baseline comorbidities, machine used for echocardiography and strain data from echocardiography results were extracted. The global longitudinal strain, circumferential strain, and right ventricular strain data was reported in the included studies. Mean strain with standard deviation (SD) was extracted along the number of participants. Statistical analysis was performed using the random effect model adopting the Hedges g equation to obtain standardized mean difference (SMD) for continuous echocardiographic outcome data. The analysis was performed using Stata 17.0.

Abstract 130 Table 1 Forest plot of the studies included in the metanalysis for noninvasive assessment of cardiac function

Study	DM/PM N	Mean	SD	Control N	Mean	SD	Hedges's g with 95% CI	Weight (%)
CS								
Diniz 2020	35	-23.9	2.8	35	-26.7	2.9	0.97 [0.48, 1.46]	12.59
Heterogeneity: τ^2 = 0.00, I^2 = .%, H^2 = .							0.97 [0.48, 1.46]	
Test of $\theta_i = \theta_j$: Q(0) = -0.00, p = .								
Test of θ = 0: z = 3.88, p = 0.00								
GLS								
Zhong 2017	60	-20.3	2.5	30	-23.4	1.7	1.36 [0.88, 1.83]	12.83
Diniz 2020	35	-22	5.35	35	-23	3.3	0.22 [-0.24, 0.69]	13.06
Guerra 2017	28	-18.7	4.2	28	-21.2	2.1	0.74 [0.21, 1.28]	11.82
Rajaei	30	-19.6	2.67	40	-21.9	2.45	0.89 [0.40, 1.38]	12.59
Liu 2022	46	-17.8	4.9	30	-22.8	2	1.23 [0.74, 1.73]	12.50
Heterogeneity: τ^2 = 0.15, I^2 = 69.87%, H^2 = 3.32							0.89 [0.49, 1.29]	
Test of $\theta_i = \theta_j$: Q(4) = 13.68, p = 0.01								
Test of θ = 0: z = 4.34, p = 0.00								
RV								
Zhong 2017	60	-19.4	4.2	30	-24.8	2	1.48 [0.99, 1.96]	12.69
Guerra 2017	28	-19.3	6.3	28	-22.5	3.8	0.61 [0.08, 1.14]	11.92
Heterogeneity: τ^2 = 0.31, I^2 = 82.30%, H^2 = 5.65							1.05 [0.20, 1.90]	
Test of $\theta_i = \theta_j$: Q(1) = 5.65, p = 0.02								
Test of θ = 0: z = 2.41, p = 0.02								
Overall							0.94 [0.64, 1.23]	
Heterogeneity: τ^2 = 0.12, I^2 = 64.68%, H^2 = 2.83								
Test of $\theta_i = \theta_j$: Q(7) = 20.19, p = 0.01								
Test of θ = 0: z = 6.25, p = 0.00								
Test of group differences: Q_b(2) = 0.14, p = 0.93								

Random-effects REML model   Favors Control   Favors DM/PM

Results After screening for duplicates and irrelevance, a total of 5 studies including 362 patients (199/163 cases/controls) were used. We found that speckle echocardiographic strain was significantly associated with dermatomyositis/polymyositis (MD: 0.94; CI: 0.64–1.23; p =0.00) when compared with patients without DM/PM. The overall heterogeneity among studies was significant (I2: 64.68%, p=0.01). We also found a significantly increased incidence of Circumferential strain (MD: 0.97, CI: 0.48–1.46, p-value =0.00), Global longitudinal strain (MD: 0.89, CI: 0.49–1.29, p-value =0.01), and right ventricular strain (MD: 1.05, CI: 0.20–1.90, p-value =0.02) in patients of dermatomyositis/polymyositis when compared to the controls. Significant heterogeneity is noted among studies. Meta-regression analysis with a random effect model reveals female gender does not affect heterogeneity. However, GLS and RVS were significantly found to decrease with fixed effect models.

Conclusion Dermatomyositis/Polymyositis patients have lower STE parameters than controls. This indicates that DM/PM patients have impaired cardiac function involving both ventricles. STE can be used to identify and diagnose these patients for early management.

131

USE OF BETA-BLOCKERS IN PATIENTS WITH APIS-MELLIFERA AND OTHER HYMENOPTERA VENOM ANAPHYLAXIS

Aamir Akram, Vaskar Mukerji, Kamil Salam, Sahana Venkatesh. *Wright State University*

Introduction/Background The Hymenoptera comprise a group of insects that includes bees, wasps, sawflies and ants. Hymenoptera stings, primarily from bees (Genus: Apis, Species: Mellifera) result in approximately 60-70 deaths in the United States annually and cause serious reactions in others. The number of deaths from bee stings exceeds that from snake bites, spiders or wild animal attacks in this country. Beta blockers represent one of the most commonly used class of drugs to treat a variety of illnesses. Due to their mechanism of action, beta-blockers may reduce the efficacy of epinephrine used to treat anaphylaxis and may also counter the body's own adrenergic response.

Objective(s) The purpose of this study was to determine whether Hymenoptera stings resulted in increased morbidity and mortality in patients receiving beta-blockers.

Methods We reviewed the published literature, via an on-line search, seeking adults over the age of 18 years with reported Hymenoptera sting reactions. The reactions were graded for severity using the Mueller scale. The use of beta-blockers in these patients was recorded. We then determined the percentage of patients on beta-blockers who developed a severe reaction of Grade 3 or higher, which was characterized by shock and severe multi-system organ damage. We also determined the number of patients not reported to be on beta-blockers who had a severe reaction and compared the two population subsets.

Results We were able to access information on more than 3000 reported cases of Hymenoptera sting reactions. Among these, the two largest studies accounted for 2749 patients of which 1400 patients were categorized as having a grade 3 or 4 reaction. These studies showed that the percentage of patients having a severe reaction following the sting was higher among those on beta-blockers compared with those not on beta-blockers. Other smaller studies had varying results.

Conclusion Statistical analysis was limited by the heterogenicity of the information presented in the various publications and the great variation in the standards used in reporting. Our data demonstrate that a large percentage of individuals on beta-blockers suffer a severe outcome after bee stings. However, further study is necessary in this area. For now, great caution should be exercised in the use of beta-blockers in patients with a known history of bee sting anaphylaxis. In these patients, a severe reaction may recur following a bee sting, and so immediate aggressive management may need to be initiated. If beta-blocker therapy is essential in the management of these patients, then "accelerated" immunotherapy should be considered as a preventive measure.

REFERENCE(S)

1. Stoevesandt J, Hain J, Kerstan A, Trautmann A. Over- and underestimated parameters in severe Hymenoptera venom-induced anaphylaxis: cardiovascular medication and absence of urticaria/angioedema. J Allergy Clin Immunol. 2012 Sep;130(3):698-704.e1. doi: 10.1016/j.jaci.2012.03.024. Epub 2012 May 1. PMID: 22554708.
2. Ruëff F, Przybilla B, Biló MB, Müller U, Scheipl F, Aberer W, Birnbaum J, Bodzenta-Lukaszyk A, Bonifazi F, Bucher C, Campi P, Darsow U, Egger C, Haeberli G, Hawranek T, Körner M, Kucharewicz I, Küchenhoff H, Lang R, Quercia O, Reider N, Severino M, Sticherling M, Sturm GJ, Wüthrich B. Predictors of severe systemic anaphylactic reactions in patients with Hymenoptera venom allergy: importance of baseline serum tryptase-a study of the European Academy of Allergology and Clinical Immunology Interest Group

on Insect Venom Hypersensitivity. J Allergy Clin Immunol. 2009 Nov;124(5):1047-54. doi: 10.1016/j.jaci.2009.08.027. PMID: 19895993.

3. Solley GO. Stinging and biting insect allergy: an Australian experience. Ann Allergy Asthma Immunol. 2004 Dec;93(6):532-7. doi: 10.1016/S1081-1206(10)61259-8. PMID: 15609761.

4. Lantner R, Reisman RE. Clinical and immunologic features and subsequent course of patients with severe insect-sting anaphylaxis. J Allergy Clin Immunol. 1989 Dec;84(6 Pt 1):900-6. doi: 10.1016/0091-6749(89)90387-4. PMID: 2600324.

Abstract 131 Table 1

	Total Patients	Patients on Beta Blockers	Patients not on Beta Blockers		
Over- and underestimated parameters in severe Hymenoptera venom–induced anaphylaxis	657	59	566	Total	
Grade 1	208	14	178		
Grade 2	277	30	238		
Grade 3	172	15	150		
Total Percentage		25.42372881	26.50176678		
Predictors of severe systemic anaphylactic reactions in patients with Hymenoptera venom allergy	962	52	868	Total	
grade 1-2	756	34	698		
grade 3-4	206	18	170		
Total Percentage		34.61538462	19.58525346		
Stinging and biting insect allergy: an Australian experience	1787	18	1769	Total	
grade 1-2	593	5	588		
grade 3-4	1194	13	1181		
Total Percentage		72.22222222	66.760882		

132

SERUM PROTEOME DIFFERENCES BETWEEN CHRONIC AND ACUTE REACTIVE ARTHRITIS PATIENTS

[1]Tarek Firzli, [1]Brooke Clemmensen, [1]Juli Petereit, [2]Chad Porter, [3]Mark Riddle, [4]Kennedy Ukadike.
[1]*University of Nevada Reno School of Medicine;* [2]*Naval Medical Research Center;* [3]*Pfizer;* [4]*Renown Health*

Introduction/Background Reactive Arthritis (ReA) is an arthitic sequela to enteric or sexually transmitted infection, commonly campylobacter jejuni, salmonella sp., shigella sp., chalmydia trachomatis and yersinia sp.[1] Symptoms appear about 2-4 weeks following such infections and may include the classic triad of urethritis, uveitis and arthritis, although more commonly patients do not present with all of these symptoms. While a majority of patient's symptoms resolve within 6 months, a subset (10-30%) may go on to develop chronic symptoms.[2, 3] Certain general inflammatory biomarkers such as ESR, CRP, IL-6, IL-13, IFN-gamma and TNF-alpha have also been described, however no specific serum protein biomarkers have been described.[1, 4] There is a paucity of data characterizing acute ReA which resolves and chronic ReA which may persist for years causing significant morbidity to patients.
**Objective(s)** Our primary aim is to investigate differences in the serum proteomes of acute and chronic ReA patients by evaluating discordant fold changes in these patients as a mainly hypothesis generating study.
Methods Serum samples were collected from 50 active component military personnel from the Department of Defense Serum Biorepository between 1998 and 2012 from a previously described cohort.[5] ICD-10 codes were used to identify ReA patients. Control serum samples were collected for each patient consisting of the closest sample prior to the ReA diagnosis, and disease serum samples were the closest sample following diagnosis. Patients were further characterized as acute ReA if they had no follow up encounters for ReA past 6 months, and chronic if they had continued encounters for ReA past 6 months. Samples were analyzed by the University of Arkansas Medical School Proteomics Center using LC/MS chromatography with data-independent acquisition to gather protein abundances. The differential expression between the pre disease samples (controls) and post disease samples were calculated for acute ReA and chronic. We set our cutoff log fold change at >= 0.1 and <= -0.1 and our unadjusted p-value threshold at p< 0.1. We grouped proteins into "significantly discordant" if they reached our significance threshold of fold change in acute and chronic ReA, but the direction of fold change differed. We labeled proteins "potentially significantly discordant" if a protein reached our threshold in one condition but not in the other, however the direction of fold change was different.
Results We identified 131 proteins met either the fold change or p value threshold in acute ReA or chronic ReA patients. Of these proteins, 22 had fold change discordance between conditions. We found 10 proteins which were significantly discordant (Figure 1) and 12 proteins that were potentially significantly discordant (Figure 2). The significantly discordant set of proteins included CRHBP (corticotropin releasing hormone binding protein), S100A7 (S100 calcium binding protein A7), BPGM (bisphosphoglycerate mutase), FN1 (fibronectin 1), ITGA2B (integrin subunit alpha 2b), GHR (growth hormone receptor), CPQ (carboxypeptidase Q), ECM2 (extracellular matrix protein 2), MMP3 (matrix metallopeptidase 3) and XYLT2 (xylosyltransferase 2). The potentially significantly discordant set of proteins included C4A (complement 4a), ADGRG6 (adhesion G protein-coupled receptor G6), C3 (complement C3), PRKCSH (protein kinase C substrate 80K-H), LAMP1 (lysosomal associated membrane protein 1), LGN2 (lipocalin 2), HEG1 (heart development protein with EGF like domains 1), CAMP (cathelicidin antimicrobial peptide), SELL (selectin L), OGN (osteoglycin), FBLN1 (fibulin 1), and ITGB3 (integrin subunit beta 3).

Significant Discordant Expression Differences Between Chronic and Acute ReA
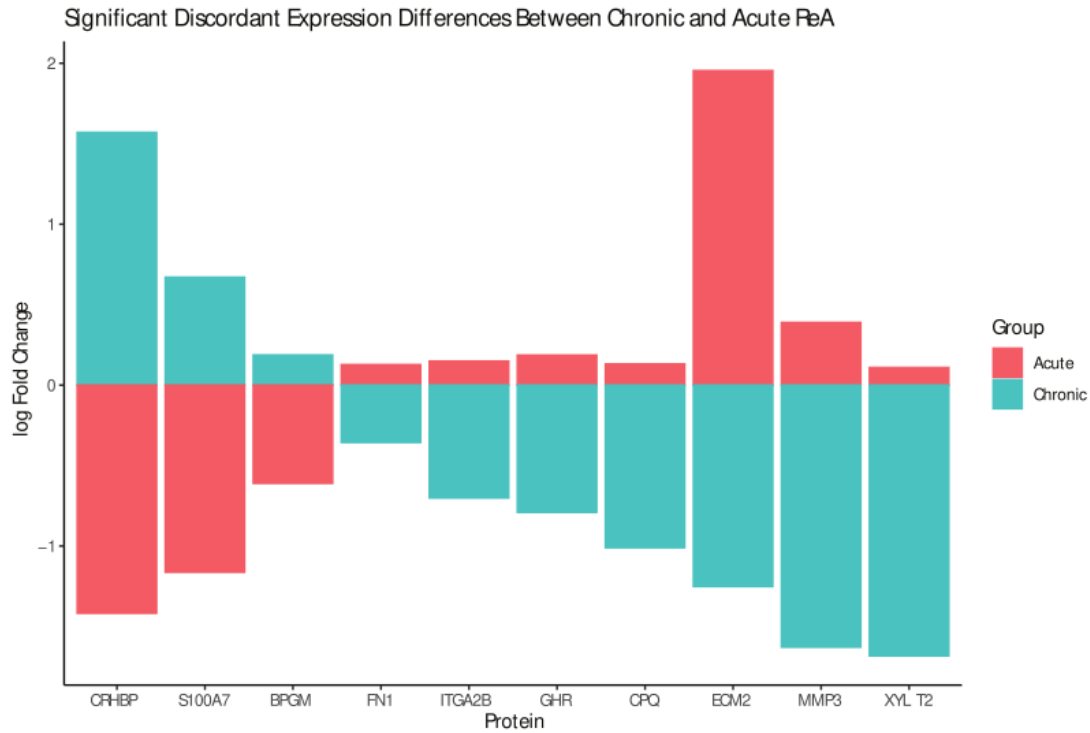
Abstract 132 Figure 1 Reported fold change differences between pre disease controls and post disease samples in chronic and acute patients, ordered in descending order of fold change in the chronic group. Significantly discordant proteins are defined as proteins showing significant fold changes in both chronic and acute patients but in different directions.

Potentially Significant Discordant Expression Differences Between Chronic and Acute ReA
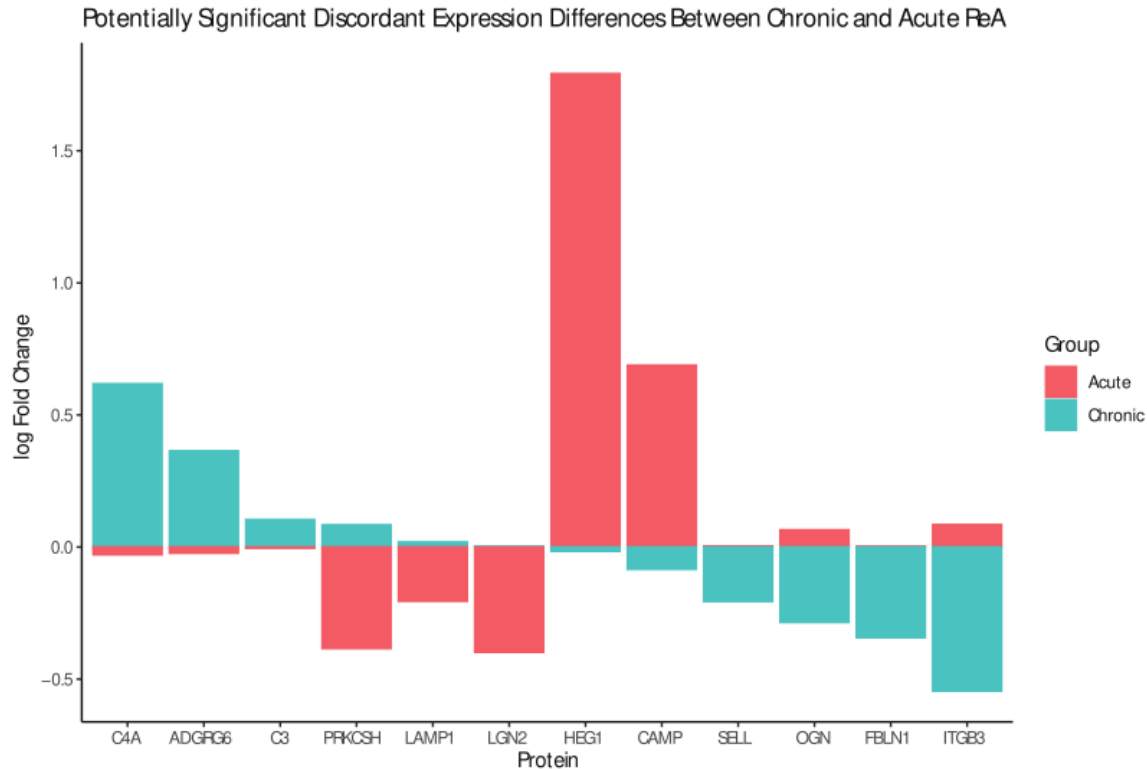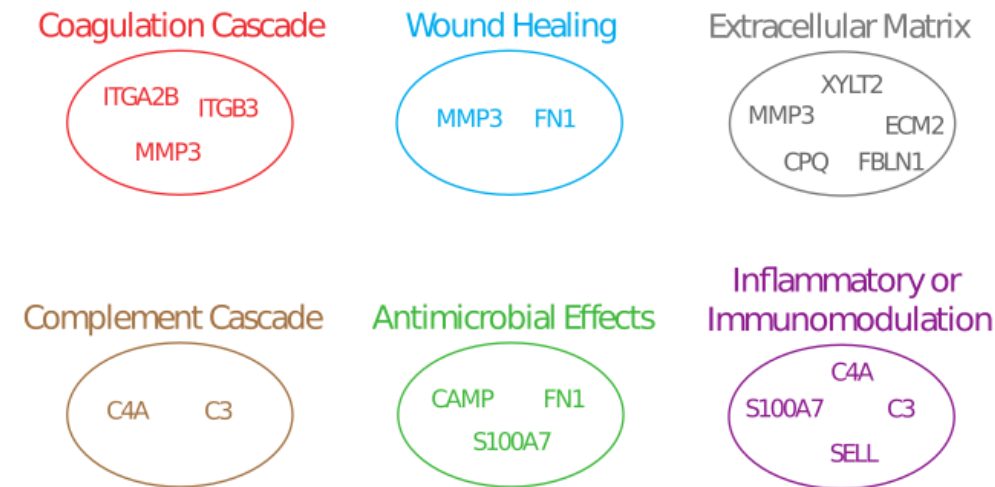
Abstract 132 Figure 2 Reported fold change differences between pre disease controls and post disease samples in chronic and acute patients, ordered in descending order of fold change in the chronic group. Potentially significantly discordant proteins are defined as proteins showing significant fold changes in either the chronic or acute patients but in different directions.

Conclusion We several potential differences between protein expression in chronic versus acute ReA. These tended to have functions such as wound repair (MMP3 and FN1) which showed decreased expression in chronic ReA patients, the coagulation cascade (ITGA2, ITGB3 and MMP3) which showed decreased expression in chronic ReA patients, complement proteins (CA4, C3) which showed increased expression in chronic ReA patients, proteins with antimicrobial effects (CAMP, S100A7, and FN1) which had variable differences, proteins with roles in inflammatory/immunomodulatory processes (S100A7, C3, SELL, and C4A) which had variable differences and proteins involved in the ECM (ECM2, CPQ, MMP3, XYLT2, FBLN1) which showed decreased expression in chronic ReA patients (Figure 3). We believe that chronic ReA may progress due to alterations in some of these functional domains, however more research is required to prove causation. What is further unclear is whether these differences in expression are the result of pre-existing genetic differences or the result of heterogenous host responses to ReA pathogenesis. Limitations of this study include low sample size which prompted the decision to utilize unadjusted p-values, and a permissive fold change threshold, and the use of a pre-existing cohort that included a paucity of metadata to utilize as controlling variables.

Functional domains of discordant proteins on chronic and acute ReA

Coagulation Cascade
ITGA2B ITGB3
MMP3

Wound Healing
MMP3 FN1

Extracellular Matrix
XYLT2
MMP3 ECM2
CPQ FBLN1

Complement Cascade
C4A C3

Antimicrobial Effects
CAMP FN1
S100A7

Inflammatory or Immunomodulation
C4A
S100A7 C3
SELL

Abstract 132 Figure 3 Groupings of selected proteins which were identified in the significantly discordant or potentially significantly discordant protein lists by functional properties. Functional properties were selected primarily where multiple proteins acted in these domains.

REFERENCE(S)
1. Garcia-Kutzbach, A., et al., Reactive arthritis: update 2018. Clin Rheumatol, 2018. 37(4): p. 869-874.
2. Carter, J.D., Reactive arthritis: defined etiologies, emerging pathophysiology, and unresolved treatment. Infect Dis Clin North Am, 2006. 20(4): p. 827-47.
3. Ngaruiya, C.M. and I.B. Martin, A case of reactive arthritis: a great masquerader. Am J Emerg Med, 2013. 31(1): p. 266 e5-7.
4. Verma, A., et al., Elucidating potential molecular signatures through host-microbe interactions for reactive arthritis and inflammatory bowel disease using combinatorial approach. Sci Rep, 2020. 10(1): p. 15131.
5. Porter, C. K., et al. (2020). Contemp Clin Trials Commun 17: 100522.

133

COMPARATIVE ANALYSIS OF DIFFERENCES IN METABOLISM AND HEPATOTOXICITY IN MURINE MODELS OF TYPE1/TYPE17 VS TYPE2 IMMUNE RESPONSES AFTER ORAL EXPOSURE TO THE HARMFUL ALGAL BLOOM CYANOTOXIN MICROCYSTIN-LR

Apurva Lad, Joshua Breidenbach, Prabhatchandra Dube, Shungang Zhang, Jason Breuler, Bivek Timalsina, Sanduni Premathilaka, Dragan Isailovic, Steven Haller, David Kennedy. *University of Toledo*

Introduction/Background Overgrowths of cyanobacteria (aka blue-green algae) are increasing in freshwater sources across the globe and referred to as Harmful Algal Blooms (cHABs). These cHABs produce bioactive secondary metabolites including microcystin-LR (MC-LR), which is one of the most frequently detected and potent cyanotoxins and poses significant health risks to exposed individuals. While the immunotoxicity of MC-LR has been demonstrated in target organs including the liver and kidney, little is known about the metabolism and fate of this common cyanotoxin as well as the role of the immune system in response to MC-LR exposure.

Objective(s) We compared the metabolism and toxicity of a single oral exposure of MC-LR in strains of mice that are predisposed to either type 1/ type 17 (C57BL/6) or type 2 (BALB/c) immune responses to xenobiotics.

Methods Ten-week-old male BALB/c and C57BL/6 mice (n=4 each per group) were gavaged with either a single dose of water (vehicle) or 500 μg/kg of MC-LR. The mice were then placed in metabolic cages for 24 hours to collect urine, followed by euthanasia and collection of blood and organs. The 24-hrs urine and plasma derived from blood were analyzed using LC-MS/MS for both MC-LR and MC-LR-Cysteine (MC-LR-Cys), an adduct formed during hepatic detoxification of MC-LR. Quantitative PCR analysis was performed on the liver and kidney tissues for markers of hepatotoxicity and nephrotoxicity, respectively, as well as the microcystin transporter – Organic Anion Transporter Protein SLCO1b2 (Slco1b2).

Results After 24 hours both MC-LR and MC-LR-Cys were below the limit of detection in the plasma of both strains of mice. Mass spectrometric analysis of the urine samples indicated that BALB/c mice excreted significantly higher (12 fold) amounts of MC-LR than C57BL/6 mice ($p \leq 0.01$). The conversion of MC-LR to MC-LR Cys was significantly lower in the BALB/c mice ($p \leq 0.01$), but the levels were still 6 times higher as compared to MC-LR-Cys levels in the C57BL/6 mice. No significant differences between mouse strains were seen for markers of nephrotoxicity including kidney injury molecule-1 (KIM-1) and neutrophil gelatinase-associated lipocalin (NGAL). Livers of BALB/c vs C57BL/6 mice demonstrated significantly higher basal expression of Slco1b2, a solute carrier that aids in the transport of MC-LR into the cells ($p \leq 0.05$). An interesting observation was that the expression of Slco1b2 was significantly reduced in the livers of BALB/c mice that were exposed to a single dose of MC-LR vs vehicle ($p \leq 0.0001$) whereas in the C57BL/6 mice, exposure to MC-LR increased the expression of this transporter vs vehicle ($p \leq 0.05$). Despite significant reduction in the Slco1b2 transporter levels after MC-LR exposure, livers of Balb/c mice showed significant increase in the markers of hepatotoxicity such as Oncostatin M Receptor (OSMR), Serpine and CD36 (all $p < 0.05$ vs vehicle). These markers showed a similar trend in the livers of C57BL/6 mice, with Serpine and CD36 being significantly upregulated following exposure to MC-LR ($p \leq 0.0001$ and $p \leq 0.001$, respectively) whereas OSMR showed an upward trend ($p=0.077$). Another marker associated with glutathione mediated detoxification of microcystins, Glutathione S-Transferase Mu 5 (Gstm5), had significantly higher basal levels in BALB/c mice compared to the C57BL/6 mice. However, MC-LR exposure led to significant reductions in Gstm5 in both strains of mice.

Conclusion These results indicate that type 1/ type 17 immune response prone C57BL/6 mice may have a reduced rate of MC-LR metabolism compared to the type 2 prone BALB/c mice. These metabolic differences appear to have significant implications for the increased hepatotoxic response seen in

BALB/c mice and suggest potential strategies for identifying novel preventative, diagnostic and therapeutic targets to combat the health effects of cyanotoxins such as MC-LR.

134

INCREASED HEPATOTOXIC AND NEPHROTOXIC RESPONSE IN A MURINE MODEL OF TYPE 1/TYPE 17 VS TYPE 2 IMMUNE RESPONSE EXPOSED TO AEROSOLIZED HARMFUL ALGAL BLOOM TOXIN MICROCYSTIN-LR

Gabriel Kleer, Joshua Breidenbach, Apurva Lad, Benjamin French, Bivek Timalsina, Prabahatchandra Dube, Dhilhani Faleel, Deepak Malhotra, David Kennedy, Steven Haller. *University of Toledo College of Medicine and Life Sciences*

Introduction/Background Cyanobacterial Harmful Algal Blooms (cHABs) are on the rise globally and pose serious health concerns due to the release of cyanotoxins, which are harmful to both humans and the environment. Microcystin-LR (MC-LR) is one of the most frequently produced cyanotoxins and has recently been detected in aerosols generated by the normal motions of affected bodies of water. However, the human health effects of MC-LR aerosols on health remain largely unknown. We have previously demonstrated that MC-LR aerosol exposure has a pro-inflammatory influence on the airways of mice, inducing a type 1/type 17 inflammatory response.

Objective(s) The objective of this study was to investigate the pro-inflammatory effects of aerosolized MC-LR in downstream target organs including the liver and kidney in strains of mice that are predisposed to either type 1/ type 17 (C57BL/6) or type 2 (BALB/c) immune responses to xenobiotics.

Methods Male C57BL/6 and BALB/c mice (13-14 weeks old) were exposed to MC-LR aerosol or control vehicle aerosol using an inExpose animal exposure system equipped with a nose-only exclusively nasal inhalation adapter and a small particle (2.5-4 µm) VMD Aeroneb Lab ultrasonic nebulizer. Exposures were 1 hour each day for 14 days and tissues were harvested within 1 hour after the final exposure. Targeted quantitative PCR (qPCR) arrays were performed on the liver and kidney tissues for markers of hepatotoxicity and nephrotoxicity, respectively, as well as the microcystin transporter – Organic Anion Transporter Protein SLCO1b2 (Slco1b2).

Results Livers of C57BL/6 vs BALB/c mice demonstrated significantly lower basal expression of Slco1b2, a solute carrier that aids in the transport of MC-LR into the cells (p≤0.05). Interestingly, livers of C57BL/6 and BALB/c mice had similar levels of Glutathione S-Transferase Mu 5 (Gstm5), which is associated with glutathione mediated detoxification of microcystins. Despite this, livers of C57BL/6 mice exposed to MC-LR aerosol demonstrated >5 fold increases in expression of markers related to inflammation mediated by chemokine and cytokine signaling (e.g. Ccl1, Ccl20, Cxcr4, Lta) as well as >10 fold increases in expression of markers related Toll receptor signaling (e.g. TLR7, TLR9, Tirap), and Interleukin signaling (e.g. IL-1 alpha, IL-1 beta, IL-6, IL-22) compared to livers of BALB/c mice. Kidneys of BALB/c vs C57BL/6 mice were not significantly different in expression of the Slco1b2 microcystin transporter. Kidneys of C57BL/6 mice exposed to MC-LR aerosol demonstrated >10 fold increases in expression of markers related to inflammation mediated by chemokine and cytokine signaling (e.g. Cxcl3, Cxcl9, Lta, TNF alpha) as well as Toll receptor signaling (e.g. TLR5, TLR6, TLR7, TLR9), and Interleukin signaling (e.g. IL-5, IL-9, IL-9, IL-22) compared to livers of BALB/c mice.

Conclusion These results indicate that type 1/ type 17 immune response prone C57BL/6 mice may have increased hepatotoxicity and nephrotoxicity compared to the type 2 prone BALB/c mice. These differences may suggest potential strategies for identifying novel preventative, diagnostic, and therapeutic targets to combat the health effects of exposure to aerosolized cyanotoxins such as MC-LR.

135

OVERLAP OF RHEUMATOID ARTHRITIS AND GRANULOMATOSIS WITH POLYANGIITIS

[1]Faria Sami, [2]Shahzad Ahmed Sami, [3]Almurtada Razok, [3]Kirtan Patolia. [1]*John H. Stroger Hospital of Cook County;* [2]*Trinity Health Oakland Campus;* [3]*Cook County Health - - Chicago, IL*

Introduction/Background Rheumatoid arthritis (RA) is an inflammatory polyarthritis with multisystem involvement. It can coexist with other autoimmune diseases and rarely even vasculitis.[1-3] Granulomatosis with polyangiitis (GPA) is necrotizing vasculitis of medium-sized vessels. GPA patients can have symmetric polyarthritis which can make it challenging to differentiate from RA.[4] The handful of cases of overlap of GPA and RA reported raise the question of possible interrelation between the two.[5] We present a case of RA with GPA with the aim to highlight diagnostic challenges and association of GPA and RA.

Case Presentation A 57-year-old gentleman presented with arthralgia, joint swelling, erythema, and stiffness for 5 months duration involving the knees, shoulders, elbows, wrists and small joints of the hands bilaterally. He also had dry eyes and episodes of epistaxis for four months. Review of other systems was negative.The exam revealed synovitis in bilateral wrists, metacarpophalangeal joints, proximal interphalangeal joints, elbows, shoulders, and knees with limited range of motion. The EULAR/ACR score for RA was 10.Labs showed hemoglobin of 9.7 g/dL, creatinine 2.2 mg/dL, ESR 83mm/hr, CRP 10.22 mg/dL, rheumatoid factor (RF) 140 IU/mL, anti-CCP antibodies (anti-CCP Ab) During treatment in following months, he developed diffuse alveolar hemorrhage, rapidly progressive glomerulonephritis and end-stage renal disease.

Discussion GPA and RA have overlapping symptoms involving the musculoskeletal, respiratory, and cardiovascular systems, with some differentiating features. For instance, arthritis is seen in GPA but erosive arthritis, a key RA feature, is rarely encountered.[6] Similarly, GPA can affect any part of the upper respiratory tract but in RA, the disease is limited to the laryngeal region.[7, 8] Hassan et al. reviewed the literature for 14 overlap cases for RA and GPA. About 88% were females and the age at diagnosis was in the 4th-5th decades. RA preceded GPA commonly and the mean interval between diagnoses was 101 months. In most cases, GPA had sinopulmonary involvement. More than 65% had ANCA antibodies and more than 80% had positive rheumatoid factor at the time of RA diagnosis.[5] Our case is unique in that the patient is a male of 59 years, diagnosed with both conditions at the same time. In a seven-year study, ANCA-positive RA patients were more likely to have rapid progression of erosive arthritis, assessed by the Larsen Grading Scale. They were also more likely to have RF.[9] However, there is a paucity of data to conclude if GPA/RA overlap confers a worse prognosis or rapid progression of GPA. In our patient, GPA was rapidly progressive. Vaishnav et al. published a case of GPA presenting as rapidly progressive DAH causing death in a patient on treatment for RA for 7 months. 10 It is also difficult to predict the renal outcomes in GPA/RA patients, as only 3/16 (19%) of the cases had renal involvement. 11More studies are needed to predict the prognosis and severity of GPA manifestations in GPA/RA patients and possibly to define diagnostic guidelines of this overlap syndrome.

REFERENCE(S)
1. Wang Y, Chen S, Chen J, Xie X, Gao S, Zhang C, Zhou S, Wang J, Mai R, Lin Q, Lin J, Matucci-Cerinic M, Zhang G, Furst DE. Germline genetic patterns underlying familial rheumatoid arthritis, systemic lupus erythematosus and primary Sjögren's syndrome highlight T cell-initiated autoimmunity. Ann Rheum Dis. 2020 Feb;79(2):268-275. doi: 10.1136/annrheumdis-2019-215533. Epub 2019 Dec 17. PMID: 31848144

2. Korkmaz C, Zubaroğlu I, Kaya T, Akay OM. Takayasu's arteritis associated with rheumatoid arthritis: a case report and review of the literature. Rheumatology (Oxford) 2001;40:1420–2.
3. Harada S, Mitsunobu F, Kodama F, Hosaki Y, Mifune T, Tsugeno H, et al. Giant cell arteritis associated with rheumatoid arthritis monitored by magnetic resonance angiography. Intern Med. 1999;38:675–8.
4. Kısacık B, Önder ME, Sayarlıoğlu M, Onat AM. Symmetric polyarthritis as an initial symptom in granulomatosis with polyangiitis: A report of six cases and review of the literature. Eur J Rheumatol. 2018 Sep;5(3):191-193. doi: 10.5152/eurjrheum.2018.17050. Epub 2018 Apr 19. PMID: 30071923; PMCID: PMC6116851.
5. Hassan AS, Edigin E, Patel AR, Manadan A. The Co-existence of Rheumatoid Arthritis and Granulomatosis With Polyangiitis: Two Cases and Review of the Literature. Cureus. 2021;13(8):e17103. Published 2021 Aug 11.doi:10.7759/cureus.17103
6. Noritake DT, Weiner SR, Bassett LW, Paulus HE, Weisbart R. Rheumatic manifestations of Wegener's granulomatosis. J Rheumatol. 1987 Oct;14(5):949-51. PMID: 3501472.
7. Trimarchi M, Sinico RA, Teggi R, Bussi M, Specks U, Meroni PL. Otorhinolaryngological manifestations in granulomatosis with polyangiitis (Wegener's). Autoimmun Rev. 2013 Feb;12(4):501-5. doi: 10.1016/j.autrev.2012.08.010. Epub 2012 Aug 23. Erratum in: Autoimmun Rev. 2015 Jan;14(1):80. PMID: 22940553.
8. Rudrappa M, Kokatnur L, Shah S. Case Report: Upper airway obstruction due to rheumatoid arthritis. F1000Res. 2020 Feb 18;9:119. doi: 10.12688/f1000research.22256.1. PMID: 34484694; PMCID: PMC8383128.'
9. Mustila A, Paimela L, Leirisalo-Repo M, Huhtala H, Miettinen A. Antineutrophil cytoplasmic antibodies in patients with early rheumatoid arthritis: an early marker of progressive erosive disease. Arthritis Rheum. 2000 Jun;43(6):1371-7. doi: 10.1002/1529-0131(200006)43:63.0.CO;2-R. PMID: 10857797.
10. Vaishnav KU, Bhatt C, Desai A. Diffuse alveolar haemorrhage in granulomatosis with polyangitis (Wegener's) with coexistent rheumatoid arthritis. BMJ Case Rep. 2012 Aug 8;2012:bcr2012006184. doi: 10.1136/bcr.2012.006184. PMID: 22878986; PMCID: PMC4543218.
11. Szilasi M, Mátyus J, File I, et al. Association of ANCA-associated vasculitis-rheumatoid arthritis overlap syndrome in four patients: rituximab may be the right choice?. Autoimmunity. 2012;45(4):304-309. doi:10.3109/08916934.2012.677078

136

GOUT AS A CELLULITIS MIMIC

Faria Sami, John Case. *John H. Stroger Hospital of Cook County*

Introduction/Background Gout is a crystalline arthropathy caused by monosodium urate deposition in joints, more commonly affecting men [1,2]. While the management is entirely different, rarely cellulitis can mimic gout and, more commonly, gout can mimic cellulitis [3, 4]. Cellulitis is a clinically diagnosed infection of subcutaneous tissue, epidermis, and dermis [5]. Distinction between the two can be a diagnostic challenge [6]. Our case highlights the significance of keeping a low threshold for gout when the presentation resembles cellulitis with desquamation.

Case Presentation A 65-year-old man with hypertension and diabetes presented with 5 days of left index finger erythema, pain and swelling, with fever and chills. He reported past episodes of similar tender erythema and swelling involving the left hand and right elbow that were treated as cellulitis with antibiotics. Review of other systems was negative. Labs were remarkable for CRP 4.1 mg/dL (normal On exam tender, warm, erythematous swelling on the dorsum of the digit was seen as were areas of desquamation. Rheumatology suspected gout & ordered X-rays. Orthopedic service advised surgical intervention. Vancomycin & ceftriaxone were started for cellulitis. Subsequently, pain & erythema improved. The patient was taken for incision & drainage, and copious amount of tophi was removed from the left 2nd PIP. Antibiotics were discontinued and prednisone 40 mg was started. Both hand X-rays showed periarticular osteopenia, degenerative changes in multiple wrist and finger joints, metacarpal head erosions. Soft tissue swelling in left hand and 2nd & 3rd digits was noted. Repeat blood & urine cultures were negative, the initial bacterial growth was concluded a contaminant.

Discussion Early on in gouty arthritis the inflammatory changes can mimic cellulitis [6]. Tendonitis from gout can also present similarly to cellulitis and effusion is often absent [7]. Pseudogout can also present similarly and should be a differential diagnosis [8]. Typical gout is abrupt and has dramatic erythema, severe pain, swelling and tenderness in the joint with sometimes fever/chills, peaking in 12-24 hours. These signs can resemble cellulitis. But gout is more likely to have recurrent attacks with spontaneous resolution. Cellulitis is insidious and oftentimes progresses from a pustule, abscess or wound. Fever & leukocytosis are nonspecific findings. It is not typically recurrent unless a predisposing factor like venous stasis edema is present. Current diagnostic approach for gout includes aspiration of synovial fluid for microscopic analysis for negatively birefringent monosodium urate crystals with or without gram staining & culture [9]. Lack of response to NSAIDs and steroids can allow deviating from gout to cellulitis, however, history of recurrent episodes as in our patient serves as a clue of gout [8]. Gradual resolution of gout can also be imitative of response to antibiotics, as in our patient, making accurate diagnosis challenging. Like cellulitis, severe gout may resolve with desquamation. Desquamation and/or ulceration localized to one joint is more likely in gout [10, 11]. In a recent study, delta neutrophil index was studied as a useful tool to differentiate gout from cellulitis, regardless of presence of hyperuricemia and monosodium urate [12]. Rarely, gout can also cause cellulitis for which ultrasound can be a useful diagnostic tool [13, 14]. Prompt diagnosis is necessary to allow for judicious use of antibiotics as well as use of acute gout therapy in setting of active infection.

REFERENCE(S)
1. Kuo CF, Grainge MJ, Zhang W, et al. Global epidemiology of gout: prevalence, incidence and risk factors. Nat Rev Rheumatol 2015;11:649–62.
2. Schlee S, Bollheimer LC, Bertsch T, Sieber CC, Härle P. Crystal arthritides - gout and calcium pyrophosphate arthritis : Part 1: Epidemiology and pathophysiology. Z Gerontol Geriatr. 2018

Jun;51(4):453-460. English. doi: 10.1007/s00391-017-1197-3. Epub 2017 Feb 23. PMID: 28233117.

3. Blumberg G, Long B, Koyfman A. Clinical Mimics: An Emergency Medicine-Focused Review of Cellulitis Mimics. J Emerg Med. 2017 Oct;53(4):475-484. doi: 10.1016/j.jemermed.2017.06.002. PMID: 29079067.

4. Falagas ME, Vergidis PI. Narrative review: diseases that masquerade as infectious cellulitis. Ann Intern Med. 2005 Jan 4;142(1):47-55. doi: 10.7326/0003-4819-142-1-200501040-00011. PMID: 15630108.

5. Boettler MA, Kaffenberger BH, Chung CG. Cellulitis: A Review of Current Practice Guidelines and Differentiation from Pseudocellulitis. Am J Clin Dermatol. 2022 Mar;23(2):153-165. doi: 10.1007/s40257-021-00659-8. Epub 2021 Dec 13. PMID: 34902109.

6. Raff AB, Kroshinsky D. Cellulitis: A Review. JAMA. 2016 Jul 19;316(3):325-37. doi: 10.1001/jama.2016.8825. PMID: 27434444.

7. Ohnishi J, Ishimaru N, Seto H, Kanzawa Y, Kinami S. Gout in the Flexor Hallucis Longus Tendon Mimicking Cellulitis: A Case Report. J Am Podiatr Med Assoc. 2020 Jan;110(1):Article8. doi: 10.7547/18-161. PMID: 32073328.

8. StuWilli, and StuWilli. "Case Report: Gout vs. Cellulitis." Journal of Urgent Care Medicine, 1 Feb. 2010, www.jucm.com/case-report-gout-vs-cellulitis/.

9. Chen LX, Schumacher HR. Current trends in crystal identification. Curr Opin Rheumatol. 2006 Mar;18(2):171-3. doi: 10.1097/01.bor.0000209430.59226.0f. PMID: 16462524.

10. Zahoor H, Patel R, El-Bahri J. Ulcerated Tophaceous Gout. Cureus. 2022 Sep 3;14(9):e28729. doi: 10.7759/cureus.28729. PMID: 36204027; PMCID: PMC9528853.

11. Eggebeen AT. Gout: an update. Am Fam Physician. 2007 Sep 15;76(6):801-8. PMID: 17910294.

12. Pyo JY, Ha YJ, Song JJ, Park YB, Lee SK, Lee SW. Delta neutrophil index contributes to the differential diagnosis between acute gout attack and cellulitis within 24 hours after hospitalization. Rheumatology (Oxford). 2017 May 1;56(5):795-801. doi: 10.1093/rheumatology/kew471. PMID: 28115599.

13. Wakefield RJ, Emery P, Pease C. Gout related upper limb cellulitis: an ultrasound study. J Rheumatol. 2003 Feb;30(2):417-9. PMID: 12563707.

14. Skedros JG, Smith JS, Henrie MK, Finlinson ED, Trachtenberg JD. Upper Extremity Compartment Syndrome in a Patient with Acute Gout Attack but without Trauma or Other Typical Causes. Case Rep Orthop. 2018 Jan 23;2018:3204714. doi: 10.1155/2018/3204714. PMID: 29796328; PMCID: PMC5896219.

STATIN-ASSOCIATED NECROTIZING AUTOIMMUNE MYOPATHY

Joel Wright, Angila Bag, Smitha Agadi, Dipal Patel. *Hackensack University Medical Center/Englewood Hospital*

Introduction/Background Statins have become a cornerstone therapy in the primary and secondary prevention of atherosclerotic cardiovascular disease with 1 in 4 Americans over the age of 40 currently taking a statin. Despite their great benefit, the most common reason for their discontinuation by patients is statin-associated muscle symptoms (SAMS). SAMS may manifest as separate and distinct entities clinically: (i) myalgia, (ii) rhabdomyolysis, (iii) Toxic Self-limited Myopathy and (iv) Statin-Associated Necrotizing Autoimmune Myopathy (SANAM), a relatively newly described disease. SANAM is less commonly recognized and occurs with an estimated incidence of 1 in 100,000 persons on a statin. It is important that clinicians are vigilant for SANAM and differentiate it from other SAMS as its management and prognosis vary from the other entities.

Case Presentation A 58-year-old male presented with a one month of progressive weakness in all extremities, intermittent thigh pain on standing and 30 lb weight loss over 6 months. His past medical history included Hypertension, Type 2 Diabetes, Hyperlipidemia and a myocardial infarction 3 years prior for which Atorvastatin was started. Examination revealed bilateral proximal upper and lower extremity as well as neck flexor weakness. He was areflexic and demonstrated a waddling gait. The remainder of his exam was unremarkable. Complete blood count and basic metabolic panel were normal. Creatine kinase (CK) was 19,365 U/L (30-200), LDH 1,203 U/L (125-220) AST 160 U/L (5-34) and ALT 321 U/L (Atorvastatin was discontinued at presentation and fluids were initiated with some improvement in weakness and downtrending CK over the 3 day course of admission. On follow-up with Rheumatology a week after discharge, he was started on Prednisone due to residual weakness.

Discussion The purpose of this case report is to highlight a rare complication of commonly prescribed statins. SANAM presents with predominantly painless symmetric proximal weakness, developing an average of 36 months following statin initiation, although it can occur at any time. CK levels typically range from 10-100 times the upper limit of normal with electromyography revealing an irritable myopathy and serology displaying elevated anti-HMGCR antibodies in all cases. While statins may cause transaminase elevation through their hepatotoxic potential, this can also be of musculoskeletal origin, clueing one into the fact that the patient may instead have muscle injury, as was the case in this patient. Rightfully, muscle specific antibodies were checked to evaluate for paraneoplastic inflammatory myopathy such as polymyositis/dermatomyositis in the setting of significant weight loss. SANAM, although less commonly, can also present with weight loss. Typical of SANAM, which differentiates it from severe forms of Toxic Self-Limited Myopathy clinically, is the lack of weakness resolution on statin discontinuation. It is paramount that the statin be discontinued and serology sent promptly to confirm SANAM, as these patients usually require immunosuppression, unlike with the other forms of statin myopathy.

138

ANGIOTENSIN II TYPE 1 RECEPTOR ANTIBODY MEDIATED KIDNEY REJECTION UNRESPONSIVE TO TREATMENT

Suhalika Sahni, David Allison, Zahraa Hajjiri, Luis Manon, Sally Campbell-Lee, Suman Setty. *University of Illinois Chicago*

Introduction/Background Antibody-mediated rejection (AMR) is a well-known complication following a kidney transplant, resulting in graft failure if not treated promptly. Many AMR cases are due to recipient antibodies against donor HLA antigens. Recently, non-HLA antibodies have been identified as causing AMR in the absence of recipient HLA sensitization. Among these, antibodies with agonistic specificity for the angiotensin II type 1 receptor (AT1R) are increasingly implicated in cases of AMR refractory to standard treatment. While some reports have suggested improvement or stabilization of graft function, we present two patients in which anti-rejection therapy including therapeutic plasma exchange was unable to salvage the allograft.

Case Presentation Patient 1A 53-year-old woman with a history of end-stage renal disease (ESRD) renal transplant 3 years ago was admitted with acute renal failure and serum creatinine (Cr) 3.4 mg/dL (baseline 1.2 mg/dL). At the time of transplant, the HLA antibody screen and crossmatch were negative. Her maintenance immunosuppression was tacrolimus and mycophenolic acid. During hospitalization, she underwent a kidney allograft core biopsy that demonstrated glomerulitis, peritubular capillaritis and acute tubular necrosis. C4d was focally positive in the peritubular capillaries via immunohistochemistry. She was administered i.v methylprednisolone 500 mg for 3 days for acute T cell-mediated rejection (TCMR), then continued oral prednisone 10 mg daily. Donor-specific antibodies were not detected. The patient underwent 2 plasma exchanges (TPE) followed by i.v immunoglobulin (IVIgG) 10 g, every other day, prior to discharge. Ten days after discharge, the AT1R antibody came positive after which she underwent 26 TPE sessions, with increasing serum Cr. She also received losartan during treatment. Unfortunately, the transplant failed, and peritoneal dialysis was restarted despite a negative AT1R antibody assay after a prolonged series of outpatient TPE. Patient 2 A 62-year-old male with a history of ESRD status renal transplant 2 years ago presented with proteinuria and elevated creatinine. The patient was on tacrolimus with prednisone and mycophenolate. The kidney allograft core biopsy showed changes of glomerulitis and peritubular capillaritis and was negative for C4d by immunohistochemistry. AT1R antibody was ordered and returned as positive >40 units/mL. The patient didn't respond to losartan. He then underwent 6 sessions of TPE and IVIgG, with worsening of serum Cr (2.97 mg/dL). His renal function further declined and he restarted hemodialysis 3 months later.

Discussion Angiotensin II type 1 receptor antibody-mediated rejection (AT1R-AMR) is increasingly being identified as the etiology of allograft rejection in kidney transplant recipients without detectable HLA antibodies. While some reports have suggested that AT1R-AMR may be refractory to standard therapy, others have reported improvement or stabilization of graft function (Table 1). Due to proposed agonistic effect of AT1R antibodies causing vasoconstriction, angiotensin receptor blockers have been suggested as adjunct therapy. Thus, we want to emphasize that there could be yet-unidentified antibodies against the donor's kidney in addition to other patient specific factors that may explain a poor therapeutic response in some cases but recovery in others. Identification of these antibodies is critical for treatment and risk stratification for patients with allogenic renal transplant rejection apart from HLA antibodies.

Abstract 138 Table 1 Summary of Cases Treated With TPE: Abbreviations: TPE, therapeutic plasma exchange; IVIgG, intravenous immunoglobulin; ARB, angiotensin receptor blocker; NR, not reported

	No. of cases	TPE sessions	IVIgG	Other immunosuppression	ARB use?	Outcome
Dragun [1]	7	Yes (NR)	Yes	NR	Yes	Graft salvage
Yamada [2]	2	8 – 11	Yes	NR	Yes	Graft salvage
Wiwattanathum [3]	1	11	Yes	Methylprednisolone, anti-thymocyte globulin, tacrolimus, rituximab	No	Graft salvage
Jobert [4]	1	6	No	Methylprednisolone, anti-thymocyte globulin	Yes	Graft salvage
Fuss [5]	11	6 - 11	Yes	Methylprednisolone, anti-thymocyte globulin	Yes	Graft salvage
Lee [6]	10	Yes (NR)	Yes	Steroids (unspecified), anti-thymocyte globulin, rituximab, bortezomib (1 case)	NR	Graft salvage
Our report	2	26 (case 1) 6 (case 2)	Yes	Methylprednisolone, tacrolimus	Yes	Graft failure
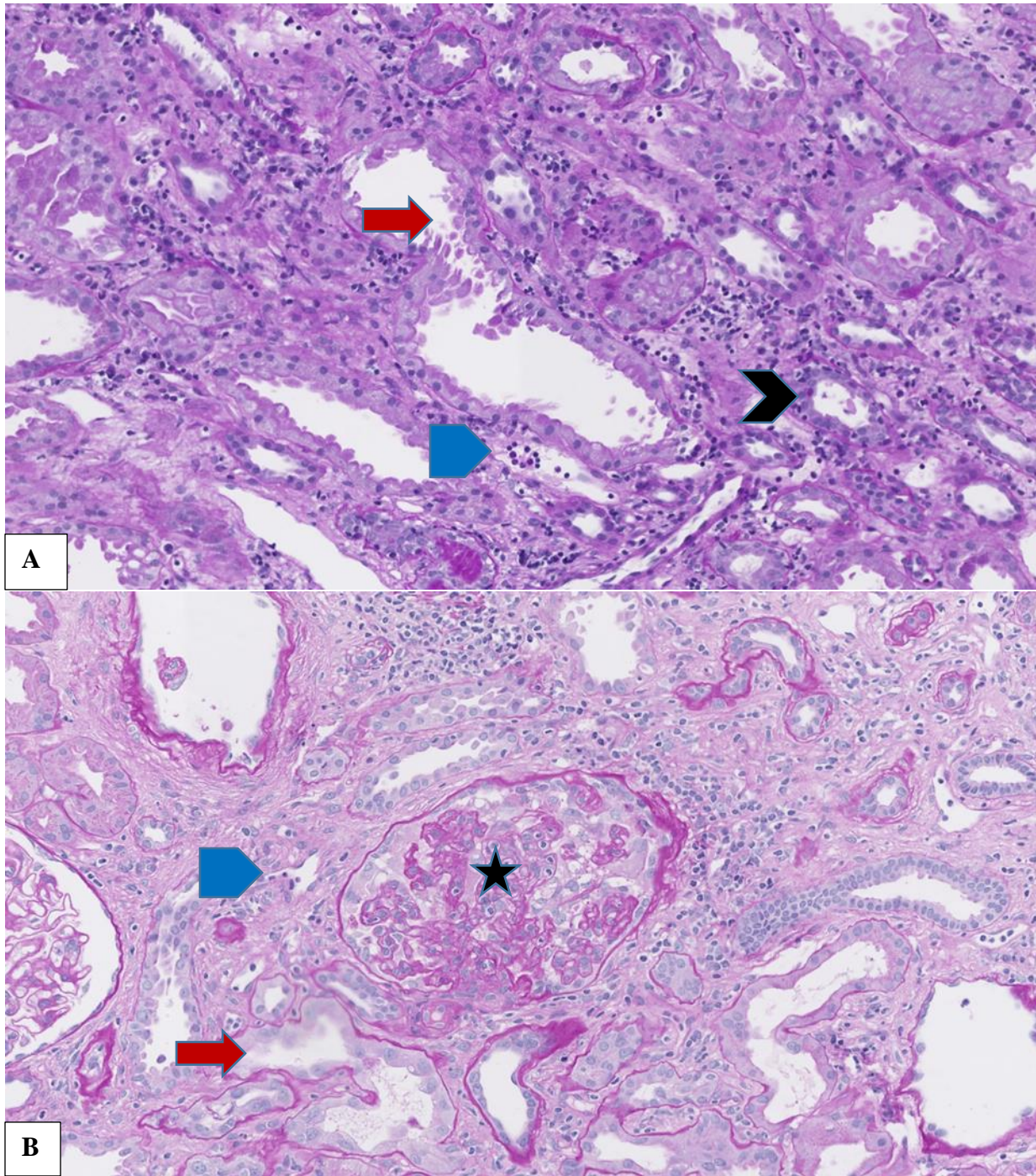
Abstract 138 Figure 1 Periodic acid Schiff stained sections of renal biopsies from pt 1 (image A) and pt 2 (image B) (original magnification 200x): A. Tubular luminal dilatation with attenuation of brush borders suggestive of acute tubular necrosis (red arrow), tubulitis (black chevron) in non-atrophic and atrophic tubules and peritubular capillaritis (blue pentagon). B. Glomerulitis (star), tubular luminal dilatation with attenuation of brush borders suggestive of acute tubular necrosis and peritubular capillaritis.

REFERENCE(S)

1. Dragun D, Muller D, Brasen J, Fritsche L, Neiminen-Kelha M, Dechend R, Kintscher U, Rudolph B, Hoebeke J, Eckert D, Mazak I, Plehm R, Schonemann C, Unger T, Budde K, Neumayer H, Luft F, Wallukat G. Angiotensin II type 1-receptor activating antibodies in renal-allograft rejection. N Engl J Med. 2005;352:558 – 569.

2. Yamada C, Huang Y, Norman S, Naik A, Moussa O, Samaniego M, Cooling L. Efficacy of therapeutic plasma exchange on angiotensin II type-1 receptor antibodies on two kidney transplant recipients. J Clin Apher. 2018 Dec;33(6):673 – 677.

3. Wiwattanathum P, Ingsathit A, Thammanichanond D, Worawichawong S. Successful treatment of anti-angiotensin II type 1 receptor antibody-associated rejection in kidney transplantation: a case report. Transplantation Proceedings. 2018;50:877 – 880.

4. Jobert A, Rao N, Deayton S, et al. Angiotensin II type 1 receptor antibody precipitating acute vascular rejection in kidney transplantation. Nephrology. 2015;20(Suppl 1):10-12.

5. Fuss A, Hope CM, Deayton S, et al. C4d-negative antibody-mediated rejection with high anti-angiotensin II type I receptor antibodies in absence of donor-specific antibodies. Nephrology. 2015;20:467-473.

6. Lee J, Park Y, Kim BS, et al. Clinical implications of angiotensin II type 1 receptor antibodies in antibody-mediated rejection without detectabledonor-specific HLA antibodies after renal transplantation. Transplant Proc. 2015;47:649-652.